SUBDUCTION ZONE-TO-MANTLE FLUXES OF TRACE ELEMENTS AT INTRAOCEANIC MARGINS AND IMPLICATIONS FOR MANTLE EVOLUTION

A Dissertation

Presented to the Faculty of the Graduate School

of Cornell University

in Partial Fulfillment of the Requirements for the Degree of

Doctor of Philosophy

by

Katherine Anne Porter

August 2005

SUBDUCTION ZONE-TO-MANTLE FLUXES OF TRACE ELEMENTS AT INTRAOCEANIC MARGINS AND IMPLICATIONS FOR MANTLE EVOLUTION

Katherine Anne Porter, Ph.D.

Cornell University 2005

Chemical and isotopic anomalies in mantle-derived rocks have been explained by invoking the presence of recycled oceanic crust (i.e., material of crustal origin that is incorporated into the mantle at subduction zones) in their mantle sources. Differences between the chemical and isotopic characteristics of the ingoing slab material and those of the inferred slab-derived mantle reservoirs have been attributed to processes within the subduction zone that alter the composition of the ingoing slab. However, there have been few studies that have specifically examined the composition of residual slab material to determine the effects of subduction zone processing. I used a mass-balance approach to calculate residual slab compositions at nine intraoceanic subduction zones. I calculated residual slab trace element ratios and modern isotopic characteristics of ancient subducted slabs in order to examine the feasibility of mantle evolution models that posit a major role for subducted slabs. Using my calculated residual slab compositions, I was unable to reproduce the chemical and isotopic characteristics of the mantle that have been attributed to the incorporation of recycled crustal material. Modifications to my model to account for variations in mantle wedge composition and in crustal addition rates do not significantly alter these conclusions. My results therefore

indicate that subduction zone processing alone is probably insufficient to produce the chemical and isotopic characteristics of inferred mantle reservoirs.

BIOGRAPHICAL SKETCH

Katherine Anne Porter grew up in New Hampshire and graduated from Hillsboro-Deering High School in June 1996. She attended the University of Delaware from August 1996 until May 2000, when she received a Bachelor of Science degree in Geology. During a field geology course in Iceland in 1999, she became interested in mantle geochemistry and the evolution of mantle plumes. This interest led her to attend graduate school at Cornell University.

For Daddy, who taught me to

"Work hard and be a leader,"

"Watch out for the crazies," and

"You gotta laugh at yourself!"

And for Mom, Ben, and Chris, who made sure that I did.

ACKNOWLEDGMENTS

This work was funded by a National Science Foundation Graduate Research Fellowship and a Cornell Science Inquiry Project Teaching Fellowship to the author and by National Science Foundation grant #EAR0309992 to Dr. William White. The modeling would not have been possible without the resources of the GEOROC, PetDB, and EarthRef databases and the Java MELTS program. The author wishes to express her gratitude to Dr. William White; Dr. Louis Derry; Dr. Francis DiSalvo; Dr. Stagg King; Dr. Robert Kay; Dr. Suzanne Kay; Adam Goss; and several anonymous reviewers for their assistance, insight, and advice on this project.

Special thanks to Dr. Christopher Maloney for fixing the computers and to the Paleogeeks for many a discussion of species concepts and other minutiae.

TABLE OF CONTENTS

LIST OF FIGURES

LIST OF TABLES

LIST OF ABBREVIATIONS

Abbreviation	**Definition**
AOC	Altered Ocean Crust
BSE	Bulk Silicate Earth (crust + mantle)
DMM	Depleted MORB Mantle
EMI	Enriched Mantle type I
EMII	Enriched Mantle type II
Fo	Forsterite (Mg_2SiO_4)
HFSE	High Field Strength Elements (Nb, Ta, Zr, Hf, [Th,U])
HIMU	High-μ mantle reservoir (μ = $^{238}U/^{204}Pb$)
IAV	Island Arc Volcanics
Kd	mineral-melt distribution coefficient
LILE	Large Ion Lithophile Elements (K, Rb, Ba, Sr)
LLOD	Liquid Line Of Descent (fractionation path)
MORB	Mid-Ocean Ridge Basalt
NMORB	Normal MORB
NMORBs	NMORB-source mantle
OIB	Ocean Island Basalt
REE	Rare Earth Elements (La, Ce, Nd, Sm, Eu, Y, Yb, Lu)

Chapter 1: Conceptual Background and Method

Conceptual Background

Many of the processes that control the chemical composition of the Earth's mantle[a] are poorly constrained. Although "pieces" are occasionally brought to the surface (for example, as xenoliths and in kimberlite pipes[b]), the mantle is generally inaccessible to direct sampling and its characteristics and evolution must be estimated using indirect methods. Since many of the rocks that are erupted at the Earth's surface are produced by melting within large regions of the mantle, their characteristics can be used to infer mantle chemistry. Chemical and isotopic analyses of mantle-derived rocks have shown that the mantle is characterized by both large- and small-scale variations in elemental and isotopic composition (e.g. Allegre *et al.*, 1986; Arai *et al.*, 1997; Hofmann, 1988; White, 1995). Assuming that the mantle was originally homogeneous (a generally valid assumption, given the probable mechanisms of Earth's formation), then it becomes necessary to account for the loss of homogeneity over the history of the planet.

---

[a] The Earth's interior can be divided into layers based either on chemistry or rheology. The core (0-2800 km) is composed primarily of nickel and iron. The mantle (2800-~6400 km) is of primarily ultramafic composition (high concentrations of Mg and Fe, and low in Si relative to the crust), and the crust (~6400-6430 km) has a generally felsic or sialic (high in Si, Al, and K) composition. In terms of rheology, the core has two layers (solid inner and liquid outer), and the mantle contains two layers: a ductile, weak asthenosphere (2800-6300 km) and a brittle lithosphere (6300-6430 km). The lithosphere includes all of the crust and part of the (compositionally defined) mantle.

[b] Xenoliths are chunks of rock whose extremely mafic composition and mineralogy are very different from the volcanic rocks in which they are embedded. Their mineralogy suggests that they may actually be pieces of the mantle – lower lithosphere or asthenosphere – that were "broken off" by the rising magma and carried to the surface. Kimberlite pipes are tube-like veins containing highly "primitive" – that is, mafic and mantle-like – rocks. The presence of diamonds in kimberlites suggests that they originate at very high (i.e. mantle-like) temperatures and pressures and ascend very rapidly.

The extraction of the crust from the mantle has played an extremely important role in the development of the chemical variations in the mantle. Almost without exception, igneous[c] rocks found at the Earth's surface are produced by small degrees of partial melting of a large mantle source region; these rocks are generally associated with volcanism in regions where the Earth's tectonic plates[d] are converging or diverging and producing new crust. Since many elements have strong thermodynamic preferences for solid or melt phases, the melts (and residues) produced by partial melting of the solid mantle exhibit different chemical compositions than their mantle source material. The melt phases produced during partial melting are generally less dense than their complementary residues; as a result, the melts tend to rise to the Earth's surface, where they are erupted to form the rocks of the crust. However, the extraction of the Earth's crust from an initially homogeneous mantle cannot completely account for all of the observed heterogeneities in the mantle. For example, an examination of the isotopic characteristics of mantle-derived rocks (MORB and OIB) shows that there are variations in mantle isotopic signatures that would not be expected to occur within the

[c] Geologists classify rocks into three primary groups based on how they form. Igneous rocks are produced by the cooling and crystallization of molten rock (magma or lava). Sedimentary rocks are produced by compaction & cementation of pieces of other rock, and metamorphic rocks are produced when a rock undergoes chemical and physical changes due to heat and pressure (but doesn't melt – then it would form an igneous rock!).

[d] The Earth's lithosphere is "broken" into many different plates, which are in constant motion. In places where the plates touch each other, extreme stresses lead to all sorts of neat geology. Where the plates are moving away from each other (divergent margins), mantle material can rise, partially melt, and erupt to form new crust (i.e. lots of volcanism – but because of the relatively low stresses and ductile material, not many large earthquakes; see Figure 1.7). This usually occurs in ocean basins deep under water, but in Iceland and East Africa one can observe surface manifestations of the process. At transform margins, where the plates slide past one another, one sees a lot of earthquakes (e.g. the San Andreas fault in California) but not much volcanism. At convergent margins, or subduction zones (see Figure 1.2), volcanism and earthquakes are quite intense. The biggest earthquakes ever have occurred on these margins (e.g. Chile, Alaska, Sumatra).

mantle had it been formed from extraction of melt over time (see Figure 1.1). Such heterogeneities suggest that some additional process or processes must be contributing to mantle chemistry.

One important process influencing the chemistry of the mantle involves the consumption of crustal material at subduction zones, where two tectonic plates collide and one sinks beneath the other. Figure 1.2 shows a diagram of the typical geometry of such a region. The incorporation of the downgoing plate (the "slab") into the convecting mantle[e] could be a major source of mantle heterogeneity. If mantle that had been mixed with crustal material were to melt and produce crustal rocks, those rocks would undoubtedly show chemical and isotopic signatures that reflected the mixture of materials in their source. Indeed, the incorporation of subducted crustal material into the mantle has been invoked to explain the characteristics of several distinct mantle "reservoirs" whose existence has been inferred from studies of the chemistry of ocean island basalts[f] (OIB; e.g. Elliott *et al.*, 1999; Hannigan *et al.*, 2001; Hart and Staudigel, 1989; Jacobsen, 1989; Marty and

[e] The chemical organization of the mantle is poorly defined. We know that the mantle convects, but there is debate as to whether there is significant exchange of material between the "lower" mantle (below ~670 km) and the "upper" mantle. I have tried to avoid tying my discussions to any particular model of mantle mixing. "Convecting mantle" simply means that part of the mantle that is tapped to produce rocks erupted at the surface. It could be upper, lower, or any other portion of the mantle.

[f] Magmas are classified primarily by their major element chemistry. Basalts have low SiO_2 (<~50 wt%), high MgO (>~6-7 wt%) and FeO (~1-3 wt%), and relatively low Al_2O_3 (that is, they have a mafic composition). As a basaltic magma cools and begins to crystallize, the residual melt "evolves" and becomes more acidic (higher in SiO_2, lower in MgO). Andesites are generally the most evolved igneous rocks; they have very high SiO_2 (up to 70 wt%) and Al_2O_3 (10-15 wt%). Most rocks erupted at mid-ocean ridges are basalts (MORB or mid-ocean ridge basalts); most rocks erupted at subduction zones are closer to the andesitic side of things. Ocean Island Basalts (OIB) are basalts that do not erupt at divergent margins, so they're not MORB; they're generally thought to be the surface expression of "plumes" of mantle material that rise from the interior of the Earth to the surface. There's a whole other thesis in explaining various ideas about OIB. For our purposes, the important thing is that they are mantle-derived (they come from below the lithosphere) but they have very different trace element and isotopic chemistry from MORB.

Dauphas, 2003; McCulloch, 1993; Paul *et al.*, 2002; Sims and DePaolo, 1997; White and Duncan, 1996).

Arguments for the presence of recycled crustal material in the mantle source for OIB have largely been based upon comparisons between inferred OIB source characteristics and the observed chemistry of sediments and other crustal material. This is certainly a logical starting point, since most subducting slabs primarily consist of sediment and oceanic crust. These inferences assume that the oceanic crust and sediment carried into the convecting mantle have the same composition as crust and sediment entering the subduction zone. However, the slab experiences substantial changes in temperature and pressure conditions as it moves through the subduction zone. The changing conditions alter the slab's composition, and the chemistry of the residual slab is therefore probably quite different from that of the material that entered the subduction zone. Since the residual slab cannot be directly sampled, estimates calculated from mass balance and isotopic studies must be used to determine the composition of the residual slab material and to examine the feasibility of the various mantle evolution models that posit a significant role for subducted crust in the development of mantle heterogeneity. As most studies of subduction zones have focused on the characteristics of the rocks erupted at the subduction zone (island arc volcanics, or IAV), estimates of residual slab chemistry are not readily available. In this project, I have used a mass-balance approach to estimate the compositions of residual slab material at nine major subduction zones. I use published data on the compositions of the ingoing slab components and erupted IAV, together with information about the various processes that

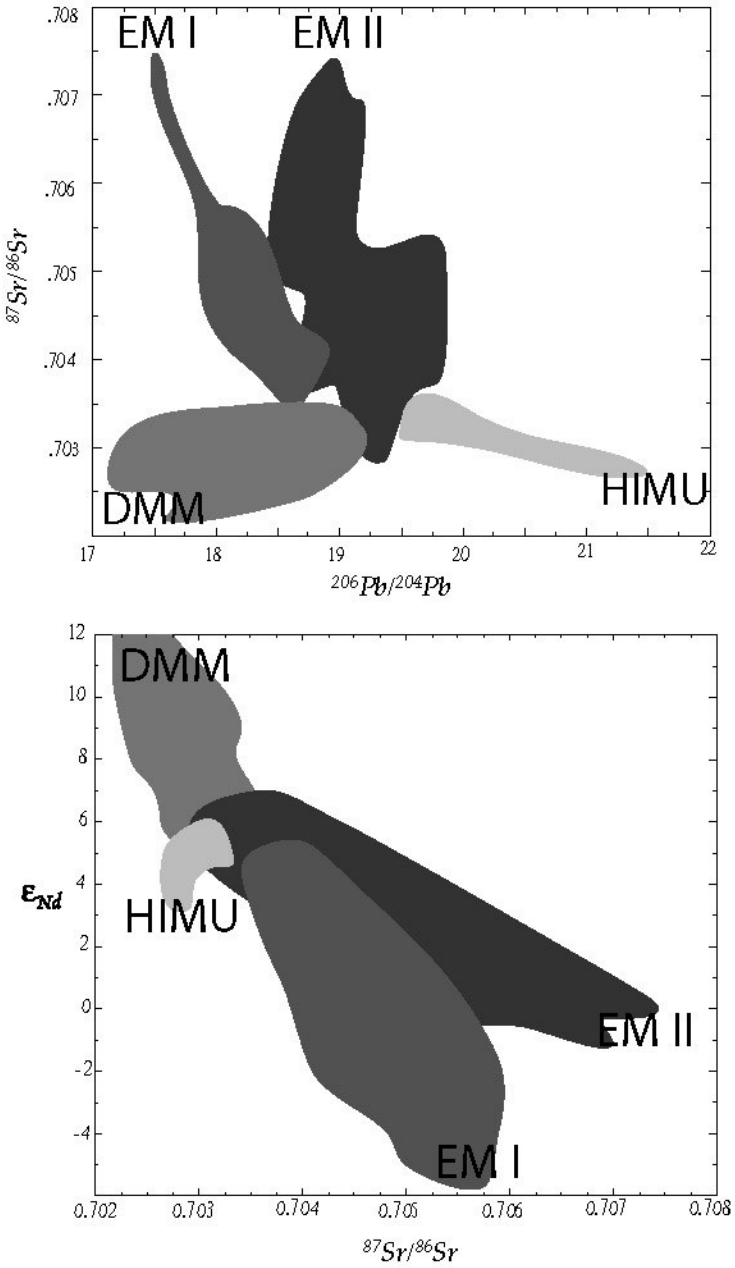

Figure 1.1 Variations in isotopic compositions in the mantle in Sr-Pb isotopic space (top) and Nd-Sr isotopic space (bottom).

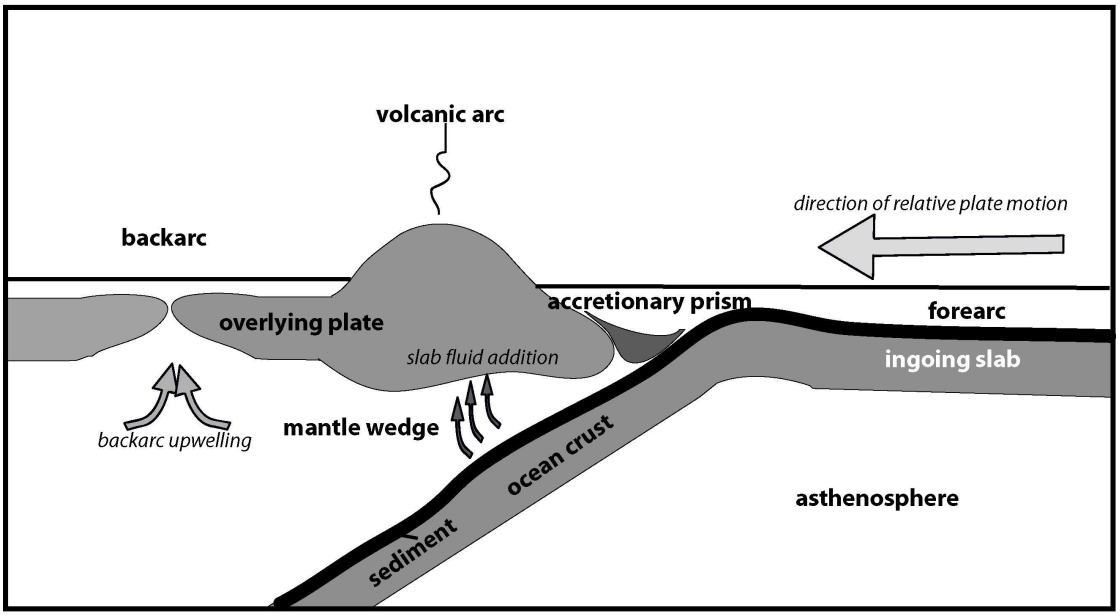

Figure 1.2 Generalized subduction zone (island arc) system. System components are in bold type; processes are in italics. Back arcs and accretionary prisms are not found in all arc systems. Not to scale.

occur within the subduction zone, to approximate the residual slab compositions.

To a first order, assuming that the subducting slab is the only input to the subduction zone and that the volcanics erupted at the island arc are the only output from the slab, the flux of material into the mantle can be computed using

1.1 $$F_{mantle} = F_{in} - F_{arc},$$

where the subscripts *mantle*, *in*, and *arc* refer to the flux of material into the mantle[g], the flux of slab material into the subduction zone, and the flux of material from the slab into the island arc volcanics (IAV), respectively. Using published data, I can calculate both F_{in} and F_{arc} for each element of interest, and I can then estimate the residual slab flux (F_{mantle}) using equation 1.1.

Preparation of data set

I obtained all data from the GEOROC database (Table 1.1) by searching for samples of volcanic glass and whole rock from each convergent margin. I filtered the data from each arc to remove all samples with >55 wt% SiO_2[h] and any samples for which SiO_2, MgO, or K_2O analyses were unavailable. I divided the samples from each arc into high-, medium-, and low-K series using the following criteria (Figure 1.3; Le Maitre, 2002; Tatsumi and Eggins, 1995[i]):

[g] This is, of course, what I'm really interested in. But in order to calculate it, I have to know the other two fluxes.

[h] I removed highly evolved (high SiO_2) samples in order to minimize inaccuracies caused by fractional crystallization.

[i] These two sources give slightly different slopes and intercepts for the dividing lines between the series; however, having tried both and seen that it doesn't really make any difference to the results, I've only included one set of equations here.

1.2a low-K: $[K_2O] < (0.045[SiO_2] - 1.86)$

1.2b medium-K: $(0.085[SiO_2] - 2.88) > [K_2O] > (0.045[SiO_2] - 1.86)$

1.2c high-K: $[K_2O] > (0.085[SiO_2] - 2.88)$

I calculated an average composition for each series at each arc using the filtered samples (see Appendix A for average major and trace element compositions for magma series at each arc). In order to reduce possible errors introduced by typographical and database inconsistencies, I examined the relative standard deviation for each trace element[j] average and removed any major outliers. I corrected the average major element compositions for fractional crystallization using a liquid line of descent calculation

The magma that is formed from melting of the wedge at the arcs undergoes fractional crystallization within the arc prior to its eruption as IAV. In order to use the compositions of the erupted IAV to estimate the contributions of the slab and wedge components to the arc, I had to correct the IAV compositions for this fractionation. I accomplished these corrections using the online version of the MELTS program (http://penmelts.geology.washington.edu/index.html; Ghiorso, 1985; Ghiorso and Sack, 1995; Sack and Ghiorso, 1994) to calculate a liquid line of descent (LLOD) for each set of data.

For each magma series (high-, medium-, and low-K) at each arc, I plotted the major elements versus wt% MgO in order to estimate the major element composition of the parental magma (e.g., Figure 1.4; see Appendix B for parental compositions and complete LLOD curves for all arcs). I then

[j] Major elements are Si, Al, Ti, Fe, Mg, K, Na (usually), P (usually), Mn, and Ca. Trace elements are pretty much everything else. Basically if the element is present in less than 0.1 wt%, it's a trace element.

Table 1.1 Sources of data used in this study.

Data Used	Source(s)
published IAV sample compositions	GEOROC database: http://georoc.mpch-mainz.gwdg.de/georoc/Entry.html
crustal addition rates	Crisp, 1984; Dimalanta *et al*, 2002; Reymer & Schubert, 1984
composition of MORB	PetDB database: http://www.petdb.org/index.jsp
composition of AOC	Kelley, 2004 and Staudigel *et al*, 1996
mineral/melt distribution coefficients	EarthRef Kd's database: http://www.earthref.org
sediment compositions, thicknesses, and densities; average arc convergence rates	Plank and Langmuir, 1998

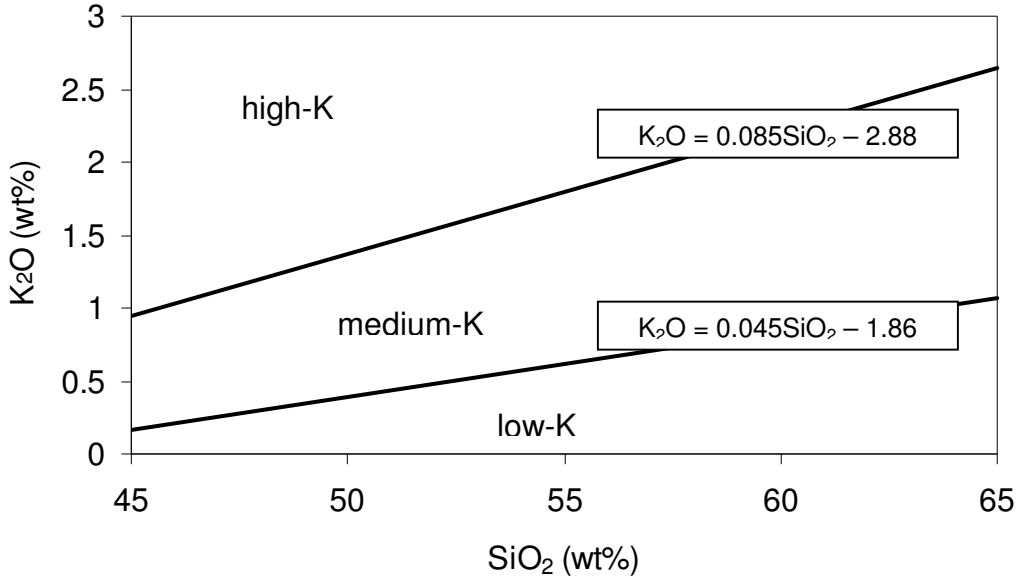

Figure 1.3 K_2O vs. SiO_2 for different magma series. After Le Maitre, 2002 and Tatsumi and Eggins, 1995.

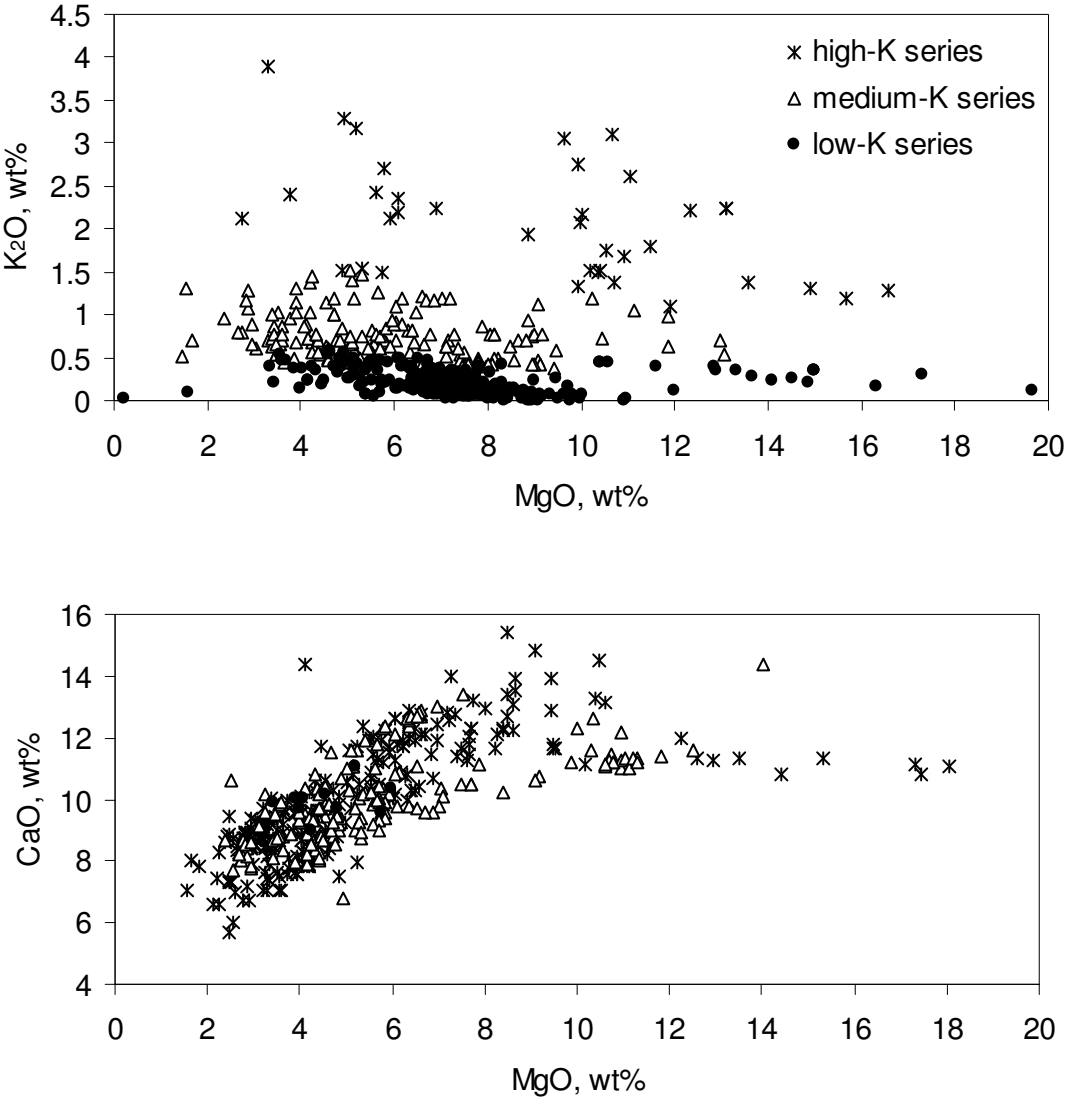

Figure 1.4 Major element plots vs. MgO for the Tonga (top) and Sunda-Java (bottom) island arcs. Similar plots of other major elements were used to infer the parental (high-MgO) composition for each magma series at each arc; these plots are shown in Appendix B.

used the Java MELTS program to calculate the composition of olivine in equilibrium with this melt. I made the assumption that any primary magma must be in equilibrium with mantle olivine (~Fo_{91}[k]), since it is formed within the mantle wedge. If the initial parental magma composition that I selected was not in equilibrium with Fo_{91} or higher, I used the MELTS program to add olivine to the parental magma composition in 1 wt% increments until the resulting composition was in equilibrium with Fo_{91}.

Using the MELTS program, I determined the liquidus temperature for the parental composition under the pressure and f_{O2} conditions applicable to the arc (2.5 kbar, QFM+1; Parkinson and Arculus, 1999); I calculated a LLOD for each sample by reducing the temperature incrementally and recording the masses and compositions of the melt and mineral phases[l] that were present at each temperature step. Once I had these data, I examined the fit of the magma evolution curves to the erupted IAV (e.g., Figure 1.5; see also Appendix B). I adjusted the parental magma composition as needed to produce a good fit to the observed IAV compositions. I used the average MgO composition for a given series to estimate the approximate degree of fractionation experienced by that series. Using the average trace element compositions for each series, mineral-melt distribution coefficients from the GERM Kd's Database (Tables 1.1 and 1.2), and the equation describing

---

[k] Fo refers to forsterite, Mg_2SiO_4, one of the endmembers of the olivine solid solution series (the other is fayalite [Fa], Fe_2SiO_4). In general, the Fo level of a magma drops as it evolves, so high Fo values indicate primitive magmas. Crystallographic data: Orthorhombic 2/*m* 2/*m* 2/*m*. Fo: a 4.758, b 10.214, c 5.984. Fa: a 4.817, b 10.477, c 6.105. No distinct cleavage.

[l] Although the MELTS program can give very useful mineral phase data for a given set of chemical and thermodynamic conditions, it does not provide information on many trace mineral phases that can have significant impact on the chemistry of the overall system. Amphibole, for example, has been found as a phenocryst phase in rocks in some subduction zone systems, but is not generated by the MELTS program. Despite this known limitation, however, I used MELTS to calculate my liquid lines of descent because it was the most complete and readily accessible tool for thermodynamic calculations available to me.

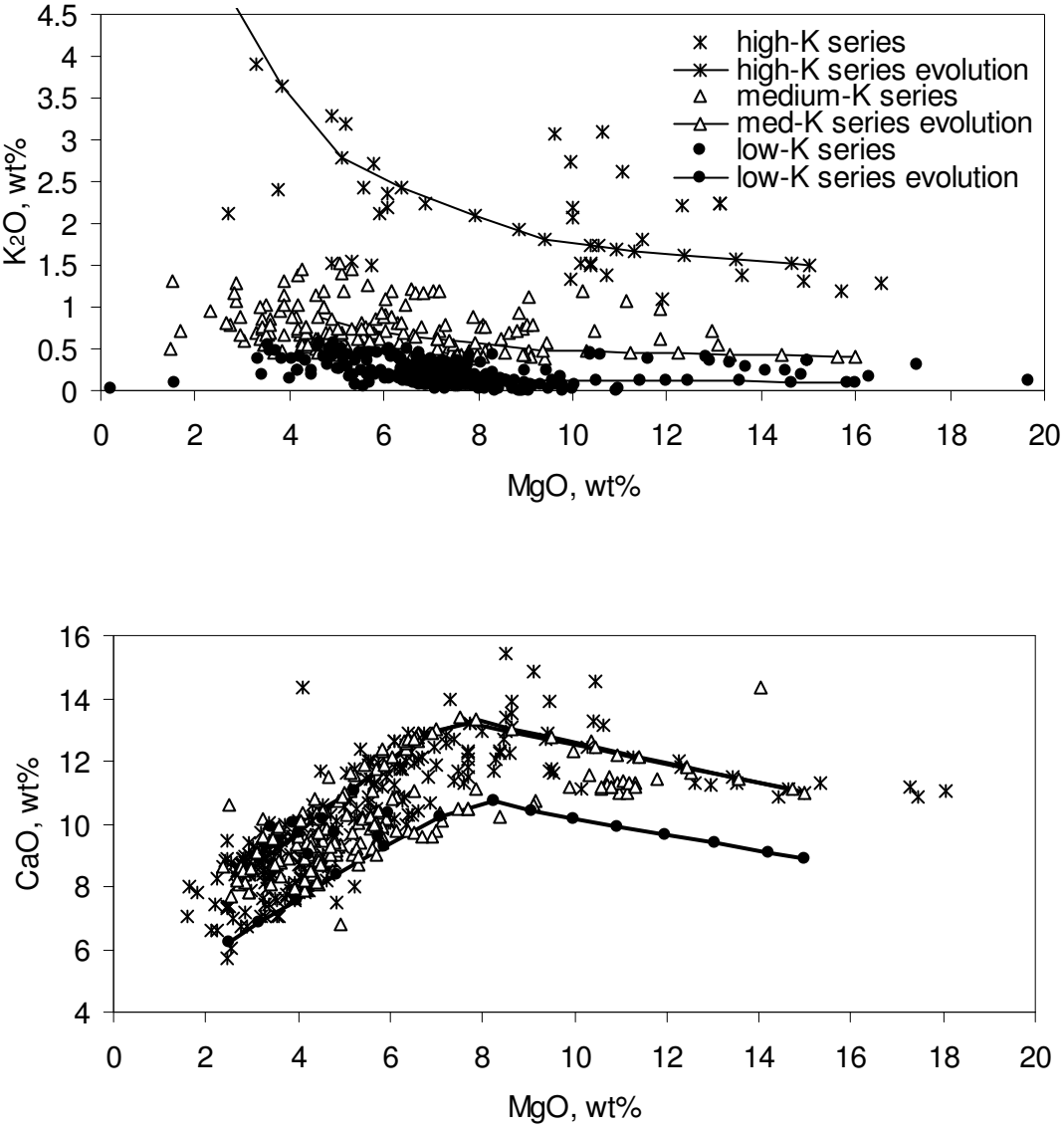

Figure 1.5 Liquid line of descent (LLOD) curves for selected major elements at the Tonga (top) and Sunda-Java (bottom) island arcs. See Appendix B for plots from other arcs.

Table 1.2 Mineral/melt partition coefficients.

	olivine	clino-pyroxene	ortho-pyroxene	feldspar	spinel	whitlockite
K	0.00017	0.0028	0.0001	0.18		
Rb	0.000044	0.0033	0.0002	0.025		
Ba	0.0000034	0.0022	0.0067	0.33		
Th	0.000052	0.014	0.0056	0.19		1.3
U	0.00002	0.013	0.015	0.34		0.5
Nb	0.00005	0.0081	0.015	0.033	0.08	
Ta	0.00005	0.013	0.015	0.11	0.06	
La	0.0000088	0.052	0.0056	0.082	0.01	
Ce	0.000019	0.108	0.0058	0.072	0.01	
Pb	0.0076	0.01	0.009	1.07	0.0005	
Sr	0.000063	0.157	0.0068	2.7		
Nd	0.00042	0.277	0.007	0.045	0.01	
Zr	0.00068	0.195	0.004	0.001	0.06	
Hf	0.001	0.223	0.021	0.02	0.05	
Sm	0.000445	0.462	0.085	0.033	0.0064	
Eu		0.458	0.0078	0.55	0.0061	
Y	0.0098	0.62	0.014	0.013	0.01	
Yb	0.0366	0.633	0.032	0.014	0.0076	
Lu	0.02	0.623	0.042	0.038	0.01	

fractional crystallization, I calculated the initial concentration of each trace element in the parental magma. Table 1.3 gives an example of the LLOD calculations for the low-K series at the Tonga arc, and Appendix B gives mineral phase data for each arc.

I used the mineral phase data generated in the liquid line of descent calculation to correct[m] trace element compositions using the distribution coefficients in Table 1.2. Figure 1.6 shows the average fractionation-corrected compositions for the arcs in this study; average compositions are given in Table 1.4, and compositions for observed and fractionation-corrected IAV from each magma series are tabulated in Appendix C.

Ingoing slab composition and flux

The ingoing slab contains three major components: unaltered oceanic crust, altered oceanic crust (AOC), and sediment. The compositions of these three components are heavily dependent on the processes by which they are formed. Oceanic crust is formed primarily at mid-ocean ridges, where extensional stresses create a decrease in overburden pressure on the underlying solid mantle and allow it to upwell toward the ridge (Figure 1.7). The mantle moves along an adiabatic path during upwelling; as the overburden pressure decreases, the mantle undergoes decompression partial melting. The partial melting produces basaltic magma, which percolates out of the solid mantle. As the magma rises, it undergoes some fractional crystallization. The solid residue of this crystallization becomes lower oceanic crust, while the remaining magma continues to rise until it

[m] Assuming fractional melting and using mass fractions from MELTS.

Table 1.3 Sample LLOD calculation for the low-K series at the Tonga arc. All concentrations in ppm. Mineral phase data for other arcs in Appendix B.

Average wt% MgO in Tonga low-K series = 7.56 wt%

Mass of minerals fractionated†:
olivine = 16.56 g clinopyroxene = 28.65 g feldspar = 2.72 g

	Composition of Average IAV	Composition of Fractionation-Corrected IAV
K	1535.85	736.13
Rb	3.93	1.88
Ba	44.23	21.20
Th	0.26	0.12
U	0.11	0.05
Nb	1.82	0.87
Ta	0.13	0.06
La	2.76	1.32
Ce	7.45	3.57
Pb	2.33	1.12
Sr	142.98	73.80
Nd	5.83	2.86
Zr	53.54	25.76
Hf	1.48	0.72
Sm	1.76	0.94
Eu	0.74	0.40
Y	22.99	13.36
Yb	1.78	1.05
Lu	0.25	0.15

† out of 100g initial mass

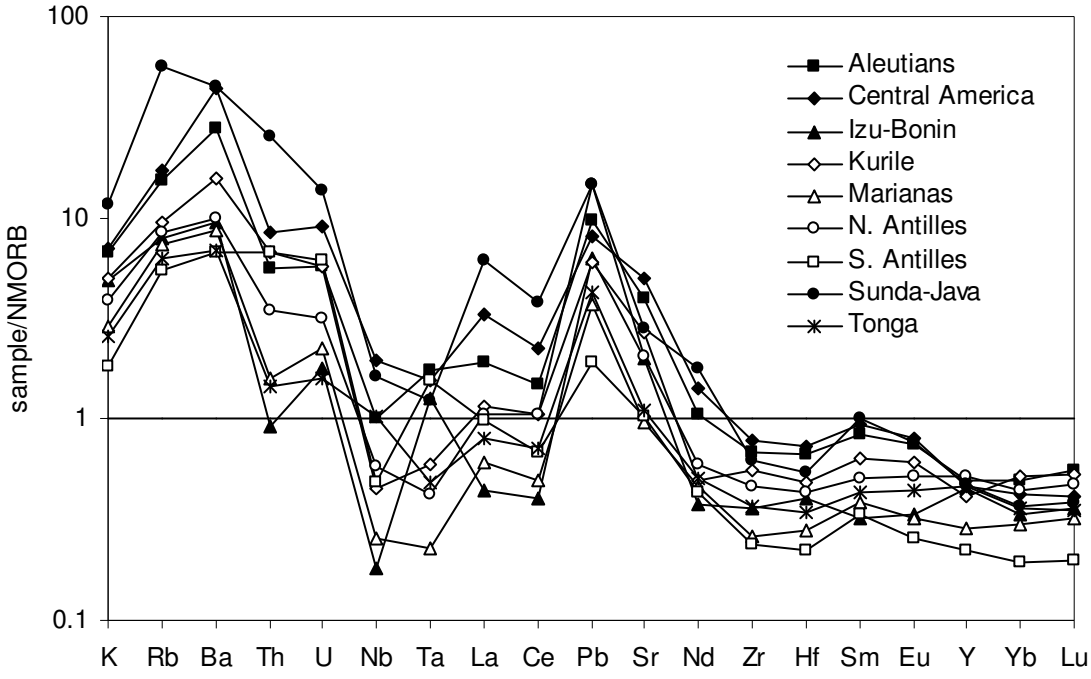

Figure 1.6 MORB-normalized trace element diagram of average fractionation-corrected IAV compositions. Normalizing values from Sun and McDonough, 1989 (Table 1.5).

Table 1.4 Compositions of average fractionation-corrected IAV. Concentrations in ppm.

	Aleutians	Central America	Izu-Bonin	Kurile	Marianas	Northern Antilles	Southern Antilles	Sunda-Java	Tonga
K	1535.51	7051.67	1102.91	2329.95	1751.26	2976.65	2898.37	4190.50	4064.54
Rb	3.48	31.93	3.04	4.77	4.15	5.26	4.41	9.63	8.51
Ba	43.04	281.71	42.85	62.09	54.97	97.71	59.06	273.79	173.28
Th	0.17	3.07	0.81	0.42	0.19	0.80	0.11	1.01	0.67
U	0.07	0.64	0.29	0.15	0.11	0.27	0.08	0.42	0.27
Nb	2.40	3.81	1.14	1.35	0.59	1.05	0.42	4.55	2.33
Ta	0.06	0.16	0.20	0.06	0.03	0.08	0.17	0.20	0.23
La	1.99	15.27	2.48	2.62	1.51	2.91	1.10	8.19	4.78
Ce	5.35	28.78	5.18	7.99	3.71	8.00	3.02	16.93	11.21
Pb	1.29	4.41	0.57	4.41	1.11	1.81	1.88	2.44	2.94
Sr	100.35	252.88	92.88	183.01	86.76	240.11	181.36	448.60	354.97
Nd	3.70	12.95	3.12	4.38	3.41	3.59	2.76	10.40	7.77
Zr	27.53	46.61	17.79	34.42	19.39	40.72	26.87	58.39	50.23
Hf	0.71	1.12	0.45	0.88	0.57	0.99	0.83	1.51	1.38
Sm	1.13	2.65	0.88	1.33	1.01	1.69	0.85	2.48	2.18
Eu	0.45	0.79	0.26	0.53	0.33	0.62	0.34	0.81	0.76
Y	13.00	13.35	6.18	14.40	7.96	11.56	12.63	13.04	13.78
Yb	1.10	1.12	0.59	1.34	0.92	1.60	1.02	1.29	1.50
Lu	0.16	0.18	0.09	0.21	0.15	0.24	0.16	0.19	0.25

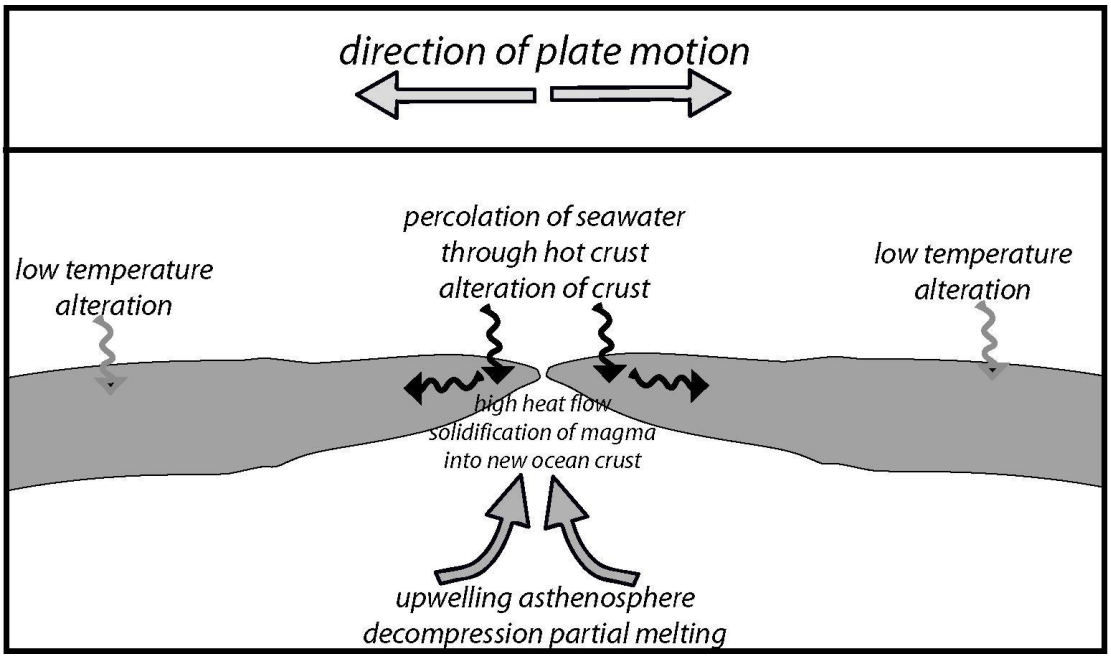

Figure 1.7 Schematic diagram of a mid-ocean ridge system. Hydrothermal alteration occurs as seawater percolates downward into the ridge crest, is heated, and migrates through and alters the surrounding oceanic crust. Low temperature alteration occurs away from the ridge crest as seawater percolates through the crust. Not to scale.

erupts at the ridge to form MORB. The composition of MORB – and, to a lesser degree, the lower crust – is fairly well established, although it does vary within and between ocean basins (e.g. Hannigan *et al.*, 2001; Hofmann, 1988; Holm, 2002; Ito *et al.*, 1987; Kinzler and Grove, 1993; Sims and DePaolo, 1997; Sun and McDonough, 1989; White and Hofmann, 1982). Studies of MORB constrain the composition of oceanic crust when it is initially erupted at a mid-ocean ridge, but the crust that is subducted includes both MORB and the lower crust. Since the MORB are produced by fractionation of the lower crust, I can estimate the composition of the "bulk" ocean crust (MORB plus lower ocean crust) using a LLOD calculation on typical MORB compositions (downloaded from the PetDB database; see Tables 1.1 and 1.5).

The calculated bulk ocean crust composition represents pristine, newly formed oceanic crust. However, the ocean crust subducted at converging margins is rarely newly erupted; it may be up to 180 million years old. A variety of processes operate upon the crust as it ages, producing substantial changes in its overall composition. Since most subducted slabs contain a significant amount of fairly old (and, presumably, altered) ocean crust, I have included an altered ocean crust (AOC) component in my estimates for ingoing slab compositions. The most important of the processes affecting AOC composition is the interaction of the crust with ocean water. At the ridge itself, the heat from upwelling magma greatly increases the temperature of ocean water that circulates through cracks in the ridge, and hydrothermal alteration[n] of the crust can occur when the

[n] Changes in chemistry due to interactions with hot water – in this case, sea water, but the general term "hydrothermal" refers to any kind of water.

heated ocean water interacts with the newly erupted basalt (e.g. Alt, 1999; Alt *et al.*, 1985; Juteau and Maury, 1999; Kelley, 2004; Staudigel *et al.*, 1996). In general, interaction of oceanic basalt with hot ocean water causes the basalt to become hydrated and enriched in some fluid-mobile elements[o] (e.g. U, Ba, Cs). As it migrates out of the high temperature zone, the oceanic crust undergoes further alteration at lower temperatures. This low temperature alteration causes additional changes in the chemistry of the ocean crust (e.g. Bach *et al.*, 2001; Elderfield *et al.*, 1999; Gillis *et al.*, 1992; Utzmann *et al.*, 2002; Figure 1.7). High- and low-temperature interactions with seawater alter only the shallower part of the oceanic crust, but the effects on its chemistry can be significant. Table 1.5 gives the compositions of altered and unaltered ocean crust.

In addition to AOC and unaltered crust, a typical subducting slab includes a layer of sediment that has been deposited on the ocean floor through time. Oceanic sediment is an important reservoir for many major and trace elements, and its chemical composition is highly variable. The chemistry of the sediment is primarily controlled by the source from which it is derived. Since the continents are enriched in many incompatible trace elements[p] (see Table 1.5; Albarede, 1998; McDonough and Sun, 1995; Wedepohl, 1995; Wedepohl and Hartmann, 1994), terrigenous sediment can be an important reservoir for these elements. The thickness of the terrigenous sedimentary layer is primarily determined by the proximity of the oceanic plate to a continental land mass drainage system (i.e., a large river

[o] Elements that tend to be mobile in aqueous fluids.
[p] Incompatible elements will tend to segregate into the melt phase very readily (they have very low solid-liquid distribution coefficients)Many trace elements are incompatible, and all of the elements I have focused on are incompatible to various degrees.

Table 1.5 Trace element compositions for various Earth reservoirs. Concentrations in ppm.

	Composition of Average MORB[Ŧ]	Composition of Bulk Ocean Crust[†]	Composition of Altered Ocean Crust[‡]	Composition of Continental Crust[§]
K	600.00	453.30	5146.91	19923.50
Rb	0.56	0.42	13.70	78.00
Ba	6.30	4.82	15.60	584.00
Th	0.12	0.09	0.17	8.50
U	0.05	0.04	0.39	1.70
Nb	2.33	1.76	2.89	19.00
Ta	0.13	0.10	0.21	1.10
La	2.50	1.89	3.40	30.00
Ce	7.50	5.67	11.40	60.00
Pb	0.30	0.23	0.44	14.80
Sr	90.00	75.72	109.00	333.00
Nd	7.30	5.57	11.30	27.00
Zr	74.00	55.91	112.00	203.00
Hf	2.05	1.55	3.07	4.90
Sm	2.63	1.99	3.95	5.30
Eu	1.02	0.77	1.34	1.30
Y	28.00	21.26	40.70	24.00
Yb	3.05	2.30	4.02	2.00
Lu	0.45	0.34	0.64	0.35

[Ŧ] From Sun and McDonough, 1989
[†] i.e., fractionation-corrected MORB
[‡] From Kelley, 2004
[§] From Wedepohl, 1995

or other outflow). Oceanic crust that is far from any continental mass (e.g., the central Pacific ocean basin) generally has a very thin terrigenous sediment layer; in contrast, regions near continental drainage basins (e.g., the Atlantic ocean basin near the Amazon river delta) can be overlain by extremely thick layers of terrigenous sediment.

A significant biogenic component is also found in most oceanic sediment. Biogenic sediment consists of the organic and inorganic waste products and remains of ocean-dwelling organisms. These materials tend to be composed primarily of calcite ($CaCO_3$)[q] and opal or other forms of biogenic silica ($SiO_2 \cdot xH_2O$)[r]. Trace elements may be incorporated to varying degrees within these materials (Sr, for example, frequently substitutes for Ca in calcite), and so biogenic sediment can also act as an important reservoir for trace elements.

The sediment layer covering the ocean floor is heterogeneous on many length scales. However, for the purposes of estimating elemental fluxes into subduction zones, the sediment input to the system can be approximated by a weighted average of the various components. Plank and Langmuir (1998) have calculated average compositions for the sediment layers entering the majority of the world's major subduction zones, and I used their estimates in the calculations throughout this study; these values are given in Table 1.6.

Once the compositions of ocean crust, AOC, and sediment at each subduction zone are known, it should be possible to calculate the "bulk"

---

[q] Hexagonal, $\bar{3}$ 2/*m*. a 4.990, c 17.064. R $\bar{3}$ *c*. Twinning on {01 $\bar{1}$ 2} and {0001}.
[r] Amorphous.

Table 1.6 Ingoing sediment compositions from Plank and Langmuir, 1998. Concentrations in ppm.

	Aleutians	Central America	Izu-Bonin	Kurile	Marianas	Northern Antilles	Southern Antilles	Sunda-Java	Tonga
K	17516.08	5644.99	6724.18	14112.48	11289.99	15025.64	23244.98	15689.76	17516.08
Rb	57.00	15.60	25.10	59.90	30.30	83.50	142.00	63.30	39.50
Ba	2074.00	2571.00	2.44	627.00	311.00	204.00	402.00	1486.00	1680.00
Th	5.49	0.93	2.43	6.22	2.62	12.08	14.94	7.73	9.89
U	2.39	1.37	1.19	1.39	0.58	1.36	4.27	0.99	1.43
Nb	7.74	1.80	3.87	7.67	11.04	18.33	21.32	8.74	8.44
Ta	0.55	0.13	0.24	0.32	0.76	1.12	1.30	0.69	0.55
La	17.96	15.75	27.26	21.94	20.78	35.54	47.91	29.80	134.47
Ce	39.03	10.62	31.35	50.11	31.54	82.83	105.41	74.53	196.18
Pb	12.91	7.36	6.82	23.68	6.00	25.54	30.46	20.60	113.30
Sr	245.00	1227.00	110.00	87.00	161.00	111.00	135.00	405.00	233.00
Nd	19.07	12.23	28.74	22.03	21.03	31.22	41.64	25.44	158.20
Zr	131.00	29.00	48.00	83.00	86.00	146.00	170.00	110.00	123.00
Hf	3.26	0.84	0.88	2.10	1.90	4.18	4.86	3.33	3.51
Sm	4.43	2.87	6.35	5.50	4.62	6.18	7.89	5.71	34.86
Eu	1.10	0.63	1.46	1.24	1.15	1.32	1.59	1.15	8.46
Y	21.60	31.70	46.00	28.90	25.90	23.90	28.70	24.60	173.00
Yb	2.31	1.84	2.90	2.82	1.86	2.39	2.76	2.43	17.01
Lu	0.34	0.28	0.42	0.43	0.27	0.36	0.40	0.39	2.58

ingoing slab composition using a simple weighted average[s]. In order to calculate the weighting factors for each component in the slab, I first assumed that the thickness of the oceanic crust (MORB + lower ocean crust + AOC) is 6 km[t], and that the total thickness of the slab (MORB + lower ocean crust + AOC + sediment) is therefore 6 km + the thickness of the sediment layer (Table 1.7). The volume fraction of sediment in the slab (weighting factor) was calculated using:

1.3 $$f_{sed} = \frac{T_{sed}}{6km + T_{sed}}$$

where T_{sed} is the thickness of the sediment layer from Plank and Langmuir (1998).

Estimation of the thickness of AOC is somewhat problematic, since a) its thickness varies substantially based on its history and age; and b) there have not been any systematic examinations of altered crust thickness worldwide[u]. In order to obtain estimates for the thickness of the AOC, I made use of the observation that short-lived U-series isotopes show a substantial disequilibrium in the IAV erupted at many subduction zones (Figure 1.8). With few exceptions, IAV plot to the right (U-enriched side) of the 1:1 line on this diagram, which implies enrichment of U over Th. The short half-lives of the U-series isotopes require that this fractionation must occur within several hundred thousand years of eruption (Hawkesworth *et al.*, 1997a; Hawkesworth *et al.*, 1997b). Such a short timescale indicates that

[s] Of course, the compositional data for the various components are for fairly specific sampling areas. But as it would take many years and dollars to sample every square inch of the Earth's surface…well, we make do with what we have.

[t] In some places oceanic crust may be up to 7 or 8 km, but 6 km is a generally accepted thickness. Again, this includes MORB, lower crust, and altered crust, but *not* sediment.

[u] Although many Ocean Drilling Program drill holes have penetrated the AOC, few have reached all the way through it to the unaltered crust below (not that this is a particularly well-defined boundary).

Table 1.7 Ingoing bulk slab compositions and component fractions for arcs in this study. Concentrations in ppm.

	Aleutians	**Central America**	**Izu-Bonin**
K	1393.77	796.72	3665.23
Rb	3.54	1.43	10.14
Ba	118.87	174.57	10.67
Th	0.39	0.15	0.35
U	0.17	0.12	0.34
Nb	2.09	1.76	2.59
Ta	0.12	0.10	0.17
La	2.77	2.81	5.05
Ce	7.51	5.99	11.23
Pb	0.93	0.70	0.94
Sr	85.05	151.88	97.57
Nd	6.32	6.01	10.90
Zr	60.05	54.13	86.76
Hf	1.64	1.50	2.34
Sm	2.13	2.05	3.49
Eu	0.79	0.76	1.15
Y	21.28	21.95	34.45
Yb	2.30	2.27	3.32
Lu	0.34	0.34	0.51
f_{sed}	0.055	0.066	0.091
f_{AOC}	0.000	0.000	0.563
f_{MORB}	0.945	0.934	0.346

Table 1.7 (continued)

	Kurile	Marianas	Northern Antilles
K	1716.43	2699.05	2529.77
Rb	5.14	6.72	7.87
Ba	40.28	30.67	15.83
Th	0.44	0.30	0.57
U	0.15	0.18	0.20
Nb	2.21	2.79	2.75
Ta	0.12	0.18	0.17
La	3.16	3.74	3.65
Ce	8.74	9.34	10.44
Pb	1.54	0.72	1.25
Sr	79.96	92.27	87.88
Nd	7.10	8.48	8.40
Zr	63.50	75.43	77.55
Hf	1.74	2.04	2.14
Sm	2.40	2.79	2.79
Eu	0.86	0.98	0.98
Y	23.80	27.60	27.69
Yb	2.52	2.80	2.87
Lu	0.38	0.43	0.44
f_{sed}	0.055	0.074	0.038
f_{AOC}	0.109	0.309	0.325
f_{MORB}	0.836	0.618	0.637

Table 1.7 (continued)

	Southern Antilles	Sunda-Java	Tonga
K	3269.83	2060.14	1234.13
Rb	14.32	6.49	2.53
Ba	37.81	119.75	25.48
Th	1.25	0.69	0.21
U	0.44	0.14	0.10
Nb	3.52	2.40	1.98
Ta	0.22	0.16	0.12
La	5.77	4.18	3.61
Ce	14.64	11.49	8.58
Pb	2.60	1.81	1.56
Sr	87.82	104.13	81.68
Nd	9.64	7.63	8.05
Zr	77.39	65.26	63.66
Hf	2.15	1.83	1.76
Sm	2.89	2.46	2.62
Eu	0.96	0.85	0.93
Y	26.24	23.32	25.43
Yb	2.73	2.47	2.69
Lu	0.41	0.37	0.41
f_{sed}	0.077	0.077	0.012
f_{AOC}	0.227	0.093	0.124
f_{MORB}	0.697	0.830	0.864

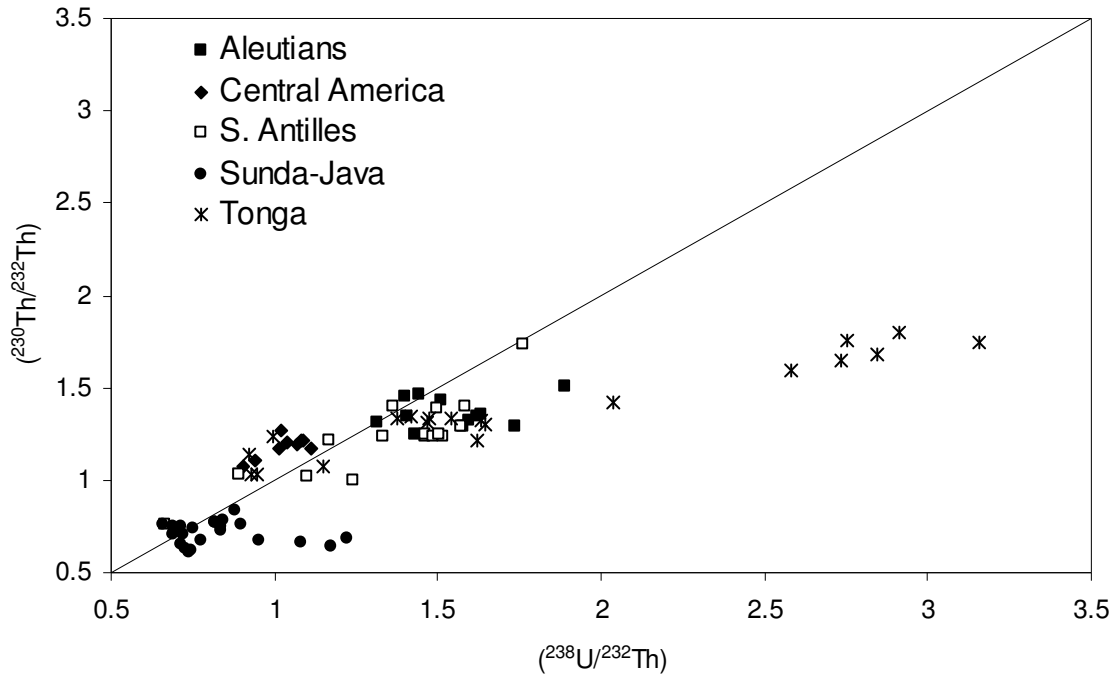

Figure 1.8 U-series isotope plot for IAV at island arcs in this study. Most samples show significant deviation to the right (U-enriched) side of the 1:1 line.

the fractionation occurs during or just prior to the melting that produces IAV, so it directly reflects the influence of the slab on the IAV. Partial melting of the IAV source (the slab-modified mantle wedge) will produce melts with lowered Th/U, so the IAV source must have a Th/U ratio that is greater than or equal to that of the IAV. The Th/U ratio in modern AOC (~0.44; Kelley, 2004) is much lower than that in sediment or ocean crust, so increasing the fraction of AOC in the slab will lower its bulk Th/U. By constraining the slab Th/U to be equal to the average IAV Th/U, I can calculate the maximum fraction of AOC in the subducting slab using

1.4 $$f_{AOC} = \frac{R_{slab} - R_{sed} f_{sed} - R_{crust} f_{crust}}{R_{AOC}},$$

where f_i denotes the fraction of component i in the bulk slab; R_i is the Th/U ratio of component i; and the subscripts *crust, sed, AOC,* and *slab* denote unaltered oceanic crust, sediment, altered oceanic crust, and bulk slab (sediment + AOC + unaltered crust), respectively. R_{slab} is set equal to the average Th/U of the IAV.

Using data on the compositions of each slab component and their relative thickness in each ingoing slab, I calculated an estimated bulk ingoing slab composition for each arc under examination using a weighted average (Table 1.7; Figure 1.9). Using published convergence rates and sediment densities (Plank and Langmuir, 1998), I estimated the total flux of material going into the arc using:

1.5 $$F_{in} = \frac{r}{T_{slab}} \left(T_{crust} \rho_{crust} + T_{AOC} \rho_{AOC} + T_{sed} \rho_{sed} \right),$$

where r represents the convergence rate; T_i represents the thickness of component i; ρ_i denotes the density of component i; and subscripts are as in equation 1.4. The flux of each element into the arc was then simply its concentration in the bulk slab multiplied by the bulk mass flux into the arc.

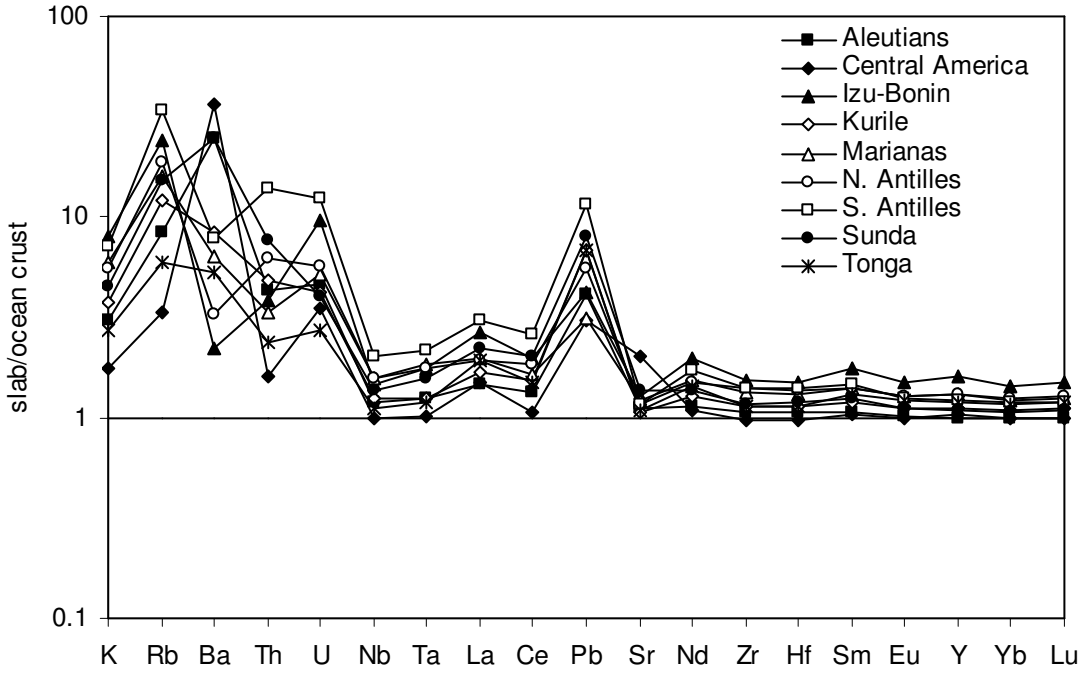

Figure 1.9 Ingoing slab compositions for arcs in this study. Concentrations normalized to bulk ocean crust (Table 1.5).

I used a mass balance (described in equation 1.1) between ingoing slab material and erupted IAV to approximate the loss of different trace elements from the subducting slab. In order to determine whether or not my calculated slab losses were reasonable, I used information about the physical and chemical processes thought to occur within subduction zones. Some of these processes are described below.

Slab component composition and flux

As the slab "enters" the subduction zone – that is, as it becomes subject to the compressional stresses that characterize these regions – the increasing pressure causes the relatively porous sedimentary layer to dewater. Because the temperature at which this dewatering occurs is fairly low, the fluid released at this stage is not considered an important transport phase for most trace elements. Only the most fluid-mobile elements, such as Cs, are transported in appreciable quantities by these fluids (Brenan *et al.*, 1998; Chan *et al.*, 1999; Johnson and Plank, 1999; Kastner *et al.*, 1991; von Huene *et al.*, 1998; You *et al.*, 1996). These highly mobile elements are not included in my models, so I will not discuss dewatering further here.

The subducting slab is also subjected to extreme shear stresses as it slides beneath the overlying plate. These stresses may cause the uppermost layers of sediment to be scraped off against the edge of the overlying plate. The off-scraped sediments can then form an accretionary prism (see Figure 1.2), which may become quite thick. Like dewatering, sediment accretion is a largely physical process; unlike dewatering, sediment off-scraping often results in significant changes in the composition of the bulk slab, since sediment is an important reservoir for many trace elements. In

their compilation, Plank and Langmuir (1998) estimated the effects of sediment accretion when they calculated the thickness and composition of the sedimentary layers at the various subduction zones. Therefore, although I do not explicitly address sediment accretion in my calculations, its effects are included indirectly through the use of the Plank and Langmuir (1998) estimates.

Processes such as dewatering and accretion can affect the composition of the slab via physical removal of material. In general, however, the most significant changes in slab composition occur because of chemical processes operating within the subduction zone. The compositions of IAV that are erupted at the arc can be used to infer the characteristics of material that is released from the slab. Although the slab supplies a significant fraction of the trace element budget of the IAV, the bulk of the magma that forms the IAV is derived from the mantle wedge. The composition of the mantle wedge before it has experienced any alteration by slab-derived materials is generally assumed to be similar to that of the upper mantle in general. Partial melting of the upper mantle at mid ocean ridges produces MORB, which has a fairly well-defined chemical signature. If IAV are produced by the same degree of partial melting of the upper mantle as are MORB, then deviations in the chemistry of the IAV from MORB should be due to the influence of the slab on the mantle wedge. Although it is difficult to constrain the exact extent of partial melting that produces MORB and IAV, the influence of the slab can still be estimated by examining deviations of IAV from a MORB-parallel trend on a trace element plot such as Figure 1.6 because different degrees of partial melting of upper mantle material will tend

to produce similar trace element patterns[v]. As is apparent from Figure 1.6 and Table 1.4, several trends are consistently observable in many island arcs. The most noticeable is the substantial enrichment in large-ion lithophile elements (LILE) relative to high field strength elements (HFSE) and rare earth elements[w] (REE – particularly the "heavy" rare earths). A second readily observable pattern is the relatively smaller degree of fractionation between the various REE. These trends are a strong indication that the phase that transports material from the slab to the wedge fractionates LILE from REE to a much greater extent than it fractionates the REE from each other. Two main possibilities exist for the nature of the transporting phase: a partial melt of the slab material or an aqueous fluid released from the slab.

The REE show a range of mineral/melt partition coefficients (Table 1.2), and melting of the slab would produce a range of REE concentrations within the IAV. In contrast, the mineral/melt partition coefficients for many LILE and HFSE are not different enough to account for the large variations in these elements within the IAV if slab melting were the only transport mechanism for trace elements. The most likely candidate for a phase that can transport LILE but not fractionate REE is an aqueous fluid[x], which forms as a result of temperature and pressure increases at depth within the subduction zone (e.g. Class *et al.*, 2000; Elliott *et al.*, 1997; Hawkesworth *et al.*, 1997a; Johnson and Plank, 1999; Peacock, 1990; Peacock *et al.*, 1994; Tatsumi and Eggins, 1995; Tatsumi *et al.*, 1983).

---

[v] Provided the variations in degree of partial melting are not extreme (>30%).

[w] LILE: K, Rb, Ba, Sr. HFSE: Nb, Ta, Zr, Hf, (Th,U). REE: La, Ce, Nd, Sm, Eu, Y, Yb, Lu.

[x] Although small-degree partial melts of the sediment or slab may contribute to IAV in some arcs, I do not explicitly consider them here. However, since the method that I employ uses observed compositions and fluxes, rather than any assumptions about processes, the results should still be valid even in arcs with a component of slab or sediment melt in the IAV.

As the slab descends through the subduction zone, increasing heat and pressure cause it to dehydrate; this is a similar process to the dewatering experienced by the sediment in the accretionary prism and upper parts of the subduction zone. However, whereas the water lost from the sediment in the shallow regions of the subduction zone is primarily interstitial water[y], that released from the slab at depth tends to be mainly structural or bound water. Due to the high pressure/temperature conditions that prevail at depth within the subduction zone, the aqueous fluids released from the slab tend to mobilize many more elements than do those released during shallow dewatering. Experimental studies have demonstrated that certain groups of elements (e.g. LILE; Ayers, 1998; Ayers and Watson, 1991; Becker *et al.*, 2000; Tatsumi, 1989) are much more mobile in aqueous fluids than others. As the fluids are released from the slab, they mobilize various elements to different degrees; the enriched fluids interact with and variably enrich the overlying mantle wedge. The input of the fluids also stimulates partial melting of the enriched wedge by lowering its melting point.

To a first order, the IAV can be modeled as a mixture between a wedge-derived component and a slab-derived component (F_{arc} in equation 1.1), and the composition of the slab component can be calculated by subtracting the composition of the wedge component from the fractionation-corrected IAV composition:

1.6 $$[i]_{slab\ component} = [i]_{IAV} - [i]_{wedge\ component}$$

As an initial approximation, I assumed that the wedge component in the IAV had the same composition as NMORB. I was then able to use the

[y] Water contained in pores or interstices between sediment particles, rather than incorporated into the crystalline structure of hydrous minerals (structural or bound water).

composition of ocean crust[z] as a "normalizing" composition in the calculation of the slab component. Yb is essentially immobile in slab-derived fluids (Brenan and Watson, 1991; Hawkesworth *et al.*, 1991; Kastner *et al.*, 1991; Tatsumi and Eggins, 1995), so I assumed that all Yb in the IAV was derived from the mantle wedge[aa]. I calculated a normalizing factor N using:

1.7 $$N = \frac{[Yb]_{IAV}}{[Yb]_{MORB}}$$

The "normalized" concentration of any other trace element i in the fractionation-corrected IAV can then be calculated using

1.8 $$[i]_{IAV,norm} = N[i]_{IAV}$$

The difference in concentration between the normalized IAV and MORB is the slab component composition[bb]:

1.9 $$[i]_{slab\,component} = \frac{[i]_{IAV,norm} - [i]_{MORB}}{N}$$

Using published estimates of crustal addition rates at each arc (Tables 1.1 and 1.8), I calculated the mass flux of material that is added to the arc through volcanism. The mass flux of a given element from the slab ($F_{i,\,arc}$) could then be calculated using equation 1.10:

1.10 $$F_{i,arc} = M_{arc}[i]_{slab\,component}\left(\frac{[i]_{slab\,component}}{[i]_{IAV}}\right)$$

where M_{arc} is the mass flux of material added to the arc. Using equation 1.1, I then calculated the mass flux of each trace element into the mantle at each arc. My calculated values of $F_{i,\,arc}$ and $F_{i,\,mantle}$ for each arc are given in Table 1.9.

---

[z] This is the total ocean crust, which includes both MORB and the lower oceanic crust.
[aa] And its concentration in the IAV should, therefore, be the same as in NMORB.
[bb] I have to divide by N to return to the same compositional space that I was in before.

Table 1.8 Model parameters for mass-balance calculations.

	fraction in high-K series†	**fraction in medium-K series**	**fraction in low-K series**	**convergence rate**‡ (mm/yr)	**arc length**‡ (km)	**crustal addition rate**‡ (km^3/yr/km arc length)
Aleutians	0.07	0.81	0.12	62	1900	40
Central America	0.21	0.72	0.07	77	1450	5.5
Izu-Bonin	0.00	0.16	0.84	50	1050	40
Kurile	0.18	0.70	0.12	90	1650	35
Marianas	0.00	0.34	0.66	47.5	1400	47
Northern Antilles	0.00	0.78	0.22	24	400	20.7
Southern Antilles	0.07	0.74	0.19	24	400	20.7
Sunda-Java	0.60	0.40	0.00	67	3010	40
Tonga	0.06	0.27	0.67	170	1350	56

† i.e., fraction of total erupted IAV that are classified as high-K.

‡ From Plank and Langmuir, 1998

‡ From Crisp, 1984 and Dimalanta *et al.*, 2002

Table 1.9 Average F_{arc} and F_{mantle} values for arcs in this study. Fluxes in kg/yr/km arc length.

	Aleutians		**Central America**		**Izu-Bonin**	
	F_{arc}	**F_{mantle}**	**F_{arc}**	**F_{mantle}**	**F_{arc}**	**F_{mantle}**
K	405550.39	1018663.35	59067.91	941576.14	291537.12	2628489.86
Rb	924.03	2694.82	146.23	1646.02	469.73	7608.24
Ba	19377.80	102087.24	4281.58	214966.17	6367.27	2134.12
Th	64.31	332.43	14.66	168.93	5.21	273.37
U	26.26	142.64	6.12	149.34	6.46	264.40
Nb	85.39	2050.17	45.37	2168.80	35.07	2026.71
Ta	13.92	113.06	1.86	125.65	10.60	128.38
La	305.92	2529.26	99.71	3424.05	7.77	4012.18
Ce	585.80	7083.34	180.01	7348.10	10.84	8934.66
Pb	307.61	638.34	35.05	842.24	195.45	556.98
Sr	30550.11	56358.94	5874.64	184874.21	14029.22	63702.05
Nd	256.74	6197.55	82.61	7469.13	6.88	8678.85
Zr	661.63	60696.01	210.52	67770.79	29.94	69090.88
Hf	12.67	1666.34	4.63	1881.70	2.93	1864.67
Sm	41.79	2132.95	12.24	2564.90	0.30	2780.88
Eu	9.74	797.75	2.87	955.11	0.00	919.61
Y	100.67	21647.44	2.79	27571.70	104.15	27343.76
Yb	0.00	2355.21	0.00	2855.83	0.00	2648.37
Lu	0.43	350.69	0.07	426.42	0.12	410.00

Table 1.9 (continued)

	Kurile		Marianas		Northern Antilles	
	F_{arc}	F_{mantle}	F_{arc}	F_{mantle}	F_{arc}	F_{mantle}
K	517832.59	2028054.02	179709.50	1896456.22	110057.53	907661.90
Rb	1411.25	6219.64	469.64	4698.39	257.67	2910.18
Ba	13962.81	45789.20	6189.24	17403.54	3398.61	2971.48
Th	134.19	514.65	15.85	216.57	19.28	209.76
U	45.33	175.23	10.44	131.84	6.70	74.07
Nb	37.89	3238.40	2.83	2144.55	4.66	1102.63
Ta	1.75	181.87	0.61	139.53	0.01	69.98
La	305.29	4379.15	55.43	2825.24	53.94	1413.97
Ce	576.41	12386.05	89.31	7094.63	169.82	4030.27
Pb	237.91	2049.59	121.40	429.59	249.03	253.51
Sr	19205.97	99395.12	4873.81	66098.49	6338.49	29014.99
Nd	186.63	10347.60	73.77	6447.05	18.17	3362.22
Zr	2157.23	92026.60	93.02	57931.02	6.91	31193.04
Hf	6.72	2580.88	1.08	1571.29	0.03	862.07
Sm	27.23	3532.38	7.25	2139.52	1.26	1120.43
Eu	4.02	1271.09	0.44	749.70	0.76	392.51
Y	21.76	35277.22	6.08	21227.35	17.34	11121.46
Yb	0.00	3736.99	0.00	2154.80	0.00	1152.97
Lu	0.06	564.39	0.04	329.57	0.05	176.78

Table 1.9 (continued)

	Southern Antilles		Sunda-Java		Tonga	
	F_{arc}	F_{mantle}	F_{arc}	F_{mantle}	F_{arc}	F_{mantle}
K	53057.36	1214199.11	767803.36	1460254.89	186672.69	3422108.35
Rb	169.88	5380.55	3656.35	3362.32	502.18	6883.84
Ba	2425.87	12229.29	32135.39	97380.66	6274.18	68230.18
Th	45.92	439.14	346.07	395.77	15.94	609.57
U	16.16	154.97	70.67	82.73	7.35	272.43
Nb	26.99	1337.55	272.63	2325.01	206.83	5576.89
Ta	9.78	74.33	9.38	158.88	1.52	345.47
La	98.19	2138.51	1568.03	2948.11	111.46	10432.27
Ce	167.79	5505.25	2745.30	9686.25	254.48	24825.21
Pb	27.79	979.85	486.34	1474.78	176.30	4376.00
Sr	3550.67	30484.92	21463.89	91156.87	6894.22	231937.17
Nd	60.19	3677.58	951.25	7302.00	74.10	23451.22
Zr	70.32	29923.41	1104.31	69479.67	21.03	186132.14
Hf	1.03	831.50	15.29	1960.34	1.13	5147.42
Sm	10.08	1110.23	127.54	2534.09	10.84	7639.89
Eu	1.23	372.27	26.56	896.86	3.19	2720.56
Y	6.96	10162.50	83.46	25139.20	115.79	74253.97
Yb	0.00	1057.35	0.00	2674.71	0.00	7858.95
Lu	0.02	160.69	0.11	404.62	0.05	1187.36

Chapter 2: Geological Background

Aleutian Arc

The Aleutian arc consists of approximately 80 islands in a chain extending for 2500 km west of Anchorage, Alaska (Figure 2.1). Significant variations in physical characteristics occur from east to west along the arc. The eastern portion of the arc is marked by a continental crust-like overlying plate, roughly normal convergence of the plates at 6 cm/yr, and relatively high magma production rates. In contrast, the western end of the arc lies on predominantly oceanic crust and is characterized by primarily strike-slip motions, with very little magma production. Volcanism in the region began approximately 70 million years ago (Ma) with the subduction of the Kula plate, which has since been completely consumed. Formation of the modern islands of the Aleutian arc began in Miocene[a] times (7-16 Ma; Harbert, 1987; Marsh, 1982); the currently active volcanoes generally lie on the northern portions of these older islands. The sedimentary layer on the ingoing slab is fairly thick (Table 1.7), owing largely to the extreme age of the subducting plate (~140 Myr). As a result, the Aleutians are generally considered to be an "accreting" margin (von Huene and Scholl, 1991), with a fairly well-established accretionary prism.

[a] Refers to a span of time on the geologic time scale. Earth's history is divided into four main eras (Precambrian, Paleozoic, Mesozoic, and Cenozoic). These eras are subdivided into progressively smaller chunks called periods and epochs. Right now we are in the Cenozoic era (65 Ma-present), Quaternary period (1.8 Ma-present), and Holocene epoch (0.01 Ma-present). The Miocene epoch occurred between 24 and 5 Ma (Cenozoic era, Tertiary period).

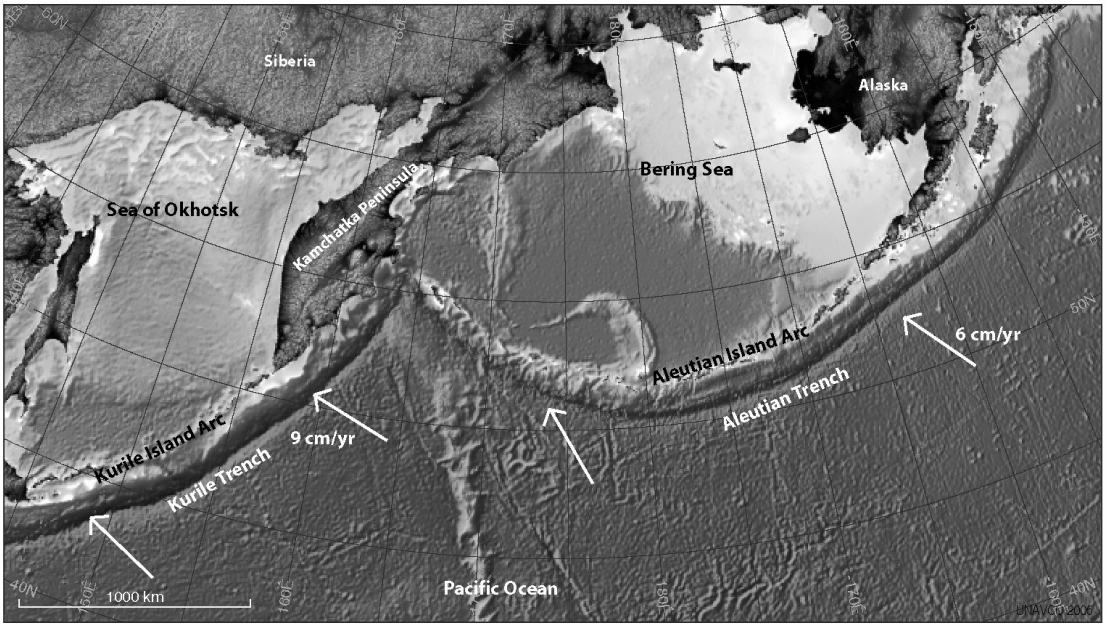

Figure 2.1 Map of Aleutian and Kurile Island Arcs. White arrows indicate direction of convergence. Topographic image from Jules Verne Voyager (http://jules.unavco.org).

Central American Arc

The 1500 km long Central American Arc is the result of subduction of the Cocos Plate beneath the Caribbean Plate (Figure 2.2). Subduction is fairly rapid, at 7.7 cm/yr, and results in high magma production rates (Shaw, 2003). Volcanism extends from Guatemala to Panama, and significant geochemical and geophysical variations occur between volcanic centers. These variations allow the modern arc to be divided into eight distinct segments, which are separated by thrusting (Carr *et al.*, 1982). Most of the currently active volcanoes are less than 100 kyr in age, although episodic volcanism has occurred in this area since the Tertiary. The overlying arc crust is primarily continental in composition, while the subducting Cocos Plate comprises fairly young (~20-30 Ma) oceanic crust (Maehr, 1997). Unlike the Aleutian arc, the Central American arc is "non-accreting" (von Huene and Scholl, 1991), with no well-developed accretionary prism.

Izu-Bonin Arc

Volcanism in the Izu-Bonin arc (Figure 2.3) began during the Eocene (40-50 Ma) with the initiation of subduction of the Pacific Plate beneath the West Philippine Sea Plate (Hochstaedter *et al.*, 2001). The modern-day convergence rate is approximately 5 cm/yr (Taylor and Nesbitt, 1998); the subducting plate forms a fairly shallow angle (45-50°) with the overlying plate (Straub, 2003). The Pacific oceanic crust being subducted is some of the oldest on Earth (140-160 Ma) and is covered by a relatively thick layer of pelagic clays and other oceanic debris (Table 1.7; Macpherson and Hall, 1999; Straub and Layne, 2003; Straub *et al.*, 2004). Subduction-related

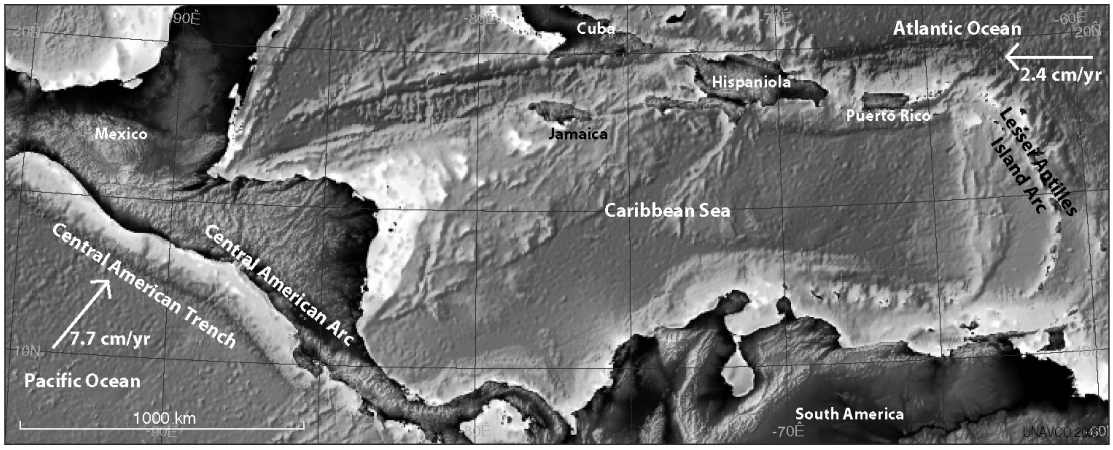

Figure 2.2 Map of Central American and Lesser Antilles arcs. White arrows indicate direction of convergence. Topographic image from Jules Verne Voyager (http://jules.unavco.org).

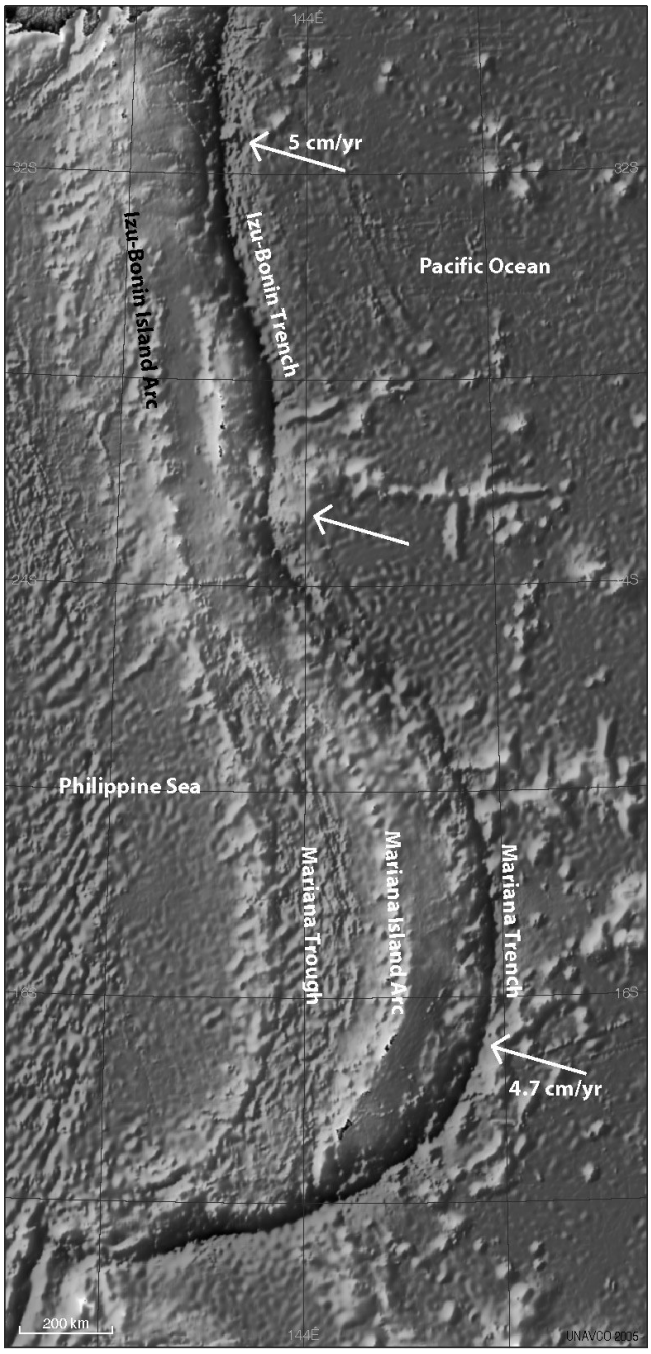

Figure 2.3 Map of Izu-Bonin and Mariana island arcs. White arrows indicate direction of convergence. Topographic image from Jules Verne Voyager (http://jules.unavco.org).

volcanism in this region has occurred during two main periods (Eocene to Oligocene and Neogene to present; Straub, 2003), and has been interspersed with periods of back-arc rifting that produced the modern-day Parece Vela and Shikoku basins. Modern volcanism occurs primarily at nine subaerial and several submarine volcanic centers (Taylor and Nesbitt, 1998).

Kurile Arc

The Kurile Arc extends for approximately 2500 km southwest of the Aleutian Arc and intersects the Northeast Honshu Arc on the island of Hokkaido (Figure 2.1). Like the nearby Izu-Bonin and Mariana arcs, volcanism in the Kurile Arc has been ongoing, though intermittent, since the Miocene (Aramaki and Ui, 1982). Studies have suggested that volcanism in this region may occur episodically, approximately every 2 Myr (e.g. Prueher and Rea, 2001). The southern part of the Kurile Arc is a double volcanic chain, which becomes a single (though somewhat wide – 270 km) volcanic arc north of the central Kurile Arc (Aramaki and Ui, 1982). The trench in this area is very deep (7000 m), and the convergence rate is fairly high (9 cm/yr). The majority of the active volcanoes in the Kurile Arc are submarine (Bindeman and Bailey, 1999).

Lesser Antilles Arc

The Lesser Antilles Arc (Figure 2.2) has formed where the Atlantic Plate is subducting beneath the Caribbean Plate, and the islands in the arc form the eastern boundary of the Caribbean Sea. The arc is often divided into northern and southern portions based on large differences in volcanic activity and arc structure. The Northern Lesser Antilles Arc, which lies north

of the island of Dominica, is composed of a double chain of islands. The "outer" (eastward) islands are the remnants of older volcanic activity (Oligocene; Rea, 1982). The westward islands comprise the northern portion of the modern, active arc[b]. The Southern Lesser Antilles Arc (south of Dominica) is characterized by active volcanism (Pleistocene to recent) overlying older, Oligocene volcanics. Due to its proximity to South America, the ingoing slab at the Southern Lesser Antilles has an extremely thick overlying sediment cover (Table 1.7; Plank and Langmuir, 1998; Rea and Ruff, 1996; Rea, 1982). Subduction in this region is fairly slow (~2.4 cm/yr), and a large accretionary prism has developed in the southern portion of the arc (up to 20 km thick; Rea, 1982).

Mariana Arc

The Mariana Arc extends southwest from the Izu-Bonin Arc to near Papua New Guinea (Figure 2.3). Like the Izu-Bonin Arc, volcanism in the Marianas has been ongoing since the Eocene and has alternated with periods of backarc rifting (Deschamps and Lallemand, 2003; Kelley, 2004; Meijer, 1982). The backarc basin, the Mariana Trough, has been formed through mid-ocean ridge-like rifting at a rate of about 3 cm/yr (fairly high compared to the subduction rate of ~4.7 cm/yr). The crust underlying the Mariana Arc is primarily oceanic in character, although it is quite thick relative to most oceanic basins (17-20 km). The active volcanoes in the arc are between 20 and 80 km apart, and lie along a very regular curve (as opposed to most other island arcs, which show small to extreme deviations from the

[b] Very active – the island of Montserrat, which has erupted several times in the past two decades, is located in the Northern Lesser Antilles.

ideal "arc" shape). Several forearc volcanoes are active in the southern portion of the Marianas (Deschamps and Lallemand, 2003; Meijer, 1982). Seismic studies indicate that the downgoing Philippine Sea Plate may be nearly vertical beneath parts of the Mariana Arc, although the dip decreases to the north toward Izu-Bonin (Kelley, 2004; Meijer, 1982).

Sunda-Java Arc

The Sunda-Java Arc extends over a distance of >3000 km between the islands of Java and Flores in Indonesia (Figure 2.4; Hutchison, 1982). This arc is part of the larger Indonesian volcanic arc, and it is characterized by subduction of Indian Ocean crust normal to Java at approximately 6.7 cm/yr (Plank and Langmuir, 1998). The age of the subducting slab increases from roughly 70 Ma in the west to over 130 Ma in the east. Volcanism in this region has been ongoing since at least the Eocene, although the current configuration has existed since only ~5 Ma. The subducting crust changes in nature from primarily continental in the west to mostly oceanic in the west. There are indications of back-arc spreading in some parts of the arc (Carn and Pyle, 2001), and several back-arc basins exist to the north of the main islands.

Tonga Arc

The Tonga Arc extends for ~1300 km from near Samoa to the Kermadec Arc in the southern Pacific Ocean (Figure 2.5; Cole, 1982). The arc formed due to the collision of the Jurassic-Cretaceous aged Pacific plate beneath the Indo-Australian plate. Volcanism has been intermittent since the Oligocene, and back-arc spreading began between 3-6 Ma when the arc split

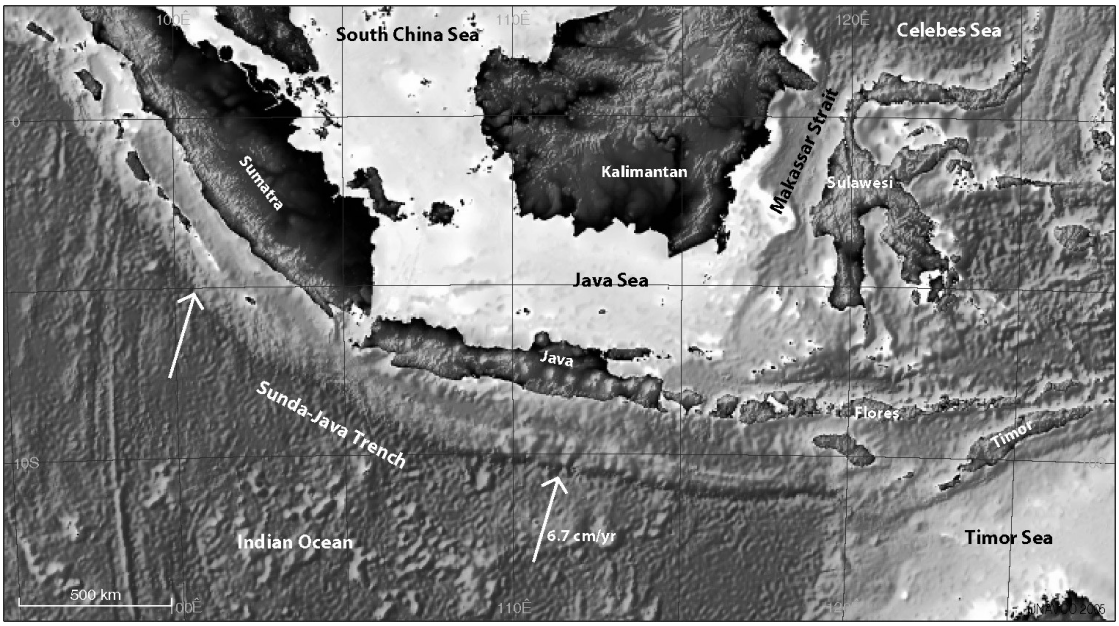

Figure 2.4 Map of Sunda-Java island arc. White arrows indicate direction of convergence. Topographic image from Jules Verne Voyager (http://jules.unavco.org).

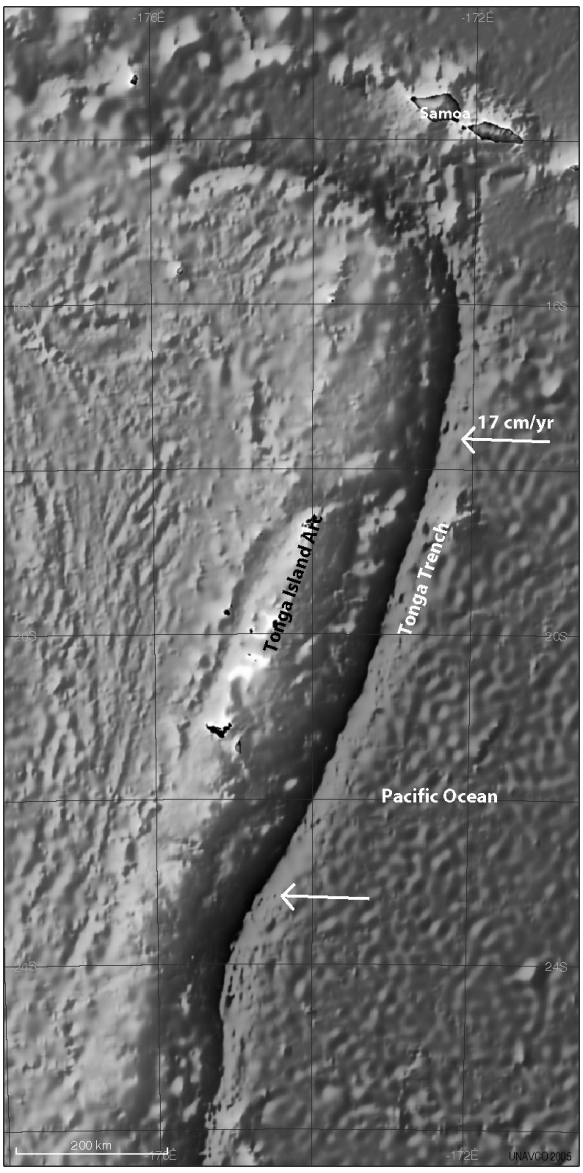

Figure 2.5 Map of Tonga island arc. White arrows indicate direction of convergence. Topographic image from Jules Verne Voyager (http://jules.unavco.org).

(Turner and Hawkesworth, 1997). Subduction most likely began in Tonga, with the arc slowly extending south toward New Zealand. The subducting slab forms an angle of roughly 40-50˚ with the overlying plate (Cole, 1982; Turner and Hawkesworth, 1997). Convergence rates are extremely high, at 17 cm/yr (Plank and Langmuir, 1998; Turner *et al*., 1997).

Chapter 3: Results, Model Variations, and Interpretation

Mobility of Trace Elements and Slab-to-Mantle Fluxes

My mass-balance model yields estimates of residual slab fluxes into the convecting mantle (Table 3.1; Figure 3.1). I used these estimates to determine the relative mobility of various trace elements within the subduction zone and to determine the trace element characteristics of the residual slab material that is incorporated into the convecting mantle. Figure 3.2 and Table 3.2 give the average residual slab flux as a fraction of the ingoing flux for each of the arcs in this study; Appendix D lists the residual slab fluxes and recycled fractions for individual magma series. Elements that are lost from the slab in significant amounts within the subduction zone have low recycled fractions (values much less than 1) in Figure 3.1. In contrast, elements that are quantitatively retained by the slab show high recycled fractions (values near 1) in Figure 3.1.

In general, my initial results support prevailing theories about the behavior of certain groups of trace elements during subduction zone processing. For example, it is generally thought that aqueous fluids released from the subducting slab are primarily responsible for transporting trace elements from the slab to the IAV (e.g. Tatsumi, 1989; Tatsumi and Eggins, 1995; Tatsumi *et al.*, 1986; Taylor and Nesbitt, 1998; Vidal *et al.*, 1989; see also chapter 1). This suggests that fluid-immobile elements should be retained by the slab during subduction zone processing, whereas fluid-mobile elements should be heavily lost by the slab. An examination of Figure 3.1 shows that, generally speaking, the results of my model agree with these predictions. Elements that are retained by the slab in all of the arcs

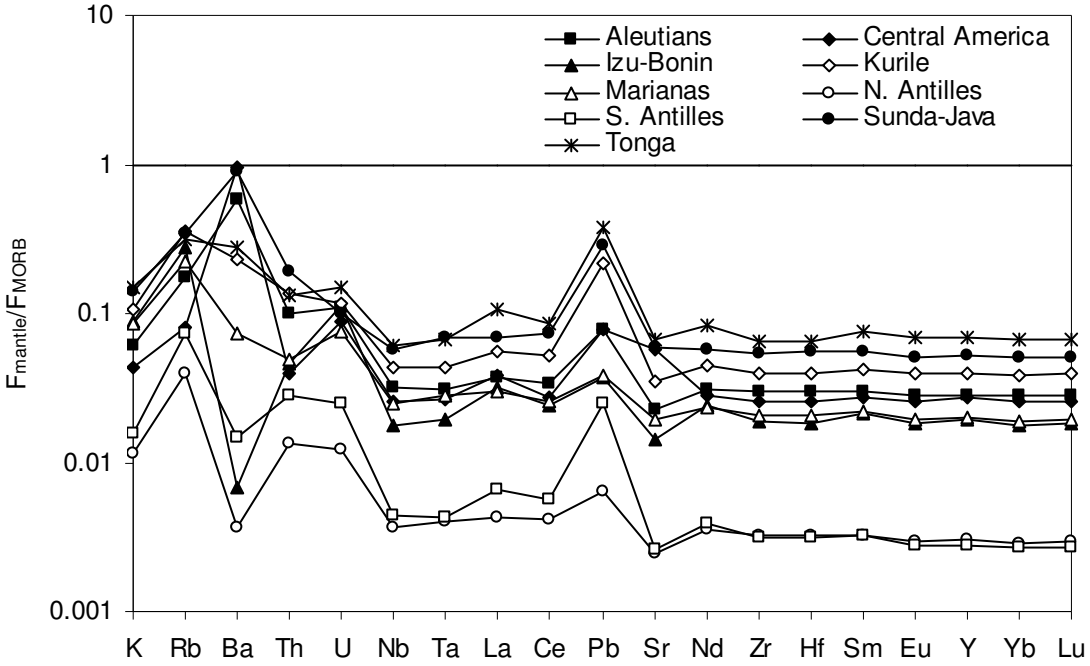

Figure 3.1 Flux of trace elements into the mantle at various subduction zones. Fluxes normalized to average normal mid-ocean ridge basalt flux.

Table 3.1 Average F_{arc} and F_{mantle} values for arcs in this study. Fluxes in kg/yr/km arc length.

	Aleutians		**Central America**		**Izu-Bonin**	
	F_{arc}	**F_{mantle}**	**F_{arc}**	**F_{mantle}**	**F_{arc}**	**F_{mantle}**
K	405550.39	1018663.35	59067.91	941576.14	291537.12	2628489.86
Rb	924.03	2694.82	146.23	1646.02	469.73	7608.24
Ba	19377.80	102087.24	4281.58	214966.17	6367.27	2134.12
Th	64.31	332.43	14.66	168.93	5.21	273.37
U	26.26	142.64	6.12	149.34	6.46	264.40
Nb	85.39	2050.17	45.37	2168.80	35.07	2026.71
Ta	13.92	113.06	1.86	125.65	10.60	128.38
La	305.92	2529.26	99.71	3424.05	7.77	4012.18
Ce	585.80	7083.34	180.01	7348.10	10.84	8934.66
Pb	307.61	638.34	35.05	842.24	195.45	556.98
Sr	30550.11	56358.94	5874.64	184874.21	14029.22	63702.05
Nd	256.74	6197.55	82.61	7469.13	6.88	8678.85
Zr	661.63	60696.01	210.52	67770.79	29.94	69090.88
Hf	12.67	1666.34	4.63	1881.70	2.93	1864.67
Sm	41.79	2132.95	12.24	2564.90	0.30	2780.88
Eu	9.74	797.75	2.87	955.11	0.00	919.61
Y	100.67	21647.44	2.79	27571.70	104.15	27343.76
Yb	0.00	2355.21	0.00	2855.83	0.00	2648.37
Lu	0.43	350.69	0.07	426.42	0.12	410.00

Table 3.1 (continued)

	Kurile		Marianas		Northern Antilles	
	F_{arc}	F_{mantle}	F_{arc}	F_{mantle}	F_{arc}	F_{mantle}
K	517832.59	2028054.02	179709.50	1896456.22	110057.53	907661.90
Rb	1411.25	6219.64	469.64	4698.39	257.67	2910.18
Ba	13962.81	45789.20	6189.24	17403.54	3398.61	2971.48
Th	134.19	514.65	15.85	216.57	19.28	209.76
U	45.33	175.23	10.44	131.84	6.70	74.07
Nb	37.89	3238.40	2.83	2144.55	4.66	1102.63
Ta	1.75	181.87	0.61	139.53	0.01	69.98
La	305.29	4379.15	55.43	2825.24	53.94	1413.97
Ce	576.41	12386.05	89.31	7094.63	169.82	4030.27
Pb	237.91	2049.59	121.40	429.59	249.03	253.51
Sr	19205.97	99395.12	4873.81	66098.49	6338.49	29014.99
Nd	186.63	10347.60	73.77	6447.05	18.17	3362.22
Zr	2157.23	92026.60	93.02	57931.02	6.91	31193.04
Hf	6.72	2580.88	1.08	1571.29	0.03	862.07
Sm	27.23	3532.38	7.25	2139.52	1.26	1120.43
Eu	4.02	1271.09	0.44	749.70	0.76	392.51
Y	21.76	35277.22	6.08	21227.35	17.34	11121.46
Yb	0.00	3736.99	0.00	2154.80	0.00	1152.97
Lu	0.06	564.39	0.04	329.57	0.05	176.78

Table 3.1 (continued)

	Southern Antilles		Sunda-Java		Tonga	
	F_{arc}	F_{mantle}	F_{arc}	F_{mantle}	F_{arc}	F_{mantle}
K	53057.36	1214199.11	767803.36	1460254.89	186672.69	3422108.35
Rb	169.88	5380.55	3656.35	3362.32	502.18	6883.84
Ba	2425.87	12229.29	32135.39	97380.66	6274.18	68230.18
Th	45.92	439.14	346.07	395.77	15.94	609.57
U	16.16	154.97	70.67	82.73	7.35	272.43
Nb	26.99	1337.55	272.63	2325.01	206.83	5576.89
Ta	9.78	74.33	9.38	158.88	1.52	345.47
La	98.19	2138.51	1568.03	2948.11	111.46	10432.27
Ce	167.79	5505.25	2745.30	9686.25	254.48	24825.21
Pb	27.79	979.85	486.34	1474.78	176.30	4376.00
Sr	3550.67	30484.92	21463.89	91156.87	6894.22	231937.17
Nd	60.19	3677.58	951.25	7302.00	74.10	23451.22
Zr	70.32	29923.41	1104.31	69479.67	21.03	186132.14
Hf	1.03	831.50	15.29	1960.34	1.13	5147.42
Sm	10.08	1110.23	127.54	2534.09	10.84	7639.89
Eu	1.23	372.27	26.56	896.86	3.19	2720.56
Y	6.96	10162.50	83.46	25139.20	115.79	74253.97
Yb	0.00	1057.35	0.00	2674.71	0.00	7858.95
Lu	0.02	160.69	0.11	404.62	0.05	1187.36

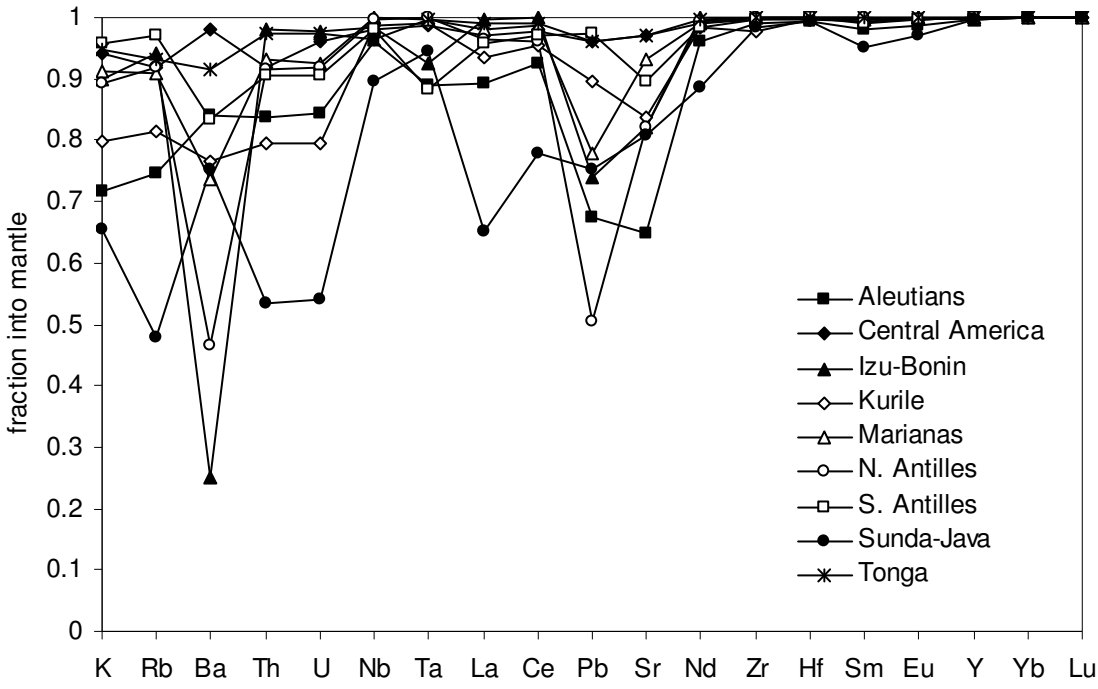

Figure 3.2 Fraction of ingoing slab material incorporated into the mantle at various subduction zones. Values near one indicate elements that are quantitatively retained by the slab during subduction zone processing, while values much less than one indicate elements that are highly mobile within the subduction zone.

Table 3.2 Fraction of ingoing slab material incorporated into the mantle at various subduction zones.

	Aleutians	Central America	Izu-Bonin	Kurile	Marianas	Northern Antilles	Southern Antilles	Sunda-Java	Tonga
K	0.7152	0.9410	0.9002	0.7966	0.9134	0.8919	0.9581	0.6554	0.9483
Rb	0.7447	0.9184	0.9419	0.8151	0.9091	0.9187	0.9694	0.4791	0.9320
Ba	0.8405	0.9805	0.2510	0.7663	0.7377	0.4665	0.8345	0.7519	0.9158
Th	0.8379	0.9201	0.9813	0.7932	0.9318	0.9158	0.9053	0.5335	0.9745
U	0.8445	0.9606	0.9761	0.7945	0.9266	0.9171	0.9056	0.5393	0.9737
Nb	0.9600	0.9795	0.9830	0.9884	0.9987	0.9958	0.9802	0.8950	0.9642
Ta	0.8904	0.9854	0.9237	0.9905	0.9957	0.9999	0.8837	0.9443	0.9956
La	0.8921	0.9717	0.9981	0.9348	0.9808	0.9633	0.9561	0.6528	0.9894
Ce	0.9236	0.9761	0.9988	0.9555	0.9876	0.9596	0.9704	0.7792	0.9899
Pb	0.6748	0.9600	0.7402	0.8960	0.7797	0.5045	0.9724	0.7520	0.9613
Sr	0.6485	0.9692	0.8195	0.8381	0.9313	0.8207	0.8957	0.8094	0.9711
Nd	0.9602	0.9891	0.9992	0.9823	0.9887	0.9946	0.9839	0.8847	0.9969
Zr	0.9892	0.9969	0.9996	0.9771	0.9984	0.9998	0.9977	0.9844	0.9999
Hf	0.9925	0.9975	0.9984	0.9974	0.9993	1.0000	0.9988	0.9923	0.9998
Sm	0.9808	0.9953	0.9999	0.9924	0.9966	0.9989	0.9910	0.9521	0.9986
Eu	0.9879	0.9970	1.0000	0.9968	0.9994	0.9981	0.9967	0.9712	0.9988
Y	0.9954	0.9999	0.9962	0.9994	0.9997	0.9984	0.9993	0.9967	0.9984
Yb	1.0000	1.0000	1.0000	1.0000	1.0000	1.0000	1.0000	1.0000	1.0000
Lu	0.9988	0.9998	0.9997	0.9999	0.9999	0.9997	0.9999	0.9997	1.0000

examined – Ta, Nb, and the rare earth elements – are fairly immobile in aqueous fluids, while more mobile elements, such as K, Rb, Ba, and Pb, have relatively low recycled fractions in all of the arcs. These results support the idea that aqueous fluids are the primary transport phase for trace elements between the slab and the mantle wedge. Although slab melts have been invoked to explain certain trace element characteristics of IAV in some of the arcs that I have considered here (e.g. Marianas: Elliott *et al.*, 1997; Johnson and Plank, 1999; Plank, 2005; Aleutians: Class *et al.*, 2000; Kay and Kay, 1988; Yogodzinski *et al.*, 1995; Yogodzinski and Keleman, 1998; Yogodzinski *et al.*, 2001), there do not appear to be any significant trends, such as large fractionations between the REE, in Figure 3.1 that might be representative of slab melting.

Implications for Mantle Pb/Ce Ratios

Trace element ratios can be used as markers of the different reservoirs that may contribute to mantle-derived volcanic rocks. For example, Newsom *et al* (1986) and Stracke *et al* (2003) have used the Pb/Ce ratio as an indicator of crustal material in the mantle source regions of various volcanic rocks. Crustal rocks have high, variable Pb/Ce, but mantle-derived rocks tend to have relatively low, invariant values (~0.04). Since Pb and Ce have similar mineral/melt distribution coefficients, Pb/Ce ratios are not significantly altered during partial melting; therefore, rocks derived from mantle sources that have been contaminated with crustal material should have Pb/Ce values that lie between the ambient mantle value of 0.04 and the (generally higher) ratio of the contaminating crustal material. Simple mixing

relations can be used to estimate the relative contribution of the crustal material.

Although the distinctive Pb/Ce ratios of mantle and crustal material can be used to elucidate crustal contamination of the mantle, they also create an apparent paradox. How can a reservoir with low, constant Pb/Ce (the mantle) give rise to material with high, variable Pb/Ce (the crust) through partial melting processes, if partial melting does not fractionate Pb/Ce? Conversely, how can the mantle maintain its low Pb/Ce if it is continually mixing with crustal material at subduction zones? One possibility is that processing within the subduction zone, which involves aqueous fluids rather than partial melting, might preferentially remove Pb from the slab. The residual slab material (which is mixed into the mantle) would therefore have a lowered Pb/Ce. The high Pb/Ce fluids would mix with the mantle wedge and produce high Pb/Ce ratios in the erupted IAV, which could then be incorporated into continental crust.

In order to examine the effects of subduction zone processing on slab Pb/Ce ratios, I compared Pb/Ce ratios in the ingoing and residual slab material (Figure 3.3 and Table 3.3). Five of the arcs (Central America, Kurile, Southern Lesser Antilles, Sunda-Java, and Tonga) show very little change in Pb/Ce during subduction zone processing, but the other four exhibit substantially decreased residual slab ratios. However, even the lowest residual slab ratios (at Izu-Bonin and the Marianas) are not as low as the ambient mantle value. These results indicate that subduction zone processing may play a role in lowering slab Pb/Ce, but it is unlikely to completely explain the Pb/Ce paradox.

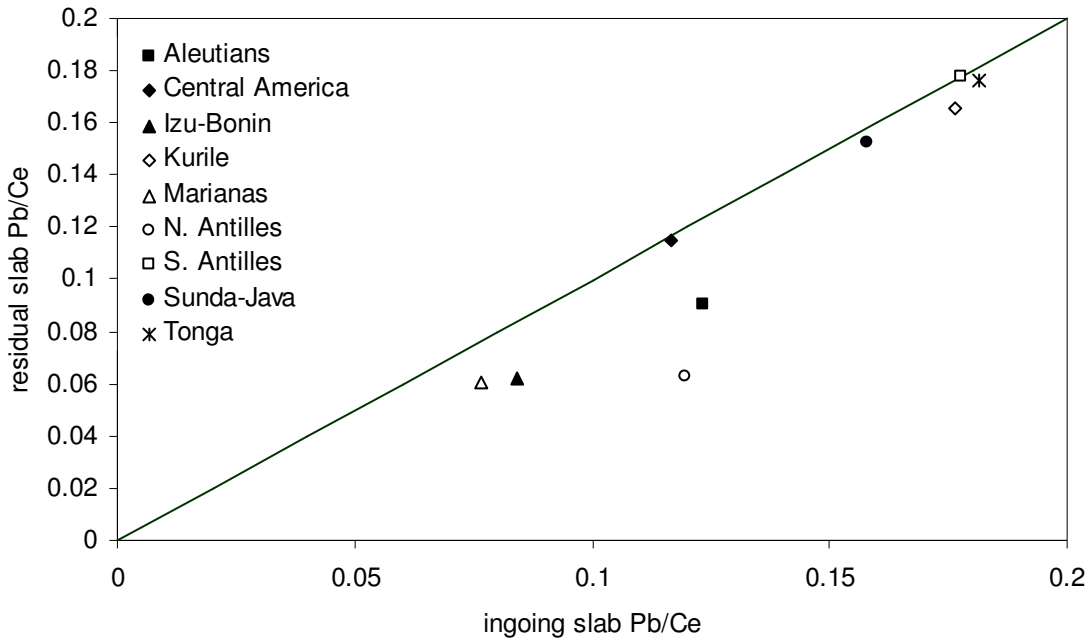

Figure 3.3 Ingoing and residual slab Pb/Ce ratios for arcs in this study.

Table 3.3 Residual slab characteristics for arcs in this study. Isotopic values are for 1.8 Ga subducted slabs.

	Aleutians	Central America	Izu-Bonin	Kurile	Marianas	Northern Antilles	Southern Antilles	Sunda-Java	Tonga
Pb/Ce	0.09	0.11	0.06	0.17	0.06	0.06	0.18	0.15	0.18
Th/U	2.33	1.13	1.03	2.94	1.64	2.83	2.83	4.78	2.24
U/Pb	0.22	0.18	0.47	0.09	0.31	0.29	0.16	0.06	0.06
Rb/Sr	0.05	0.01	0.12	0.06	0.07	0.10	0.18	0.04	0.03
Sm/Nd	0.34	0.34	0.32	0.34	0.33	0.33	0.30	0.35	0.33
$^{206}Pb/^{204}Pb$	19.74	19.36	25.27	17.54	21.93	21.66	18.97	16.94	17.13
$^{87}Sr/^{86}Sr$	0.7050	0.7029	0.7120	0.7069	0.7079	0.7097	0.7158	0.7052	0.7038
ε_{Nd}	8.4	6.2	2.9	6.4	4.7	5.8	0.4	6.6	5.5

The Kappa Conundrum and Mantle Th/U Ratios

The time-integrated mantle Th/U ratio, as inferred from lead isotopes, is roughly 3.6-3.8[a]. Modern mantle-derived rocks, however, have Th/U ratios of only 2.55-2.75. Modeling of the isotopic evolution of the mantle suggests that incorporation of very low Th/U material starting roughly 2 billion years ago (Ga) could produce this discrepancy, the so-called "kappa[b] conundrum." Collerson and Kamber (1999) and Elliott *et al* (1999) suggested that recycling of oxidized altered oceanic crust into the convecting mantle could explain the kappa conundrum.

Prior to roughly 2 Ga, Earth's atmosphere and oceans were highly reducing. Both Th and U are highly insoluble in water under reducing conditions, so hydrothermal alteration of oceanic crust at this time would have had little to no effect on the Th/U ratio of altered oceanic crust. At approximately 2 Ga, the concentration of oxygen in Earth's atmosphere began to increase. Earth's oceans became less reducing as the concentration of oxygen in the atmosphere increased. Oxidized uranium is highly soluble in aqueous solution, so the oxidation of Earth's oceans led to high oceanic U concentrations. Hydrothermal alteration of oceanic crust by high-U seawater produces AOC with very low Th/U (e.g., modern oceans are quite oxidizing, and the Th/U of modern AOC is ~0.44; Kelley, 2004). Collerson and Kamber (1999) and Elliott *et al* (1999) suggested that incorporation of such low Th/U AOC could be responsible for the mismatch between time-integrated and modern mantle Th/U.

---

[a] Since ^{208}Pb is produced by the decay of ^{232}Th and ^{206}Pb from ^{238}U decay, the ratio of the two Pb isotopes in mantle-derived rocks can be used to calculate the time-integrated Th/U ratio of the mantle.

[b] $\kappa = {}^{232}Th/{}^{238}U$.

The theory that recycling of oxidized AOC could explain the kappa conundrum requires that the Earth's oceans were sufficiently oxidized at 2 Ga to produce low Th/U AOC[c] at that time and/or that processing within subduction zones could lower the Th/U ratio of the slab prior to its being incorporated into the mantle. Several studies have indicated that the oceans were not significantly oxidized until 1.3 Ga (e.g. Arnold *et al.*, 2004; Canfield, 1998; Kah *et al.*, 2001; Shen *et al.*, 2003). If these studies are accurate, the average Th/U of ancient ingoing slabs may not have been significantly lower than it is today[d]. Using my estimated residual slab compositions, I calculated residual slab Th/U ratios for each arc. Figure 3.4 and Table 3.3 give the results of these calculations.

Of the arcs that I examined, none exhibit substantial changes in slab Th/U during subduction zone processing. Moreover, although AOC has a very low Th/U ratio, ingoing slabs generally have much higher ratios (the average of the arcs examined is 2.3) due to the presence of sediment (with very high Th/U) and unaltered oceanic crust (Th/U ~2.5) in addition to the AOC in the slab. These results suggest that the Th/U ratios of ancient ingoing slabs would have had to have been significantly lower than they are today in order for incorporation of AOC to have had a major lowering effect on mantle Th/U. Incorporation of altered oceanic crust into the mantle can therefore probably not fully explain the kappa conundrum.

[c] And, by extension, low Th/U subducting slabs.
[d] In fact, it may even have been higher, since the Th/U of AOC at that time would have been higher and would not have had the substantial lowering effect on the slab that it does today.

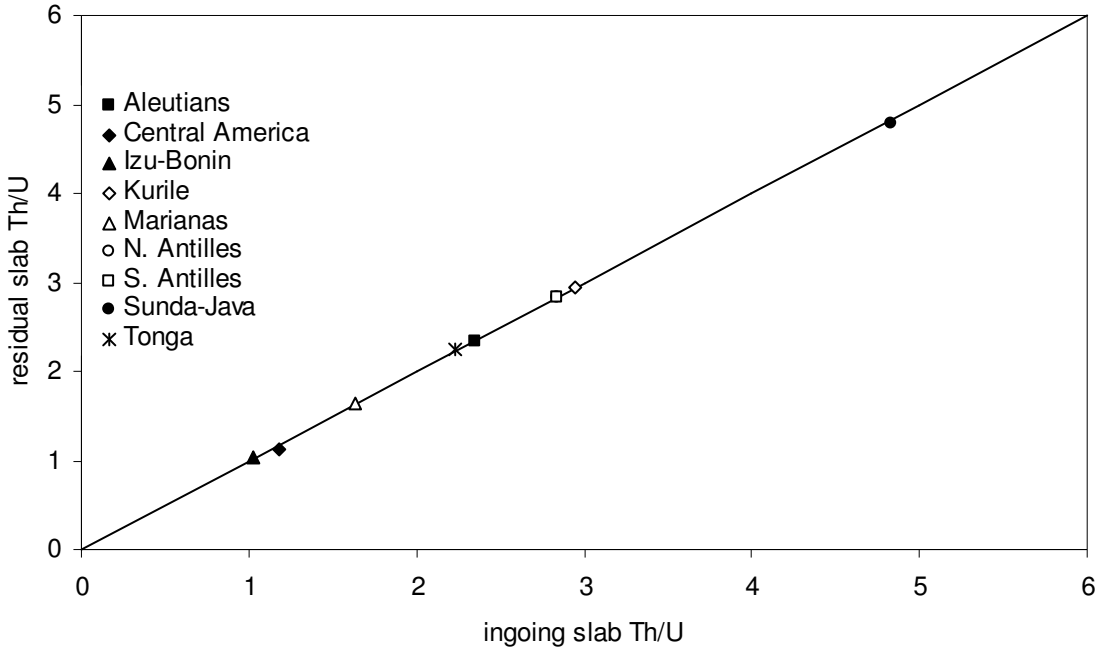

Figure 3.4 Ingoing and residual slab Th/U ratios for arcs in this study.

Estimation of Mantle Reservoir Isotopic Characteristics

Several researchers have noted the well-defined and distinctive fields that are formed by ocean island basalts (OIB) on Pb, Sr, and Nd isotopic diagrams (e.g. Hart and Staudigel, 1989; Hart and Zindler, 1989; White, 1989; see also Figure 1.1). They suggest that the OIB on these diagrams are produced by mixing between several isotopically distinct reservoirs within the mantle. Two of these reservoirs, the so-called "HIMU" and "EMII," are thought to be derived from crustal material that has been mixed into the convecting mantle. The HIMU reservoir is characterized by high $^{206}Pb/^{204}Pb$ and low $^{87}Sr/^{86}Sr$ ratios, while the EMII reservoir shows high $^{87}Sr/^{86}Sr$ and relatively low and $^{206}Pb/^{204}Pb$ ratios and ε_{Nd} values[e].

In order to examine whether or not recycled subducted material might be able to generate the HIMU and EMII signatures, I used calculated residual slab U/Pb, Rb/Sr, and Sm/Nd ratios to predict the modern isotopic composition of crustal material subducted at 1.8 Ga. I assumed that the anciently subducted residual slabs had the same parent/daughter elemental ratios (Figure 3.5 and Table 3.3) and relative proportions of sediment, AOC, and unaltered crust (Table 1.7) as do modern residual slabs. I used an inferred continental crustal composition from 1.8 Ga (Table 3.4) for the composition of 1.8 Ga sediment and 1.8 Ga depleted mantle isotopic ratios for unaltered oceanic crust and for AOC Nd and Pb isotopic ratios. Interaction with seawater, which contains relatively high concentrations of Sr,

[e] ε_{Nd} is calculated using the following equation:
$$\frac{\left(^{143}Nd/^{144}Nd\right)_{sample} - \left(^{143}Nd/^{144}Nd\right)_{chondrite}}{\left(^{143}Nd/^{144}Nd\right)_{chondrite}} x\,10^{4}$$, where "chondrite" refers to the Nd isotopic composition of a chondritic meteorite of the same age as the sample.

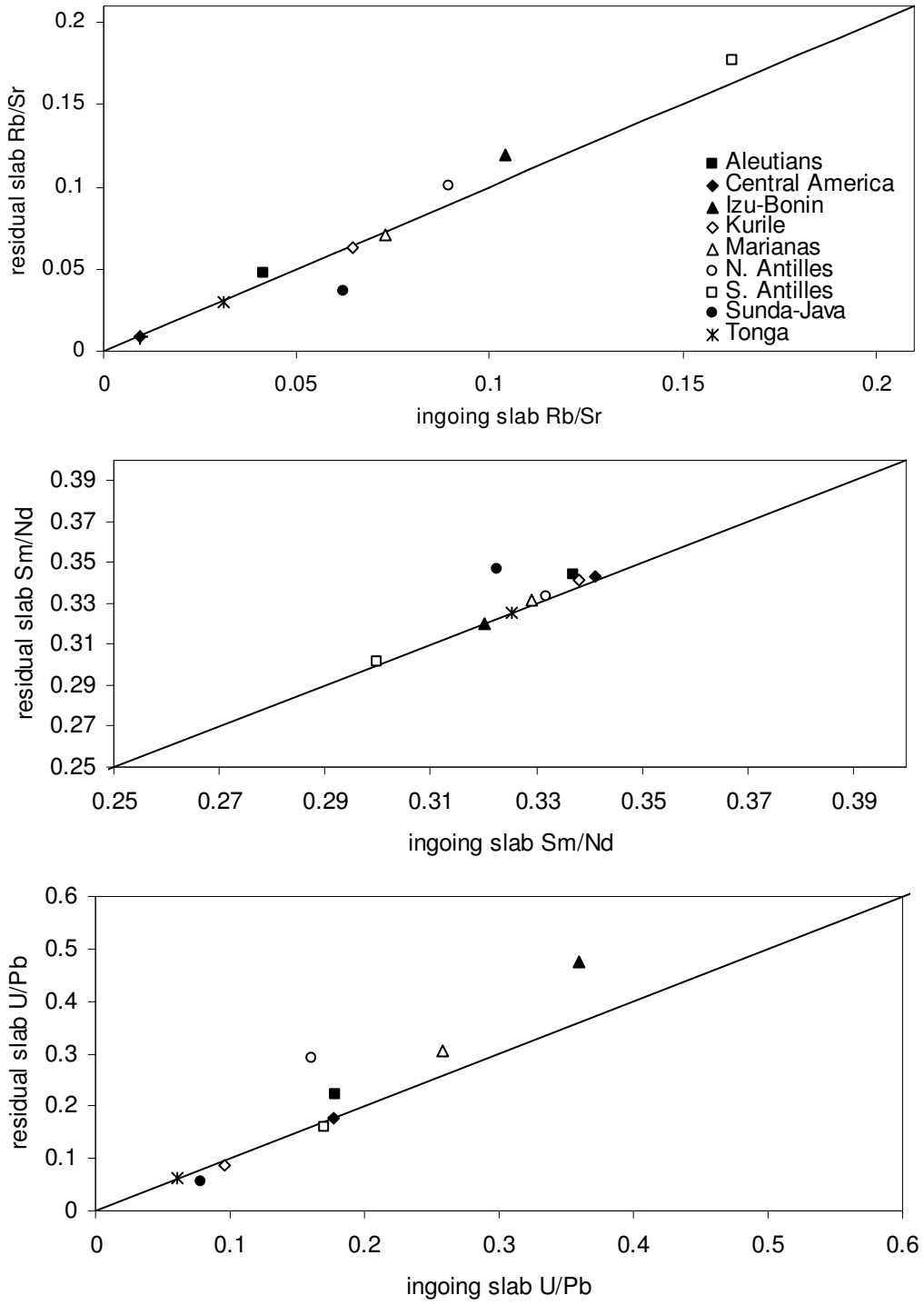

Figure 3.5 Parent/daughter ratios for residual slabs at various subduction zones.

Table 3.4 Input parameters for isotopic modeling of residual slab compositions. Values from EarthRef (Table 1.1) except where noted.

	$^{87}Sr/^{86}Sr$	$^{143}Nd/^{144}Nd$	$^{206}Pb/^{204}Pb$
initial bulk Earth ratio†	0.69898	0.50670	9.3140
present depleted mantle ratio	0.70265	0.51313	18.9667
present continental crust ratio	0.71366	0.51192	18.7000
depleted mantle ratio at 1.8 Ga†	0.70123	0.51061	15.9347
continental crust ratio at 1.8 Ga†	0.70611	0.51008	15.8017
present seawater ratio	0.70924	n/a	n/a
seawater ratio at 1.8 Ga‡	0.70510	n/a	n/a
present AOC ratio⁋	0.70458	n/a	n/a
AOC ratio at 1.8 Ga⁋	0.70236	n/a	n/a

† calculated from present-day chondrites assuming 4.55 Ga terrestrial age

‡ from Jacobsen and Kaufman, 1999; Jiedong *et al.*, 1999; Kah *et al.*, 2001; and Veizer *et al.*, 1999

⁋ from Kelley, 2004

⁋ calculated from ancient seawater and ocean crust ratios assuming the same ratios of seawater to MORB isotopes as occur today

can affect the Sr isotopic ratios of AOC[f]; I inferred the Sr isotopic composition of ancient seawater from published Sr isotope curves (Jacobsen and Kaufman, 1999; Jiedong *et al.*, 1999; Kah *et al.*, 2001; Veizer *et al.*, 1999). Starting with these inferred initial slab isotopic ratios at 1.8 Ga, I calculated the hypothetical modern-day isotopic composition of the ancient residual slab material. Figures 3.6 and 3.7 show the resulting range of possible residual slab compositions, and Table 3.3 gives the isotopic characteristics of the residual slabs after 1.8 Ga.

Of the arcs that I examined, only Izu-Bonin and the Marianas have sufficiently high residual slab U/Pb ratios to produce HIMU-like Pb isotopes after 1.8 Ga. However, in both of these arcs, residual slab Rb/Sr is far too high to produce the low Sr isotopic ratios that are characteristic of the HIMU reservoir. Similarly, although Izu-Bonin and Tonga have sufficiently low ε_{Nd} to form the EMII reservoir, their Pb and Sr isotopic ratios are not consistent with EMII characteristics.

Sensitivity of Results to Model Variations

During the development of my mass-balance model, I made several assumptions about compositions and processes within the subduction zone. These assumptions, while necessary, obviously introduced a certain degree of uncertainty into my results. I therefore explored the sensitivity of my model to variations in the two input parameters with the highest amount of uncertainty: mantle wedge composition and crustal addition rate. Overall, the model does not appear to be highly sensitive to these variations.

[f] Seawater contains almost no Nd or Pb, so these isotopic ratios are not affected by alteration.

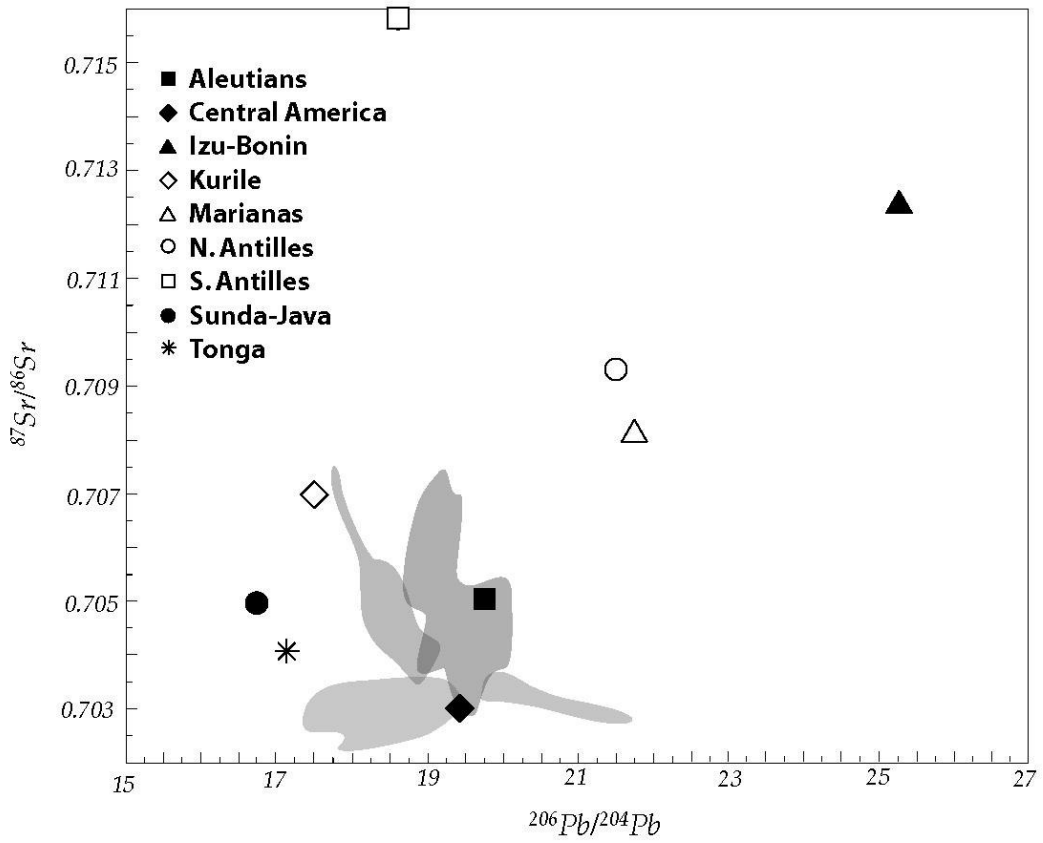

Figure 3.6 Residual slab Sr and Pb isotopic compositions for 1.8 Ga subducted slabs.

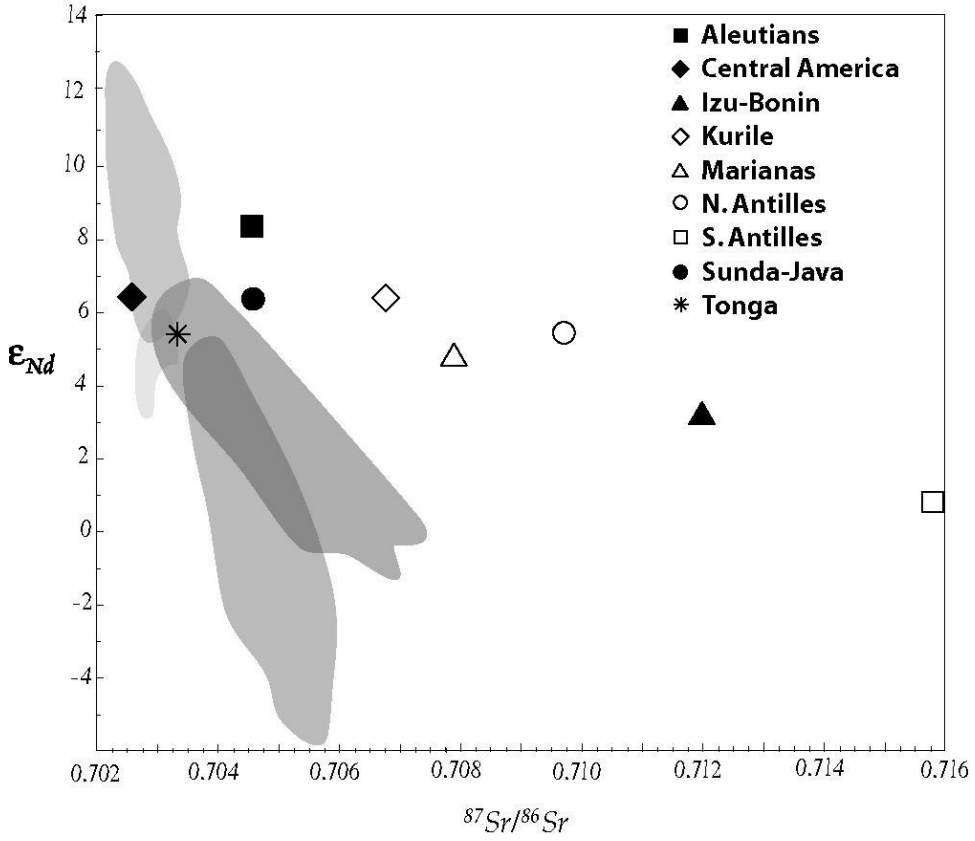

Figure 3.7 Residual slab Nd and Sr isotopic compositions for 1.8 Ga subducted slabs.

The procedure that I used to calculate the composition of the slab-derived component in the IAV assumed that a) the mantle wedge has a composition approximately the same as NMORB-source mantle and b) the IAV are produced by similar degrees of partial melting to NMORB. These assumptions are incorporated into the model in the form of a "normalizing composition" (see chapter 1) that I subtract from the average IAV compositions to remove the contribution of the mantle wedge. However, several studies have suggested that some of the arcs that I examined might have a more depleted composition than that of NMORB source mantle (e.g. Elliott *et al.*, 1997; Kamenetsky *et al.*, 1997; McCulloch and Gamble, 1991; Pearce, 1982). Such a depletion could, in theory, substantially change my calculated residual slab compositions.

To address this concern, I recalculated the residual slab compositions using a highly depleted mantle wedge component composition. I chose somewhat extreme extents of depletion in order to maximize the effect of this variation on my calculated results. To estimate the composition of a previously depleted mantle wedge, I started with the "depleted mantle" composition of Salters & Stracke (2004). I assumed that this depleted mantle composition represented NMORB-source mantle (that is, the composition of the mantle material that melts to produce NMORB[g]). To determine the composition of a wedge that has been affected by prior depletion events, I removed a 5% partial melt[h] from the Salters & Stracke (2004) composition and calculated the trace element concentrations in the

[g] I assumed that an undepleted mantle wedge would have this composition, and then I depleted it before generating the mantle wedge component of the IAV.
[h] Using a 1% porosity value in the continuous partial melting equation.

residual material. I then used a 20% partial melt of this residual material as the normalizing composition in the calculation of the residual slab. The compositions of the depleted mantle, depleted wedge, and wedge-derived component in the IAV are given in Table 3.5. Figure 3.8 and Table 3.6 give the average flux of residual slab material at each arc calculated using these normalizing values, and the resulting recycled fractions for each arc are given in Figure 3.9 and Table 3.7[i].

Most studies indicate that NMORB are produced by approximately 10% melting of their source region material, but IAV may be produced by different degrees of partial melting. I calculated two normalizing compositions from the depleted mantle composition of Salters & Stracke (2004), corresponding to partial melts of 5% and 20%[j] (Table 3.8). Figure 3.10 and Tables 3.9 & 3.10 show average residual slab fluxes calculated using high- and low-degree partial melting of the mantle wedge; Figure 3.11 and Tables 3.11 & 3.12 give recycled fractions using these values[j]. The variations in residual slab compositions that are produced by changing the normalizing values for the mantle wedge are generally small, and the overall trace element patterns do not change significantly. This suggests that any errors introduced into the results by the assumptions about the composition of the mantle wedge and/or the wedge component are also small.

Aside from the composition of the mantle wedge, the least well constrained input parameter is the rate at which volcanic material (both intrusive and extrusive) is added to the overlying plate. To examine the

[i] Values for each magma series are given in Appendix E.
[j] I chose the values of 5% and 20% partial melting to correspond to the maximum reasonable range in MORB partial melting extents.

Table 3.5 Depleted mantle, depleted wedge, and wedge-derived component for prior wedge depletion. Concentrations in ppm.

	"Depleted Mantle" Composition†	Composition of Depleted Wedge	Composition of Wedge-Derived Component in IAV
K	60	54.61	273.03
Rb	0.088	0.08	0.40
Ba	1.2	1.11	5.53
Th	0.0137	0.01	0.06
U	0.0047	0.00	0.02
Nb	0.21	0.16	0.81
Ta	0.0138	0.01	0.05
La	0.234	0.14	0.69
Ce	0.772	0.44	2.18
Pb	0.0232	0.02	0.09
Sr	9.8	5.88	28.90
Nd	0.713	0.52	2.24
Zr	7.94	6.44	23.34
Hf	0.199	0.15	0.61
Sm	0.27	0.23	0.73
Eu	0.107	0.09	0.27
Y	4.07	3.87	7.10
Yb	0.401	0.38	0.76
Lu	0.063	0.06	0.12

† From Salters and Stracke, 2004

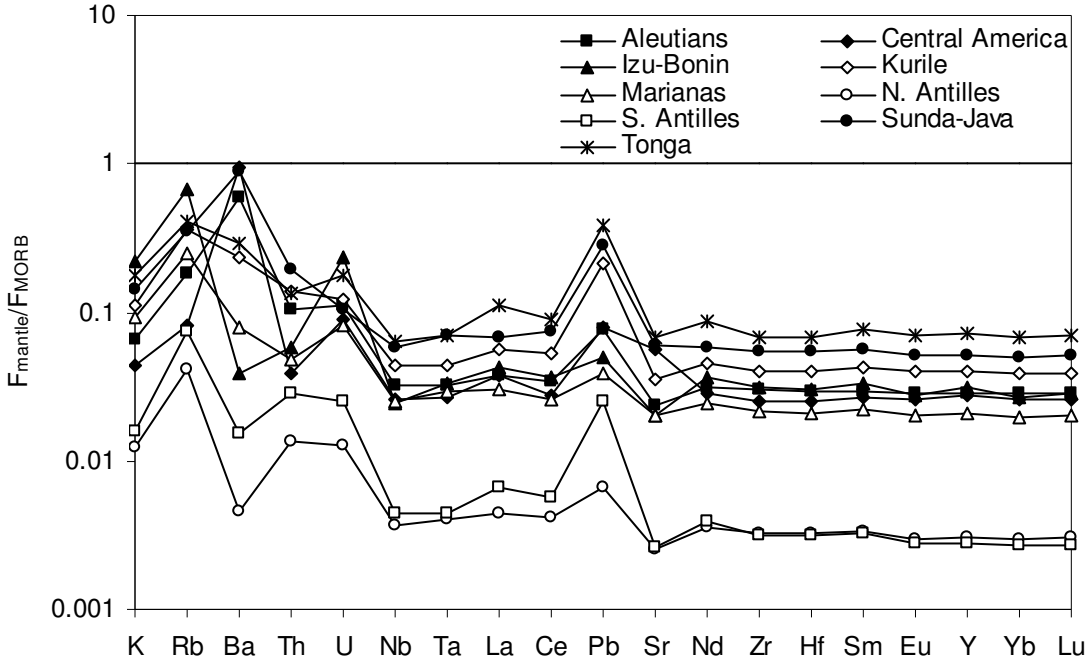

Figure 3.8 Flux of trace elements into the mantle at various subduction zones calculated assuming prior wedge depletion. Fluxes normalized to average normal mid-ocean ridge basalt flux.

Table 3.6 Flux of trace elements into the mantle at various subduction zones assuming prior wedge depletion. Fluxes in kg/yr/km arc length.

	Aleutians	Central America	Izu-Bonin	Kurile	Marianas	Northern Antilles	Southern Antilles	Sunda-Java	Tonga
K	1069058.08	947552.13	6485032.14	2098616.19	2050037.28	967205.08	1238599.50	1491824.21	4117948.04
Rb	2807.96	1659.48	18495.01	6390.44	5185.75	3066.79	5445.09	3427.03	8841.76
Ba	103820.64	215173.76	12035.80	47362.58	18402.32	3807.28	12601.41	98680.45	71256.98
Th	342.29	170.05	344.22	524.67	218.98	214.75	441.60	404.04	628.17
U	145.40	149.67	554.68	179.68	142.82	78.10	156.68	84.34	324.04
Nb	2077.72	2177.30	2861.33	3258.37	2175.89	1116.06	1350.13	2372.85	5757.27
Ta	117.02	126.01	221.11	183.62	142.74	70.09	75.36	161.59	360.62
La	2552.18	3427.14	5247.18	4407.11	2844.31	1434.13	2147.92	2966.64	10656.76
Ce	7175.72	7361.13	13613.65	12497.92	7275.56	4111.62	5541.22	9766.85	25677.44
Pb	642.88	842.74	731.33	2054.68	438.35	257.33	981.38	1477.91	4409.78
Sr	57876.33	185063.31	91770.32	100855.14	68428.61	29896.59	30850.97	92207.96	237640.56
Nd	6285.90	7483.27	13343.19	10427.20	6641.31	3423.44	3711.70	7392.11	24276.50
Zr	60958.09	67870.25	114705.55	92814.81	59711.89	31570.82	30120.34	69843.03	193733.20
Hf	1674.96	1883.66	3106.31	2588.50	1618.90	871.58	836.36	1966.25	5352.54
Sm	2145.79	2567.00	4371.54	3551.90	2211.48	1137.33	1118.97	2545.55	7915.35
Eu	800.15	955.51	1381.84	1275.50	770.01	397.52	374.37	898.58	2800.93
Y	21644.56	27572.06	43176.85	35376.74	21914.50	11279.85	10224.70	25111.30	76975.33
Yb	2355.21	2855.83	4045.31	3746.04	2215.52	1166.74	1062.77	2671.71	8098.44
Lu	351.00	426.38	647.95	565.63	339.91	179.17	161.59	404.14	1227.83

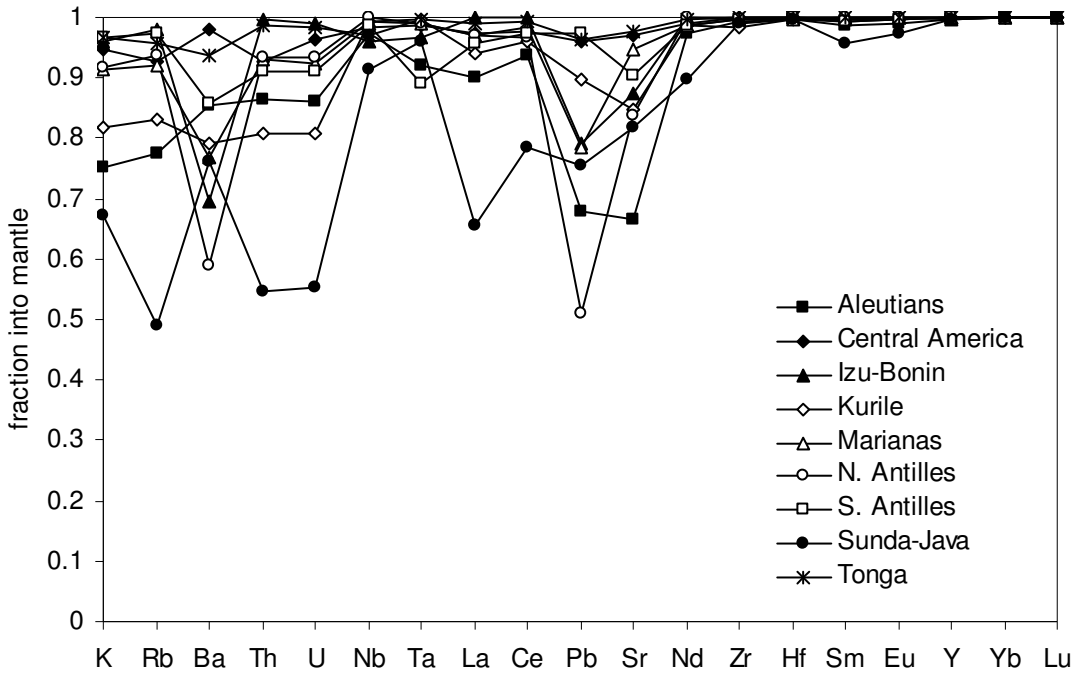

Figure 3.9 Fraction of ingoing slab material incorporated into the mantle at various subduction zones assuming prior wedge depletion.

Table 3.7 Fraction of ingoing slab material incorporated into the mantle assuming prior wedge depletion.

	Aleutians	Central America	Izu-Bonin	Kurile	Marianas	Northern Antilles	Southern Antilles	Sunda-Java	Tonga
K	0.7506	0.9469	0.9619	0.8164	0.9143	0.9164	0.9661	0.6720	0.9657
Rb	0.7759	0.9259	0.9791	0.8298	0.9198	0.9366	0.9737	0.4899	0.9569
Ba	0.8547	0.9814	0.6965	0.7919	0.7676	0.5897	0.8579	0.7620	0.9375
Th	0.8628	0.9262	0.9959	0.8081	0.9305	0.9349	0.9099	0.5447	0.9861
U	0.8609	0.9627	0.9913	0.8078	0.9225	0.9341	0.9096	0.5520	0.9841
Nb	0.9729	0.9833	0.9596	0.9927	0.9948	0.9997	0.9869	0.9142	0.9690
Ta	0.9216	0.9882	0.9665	0.9968	0.9909	0.9888	0.8922	0.9614	0.9951
La	0.9002	0.9726	0.9993	0.9392	0.9694	0.9690	0.9583	0.6573	0.9909
Ce	0.9357	0.9778	0.9999	0.9619	0.9849	0.9683	0.9737	0.7863	0.9922
Pb	0.6796	0.9606	0.7917	0.8978	0.7850	0.5103	0.9733	0.7537	0.9625
Sr	0.6659	0.9702	0.8754	0.8491	0.9484	0.8393	0.9036	0.8192	0.9760
Nd	0.9739	0.9909	0.9995	0.9870	0.9878	0.9991	0.9882	0.8967	0.9980
Zr	0.9935	0.9984	0.9992	0.9824	0.9950	0.9975	0.9983	0.9909	0.9987
Hf	0.9976	0.9986	1.0000	0.9973	0.9955	0.9969	0.9988	0.9966	0.9984
Sm	0.9867	0.9961	0.9994	0.9949	0.9980	0.9999	0.9933	0.9576	0.9989
Eu	0.9909	0.9974	0.9999	0.9980	0.9997	0.9992	0.9976	0.9742	0.9993
Y	0.9952	0.9999	0.9977	0.9993	0.9997	0.9987	0.9994	0.9969	0.9986
Yb	1.0000	1.0000	1.0000	1.0000	1.0000	1.0000	1.0000	1.0000	1.0000
Lu	0.9997	0.9997	1.0000	0.9994	0.9999	1.0000	0.9998	0.9998	0.9997

Table 3.8 Normalizing wedge compositions for 5% and 20% partial melting of the mantle wedge.

	5% Partial Melting	20% Partial Melting
K	906.600	226.650
Rb	0.846	0.212
Ba	9.638	2.410
Th	0.181	0.045
U	0.071	0.018
Nb	3.519	0.880
Ta	0.197	0.050
La	3.539	0.948
Ce	8.794	3.047
Pb	0.452	0.113
Sr	108.001	43.517
Nd	6.705	3.958
Zr	62.900	44.412
Hf	1.799	1.165
Sm	2.180	1.668
Eu	0.831	0.666
Y	21.852	20.094
Yb	2.385	2.147
Lu	0.357	0.319

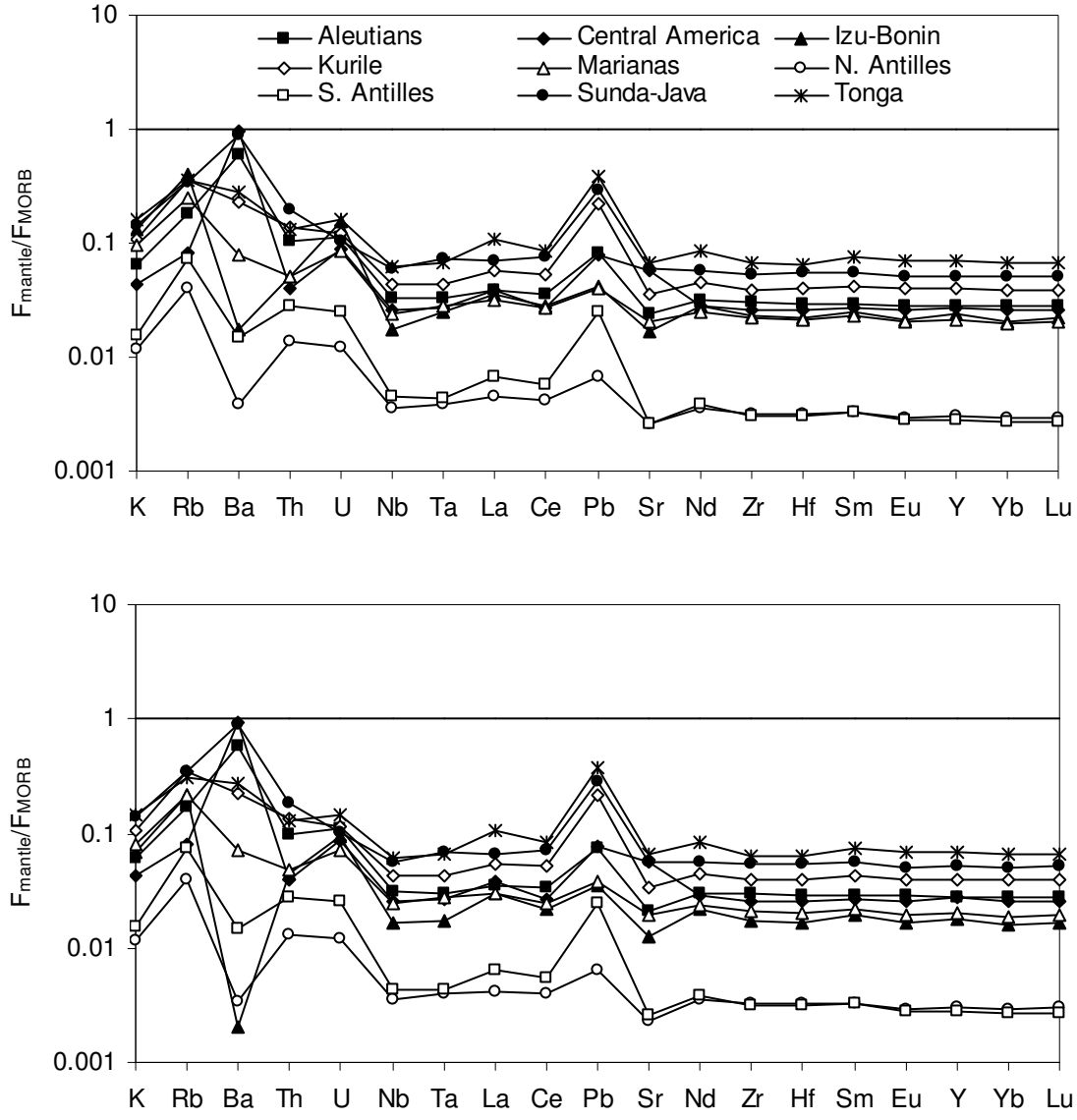

Figure 3.10 Flux of trace elements into the mantle at various subduction zones calculated assuming 5% partial melting (top) and 20% partial melting (bottom) of the IAV source. Fluxes normalized to average normal mid-ocean ridge basalt flux.

Table 3.9 Flux of trace elements into the mantle at various subduction zones assuming 5% partial melting of the IAV source. Fluxes in kg/yr/km arc length.

	Aleutians	Central America	Izu-Bonin	Kurile	Marianas	Northern Antilles	Southern Antilles	Sunda-Java	Tonga
K	1075296.85	948294.59	3961811.18	2059241.68	2129477.75	912302.93	1217206.44	1478701.12	3701878.36
Rb	2751.68	1652.76	11308.32	6212.69	5305.33	2879.41	5370.15	3331.56	7601.62
Ba	102749.46	215044.95	5543.16	46324.47	18228.69	3218.83	12342.85	97820.84	69384.37
Th	343.26	170.16	300.14	524.85	225.16	214.16	441.43	404.58	621.38
U	146.98	149.85	364.65	177.78	149.36	74.41	155.31	84.27	293.32
Nb	2074.30	2186.91	2052.47	3224.64	2099.53	1084.72	1350.47	2421.63	5642.09
Ta	120.55	126.24	164.53	182.23	137.44	66.19	75.33	163.69	347.47
La	2675.13	3445.02	4419.45	4498.76	2930.50	1450.12	2165.43	3087.94	10560.67
Ce	7333.60	7384.95	10505.51	12582.15	7404.40	4096.55	5543.50	9914.83	25221.89
Pb	667.75	845.43	634.85	2074.40	453.76	266.49	984.96	1496.52	4414.52
Sr	59942.79	185324.02	75151.25	102266.99	68957.34	30300.45	31032.14	93582.42	235954.01
Nd	6264.59	7479.71	10261.25	10361.43	6719.08	3350.58	3680.41	7344.44	23759.71
Zr	60833.58	67807.75	84583.28	91984.21	60296.73	30960.49	29849.07	69348.10	188926.74
Hf	1672.44	1882.97	2286.65	2574.95	1635.52	854.51	829.24	1957.62	5220.24
Sm	2139.55	2565.96	3319.70	3528.72	2226.41	1112.94	1108.33	2530.57	7739.32
Eu	799.23	955.35	1076.17	1269.52	774.50	390.40	371.53	895.33	2749.67
Y	21648.91	27571.47	32700.87	35194.58	22071.36	11037.73	10130.07	25026.50	75220.89
Yb	2355.21	2855.83	3121.55	3729.55	2229.21	1145.71	1054.53	2665.08	7944.73
Lu	350.70	426.42	490.57	563.12	342.24	175.54	160.21	402.99	1201.96

Table 3.10 Flux of trace elements into the mantle at various subduction zones assuming 20% partial melting of the IAV source. Fluxes in kg/yr/km arc length.

	Aleutians	Central America	Izu-Bonin	Kurile	Marianas	Northern Antilles	Southern Antilles	Sunda-Java	Tonga
K	988781.57	938048.51	2052331.60	2010753.62	1808595.70	902352.70	1212004.10	1450115.71	3326117.20
Rb	2665.89	1642.60	6016.44	6220.90	4479.37	2919.82	5385.12	3376.69	6660.79
Ba	101753.91	214926.76	635.34	45516.98	17056.26	2839.51	12170.74	97159.48	67747.62
Th	326.59	168.26	260.52	509.39	212.32	207.27	437.95	391.32	603.27
U	140.32	149.07	220.98	173.84	125.20	73.65	154.76	81.90	265.19
Nb	1985.09	2157.18	1927.71	3190.91	2119.16	1080.89	1322.59	2257.32	5498.00
Ta	107.75	125.11	111.56	179.28	137.85	69.54	73.43	155.26	341.42
La	2424.12	3410.51	3795.86	4290.01	2756.63	1375.79	2118.35	2861.41	10332.65
Ce	6815.85	7312.70	8170.88	12161.10	6900.02	3930.04	5456.97	9462.64	24545.64
Pb	623.09	840.52	521.76	2036.59	418.24	246.76	977.04	1463.71	4357.87
Sr	52484.98	184399.28	57248.44	96139.85	63834.59	27441.68	29809.58	88397.77	228392.35
Nd	6080.67	7452.18	7972.44	10280.35	6310.78	3339.92	3659.94	7201.18	23303.04
Zr	60349.46	67698.91	62322.88	91715.37	57096.12	31217.20	29912.06	69253.60	185181.82
Hf	1651.43	1879.20	1676.78	2577.13	1546.65	863.09	831.01	1951.67	5122.61
Sm	2119.64	2562.87	2548.81	3526.27	2104.91	1121.37	1109.09	2525.31	7606.10
Eu	794.66	954.61	852.16	1270.25	740.46	392.75	372.27	895.14	2710.50
Y	21643.92	27572.12	25049.59	35312.98	20927.81	11157.63	10178.70	25199.57	73978.79
Yb	2355.21	2855.83	2445.21	3740.47	2128.56	1155.91	1058.70	2679.40	7833.81
Lu	350.66	426.43	375.40	564.99	325.09	177.27	160.91	405.41	1183.09

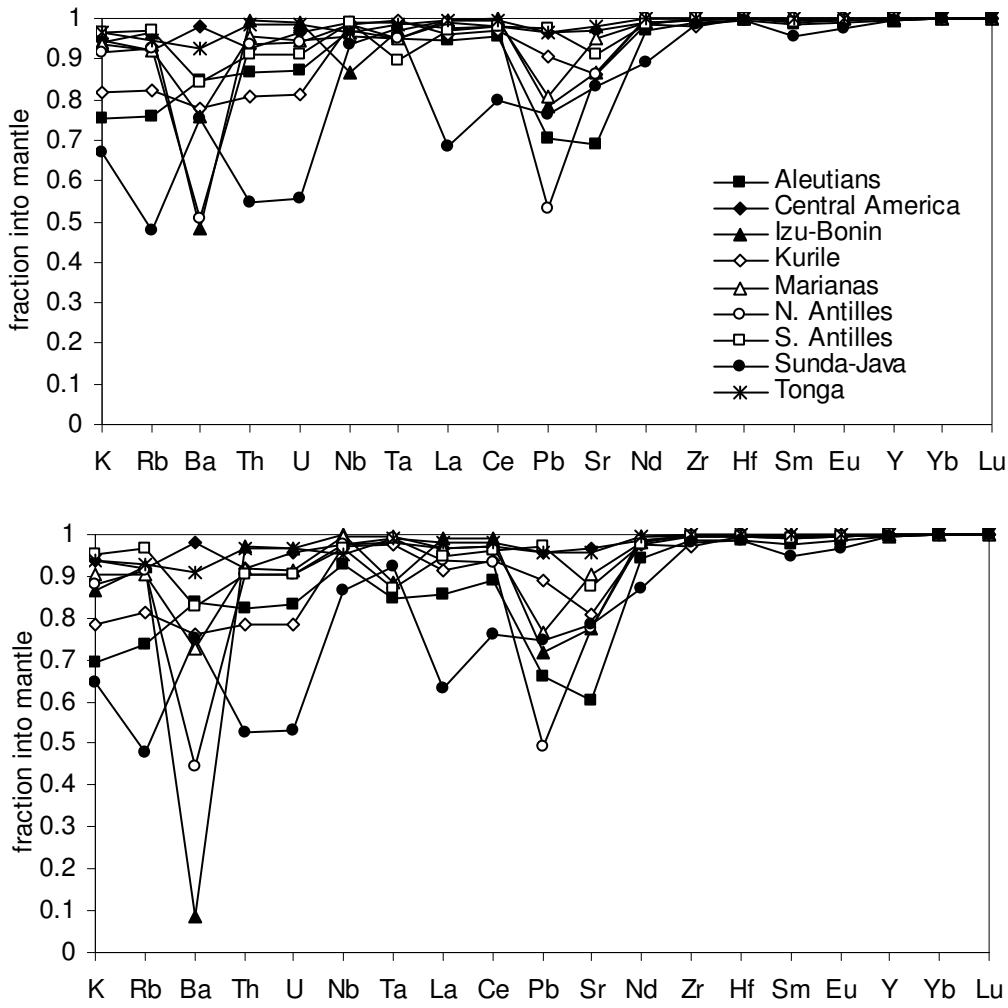

Figure 3.11 Fraction of ingoing slab material incorporated into the mantle at various subduction zones assuming 5% partial melting (top) and 20% partial melting (bottom) of the IAV source.

Table 3.11 Fraction of ingoing slab material incorporated into the mantle assuming 5% partial melting of the IAV source.

	Aleutians	Central America	Izu-Bonin	Kurile	Marianas	Northern Antilles	Southern Antilles	Sunda-Java	Tonga
K	0.7550	0.9477	0.9400	0.8154	0.9341	0.9143	0.9664	0.6716	0.9632
Rb	0.7604	0.9222	0.9632	0.8203	0.9236	0.9254	0.9713	0.4798	0.9443
Ba	0.8459	0.9808	0.4831	0.7759	0.7576	0.5090	0.8432	0.7556	0.9246
Th	0.8652	0.9268	0.9962	0.8093	0.9541	0.9365	0.9103	0.5457	0.9869
U	0.8702	0.9639	0.9891	0.8117	0.9474	0.9387	0.9107	0.5565	0.9859
Nb	0.9713	0.9877	0.8648	0.9857	0.9559	0.9839	0.9910	0.9345	0.9661
Ta	0.9494	0.9900	0.9712	0.9950	0.9484	0.9521	0.8975	0.9765	0.9857
La	0.9435	0.9777	0.9961	0.9617	0.9947	0.9922	0.9692	0.6850	0.9945
Ce	0.9562	0.9810	0.9980	0.9725	0.9962	0.9810	0.9788	0.7996	0.9943
Pb	0.7059	0.9637	0.7833	0.9072	0.8101	0.5312	0.9778	0.7636	0.9675
Sr	0.6897	0.9716	0.8647	0.8633	0.9522	0.8605	0.9132	0.8323	0.9811
Nd	0.9706	0.9905	0.9996	0.9859	0.9926	0.9983	0.9871	0.8934	0.9978
Zr	0.9915	0.9974	0.9999	0.9792	0.9973	0.9999	0.9982	0.9869	0.9998
Hf	0.9961	0.9982	0.9998	0.9977	0.9983	0.9987	0.9990	0.9952	0.9992
Sm	0.9838	0.9957	0.9997	0.9937	0.9977	0.9996	0.9922	0.9547	0.9988
Eu	0.9898	0.9973	0.9999	0.9975	0.9996	0.9988	0.9972	0.9729	0.9991
Y	0.9954	0.9999	0.9967	0.9994	0.9998	0.9983	0.9993	0.9965	0.9984
Yb	1.0000	1.0000	1.0000	1.0000	1.0000	1.0000	1.0000	1.0000	1.0000
Lu	0.9988	0.9998	0.9998	0.9999	0.9999	0.9997	0.9999	0.9997	1.0000

Table 3.12 Fraction of ingoing slab material incorporated into the mantle assuming 20% partial melting of the IAV source.

	Aleutians	Central America	Izu-Bonin	Kurile	Marianas	Northern Antilles	Southern Antilles	Sunda-Java	Tonga
K	0.6943	0.9374	0.8681	0.7869	0.9023	0.8797	0.9536	0.6471	0.9396
Rb	0.7367	0.9165	0.9248	0.8124	0.9022	0.9151	0.9684	0.4786	0.9262
Ba	0.8377	0.9803	0.0879	0.7615	0.7280	0.4445	0.8300	0.7500	0.9112
Th	0.8232	0.9165	0.9691	0.7849	0.9185	0.9044	0.9028	0.5273	0.9663
U	0.8308	0.9589	0.9655	0.7856	0.9148	0.9051	0.9029	0.5305	0.9658
Nb	0.9295	0.9743	0.9999	0.9733	0.9949	0.9745	0.9686	0.8680	0.9533
Ta	0.8486	0.9811	0.8859	0.9752	0.9956	0.9908	0.8721	0.9211	0.9885
La	0.8550	0.9679	0.9883	0.9152	0.9647	0.9356	0.9466	0.6330	0.9820
Ce	0.8887	0.9714	0.9884	0.9373	0.9724	0.9335	0.9612	0.7602	0.9820
Pb	0.6587	0.9581	0.7172	0.8901	0.7635	0.4907	0.9695	0.7461	0.9579
Sr	0.6039	0.9667	0.7758	0.8102	0.9059	0.7750	0.8752	0.7843	0.9582
Nd	0.9421	0.9868	0.9956	0.9748	0.9810	0.9852	0.9780	0.8709	0.9941
Zr	0.9836	0.9958	0.9975	0.9726	0.9988	0.9975	0.9958	0.9790	0.9992
Hf	0.9836	0.9962	0.9937	0.9948	0.9984	0.9981	0.9967	0.9858	0.9993
Sm	0.9747	0.9945	0.9997	0.9895	0.9944	0.9967	0.9886	0.9469	0.9979
Eu	0.9841	0.9965	0.9998	0.9953	0.9987	0.9962	0.9955	0.9678	0.9982
Y	0.9952	0.9999	0.9962	0.9993	0.9996	0.9987	0.9994	0.9970	0.9986
Yb	1.0000	1.0000	1.0000	1.0000	1.0000	1.0000	1.0000	1.0000	1.0000
Lu	0.9987	0.9998	0.9996	0.9999	0.9999	0.9997	0.9999	0.9997	1.0000

sensitivity of the model to errors in this parameter, I calculated residual slab compositions using three values for the crustal addition rate at each arc: the value from published sources (Table 1.1 and 1.8); one-half the published value; and twice the published value. Figure 3.12 and Tables 3.13 & 3.14 show the average residual slab fluxes calculated using the high and low crustal addition rates, and recycled fractions are given in Figure 3.13 and Tables 3.15 & 3.16. Variations in crustal addition rate have a significantly larger impact on calculated residual slab compositions than do variations in mantle wedge composition. Doubling the crustal accretion rate lowers the residual slab flux of all elements at all of the arcs, and produces negative fluxes in several elements (e.g. Ba, Pb). As with variations in mantle wedge composition, however, changes in crustal addition rate do not significantly affect overall trace element patterns for residual slab materials.

Using combinations of variable values for mantle wedge composition and crustal addition rate, I calculated the maximum and minimum residual slab values for five trace element ratios at each arc: Pb/Ce, Th/U, U/Pb, Rb/Sr, and Sm/Nd[k]. Figures 3.14 and 3.15 show the maximum and minimum values for Pb/Ce and Th/U ratios, respectively, as error bars around the central values[l]; these values are also given in Tables 3.17 and 3.18. Despite fairly large error bars in some of the arcs, the overall conclusions regarding the influence of subduction zone processing on slab Pb/Ce and Th/U ratios

[k] Although I only give the maximum and minimum values for these ratios here, a complete list of residual slab characteristics for each variation is given in Appendix E.
[l] The central values are the same as those in Figures 3.3 and 3.4.

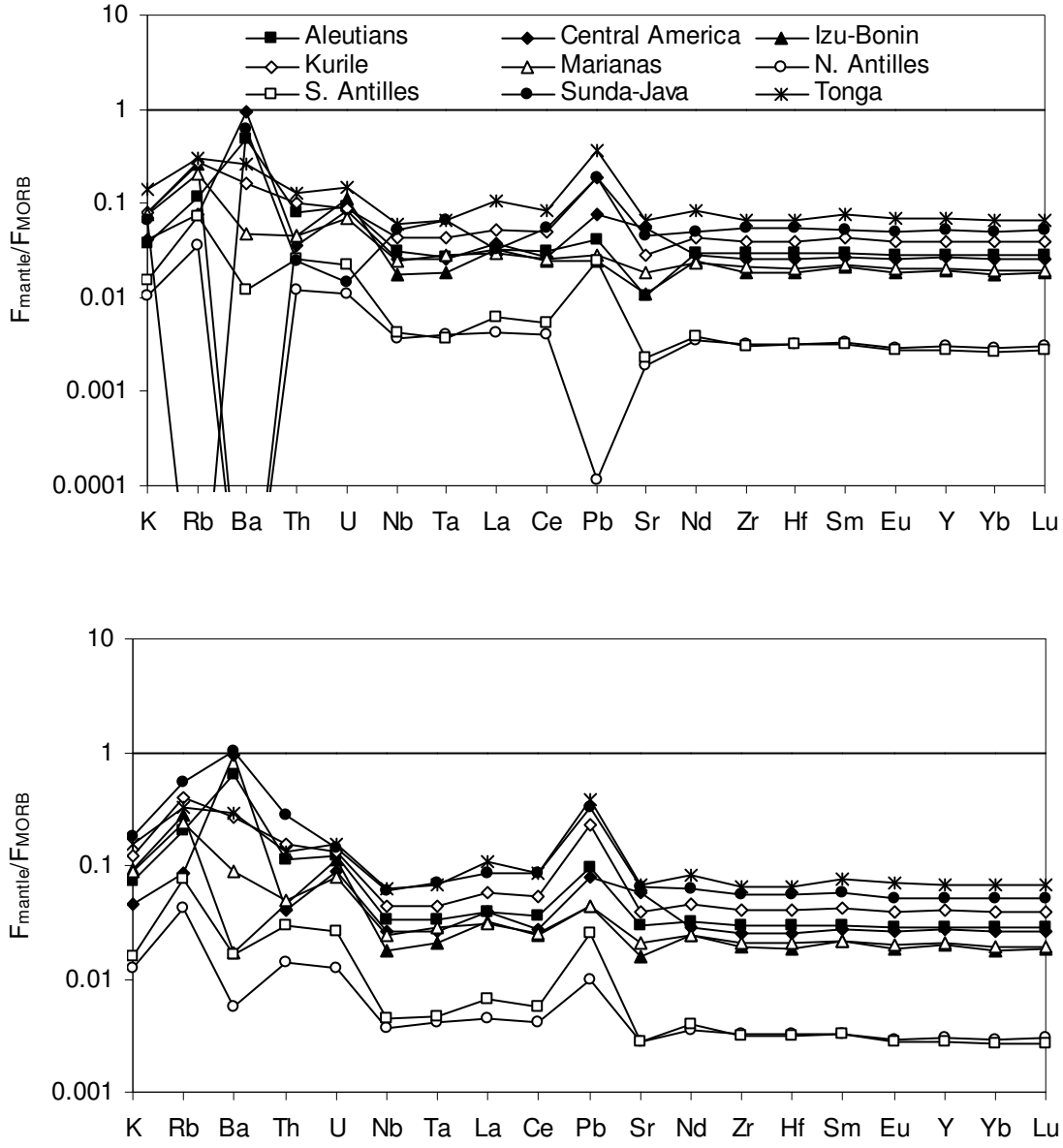

Figure 3.12 Flux of trace elements into the mantle at various subduction zones calculated assuming doubled crustal addition rate (top) and halved crustal addition rate (bottom). Fluxes normalized to average normal mid-ocean ridge basalt flux**.**

Table 3.13 Flux of trace elements into the mantle at various subduction zones assuming doubled crustal addition rate. Fluxes in kg/yr/km arc length.

	Aleutians	Central America	Izu-Bonin	Kurile	Marianas	Northern Antilles	Southern Antilles	Sunda-Java	Tonga
K	613112.96	882508.23	2336952.74	1510221.43	1716746.72	797604.37	1161141.75	692451.53	3235435.66
Rb	1770.79	1499.79	7138.50	4808.39	4228.75	2652.52	5210.66	-294.03	6381.66
Ba	82709.44	210684.60	-4233.15	31826.39	11214.30	-427.13	9803.41	65245.27	61956.00
Th	268.12	154.27	268.16	380.46	200.72	190.48	393.21	49.71	593.62
U	116.38	143.22	257.94	129.90	121.40	67.37	138.81	12.06	265.07
Nb	1964.78	2123.43	1991.64	3200.51	2141.72	1097.98	1310.56	2052.37	5370.06
Ta	99.15	123.79	117.78	180.12	138.92	69.98	64.55	149.51	343.96
La	2223.35	3324.34	4004.41	4073.86	2769.82	1360.04	2040.32	1380.09	10320.80
Ce	6497.54	7168.09	8923.82	11809.64	7005.32	3860.46	5337.46	6940.95	24570.74
Pb	330.73	807.19	361.53	1811.69	308.20	4.49	952.06	988.45	4199.70
Sr	25808.83	178999.57	49672.83	80189.15	61224.68	22676.50	26934.25	69692.98	225042.95
Nd	5940.81	7386.52	8671.97	10160.96	6373.28	3344.04	3617.39	6350.75	23377.12
Zr	60034.38	67560.27	69060.94	89869.36	57838.00	31186.13	29853.09	68375.36	186111.12
Hf	1653.67	1877.06	1861.74	2574.16	1570.21	862.05	830.47	1945.05	5146.30
Sm	2091.17	2552.66	2780.58	3505.16	2132.28	1119.17	1100.15	2406.55	7629.05
Eu	788.01	952.23	919.60	1267.07	749.26	391.75	371.04	870.30	2717.38
Y	21546.77	27568.91	27239.61	35255.46	21221.27	11104.12	10155.55	25055.75	74138.18
Yb	2355.21	2855.83	2648.37	3736.99	2154.80	1152.97	1057.35	2674.71	7858.95
Lu	350.26	426.35	409.88	564.33	329.53	176.73	160.67	404.51	1187.30

Table 3.14 Flux of trace elements into the mantle at various subduction zones assuming halved crustal addition rate. Fluxes in kg/yr/km arc length.

	Aleutians	Central America	Izu-Bonin	Kurile	Marianas	Northern Antilles	Southern Antilles	Sunda-Java	Tonga
K	1221438.54	971110.10	2774258.42	2286970.32	1986310.97	962690.66	1240727.79	1844156.57	3515444.70
Rb	3156.84	1719.13	7843.11	6925.27	4933.21	3039.02	5465.49	5190.50	7134.93
Ba	111776.14	217106.96	5317.76	52770.61	20498.15	4670.78	13442.23	113448.35	71367.27
Th	364.59	176.26	275.97	581.75	224.49	219.40	462.10	568.81	617.54
U	155.76	152.40	267.63	197.90	137.06	77.42	163.05	118.07	276.10
Nb	2092.86	2191.49	2044.25	3257.34	2145.97	1104.96	1351.04	2461.32	5680.30
Ta	120.02	126.59	133.68	182.75	139.84	69.99	79.22	163.57	346.23
La	2682.22	3473.91	4016.06	4531.80	2852.96	1440.94	2187.60	3732.12	10488.00
Ce	7376.24	7438.10	8940.08	12674.25	7139.28	4115.18	5589.14	11058.90	24952.45
Pb	792.15	859.77	654.70	2168.54	490.29	378.02	993.74	1717.95	4464.15
Sr	71633.99	187811.53	70716.66	108998.10	68535.39	32184.24	32260.25	101888.81	235384.28
Nd	6325.92	7510.43	8682.29	10440.91	6483.94	3371.30	3707.68	7777.62	23488.27
Zr	61026.83	67876.05	69105.85	93105.22	57977.53	31196.49	29958.57	70031.83	186142.66
Hf	1672.67	1884.01	1866.14	2584.24	1571.83	862.09	832.02	1967.98	5147.99
Sm	2153.85	2571.02	2781.03	3546.00	2143.15	1121.06	1115.26	2597.86	7645.31
Eu	802.62	956.54	919.61	1273.10	749.92	392.89	372.88	910.14	2722.16
Y	21697.78	27573.10	27395.84	35288.10	21230.40	11130.13	10165.98	25180.93	74311.87
Yb	2355.21	2855.83	2648.37	3736.99	2154.80	1152.97	1057.35	2674.71	7858.95
Lu	350.91	426.46	410.06	564.42	329.58	176.80	160.69	404.68	1187.39

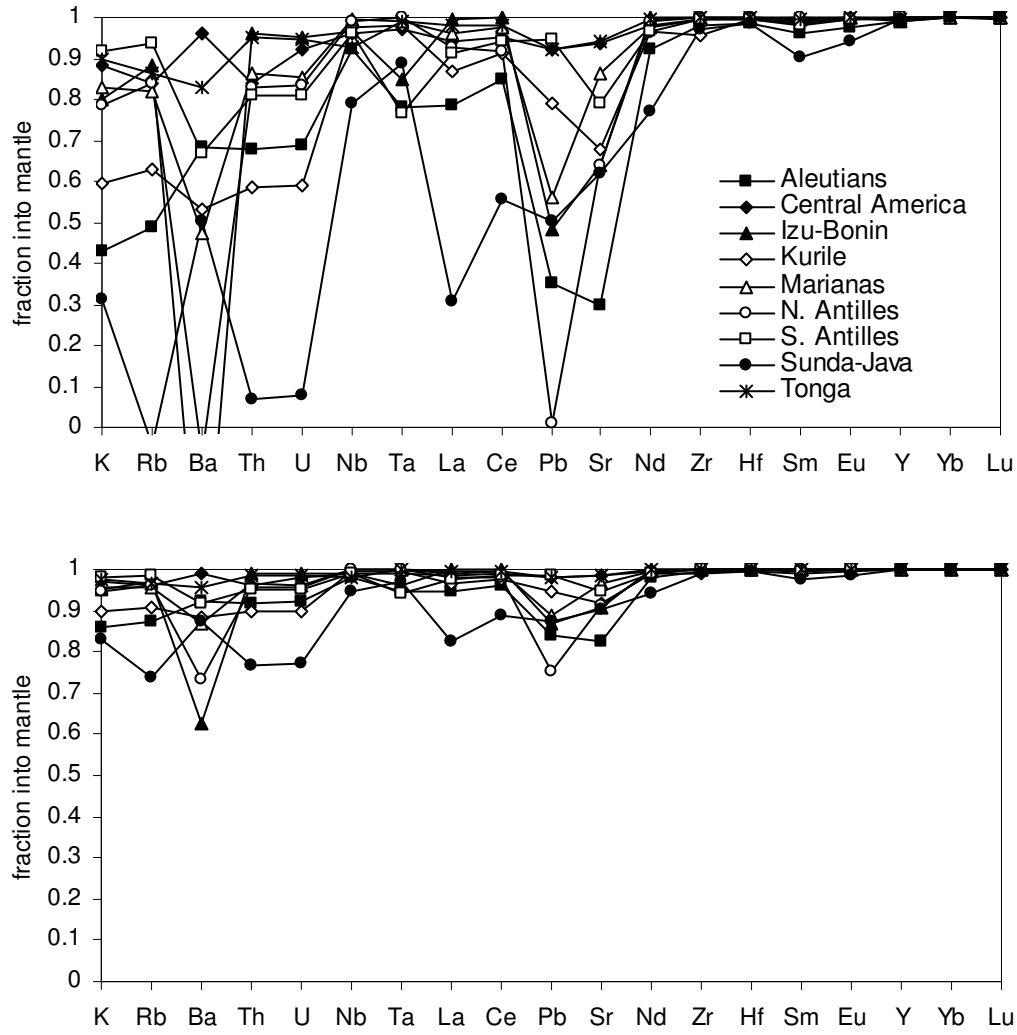

Figure 3.13 Fraction of ingoing slab material incorporated into the mantle at various subduction zones assuming doubled (top) and halved (bottom) crustal addition rates.

Table 3.15 Fraction of ingoing slab material incorporated into the mantle assuming doubled crustal addition rates.

	Aleutians	Central America	Izu-Bonin	Kurile	Marianas	Northern Antilles	Southern Antilles	Sunda-Java	Tonga
K	0.4305	0.8819	0.8003	0.5932	0.8269	0.7837	0.9163	0.3108	0.8965
Rb	0.4893	0.8368	0.8837	0.6301	0.8183	0.8373	0.9388	-0.0419	0.8640
Ba	0.6809	0.9609	-0.4979	0.5326	0.4753	-0.0671	0.6689	0.5038	0.8316
Th	0.6758	0.8403	0.9626	0.5864	0.8636	0.8316	0.8106	0.0670	0.9490
U	0.6890	0.9212	0.9523	0.5889	0.8532	0.8341	0.8112	0.0786	0.9474
Nb	0.9200	0.9590	0.9660	0.9769	0.9974	0.9916	0.9604	0.7901	0.9285
Ta	0.7808	0.9708	0.8474	0.9809	0.9913	0.9997	0.7674	0.8886	0.9913
La	0.7842	0.9434	0.9961	0.8697	0.9615	0.9265	0.9122	0.3056	0.9789
Ce	0.8472	0.9522	0.9976	0.9111	0.9751	0.9191	0.9408	0.5583	0.9797
Pb	0.3496	0.9201	0.4805	0.7920	0.5594	0.0089	0.9448	0.5040	0.9225
Sr	0.2970	0.9384	0.6390	0.6761	0.8627	0.6414	0.7914	0.6188	0.9423
Nd	0.9204	0.9781	0.9984	0.9646	0.9774	0.9892	0.9678	0.7695	0.9937
Zr	0.9784	0.9938	0.9991	0.9542	0.9968	0.9996	0.9953	0.9687	0.9998
Hf	0.9849	0.9951	0.9969	0.9948	0.9986	0.9999	0.9975	0.9845	0.9996
Sm	0.9616	0.9905	0.9998	0.9847	0.9932	0.9977	0.9820	0.9042	0.9972
Eu	0.9759	0.9940	1.0000	0.9937	0.9988	0.9961	0.9934	0.9425	0.9977
Y	0.9907	0.9998	0.9924	0.9988	0.9994	0.9969	0.9986	0.9934	0.9969
Yb	1.0000	1.0000	1.0000	1.0000	1.0000	1.0000	1.0000	1.0000	1.0000
Lu	0.9975	0.9996	0.9994	0.9998	0.9998	0.9994	0.9998	0.9994	0.9999

Table 3.16 Fraction of ingoing slab material incorporated into the mantle assuming halved crustal addition rates.

	Aleutians	Central America	Izu-Bonin	Kurile	Marianas	Northern Antilles	Southern Antilles	Sunda-Java	Tonga
K	0.8576	0.9705	0.9501	0.8983	0.9567	0.9459	0.9791	0.8277	0.9741
Rb	0.8723	0.9592	0.9709	0.9075	0.9546	0.9593	0.9847	0.7395	0.9660
Ba	0.9202	0.9902	0.6255	0.8832	0.8688	0.7332	0.9172	0.8759	0.9579
Th	0.9190	0.9601	0.9906	0.8966	0.9659	0.9579	0.9527	0.7668	0.9873
U	0.9223	0.9803	0.9881	0.8972	0.9633	0.9585	0.9528	0.7697	0.9869
Nb	0.9800	0.9898	0.9915	0.9942	0.9993	0.9979	0.9901	0.9475	0.9821
Ta	0.9452	0.9927	0.9619	0.9952	0.9978	0.9999	0.9419	0.9721	0.9978
La	0.9460	0.9859	0.9990	0.9674	0.9904	0.9816	0.9781	0.8264	0.9947
Ce	0.9618	0.9880	0.9994	0.9778	0.9938	0.9798	0.9852	0.8896	0.9949
Pb	0.8374	0.9800	0.8701	0.9480	0.8898	0.7522	0.9862	0.8760	0.9806
Sr	0.8242	0.9846	0.9098	0.9190	0.9657	0.9104	0.9478	0.9047	0.9856
Nd	0.9801	0.9945	0.9996	0.9911	0.9943	0.9973	0.9919	0.9424	0.9984
Zr	0.9946	0.9985	0.9998	0.9885	0.9992	0.9999	0.9988	0.9922	0.9999
Hf	0.9962	0.9988	0.9992	0.9987	0.9997	1.0000	0.9994	0.9961	0.9999
Sm	0.9904	0.9976	0.9999	0.9962	0.9983	0.9994	0.9955	0.9760	0.9993
Eu	0.9940	0.9985	1.0000	0.9984	0.9997	0.9990	0.9984	0.9856	0.9994
Y	0.9977	0.9999	0.9981	0.9997	0.9999	0.9992	0.9997	0.9983	0.9992
Yb	1.0000	1.0000	1.0000	1.0000	1.0000	1.0000	1.0000	1.0000	1.0000
Lu	0.9994	0.9999	0.9999	1.0000	0.9999	0.9999	0.9999	0.9999	1.0000

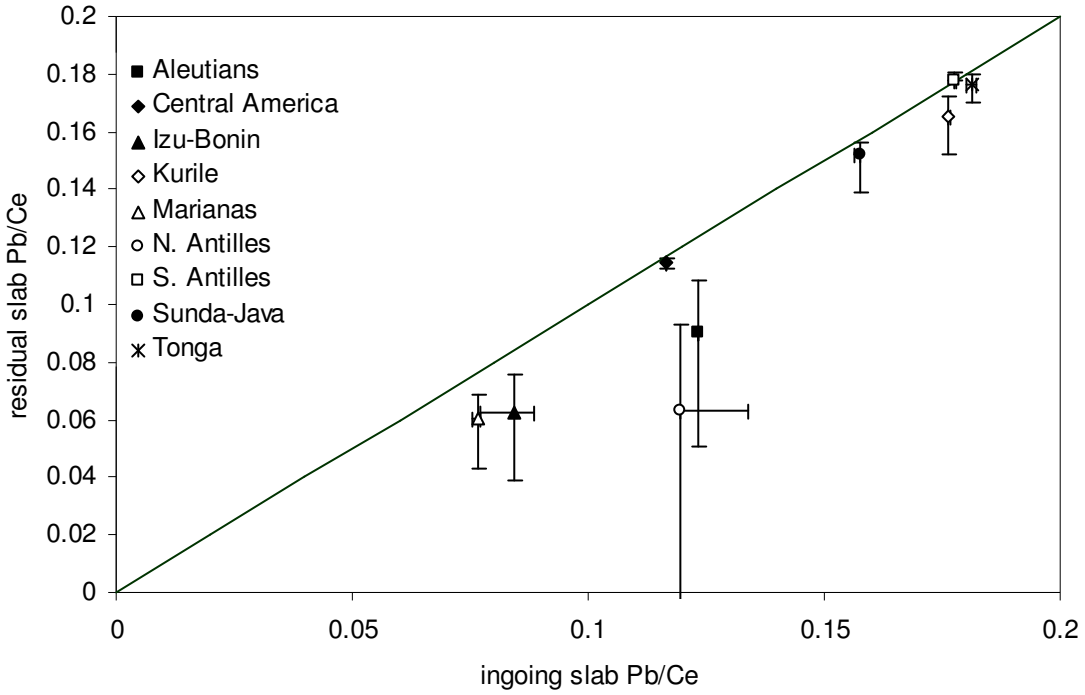

Figure 3.14 Ingoing and residual slab Pb/Ce ratios with error bars for arcs in this study.

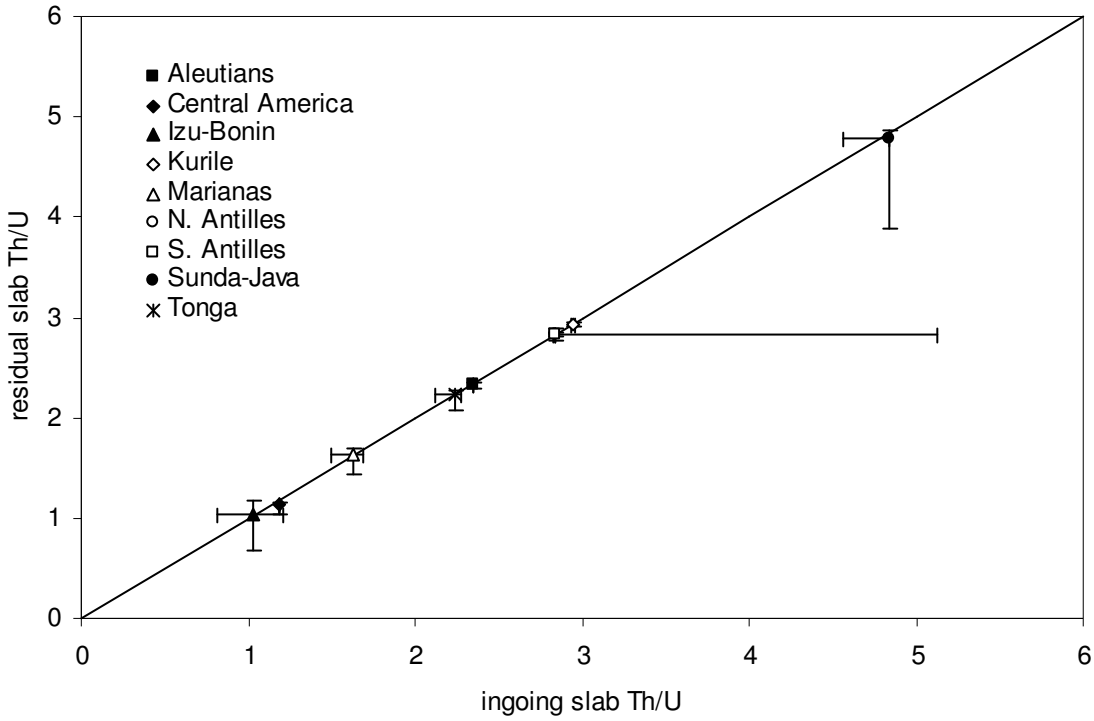

Figure 3.15 Ingoing and residual slab Th/U ratios with error bars for arcs in this study.

Table 3.17 Maximum calculated residual slab ratios and isotopic characteristics.

	Aleutians	Central America	Izu-Bonin	Kurile	Marianas	Northern Antilles	Southern Antilles	Sunda-Java	Tonga
Pb/Ce	0.11	0.12	0.08	0.17	0.07	0.09	0.18	0.16	0.18
Th/U	2.34	1.16	1.18	2.96	1.70	2.88	2.84	4.86	2.28
U/Pb	0.37	0.18	0.79	0.09	0.41	15.02	0.16	0.07	0.07
Rb/Sr	0.09	0.01	0.17	0.06	0.08	0.14	0.20	0.05	0.03
Sm/Nd	0.36	0.35	0.32	0.35	0.34	0.34	0.31	0.39	0.33
$^{206}Pb/^{204}Pb$	19.80	19.36	31.44	17.65	23.90	23.92	19.10	17.20	17.24
$^{87}Sr/^{86}Sr$	0.7056	0.7029	0.7160	0.7071	0.7085	0.7124	0.7179	0.7064	0.7041
ε_{Nd}	13.8	6.7	3.6	7.3	5.6	6.8	1.0	12.4	5.8

Table 3.18 Minimum calculated residual slab ratios and isotopic characteristics.

	Aleutians	Central America	Izu-Bonin	Kurile	Marianas	Northern Antilles	Southern Antilles	Sunda-Java	Tonga
Pb/Ce	0.05	0.11	0.04	0.15	0.04	0.00	0.18	0.14	0.17
Th/U	2.29	1.07	0.82	2.93	1.50	2.81	2.83	3.96	2.12
U/Pb	0.20	0.18	0.36	0.07	0.27	-7.03	0.15	0.01	0.06
Rb/Sr	0.04	0.01	0.10	0.06	0.07	0.09	0.17	0.00	0.03
Sm/Nd	0.34	0.34	0.32	0.34	0.33	0.33	0.30	0.33	0.33
$^{206}Pb/^{204}Pb$	19.38	19.35	22.99	17.24	21.22		18.72	16.02	17.09
$^{87}Sr/^{86}Sr$	0.7029	0.7029	0.7100	0.7064	0.7078	0.7090	0.7151	0.7021	0.7037
ε_{Nd}	6.72	6.1	2.6	6.1	4.6	5.7	0.2	4.6	5.5

remain unchanged. Residual slab Pb/Ce is generally too high to completely explain the Pb/Ce paradox, and slab Th/U ratios are not significantly altered within the subduction zone. The isotopic compositions of ancient residual slabs (Figures 3.16 and 3.17 and Tables 3.17 and 3.18) are slightly more affected by these variations, but are still not consistent with the HIMU and EMII reservoirs.

In calculating the isotopic compositions of residual slab material subducted at 1.8 Ga, I used a continental crust composition as a proxy for the composition of 1.8 Ga subducted sediment. Since sediment often has very high concentrations of trace elements, its presence or absence in a subducting slab can have profound implications for residual slab compositions. My use of 1.8 Ga continental crust in the estimates of residual slab isotopic composition might, therefore, significantly change the calculated residual slab compositions. I therefore repeated the isotopic computations using a residual slab with no sedimentary component to examine the effects of removing the sediment composition. The resulting residual slab characteristics are shown in Figures 3.18 and 3.19 and listed in Table 3.19. As is apparent from these data, removal of the sediment component has little to no effect on the ultimate isotopic characteristics of the subducted slab.

I also examined the effects of varying the age of the subducted slab. My original calculations assumed a subduction age of 1.8 Ga based on Pb isotope modeling of mantle reservoir ages, but I recalculated the isotopic compositions using subduction ages ranging from 200 Ma to 1.8 Ga. Figures 3.20 and 3.21 show the changes in isotopic characteristics with varying subduction ages. Although the differing subduction ages caused significant

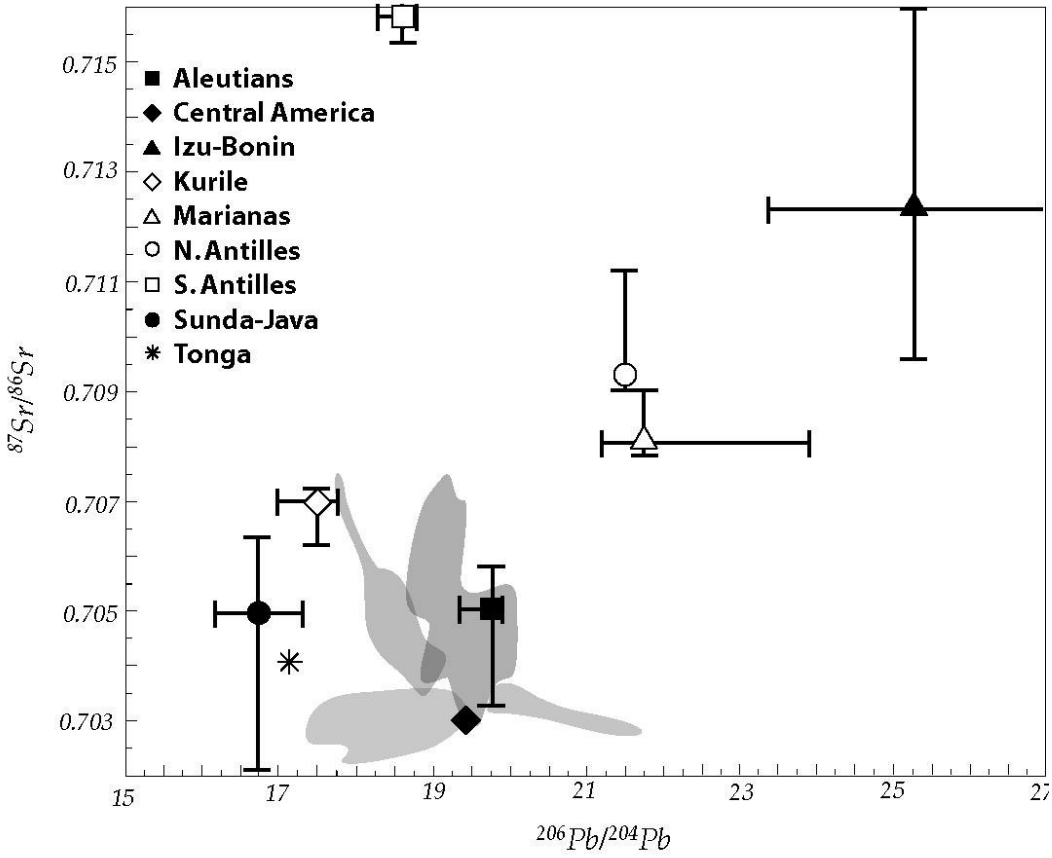

Figure 3.16 Residual slab Sr and Pb isotopic compositions with error bars for 1.8 Ga subducted slabs.

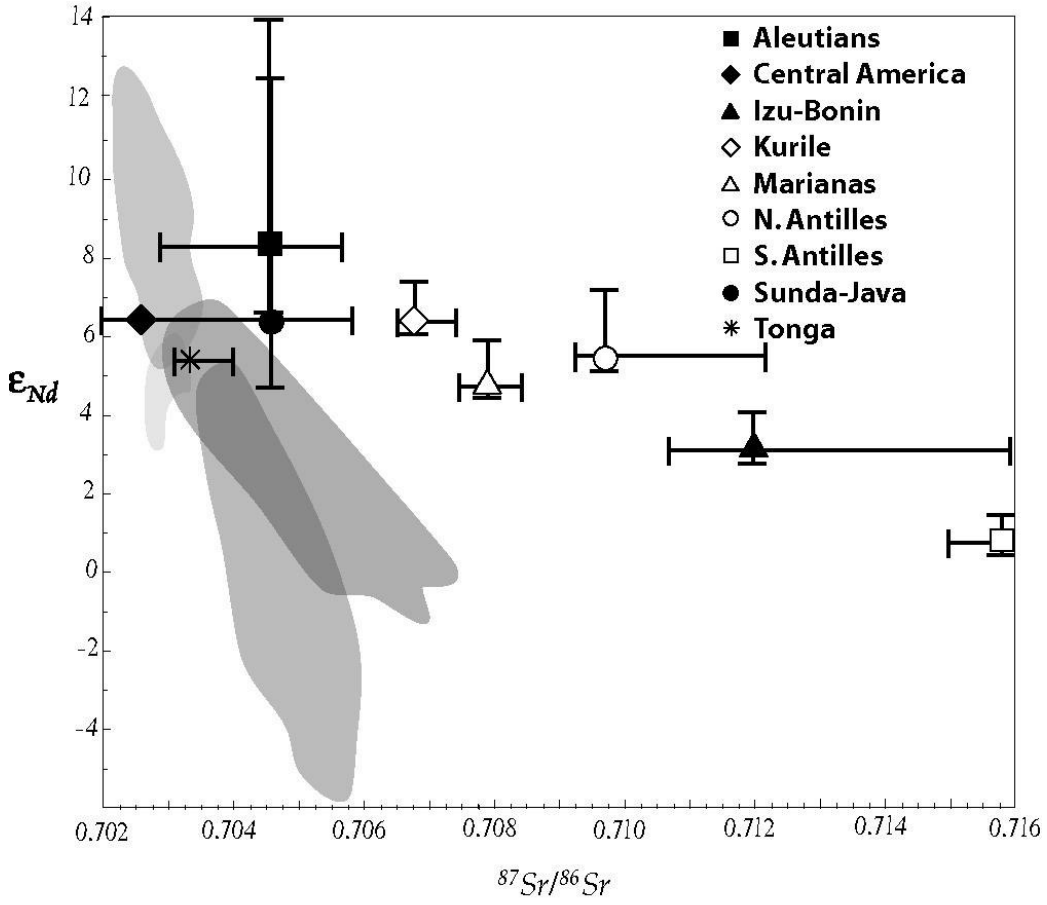

Figure 3.17 Residual slab Nd and Sr isotopic compositions with error bars for 1.8 Ga subducted slabs.

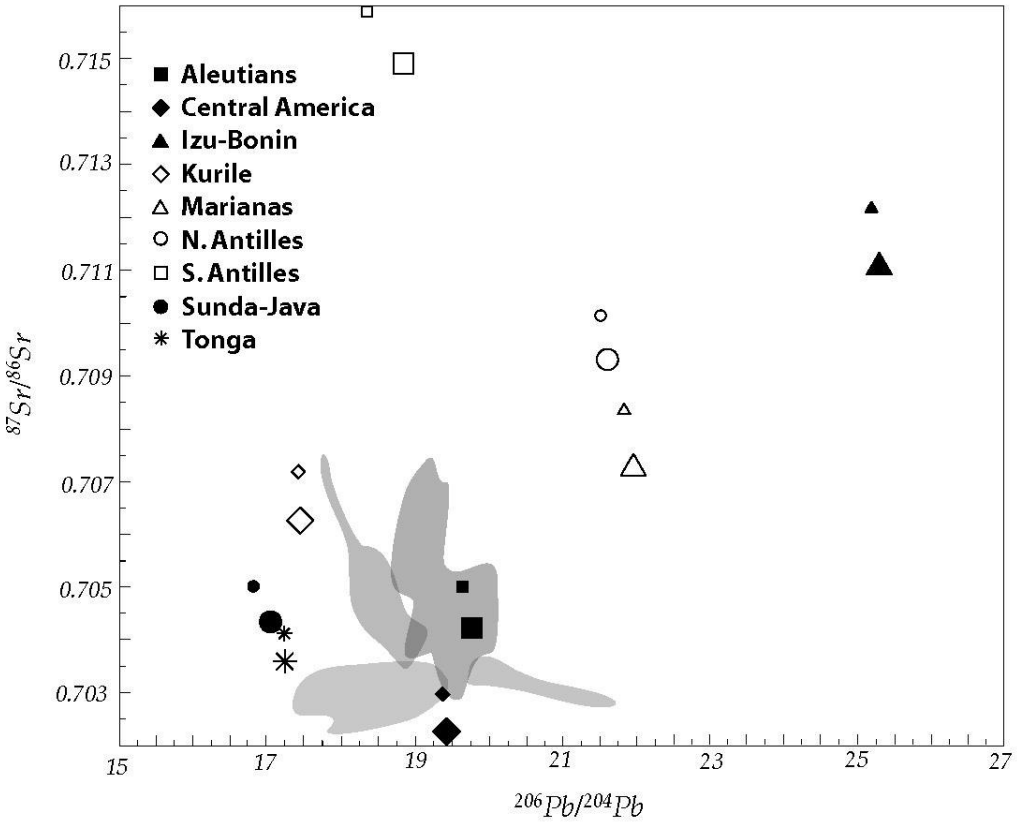

Figure 3.18 Residual slab Sr and Pb isotopic compositions for 1.8 Ga subducted slabs assuming no sediment subduction (large symbols). Small symbols show residual slab compositions calculated with sediment (see Figure 3.6).

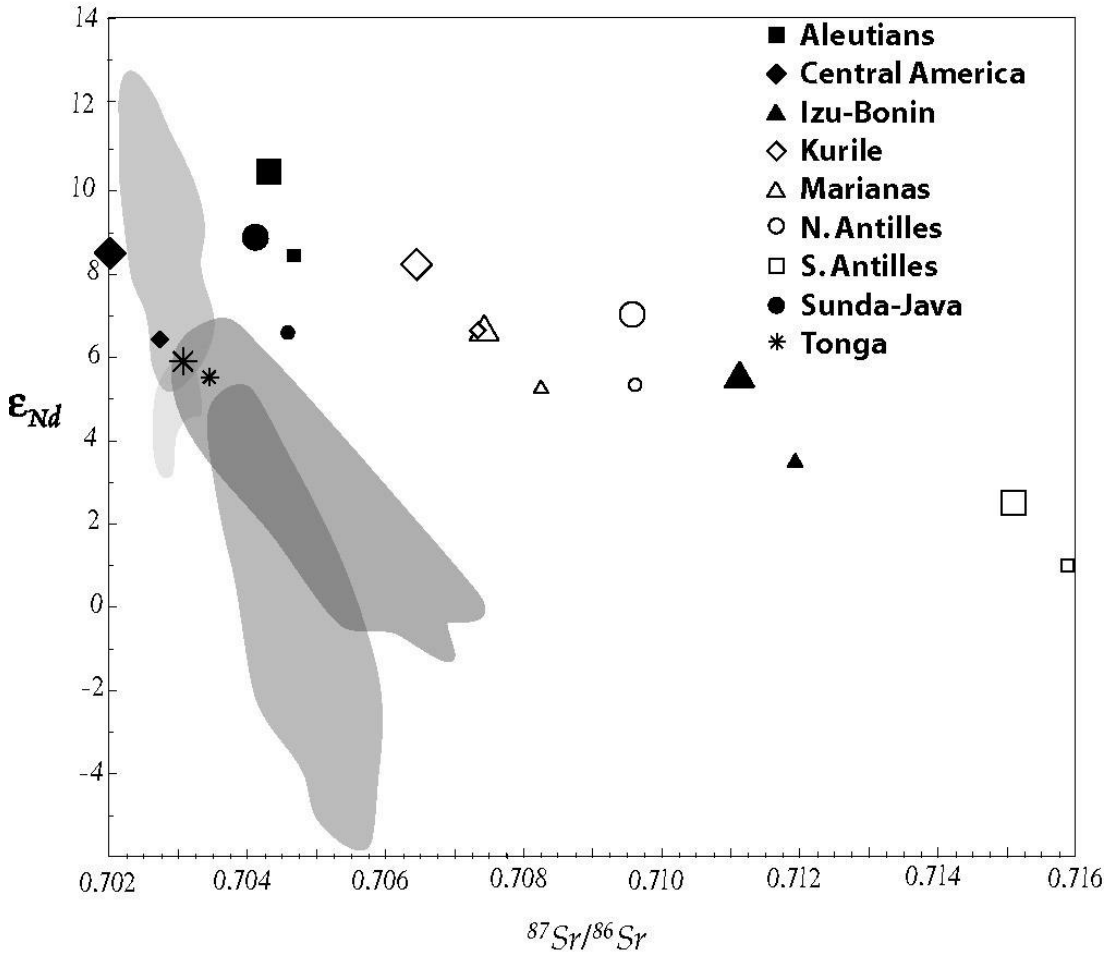

Figure 3.19 Residual slab Nd and Sr isotopic compositions for 1.8 Ga subducted slabs assuming no sediment subduction (large symbols). Small symbols show residual slab compositions calculated with sediment (see Figure 3.7).

Table 3.19 Residual slab parent/daughter ratios and isotopic compositions for 1.8 Ga subducted slabs assuming no sediment subduction.

	Aleutians	Central America	Izu-Bonin	Kurile	Marianas	Northern Antilles	Southern Antilles	Sunda-Java	Tonga
U/Pb	0.20	0.18	0.47	0.09	0.31	0.29	0.16	0.06	0.06
Rb/Sr	0.04	0.01	0.12	0.06	0.07	0.10	0.18	0.04	0.03
Sm/Nd	0.36	0.34	0.32	0.34	0.33	0.33	0.30	0.35	0.33
$^{206}Pb/^{204}Pb$	19.84	19.46	25.37	17.63	22.04	21.74	19.08	17.05	17.17
$^{87}Sr/^{86}Sr$	0.7041	0.7019	0.7108	0.7060	0.7069	0.7091	0.7147	0.7041	0.7036
ε_{Nd}	10.2	8.4	5.2	8.1	6.8	7.0	2.6	8.9	5.9

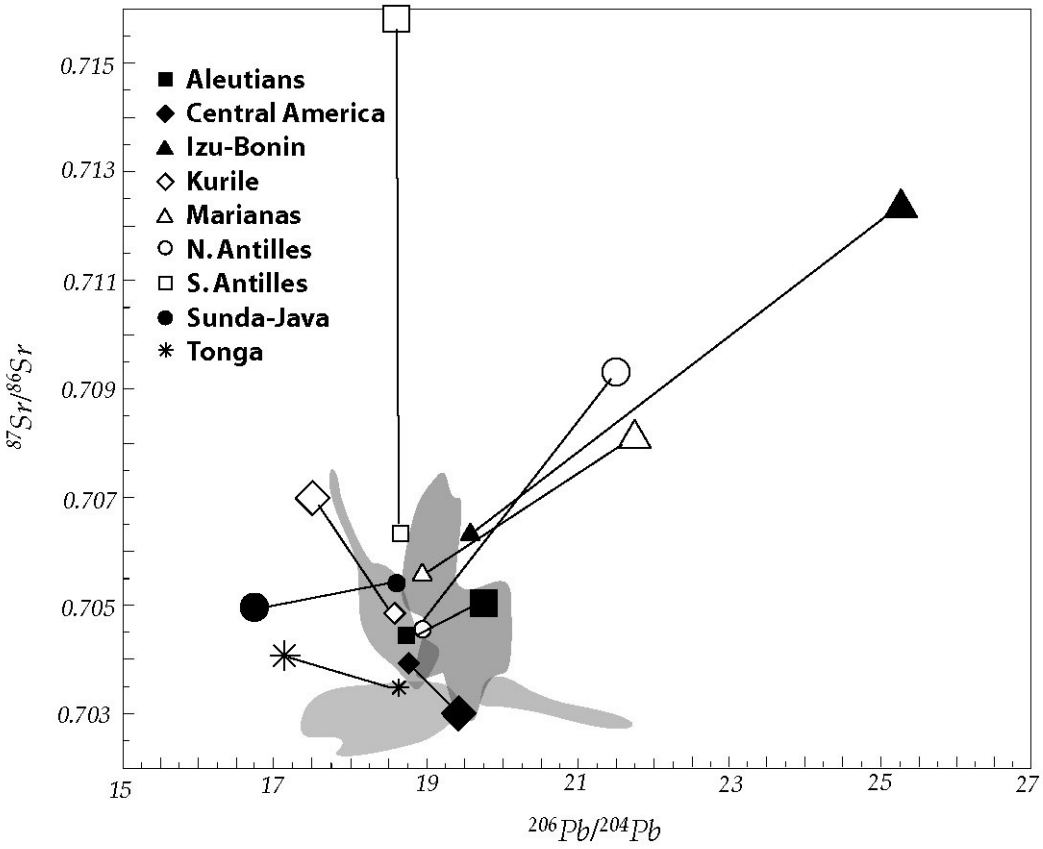

Figure 3.20 Residual slab Sr and Pb isotopic characteristics for different subduction ages. Large symbols denote 1.8 Ga compositions; small symbols denote 200 Ma compositions; lines show evolutionary path of residual slab material.

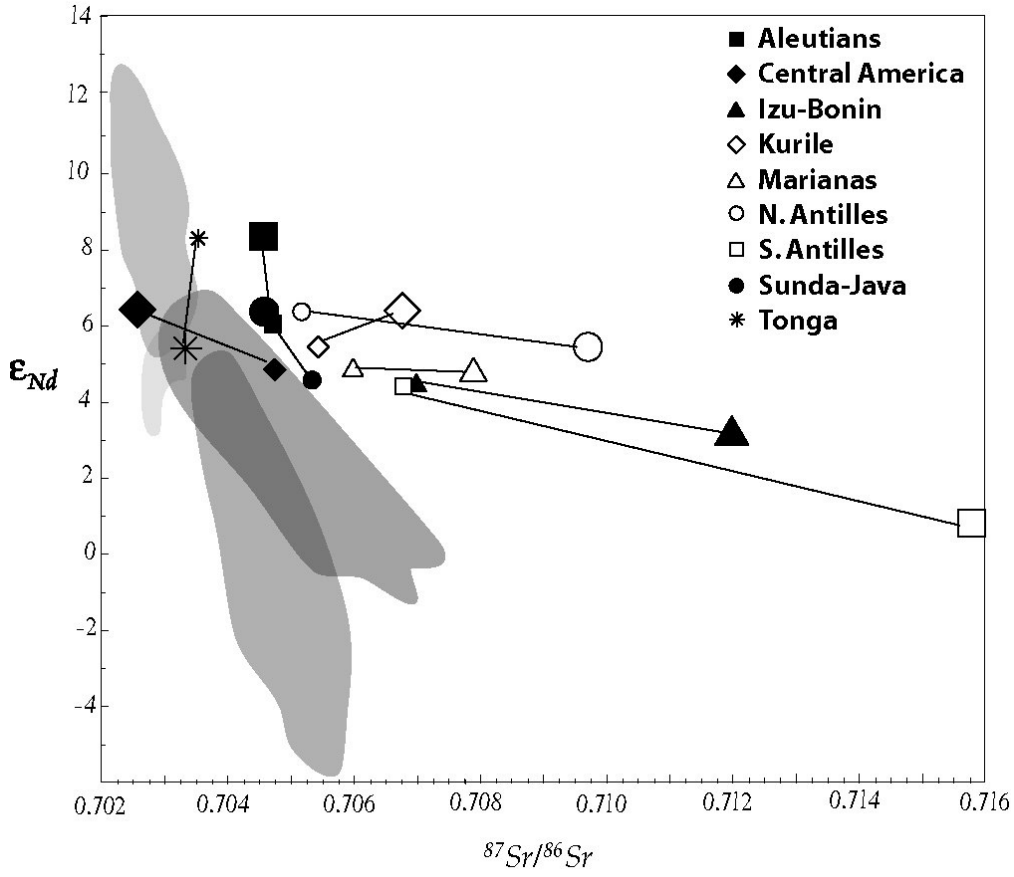

Figure 3.21 Residual slab Nd and Sr isotopic characteristics for different subduction ages. Large symbols denote 1.8 Ga compositions; small symbols denote 200 Ma compositions; lines show evolutionary path of residual slab material.

variations in the residual slab isotopic compositions, I was still unable to reproduce the characteristics of the HIMU and EMII reservoirs.

Conclusions

In order to examine the feasibility of various mantle evolution models and theories about the origin of certain mantle chemical and isotopic characteristics, I calculated residual slab fluxes for 19 trace elements at nine subduction zones. Overall, although my results support theories about the nature of some subduction zone processes, they do not support several of the ideas regarding the effects of subduction zone processing on the subducted slab and the origins of isotopically distinct mantle reservoirs. I find that, although subduction zone processing can lower ingoing slab Pb/Ce, residual slab ratios are still significantly higher than the ambient mantle value in most arcs (Figures 3.3 and 3.14). This suggests that either the depleted mantle Pb/Ce ratio is not as consistent as is currently believed, or that some process(es) – such as subduction erosion or delamination – in addition to subduction zone processing are important in maintaining the constancy of mantle Pb/Ce ratios.

The results of my examination of residual slab Th/U ratios also disagree with some currently accepted theories regarding mantle evolution. Subduction zone processing causes little to no alteration of slab Th/U ratios (Figures 3.4 and 3.15), implying that incorporation of low Th/U material at ancient subduction zones could not have significantly lowered mantle Th/U unless ancient ingoing slabs were enriched in U relative to Th. However, based on models of the oxidation of Earth's oceans in the Archean, it appears unlikely that ancient ingoing slab Th/U ratios were significantly lower

than those of modern slabs. My results support the theory that the so-called "kappa conundrum" was produced as a result of differential fractionation during the creation of the continents (e.g. Paul *et al.*, 2002).

Using modern-day residual slab parent/daughter ratios and slab compositions, I predicted the modern composition of hypothetical slab material subducted at 1.8 Ga (Figures 3.6, 3.7, 3.16 – 3.21). My calculated residual slab isotopic compositions were, in general, not consistent with the theory that the HIMU and EMII mantle reservoirs represent ancient subducted slabs. Most of the arcs that I examined could not reproduce the high Pb isotopic ratios of the HIMU reservoir or the low Sr and Nd isotopic ratios of the EMII reservoir. Those arcs that did reproduce one or two of the characteristics of the reservoirs (e.g., the Izu-Bonin and Marianas Nd and Pb isotopic compositions are similar to HIMU) lay far outside of the reservoir fields for the remaining isotopic ratio(s).

Although my model made a number of assumptions about compositions and processes within the subduction zone, these assumptions did not seem to introduce a large amount of error into my estimates of residual slab compositions. For example, varying the composition of the underlying mantle wedge to account for prior depletion or different degrees of partial melting did not significantly change the overall conclusions that I reached based on the initial model results. Despite showing a range of compositions when different model parameters were varied, Pb/Ce and Th/U ratios were still inconsistent with several of the mantle evolution theories that have been proposed (Figures 3.14 and 3.15). Isotopic characteristics of the various residual slabs were inconsistent with HIMU and EMII reservoirs when model parameters were varied (Figures 3.16 – 3.21).

Although the model variations that I examined did not produce sufficient changes in the results to account for mantle reservoir characteristics, the fact that variations in mantle composition are observed requires that some process(es) *are* able to produce these characteristics. My model assumes that the only loss of material from the slab occurs within the subduction zone, and that all of the material that is lost from the slab is incorporated into the mantle wedge. However, some studies have indicated that the slab may lose (or even gain) material well outside the zone in which IAV are produced, and that some material that is lost from the slab may not be erupted in the island arc. If these theories are valid, they could help to explain the observed mantle heterogeneities for which my model is unable to account.

It has been suggested that the efficiency of dehydration and mantle wedge metasomatism within subduction zones may be reduced if subduction velocities are very high (>12 cm/yr; Staudigel and King, 1992). Such very high convergence rates are thought to have occurred periodically throughout the history of the planet. The high subduction rates would allow cold, hydrated slab material to be mixed into the mantle (in contrast to the dehydrated material that is mixed into the mantle at modern subduction zones). Since dehydration is the primary mechanism by which many trace elements are released from the slab, retention of water by the slab could significantly increase the residual slab budget of these trace elements. U, for example, is thought to be fairly mobile in subduction zone fluids (e.g. Kogiso *et al.*, 1997; Peacock, 1990; Saunders *et al.*, 1991; Staudigel and King, 1992; You *et al.*, 1996); retention of hydrous silicates to depth could therefore

produce reservoirs with low Th/U. These low Th/U reservoirs could, if they were mixed with the convecting mantle, effectively lower the mantle Th/U ratio and partly explain the kappa conundrum. However, Staudigel & King (1992) suggest that such hydrated slab material would be likely to retain its coherence within the mantle, implying that ultrafast subduction would produce distinct reservoirs with low Th/U as opposed to lowering the overall mantle ratio. Retention of U within specific reservoirs could be responsible for the formation of HIMU-like Pb isotopic compositions, although Rb/Sr ratios in such material would probably be too high to produce HIMU-like Sr isotopes.

While the ultrafast subduction hypothesis of Staudigel and King (1992) provides a possible mechanism for the production of the HIMU reservoir, Workman *et al* (2004) have proposed a possible formation mechanism for EMII-type mantle. They note that incorporation of dehydrated slab material and terrigenous sediment is unable to produce EMII-like isotopic compositions and suggest instead that EMII is created as a result of ancient (2.5 Ga) metasomatism of lithospheric material with small degree partial melts (0.5% or less; Workman *et al.*, 2004).

Other possible explanations for the existence of mantle chemical and isotopic heterogeneities include subduction erosion (e.g. Kay *et al.*, 2005; von Huene *et al.*, 2004; von Huene and Scholl, 1991) and crustal delamination (Foley *et al.*, 2003; Morency *et al.*, 2002; Tatsumi, 2000; van Thienen *et al.*, 2004). These theories are similar in that they require the incorporation of non-slab material into the mantle. During subduction erosion, material from the overriding plate (see Figure 1.2) is removed and accreted to the subducting slab. As the slab descends into the subduction

zone, the accreted material experiences the same processing as the rest of the slab. It could therefore act as an additional source for trace elements in the IAV, increasing the residual slab flux into the convecting mantle and altering its effect on mantle chemistry. For example, if the eroded crust were enriched in Ce relative to Pb, or in U relative to Th, then removal of the "slab component" of the IAV from the combined slab-accreted crust material could lead to lowered Pb/Ce and Th/U ratios in the residual slab material. Similarly, enrichment of the eroded crust in Sr relative to Rb could produce lower residual slab Rb/Sr ratios and, ultimately, the decreased Sr isotopic characteristics that are seen in the HIMU reservoir.

Crustal delamination involves the removal of lithosphere beneath (usually) continental crust. Due to convective, thermal, or density instabilities, parts of the lower crustal "root" detach from the upper crust and sink into the convecting mantle. Mantle material upwells into the region and solidifies (with or without partial melting) to replace all or part of the detached root. The delaminated material is then incorporated into the mantle at varying depths (e.g. Foley *et al.*, 2003; Tatsumi, 2000). Lithosphere removed and incorporated into the mantle in this way could produce fairly large, chemically distinct reservoirs within the convecting mantle. Tatsumi (2000) suggested that such material might be the source of the EMI mantle reservoir based on trace and major element characteristics.

Appendix A: Average Major and Trace Element Compositions

Table A.1 Average major and trace element compositions for high-K series at various arcs.

	Aleutians			Central America			Izu-Bonin		
	mean	**rsd**	**n**	**mean**	**rsd**	**n**	**mean**	**rsd**	**n**
SiO_2	49.26	0.075	21	50.96	0.053	76	n.d.	n.d.	n.d.
TiO_2	1.89	0.460	21	1.40	0.441	63	n.d.	n.d.	n.d.
Al_2O_3	15.56	0.136	21	17.14	0.084	63	n.d.	n.d.	n.d.
Fe_2O_3	5.81	0.224	8	5.80	0.563	15	n.d.	n.d.	n.d.
FeO	6.30	0.223	4	4.98	0.153	12	n.d.	n.d.	n.d.
CaO	8.98	0.227	21	8.99	0.124	63	n.d.	n.d.	n.d.
MgO	5.57	0.361	21	5.84	0.366	76	n.d.	n.d.	n.d.
MnO	0.17	0.291	20	0.17	0.367	63	n.d.	n.d.	n.d.
K_2O	1.90	0.278	21	1.69	0.343	76	n.d.	n.d.	n.d.
Na_2O	3.64	0.212	21	3.22	0.182	63	n.d.	n.d.	n.d.
P_2O_5	0.49	0.570	18	0.45	0.290	59	n.d.	n.d.	n.d.
H_2O	1.93	0.669	11	0.79	1.052	32	n.d.	n.d.	n.d.
Rb	33.20	0.462	7	36.65	0.647	61	n.d.	n.d.	n.d.
Ba	607.00	0.530	15	727.21	0.530	74	n.d.	n.d.	n.d.
Th	3.45	0.718	6	6.74	0.589	17	n.d.	n.d.	n.d.
U	0.62	1.451	3	2.20	0.538	17	n.d.	n.d.	n.d.
Nb	2.77	0.362	3	22.27	0.622	51	n.d.	n.d.	n.d.
Ta	0.26	0.952	3	1.26	0.437	11	n.d.	n.d.	n.d.
La	20.01	0.843	12	38.80	0.536	56	n.d.	n.d.	n.d.
Ce	45.10	0.659	12	70.06	0.493	43	n.d.	n.d.	n.d.
Pb	4.49	0.827	3	5.63	0.278	15	n.d.	n.d.	n.d.
Sr	598.57	0.431	14	689.07	0.395	63	n.d.	n.d.	n.d.
Nd	28.61	0.424	10	36.06	0.393	43	n.d.	n.d.	n.d.
Zr	191.62	0.389	13	182.91	0.278	63	n.d.	n.d.	n.d.
Hf	2.87	0.343	3	4.86	0.177	11	n.d.	n.d.	n.d.
Sm	6.17	0.388	10	7.55	0.294	40	n.d.	n.d.	n.d.
Eu	1.92	0.356	10	2.00	0.321	40	n.d.	n.d.	n.d.
Y	32.08	0.379	12	32.16	0.371	51	n.d.	n.d.	n.d.
Yb	2.84	0.547	9	2.70	0.324	40	n.d.	n.d.	n.d.
Lu	0.46	0.587	7	0.32	0.214	12	n.d.	n.d.	n.d.

Table A.1 (continued)

	Kurile			Marianas			Northern Antilles		
	mean	**rsd**	**n**	**mean**	**rsd**	**n**	**mean**	**rsd**	**n**
SiO_2	50.32	0.059	40	n.d.	n.d.	n.d.	n.d.	n.d.	n.d.
TiO_2	0.84	0.333	28	n.d.	n.d.	n.d.	n.d.	n.d.	n.d.
Al_2O_3	16.96	0.108	28	n.d.	n.d.	n.d.	n.d.	n.d.	n.d.
Fe_2O_3	4.81	0.474	28	n.d.	n.d.	n.d.	n.d.	n.d.	n.d.
FeO	4.60	0.287	27	n.d.	n.d.	n.d.	n.d.	n.d.	n.d.
CaO	8.23	0.256	28	n.d.	n.d.	n.d.	n.d.	n.d.	n.d.
MgO	5.42	0.333	40	n.d.	n.d.	n.d.	n.d.	n.d.	n.d.
MnO	0.18	0.251	28	n.d.	n.d.	n.d.	n.d.	n.d.	n.d.
K_2O	2.21	0.469	40	n.d.	n.d.	n.d.	n.d.	n.d.	n.d.
Na_2O	3.33	0.179	28	n.d.	n.d.	n.d.	n.d.	n.d.	n.d.
P_2O_5	0.34	0.427	25	n.d.	n.d.	n.d.	n.d.	n.d.	n.d.
H_2O	1.26	0.889	46	n.d.	n.d.	n.d.	n.d.	n.d.	n.d.
Rb	37.87	0.527	10	n.d.	n.d.	n.d.	n.d.	n.d.	n.d.
Ba	498.72	0.487	18	n.d.	n.d.	n.d.	n.d.	n.d.	n.d.
Th	2.07	0.326	7	n.d.	n.d.	n.d.	n.d.	n.d.	n.d.
U	n.d.	n.d.	n.d.	n.d.	n.d.	n.d.	n.d.	n.d.	n.d.
Nb	3.22	0.532	11	n.d.	n.d.	n.d.	n.d.	n.d.	n.d.
Ta	n.d.	n.d.	n.d.	n.d.	n.d.	n.d.	n.d.	n.d.	n.d.
La	11.39	0.156	10	n.d.	n.d.	n.d.	n.d.	n.d.	n.d.
Ce	23.66	0.198	5	n.d.	n.d.	n.d.	n.d.	n.d.	n.d.
Pb	4.17	0.386	3	n.d.	n.d.	n.d.	n.d.	n.d.	n.d.
Sr	610.00	0.243	10	n.d.	n.d.	n.d.	n.d.	n.d.	n.d.
Nd	14.45	0.206	5	n.d.	n.d.	n.d.	n.d.	n.d.	n.d.
Zr	57.00	0.393	7	n.d.	n.d.	n.d.	n.d.	n.d.	n.d.
Hf	1.41	0.252	3	n.d.	n.d.	n.d.	n.d.	n.d.	n.d.
Sm	3.75	0.185	5	n.d.	n.d.	n.d.	n.d.	n.d.	n.d.
Eu	1.16	0.205	5	n.d.	n.d.	n.d.	n.d.	n.d.	n.d.
Y	19.00	0.334	7	n.d.	n.d.	n.d.	n.d.	n.d.	n.d.
Yb	1.84	0.224	5	n.d.	n.d.	n.d.	n.d.	n.d.	n.d.
Lu	0.27	0.307	3	n.d.	n.d.	n.d.	n.d.	n.d.	n.d.

Table A.1 (continued)

	Southern Antilles			Sunda-Java			Tonga		
	mean	**rsd**	**n**	**mean**	**rsd**	**n**	**mean**	**rsd**	**n**
SiO_2	46.37	0.038	13	50.19	0.060	269	47.26	0.071	37
TiO_2	1.09	0.284	13	0.99	0.275	269	1.77	0.803	37
Al_2O_3	15.54	0.105	13	17.14	0.138	264	13.97	0.212	37
Fe_2O_3	1.09	0.020	2	7.57	0.442	115	8.12	0.351	22
FeO	7.80	0.019	2	5.95	0.298	46	3.86	0.483	11
CaO	11.29	0.178	13	9.82	0.190	264	9.56	0.329	37
MgO	9.68	0.399	13	5.02	0.547	269	9.13	0.394	37
MnO	0.21	0.326	13	0.19	0.139	259	0.17	0.286	33
K_2O	1.27	0.224	13	2.98	0.516	269	2.07	0.325	37
Na_2O	3.12	0.292	13	3.01	0.259	264	2.64	0.287	37
P_2O_5	0.27	0.416	13	0.48	0.477	242	0.49	0.488	37
H_2O	n.d.	n.d.	n.d.	1.35	0.718	31	1.64	n/a	1
Rb	29.83	0.358	12	120.86	0.994	252	38.73	0.479	23
Ba	412.38	0.350	11	974.87	0.704	238	488.78	0.300	23
Th	10.56	0.218	5	10.95	0.581	190	1.00	0.301	18
U	3.22	0.235	5	2.30	0.553	68	0.50	0.415	16
Nb	11.62	0.544	12	13.22	0.936	236	20.92	0.930	11
Ta	0.48	0.597	3	0.51	0.949	46	0.41	1.412	13
La	25.66	0.168	5	55.84	0.592	159	23.04	0.835	26
Ce	58.43	0.206	7	103.56	0.536	169	46.86	0.828	26
Pb	4.36	0.467	5	13.47	0.503	156	6.38	0.597	19
Sr	802.50	0.710	12	808.06	0.438	257	492.34	0.835	23
Nd	27.09	0.165	7	42.08	0.486	138	22.40	0.581	21
Zr	130.09	0.345	12	145.65	0.482	254	81.84	0.619	23
Hf	3.24	0.248	3	3.21	0.340	82	1.79	0.694	14
Sm	5.39	0.139	7	7.49	0.450	91	4.84	0.456	22
Eu	1.54	0.114	7	2.18	0.415	94	1.53	0.390	22
Y	28.66	1.011	12	29.79	0.314	246	20.20	0.247	23
Yb	1.65	0.061	7	2.31	0.211	96	1.74	0.279	22
Lu	0.27	0.063	3	0.35	0.196	63	0.27	0.259	21

Table A.2 Average major and trace element compositions for medium-K series at various arcs.

	Aleutians			Central America			Izu-Bonin		
	mean	**rsd**	**n**	**mean**	**rsd**	**n**	**mean**	**rsd**	**n**
SiO_2	51.60	0.043	232	51.79	0.040	265	50.90	0.058	26
TiO_2	1.15	0.409	232	0.93	0.245	219	0.90	0.402	25
Al_2O_3	17.72	0.109	232	18.21	0.090	219	16.87	0.146	26
Fe_2O_3	3.65	0.537	53	3.01	0.567	52	3.39	0.668	14
FeO	6.05	0.336	53	6.31	0.199	51	7.15	0.241	14
CaO	9.53	0.155	232	9.62	0.140	219	9.71	0.220	26
MgO	5.15	0.417	232	4.99	0.277	265	5.96	0.401	26
MnO	0.18	0.221	231	0.17	0.195	185	0.20	0.187	25
K_2O	0.91	0.308	232	0.81	0.378	265	0.60	0.406	26
Na_2O	3.14	0.184	232	3.05	0.190	219	2.40	0.310	26
P_2O_5	0.23	0.432	198	0.21	0.417	170	0.12	0.526	22
H_2O	0.78	0.960	41	0.65	1.020	157	2.07	0.938	15
Rb	15.49	0.478	98	14.21	0.549	204	7.51	0.471	10
Ba	318.61	0.376	160	470.28	0.324	223	160.07	0.568	9
Th	1.23	0.794	43	0.94	0.478	36	0.32	0.249	3
U	0.52	0.592	28	0.52	0.638	30	0.19	0.242	3
Nb	4.63	0.380	36	5.58	0.535	82	0.68	0.162	3
Ta	0.36	0.840	19	0.20	0.752	4	0.09	0.040	3
La	8.65	0.525	76	10.64	0.636	109	3.13	0.234	4
Ce	20.11	0.366	75	23.91	0.394	66	9.26	0.290	4
Pb	5.20	0.326	2	4.21	0.422	22	3.94	0.171	3
Sr	455.93	0.270	179	542.50	0.209	205	421.44	0.525	9
Nd	13.75	0.380	65	15.88	0.343	56	8.43	0.269	4
Zr	92.95	0.418	153	92.76	0.397	169	27.20	0.864	5
Hf	2.49	0.518	38	2.34	0.361	8	2.10	0.029	3
Sm	3.75	0.359	70	3.80	0.309	58	2.93	0.240	4
Eu	1.20	0.312	70	1.22	0.232	58	1.06	0.204	4
Y	23.95	0.330	123	20.17	0.291	120	19.53	0.494	8
Yb	2.48	0.376	72	2.08	0.229	55	3.06	0.131	4
Lu	0.43	0.343	43	0.31	0.175	16	0.49	0.104	4

Table A.2 (continued)

	Kurile			Marianas			Northern Antilles		
	mean	**rsd**	**n**	**mean**	**rsd**	**n**	**mean**	**rsd**	**n**
SiO_2	51.66	0.043	153	52.22	0.034	144	51.49	0.041	29
TiO_2	1.07	0.302	145	0.82	0.392	144	0.89	0.150	29
Al_2O_3	17.80	0.102	146	16.44	0.156	143	19.11	0.047	29
Fe_2O_3	5.04	0.512	102	4.81	0.769	48	6.37	0.500	24
FeO	6.09	0.199	79	8.08	0.384	56	5.88	0.164	13
CaO	9.82	0.128	146	9.71	0.187	144	10.14	0.110	29
MgO	5.62	0.324	153	5.88	0.585	144	4.81	0.250	29
MnO	0.17	0.435	145	0.18	0.256	137	0.18	0.148	29
K_2O	0.90	0.355	153	0.86	0.285	144	0.55	0.249	29
Na_2O	2.85	0.190	146	2.59	0.241	143	2.84	0.168	29
P_2O_5	0.20	0.476	124	0.15	0.453	135	0.11	0.263	29
H_2O	0.36	0.979	75	0.78	1.568	45	n.d.	n.d.	n.d.
Rb	17.88	0.397	25	16.37	0.373	107	9.35	0.409	17
Ba	241.12	0.482	26	210.49	0.633	103	116.75	0.296	20
Th	1.69	0.487	25	0.73	0.793	27	0.85	0.694	6
U	0.74	0.874	19	0.44	0.522	28	0.29	0.310	5
Nb	3.34	0.586	26	1.91	0.743	51	2.44	0.583	9
Ta	0.25	0.541	13	0.11	0.970	32	0.10	0.292	5
La	10.40	0.370	26	5.37	0.662	32	5.14	0.541	9
Ce	24.09	0.387	26	12.78	0.476	36	16.07	0.699	9
Pb	5.10	0.300	6	4.69	0.793	20	9.50	0.251	4
Sr	370.56	0.316	25	314.08	0.592	108	312.05	0.290	20
Nd	12.63	0.246	11	11.93	0.375	34	8.14	0.196	5
Zr	104.90	0.358	20	63.66	0.337	111	62.40	0.219	20
Hf	2.31	0.286	25	1.81	0.298	35	1.61	0.190	5
Sm	3.81	0.206	30	3.05	0.317	26	2.32	0.223	5
Eu	1.21	0.218	25	0.99	0.381	41	0.90	0.178	5
Y	24.50	0.204	20	21.19	0.364	104	23.69	0.230	16
Yb	2.79	0.237	25	2.46	0.285	25	2.17	0.248	5
Lu	0.39	0.219	25	0.39	0.314	21	0.35	0.263	5

Table A.2 (continued)

	Southern Antilles			Sunda-Java			Tonga		
	mean	**rsd**	**n**	**mean**	**rsd**	**n**	**mean**	**rsd**	**n**
SiO_2	48.65	0.062	138	50.62	0.055	183	50.63	0.042	162
TiO_2	0.92	0.200	138	1.05	0.235	183	1.18	0.397	162
Al_2O_3	16.38	0.120	138	18.11	0.086	176	17.74	0.133	162
Fe_2O_3	5.37	0.748	44	4.93	0.612	53	5.83	0.467	135
FeO	6.50	0.225	26	5.86	0.255	42	5.21	0.365	110
CaO	10.87	0.169	138	10.01	0.138	176	10.53	0.120	162
MgO	8.61	0.444	138	5.71	0.423	183	6.01	0.473	162
MnO	0.18	0.531	138	0.24	1.949	175	0.16	0.223	154
K_2O	0.71	0.391	138	0.77	0.367	183	0.75	0.358	162
Na_2O	2.71	0.321	138	2.90	0.183	176	2.60	0.214	162
P_2O_5	0.21	0.651	127	0.17	0.429	149	0.24	0.428	161
H_2O	n.d.	n.d.	n.d.	0.49	0.961	25	0.29	0.831	26
Rb	16.79	0.616	126	15.05	0.655	109	12.90	0.596	96
Ba	245.54	0.635	118	279.37	0.569	123	169.99	0.586	108
Th	4.84	0.700	74	2.54	0.638	34	0.60	0.941	26
U	1.81	0.653	61	0.53	0.637	30	0.26	0.847	12
Nb	6.20	0.606	102	3.71	0.881	99	12.11	1.363	32
Ta	0.27	0.436	20	0.25	0.704	18	0.23	0.634	13
La	14.39	0.568	80	10.31	0.617	39	5.86	0.500	57
Ce	28.87	0.478	84	22.19	0.551	39	17.81	0.919	61
Pb	2.96	0.416	61	7.26	0.411	51	4.92	0.780	42
Sr	535.36	0.618	126	355.40	0.256	139	349.99	0.430	100
Nd	15.93	0.359	67	14.96	0.497	28	11.07	0.394	21
Zr	85.36	0.449	121	69.33	0.737	138	72.45	0.667	89
Hf	2.05	0.247	22	2.11	0.479	30	1.61	0.699	26
Sm	3.77	0.279	77	3.33	0.478	34	2.90	0.455	24
Eu	1.18	0.225	77	1.09	0.317	34	1.06	0.385	25
Y	20.98	0.226	123	21.57	0.245	120	23.19	0.313	90
Yb	1.86	0.202	76	1.98	0.296	34	2.23	0.436	26
Lu	0.29	0.233	50	0.34	0.306	7	0.34	0.294	19

Table A.3 Average major and trace element compositions for low-K series at various arcs.

	Aleutians			Central America			Izu-Bonin		
	mean	**rsd**	**n**	**mean**	**rsd**	**n**	**mean**	**rsd**	**n**
SiO_2	51.73	0.026	33	49.62	0.041	26	51.84	0.039	127
TiO_2	0.78	0.379	33	1.09	0.191	23	1.02	0.308	126
Al_2O_3	18.97	0.091	33	17.06	0.117	23	15.98	0.138	127
Fe_2O_3	2.41	0.626	27	9.17	0.296	7	3.42	0.429	32
FeO	5.20	0.296	28	7.65	n/a	1	7.95	0.260	32
CaO	10.90	0.107	33	10.99	0.122	23	10.40	0.154	127
MgO	6.08	0.258	33	6.61	0.343	26	5.24	0.373	127
MnO	0.15	0.181	33	0.18	0.235	23	0.20	0.158	125
K_2O	0.32	0.341	33	0.18	0.610	26	0.33	0.381	127
Na_2O	2.55	0.333	33	2.80	0.290	23	1.95	0.248	127
P_2O_5	0.13	0.163	28	0.13	0.416	23	0.09	0.577	123
H_2O	n.d.	n.d.	n.d.	1.18	0.825	21	0.64	1.232	30
Rb	8.34	0.485	28	7.07	0.451	18	3.86	0.541	57
Ba	166.19	0.455	27	194.01	0.836	21	113.02	0.596	61
Th	0.30	0.471	4	0.09	n/a	1	0.14	0.467	19
U	0.22	0.434	3	0.05	n/a	1	0.11	0.823	19
Nb	1.16	n/a	1	4.61	0.474	11	0.39	0.720	19
Ta	0.30	0.676	5	0.07	n/a	1	0.05	0.341	18
La	4.68	0.326	7	3.70	0.430	9	1.47	0.414	24
Ce	12.73	0.314	7	10.69	0.221	6	4.93	0.418	27
Pb	4.15	0.699	2	0.24	n/a	1	2.18	0.416	21
Sr	315.75	0.129	32	324.58	0.516	23	170.13	0.237	61
Nd	8.91	0.315	6	8.77	0.209	6	5.91	0.611	28
Zr	34.32	0.571	28	62.08	0.257	17	39.53	0.310	36
Hf	2.10	0.341	5	2.03	n/a	1	1.12	0.428	19
Sm	2.73	0.324	7	2.84	0.085	6	1.93	0.406	26
Eu	1.03	0.351	7	1.02	0.066	6	0.74	0.362	26
Y	8.76	0.310	28	19.37	0.276	11	19.85	0.293	55
Yb	1.99	0.397	7	1.83	0.272	6	2.21	0.394	26
Lu	0.29	0.413	7	0.42	n/a	1	0.35	0.397	26

Table A.3 (continued)

	Kurile			Marianas			Northern Antilles		
	mean	**rsd**	**n**	**mean**	**rsd**	**n**	**mean**	**rsd**	**n**
SiO_2	52.46	0.032	27	51.65	0.034	75	52.09	0.036	8
TiO_2	0.95	0.239	26	0.96	0.440	75	0.91	0.094	8
Al_2O_3	17.78	0.050	26	16.49	0.140	74	19.36	0.046	8
Fe_2O_3	6.40	0.501	21	4.94	0.620	22	5.99	0.668	5
FeO	7.06	0.320	12	6.08	0.303	20	5.80	0.094	3
CaO	9.65	0.126	26	10.66	0.105	74	9.93	0.108	8
MgO	5.40	0.215	27	6.52	0.441	75	4.24	0.064	8
MnO	0.17	0.235	25	0.17	0.173	53	0.19	0.110	8
K_2O	0.36	0.273	27	0.34	0.391	75	0.41	0.135	8
Na_2O	2.78	0.172	26	2.62	0.256	73	3.18	0.114	8
P_2O_5	0.14	0.381	21	0.12	0.399	71	0.11	0.238	8
H_2O	0.27	0.825	12	0.95	0.772	17	n.d.	n.d.	n.d.
Rb	3.37	0.603	6	7.42	0.443	52	7.00	0.350	6
Ba	88.25	0.654	8	109.28	0.598	46	110.88	0.302	8
Th	0.54	0.431	4	0.37	0.446	14	0.51	0.159	3
U	0.35	0.364	4	0.16	0.345	10	0.25	0.136	3
Nb	1.57	0.614	7	1.82	0.956	20	2.75	0.182	4
Ta	0.14	0.367	2	0.07	0.245	12	0.12	0.049	3
La	3.14	0.861	8	3.73	0.456	29	3.85	0.188	4
Ce	8.67	0.635	8	9.88	0.372	34	10.10	0.120	3
Pb	2.58	0.542	4	1.44	0.490	13	3.00	n/a	1
Sr	248.83	0.351	6	203.88	0.443	57	273.75	0.040	8
Nd	5.25	0.434	4	8.48	0.335	25	7.93	0.134	3
Zr	58.67	0.741	6	56.67	0.423	49	70.50	0.222	8
Hf	1.21	0.726	7	1.80	0.418	23	1.75	0.122	3
Sm	2.29	0.395	8	2.86	0.343	29	2.42	0.110	3
Eu	0.85	0.377	8	0.98	0.245	31	0.95	0.111	3
Y	21.67	0.254	6	24.19	0.499	47	25.00	0.233	5
Yb	2.36	0.216	8	2.61	0.250	29	2.34	0.109	3
Lu	0.35	0.235	8	0.43	0.244	23	0.38	0.125	3

Table A.3 (continued)

	Southern Antilles			Sunda-Java			Tonga		
	mean	**rsd**	**n**	**mean**	**rsd**	**n**	**mean**	**rsd**	**n**
SiO_2	52.28	0.046	35	n.d.	n.d.	n.d.	50.78	0.031	411
TiO_2	0.95	0.267	35	n.d.	n.d.	n.d.	1.26	0.589	410
Al_2O_3	18.70	0.123	35	n.d.	n.d.	n.d.	14.99	0.137	411
Fe_2O_3	9.24	0.034	16	n.d.	n.d.	n.d.	8.24	0.483	173
FeO	n.d.	n.d.	n.d.	n.d.	n.d.	n.d.	8.17	0.264	97
CaO	9.30	0.231	35	n.d.	n.d.	n.d.	11.64	0.279	411
MgO	4.79	0.487	35	n.d.	n.d.	n.d.	7.56	0.313	411
MnO	0.17	0.242	35	n.d.	n.d.	n.d.	0.19	0.261	399
K_2O	0.42	0.304	35	n.d.	n.d.	n.d.	0.19	0.676	411
Na_2O	3.23	0.306	35	n.d.	n.d.	n.d.	2.42	0.274	411
P_2O_5	52.28	0.046	35	n.d.	n.d.	n.d.	0.11	0.493	402
H_2O	n.d.	n.d.	n.d.	n.d.	n.d.	n.d.	0.40	1.200	150
Rb	8.52	0.456	34	n.d.	n.d.	n.d.	3.93	0.569	201
Ba	105.84	0.259	31	n.d.	n.d.	n.d.	44.23	0.776	227
Th	1.33	0.451	26	n.d.	n.d.	n.d.	0.26	0.541	30
U	0.37	0.615	7	n.d.	n.d.	n.d.	0.11	0.320	25
Nb	3.23	0.469	23	n.d.	n.d.	n.d.	1.82	0.936	65
Ta	0.15	0.189	2	n.d.	n.d.	n.d.	0.09	1.007	26
La	5.57	0.347	26	n.d.	n.d.	n.d.	2.76	0.658	51
Ce	13.05	0.347	26	n.d.	n.d.	n.d.	7.45	0.709	45
Pb	2.10	0.343	12	n.d.	n.d.	n.d.	1.83	0.694	33
Sr	228.10	0.297	34	n.d.	n.d.	n.d.	142.98	0.486	221
Nd	9.94	0.143	19	n.d.	n.d.	n.d.	5.83	0.680	42
Zr	74.46	0.387	23	n.d.	n.d.	n.d.	53.54	0.664	118
Hf	2.08	0.187	9	n.d.	n.d.	n.d.	1.48	0.838	45
Sm	3.20	0.250	20	n.d.	n.d.	n.d.	1.76	0.643	43
Eu	0.98	0.150	14	n.d.	n.d.	n.d.	0.74	0.642	42
Y	24.80	0.225	24	n.d.	n.d.	n.d.	22.99	0.538	118
Yb	2.43	0.156	14	n.d.	n.d.	n.d.	1.78	0.571	45
Lu	0.40	0.199	12	n.d.	n.d.	n.d.	0.25	0.556	26

Appendix B: Liquid Line of Descent Calculation Data

Table B.1 Mineral phase data for high-K series fractionation corrections. Masses of minerals given in g; 100 g initial starting mass of magma.

	Aleutians	Central America	Izu-Bonin	Kurile	Marianas	Northern Antilles	Southern Antilles	Sunda-Java	Tonga
average wt% MgO	5.57	5.84	n/a	5.42	n/a	n/a	9.68	5.02	9.13
olivine	10.14	18.71	n/a	11.87	n/a	n/a	13.75	18.83	10.83
clino-pyroxene	14.30	18.88	n/a	17.99	n/a	n/a	0.00	21.33	11.09
ortho-pyroxene	0.00	0.00	n/a	0.00	n/a	n/a	0.00	0.00	6.29
feldspar	0.00	5.90	n/a	0.00	n/a	n/a	0.00	0.00	0.00
spinel	0.00	0.00	n/a	0.00	n/a	n/a	0.00	1.02	0.00
whitlockite	0.00	0.00	n/a	0.00	n/a	n/a	0.00	0.00	0.00

Table B.2 Mineral phase data for medium-K series fractionation corrections. Masses of minerals given in g; 100 g initial starting mass of magma.

	Aleutians	Central America	Izu-Bonin	Kurile	Marianas	Northern Antilles	Southern Antilles	Sunda-Java	Tonga
average wt% MgO	5.15	4.99	5.96	5.62	5.88	4.81	8.61	5.71	6.01
olivine	15.44	18.03	15.44	17.08	13.26	16.88	13.35	18.54	16.87
clino-pyroxene	28.09	24.47	28.09	22.46	4.54	30.76	3.56	19.24	27.93
ortho-pyroxene	0.00	0.00	0.00	0.00	12.85	1.96	0.00	0.00	0.00
feldspar	15.13	16.89	15.13	13.37	0.00	5.00	0.00	0.00	0.19
spinel	0.00	0.00	0.00	0.00	0.00	0.00	0.00	0.00	0.00
whitlockite	0.00	0.00	0.00	0.00	0.00	0.19	0.00	0.00	0.19

Table B.3 Mineral phase data for low-K series fractionation corrections. Masses of minerals given in g; 100 g initial starting mass of magma.

	Aleutians	Central America	Izu-Bonin	Kurile	Marianas	Northern Antilles	Southern Antilles	Sunda-Java	Tonga
average wt% MgO	6.08	6.61	5.24	5.40	6.52	4.24	4.79	n/a	7.56
olivine	8.81	16.56	17.05	17.05	15.81	15.79	15.79	n/a	16.56
clino-pyroxene	36.55	28.65	15.14	15.14	14.34	24.71	20.13	n/a	28.65
ortho-pyroxene	2.46	0.00	1.85	1.85	3.38	3.82	3.82	n/a	0.00
feldspar	8.37	2.72	25.35	25.35	0.00	5.55	0.80	n/a	2.72
spinel	0.00	0.00	0.00	0.00	0.00	0.00	0.00	n/a	0.00
whitlockite	0.00	0.00	0.00	0.00	0.00	0.00	0.00	n/a	0.00

Table B.4 Starting compositions for LLOD calculations, high –K series. Concentrations in wt%.

	Aleutians	Central America	Izu-Bonin	Kurile	Marianas	Northern Antilles	Southern Antilles	Sunda-Java	Tonga
SiO_2	48.00	48.00	n.d.	48.90	n.d.	n.d.	48.00	45.00	50.15
TiO_2	2.00	0.20	n.d.	0.50	n.d.	n.d.	0.20	0.80	2.00
Al_2O_3	14.00	15.00	n.d.	15.00	n.d.	n.d.	15.00	10.48	11.00
Fe_2O_3	2.50	2.00	n.d.	2.30	n.d.	n.d.	2.00	3.00	3.00
FeO	4.52	5.00	n.d.	5.00	n.d.	n.d.	5.00	6.00	6.00
CaO	0.18	0.10	n.d.	0.10	n.d.	n.d.	0.10	0.17	0.15
MgO	12.00	15.00	n.d.	12.00	n.d.	n.d.	15.00	15.00	15.00
MnO	11.00	10.00	n.d.	10.00	n.d.	n.d.	10.00	11.00	10.00
K_2O	3.00	2.50	n.d.	3.00	n.d.	n.d.	2.50	3.00	1.00
Na_2O	1.50	1.20	n.d.	1.80	n.d.	n.d.	1.20	1.80	1.50
P_2O_5	0.50	0.20	n.d.	0.40	n.d.	n.d.	0.20	0.75	0.20
H_2O	0.80	0.80	n.d.	1.00	n.d.	n.d.	0.80	3.00	50.15
liquidus temp. (ºC)	1314.98	1378.81	n/a	1329.98	n/a	n/a	1378.81	1358.98	1383.50
pressure (kbar)	2.5	2.5	n/a	2.5	n/a	n/a	2.5	2.5	2.5
fO_2	QFM+1	QFM+1	n/a	QFM+1	n/a	n/a	QFM+1	QFM+1	QFM+1
temperature increment (ºC)	25	25	n/a	25	n/a	n/a	25	25	25

Table B.5 Starting compositions for LLOD calculations, medium –K series. Concentrations in wt%.

	Aleutians	Central America	Izu-Bonin	Kurile	Marianas	Northern Antilles	Southern Antilles	Sunda-Java	Tonga
SiO_2	48.00	48.00	48.00	48.00	51.40	49.00	48.00	47.00	49.00
TiO_2	0.80	0.70	0.80	0.70	0.10	1.00	0.70	0.80	1.00
Al_2O_3	15.00	15.00	15.00	15.00	13.00	11.00	15.00	11.50	11.00
Fe_2O_3	1.50	3.00	1.50	3.00	2.00	3.00	3.00	3.00	3.00
FeO	5.35	5.00	5.35	5.00	8.00	7.00	5.00	6.00	7.00
CaO	0.15	0.20	0.15	0.20	0.15	0.15	0.20	0.17	0.15
MgO	14.00	14.00	14.00	14.00	15.00	16.00	14.00	15.00	16.00
MnO	12.00	10.70	12.00	10.70	7.00	10.00	10.70	11.00	10.00
K_2O	1.80	2.00	1.80	2.00	1.60	1.80	2.00	1.18	1.80
Na_2O	0.50	0.50	0.50	0.50	0.70	0.40	0.50	0.60	0.40
P_2O_5	0.20	0.10	0.20	0.10	0.05	0.10	0.10	0.75	0.10
H_2O	0.70	0.80	0.70	0.80	1.00	0.55	0.80	3.00	0.55
liquidus temp. (ºC)	1333.11	1331.15	1333.11	1331.15	1386.23	1384.27	1331.15	1331.93	1331.93
pressure (kbar)	2.5	2.5	2.5	2.5	2.5	2.5	2.5	2.5	2.5
fO_2	QFM+1	QFM+1	QFM+1	QFM+1	QFM+1	QFM+1	QFM+1	QFM+1	QFM+1
temperature increment (ºC)	25	25	25	25	25	25	25	25	25

Table B.6 Starting compositions for LLOD calculations, low –K series. Concentrations in wt%.

	Aleutians	Central America	Izu-Bonin	Kurile	Marianas	Northern Antilles	Southern Antilles	Sunda-Java	Tonga
SiO_2	52.00	49.00	48.00	48.00	50.00	50.00	50.00	n.d.	49.00
TiO_2	0.60	1.00	0.80	0.80	0.70	0.70	0.70	n.d.	1.00
Al_2O_3	12.00	11.00	15.00	15.00	12.00	12.00	12.00	n.d.	11.00
Fe_2O_3	1.62	3.00	1.50	1.50	2.00	2.00	2.00	n.d.	3.00
FeO	5.00	7.35	5.35	5.35	8.00	8.00	8.00	n.d.	7.35
CaO	0.13	0.15	0.15	0.15	0.12	0.12	0.12	n.d.	0.15
MgO	14.00	16.00	14.00	14.00	15.00	15.00	15.00	n.d.	16.00
MnO	12.00	10.00	12.00	12.00	8.88	8.88	8.88	n.d.	10.00
K_2O	1.80	1.80	1.80	1.80	2.00	2.00	2.00	n.d.	1.80
Na_2O	0.25	0.10	0.50	0.50	0.20	0.20	0.20	n.d.	0.10
P_2O_5	0.10	0.05	0.20	0.20	0.10	0.10	0.10	n.d.	0.05
H_2O	0.50	0.55	0.70	0.70	1.00	1.00	1.00	n.d.	0.55
liquidus temp. (ºC)	1333.89	1379.68	1318.17	1318.17	1367.69	1367.69	1367.69	n/a	1379.68
pressure (kbar)	2.5	2.5	2.5	2.5	2.5	2.5	2.5	n/a	2.5
fO_2	QFM+1	QFM+1	QFM+1	QFM+1	QFM+1	QFM+1	QFM+1	n/a	QFM+1
temperature increment (ºC)	25	25	25	25	25	25	25	n/a	25

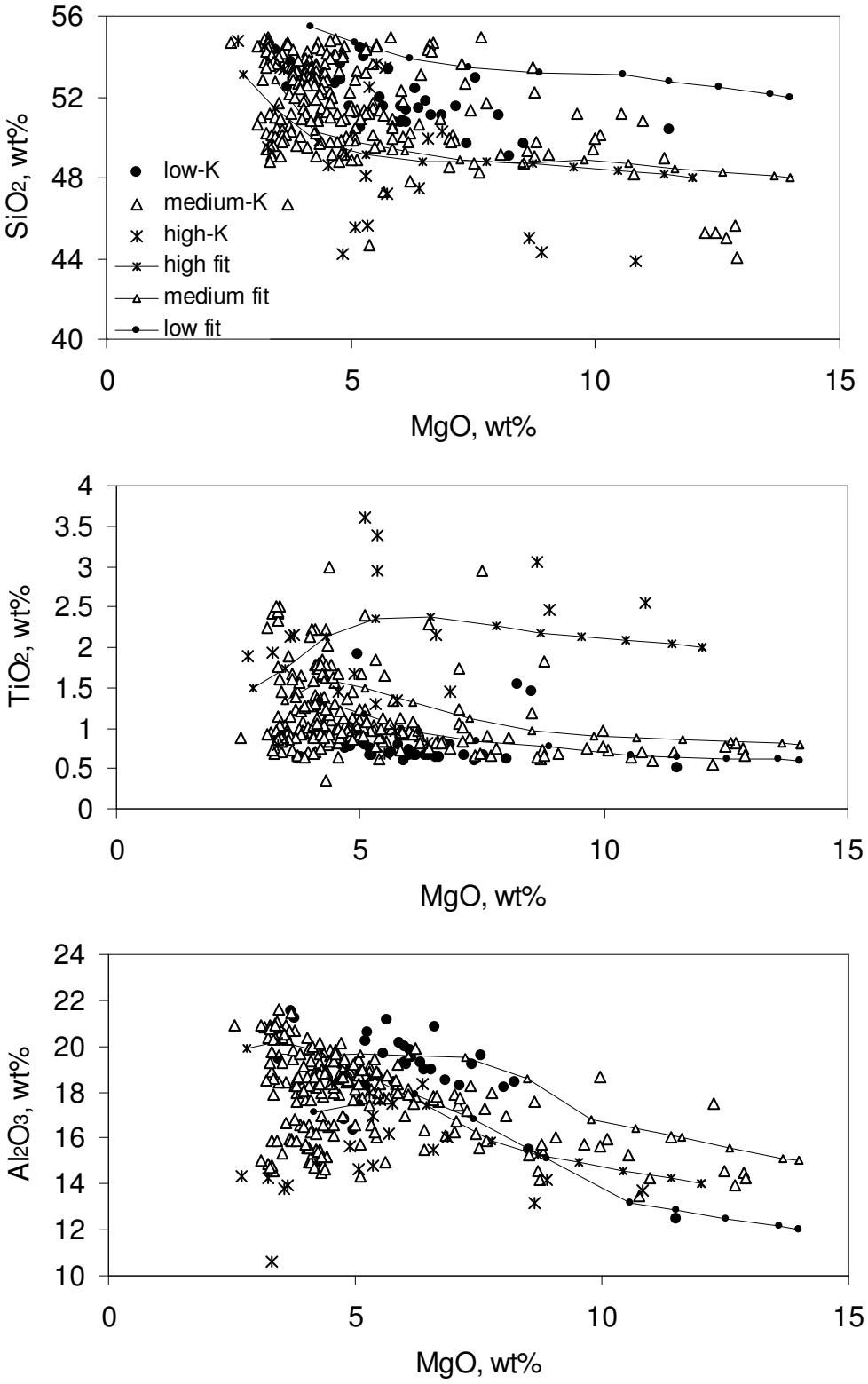

Figure B.1 Major element vs. MgO plots for the Aleutian arc.

Figure B.1 (continued)

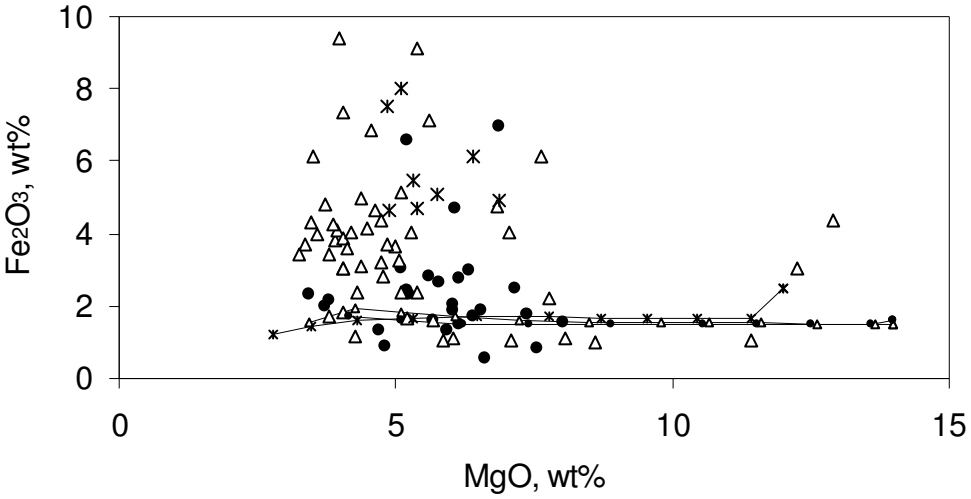

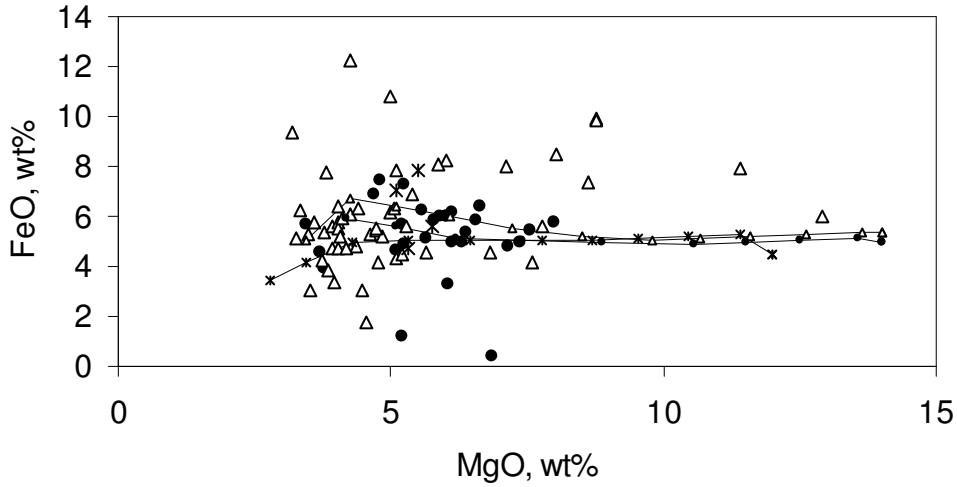

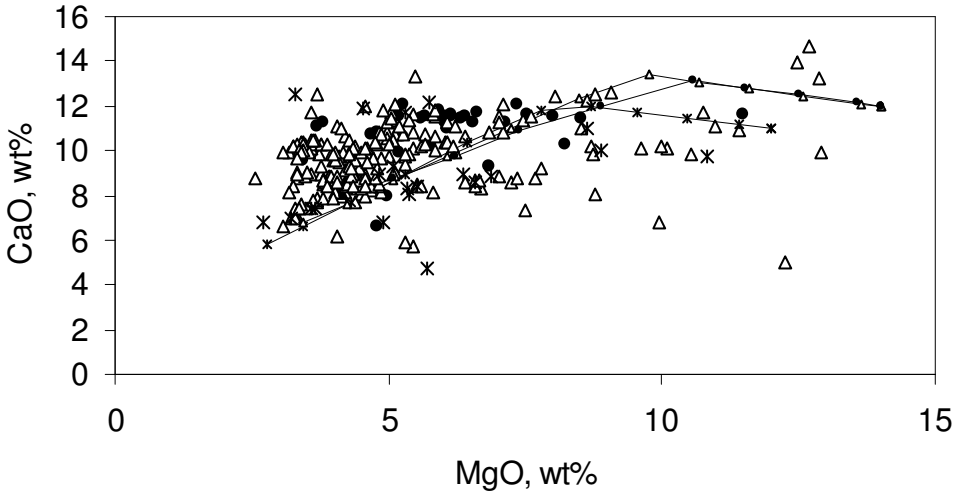

Figure B.1 (continued)

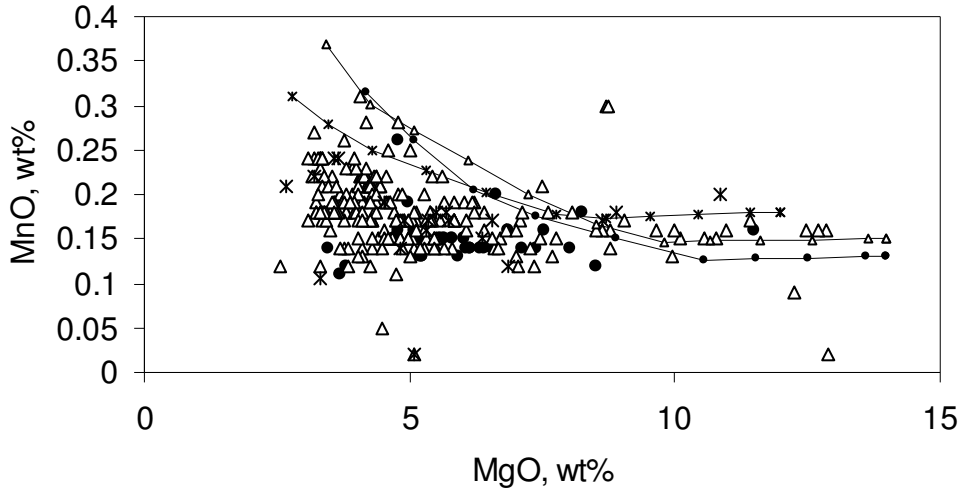

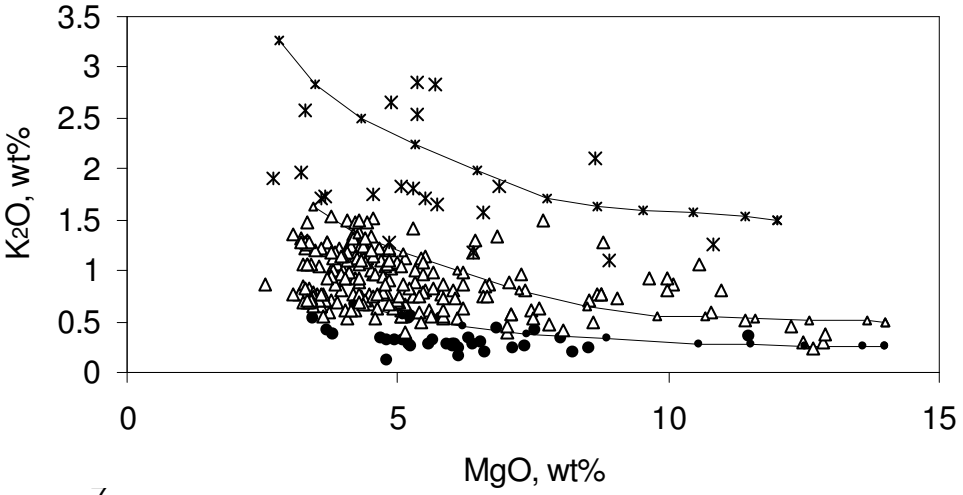

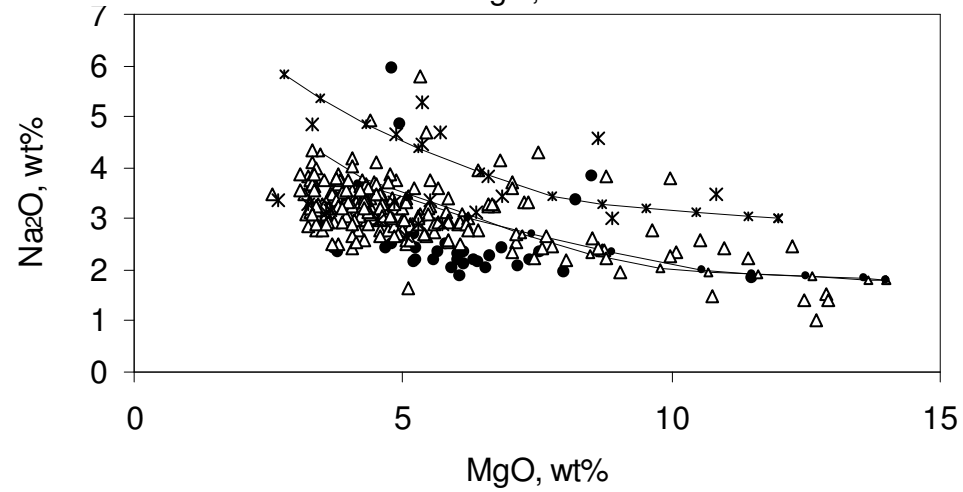

Figure B.1 (continued)

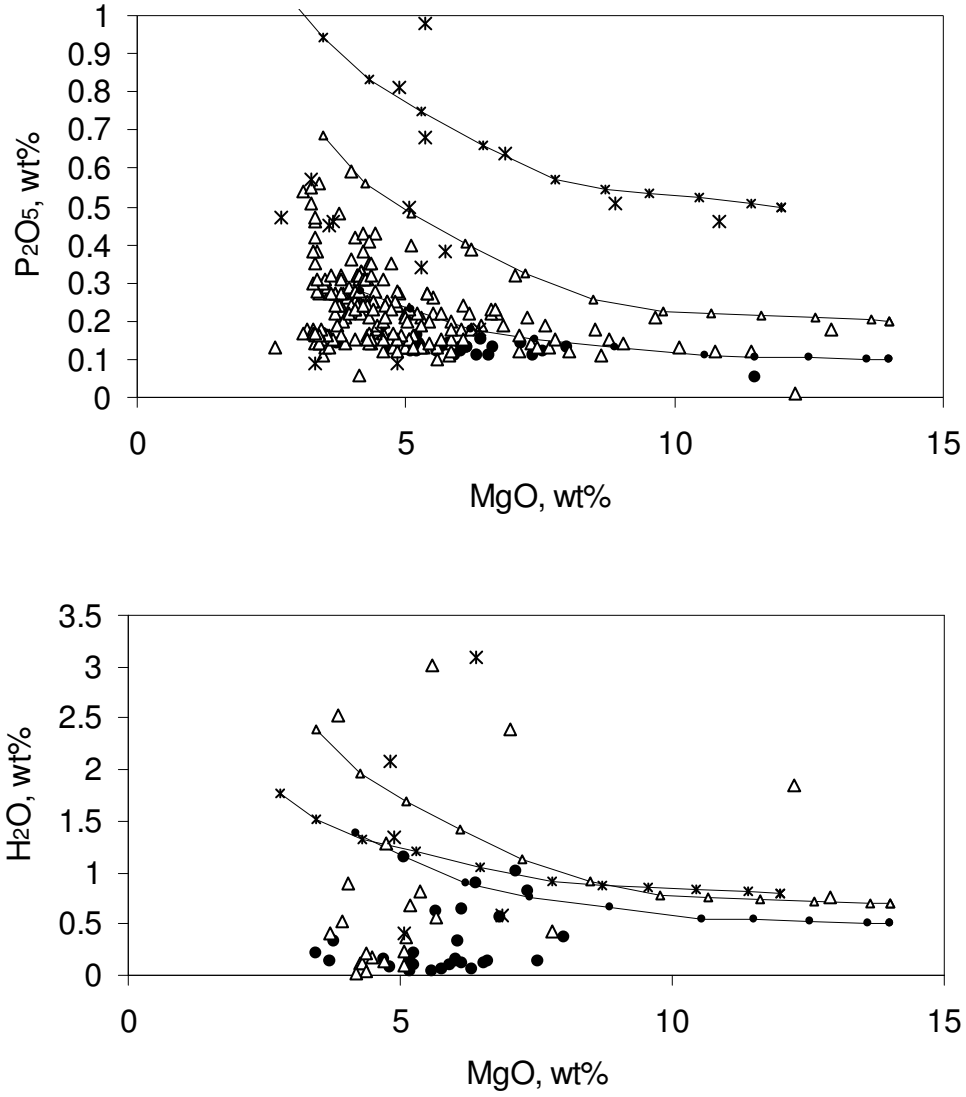

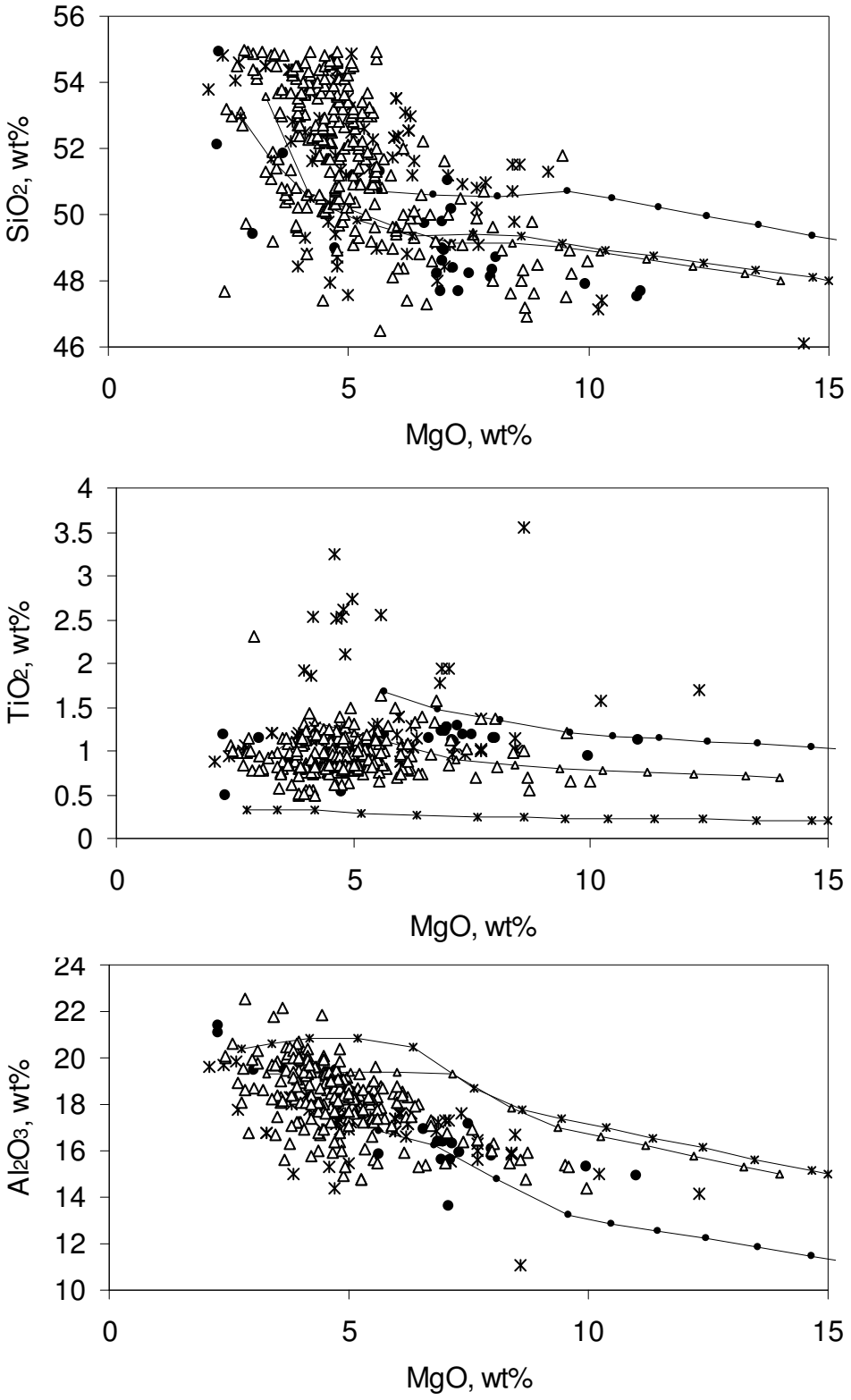

Figure B.2 Major element vs. MgO plots for Central America. Symbols as in Figure B.1.

Figure B.2 (continued)

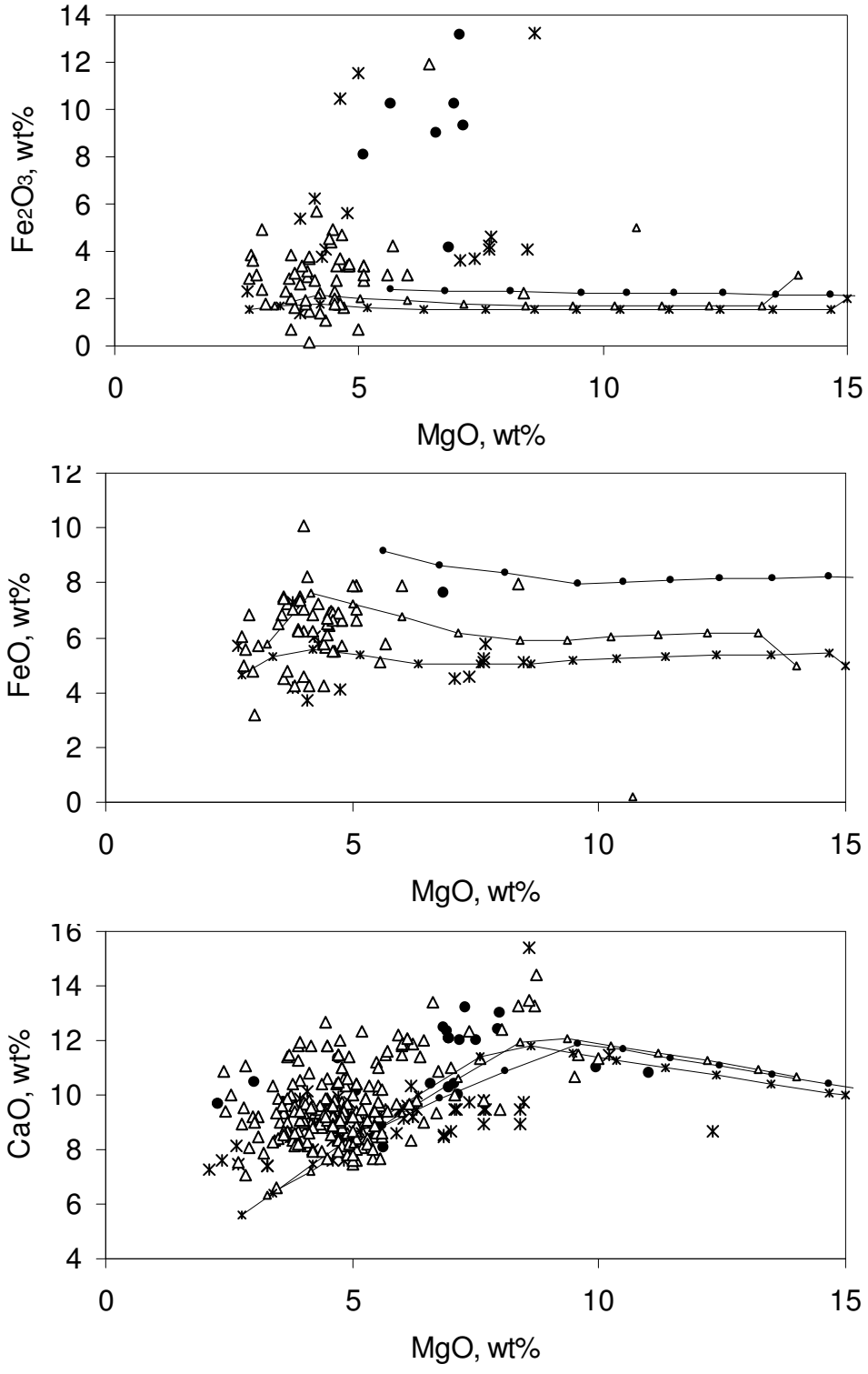

Figure B.2 (continued)

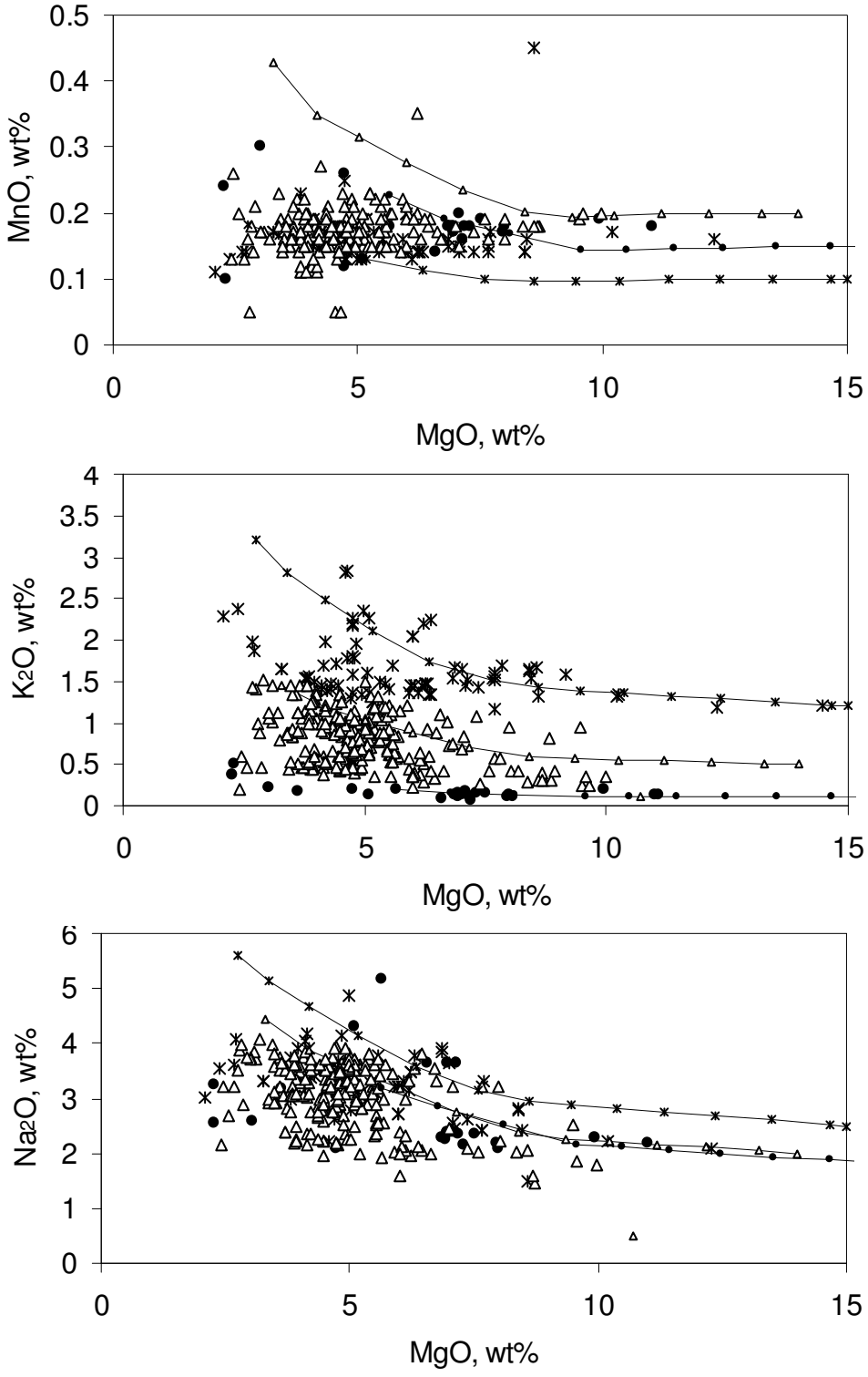

Figure B.2 (continued)

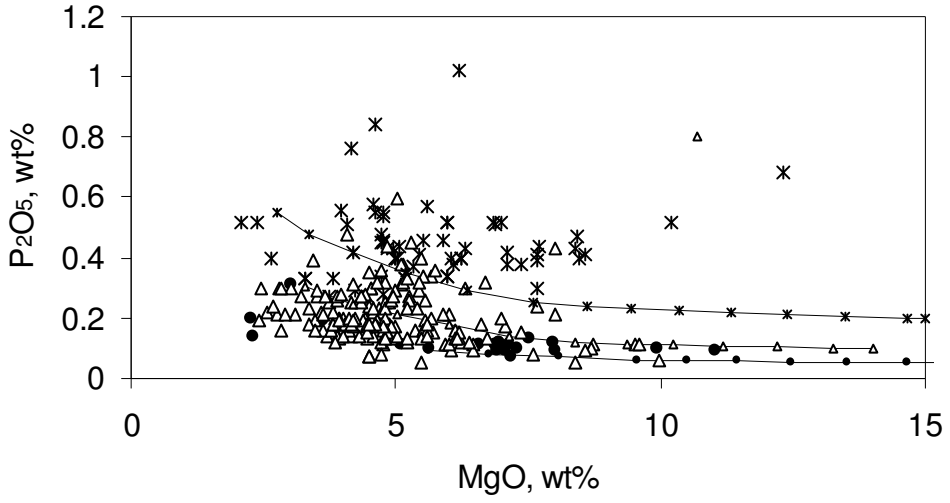

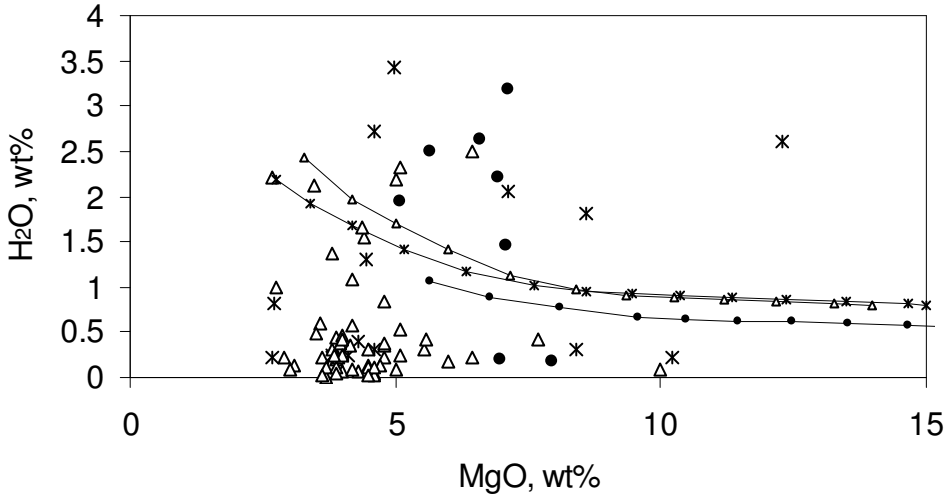

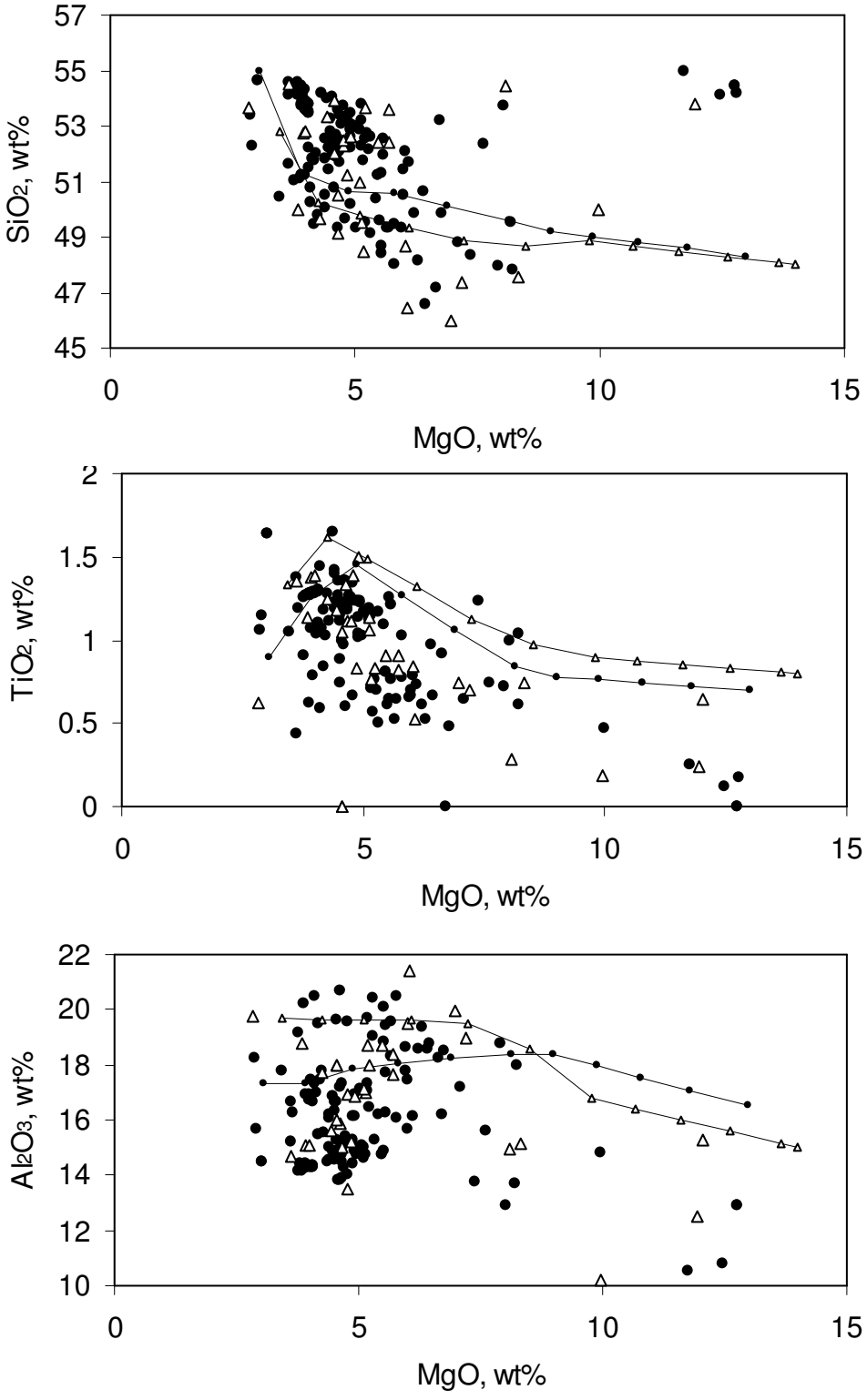

Figure B.3 Major element vs. MgO plots for the Izu-Bonin arc. Symbols as in Figure B.1.

Figure B.3 (continued)

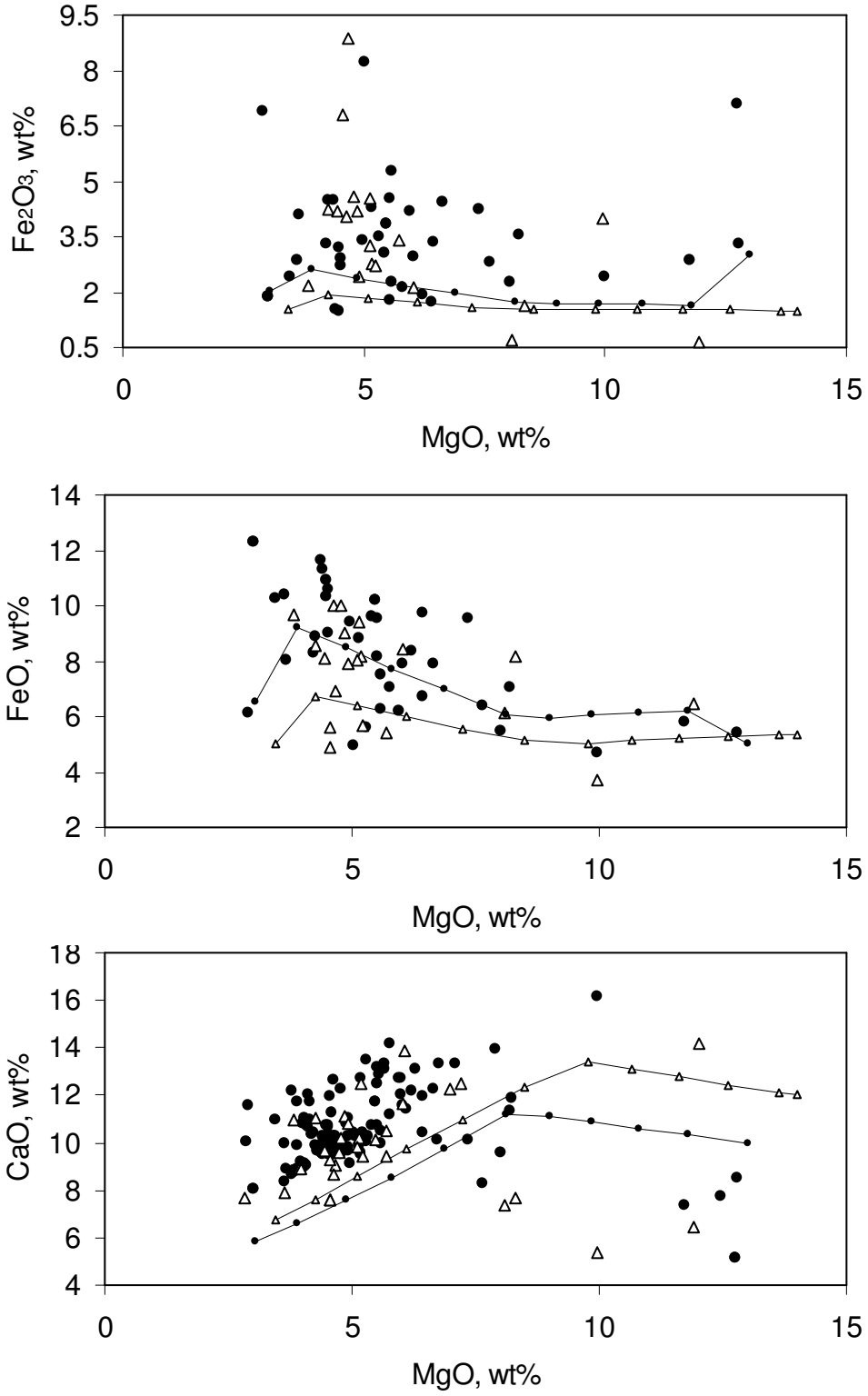

Figure B.3 (continued)

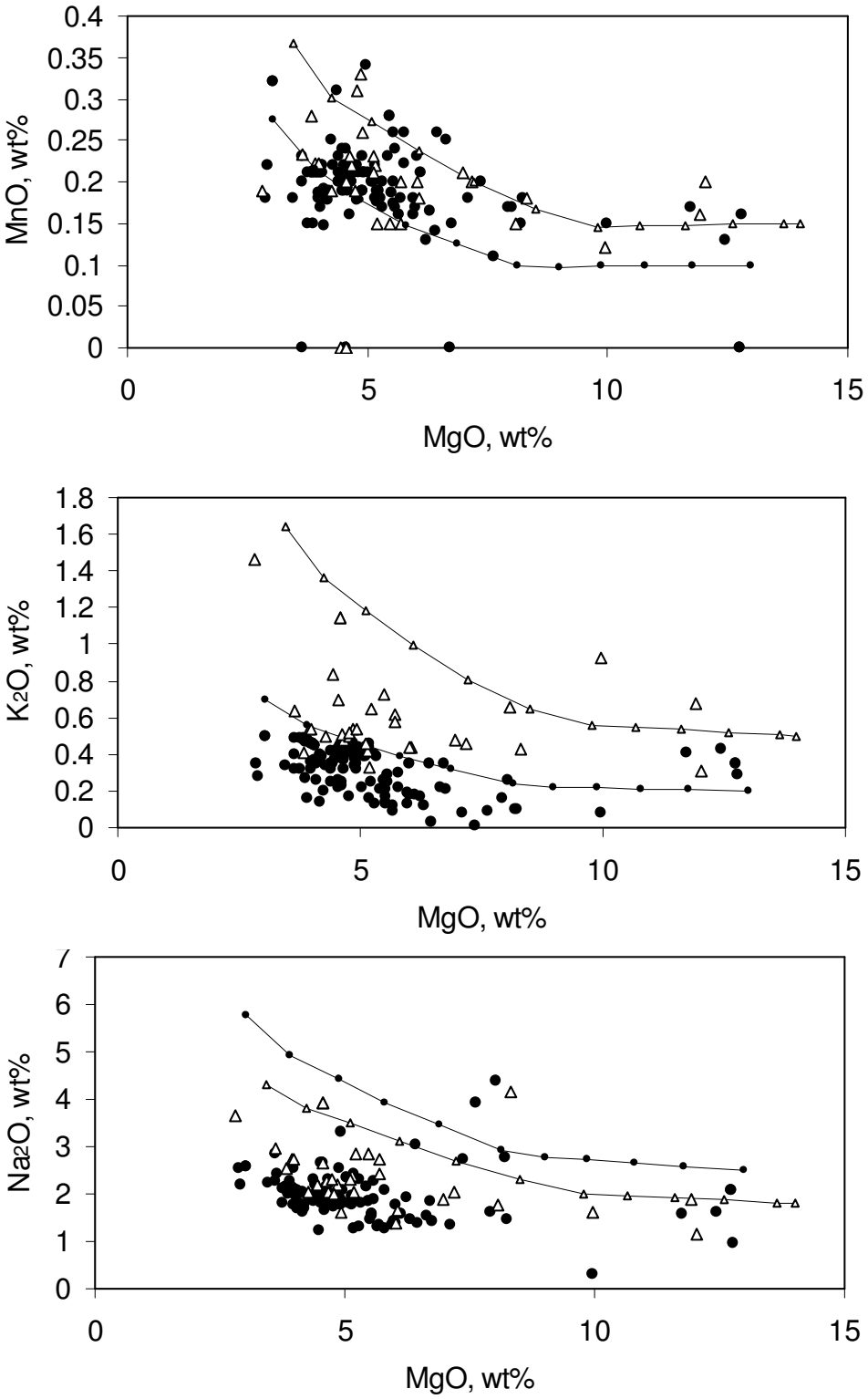

Figure B.3 (continued)

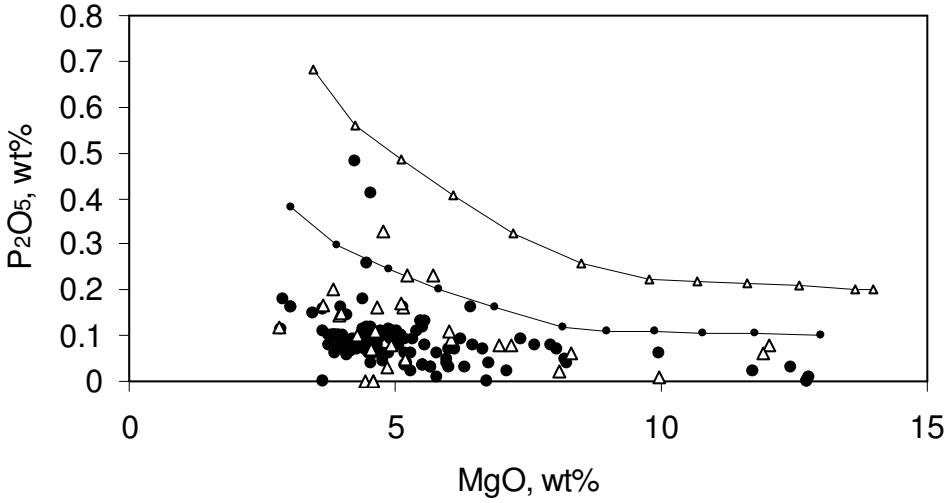

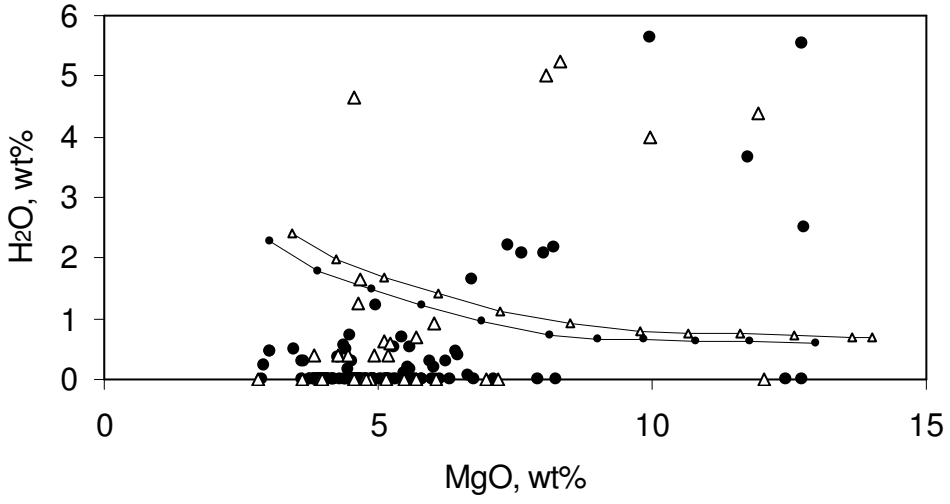

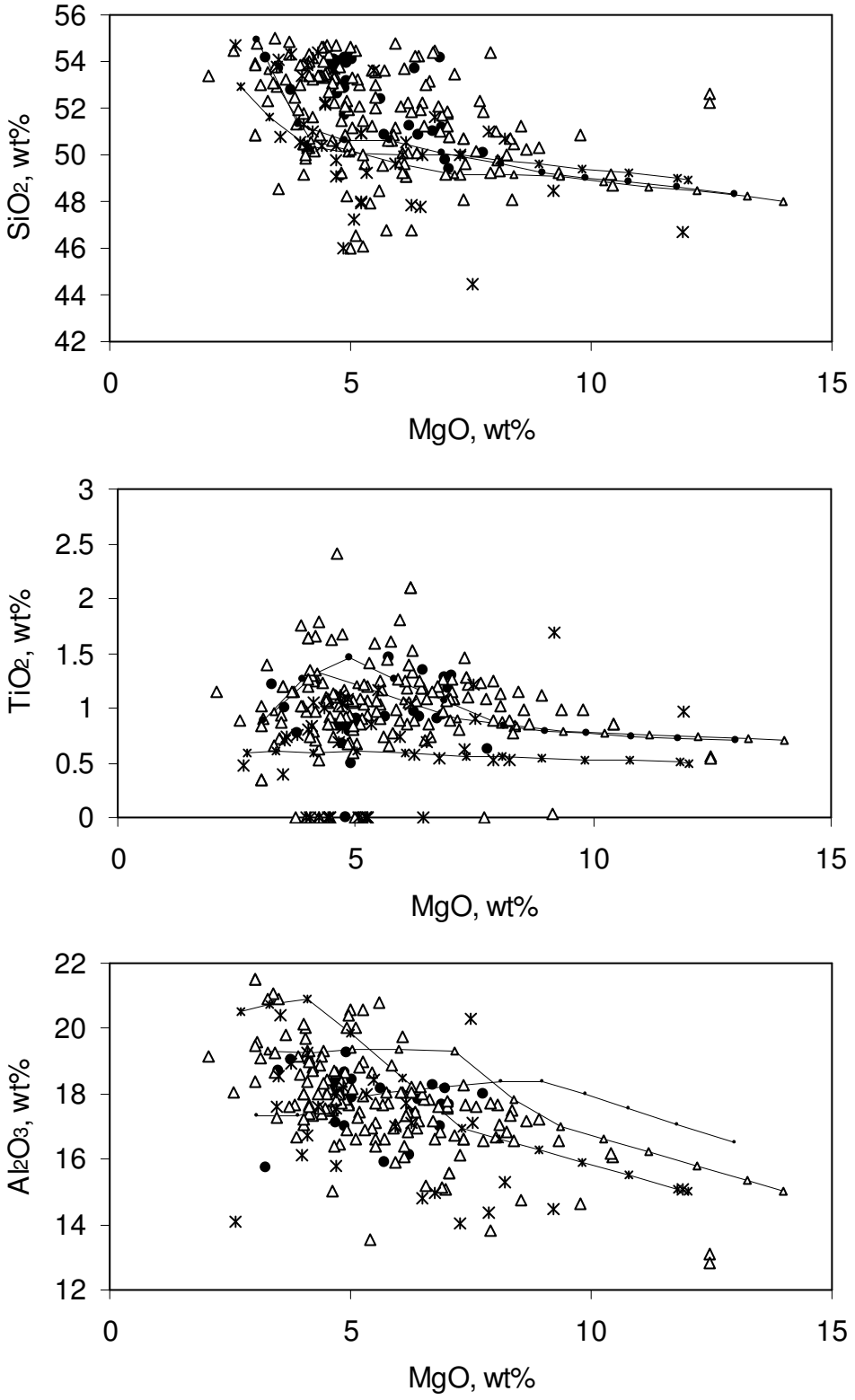

Figure B.4 Major element vs. MgO plots for the Kurile arc. Symbols as in Figure B.1.

Figure B.4 (continued)

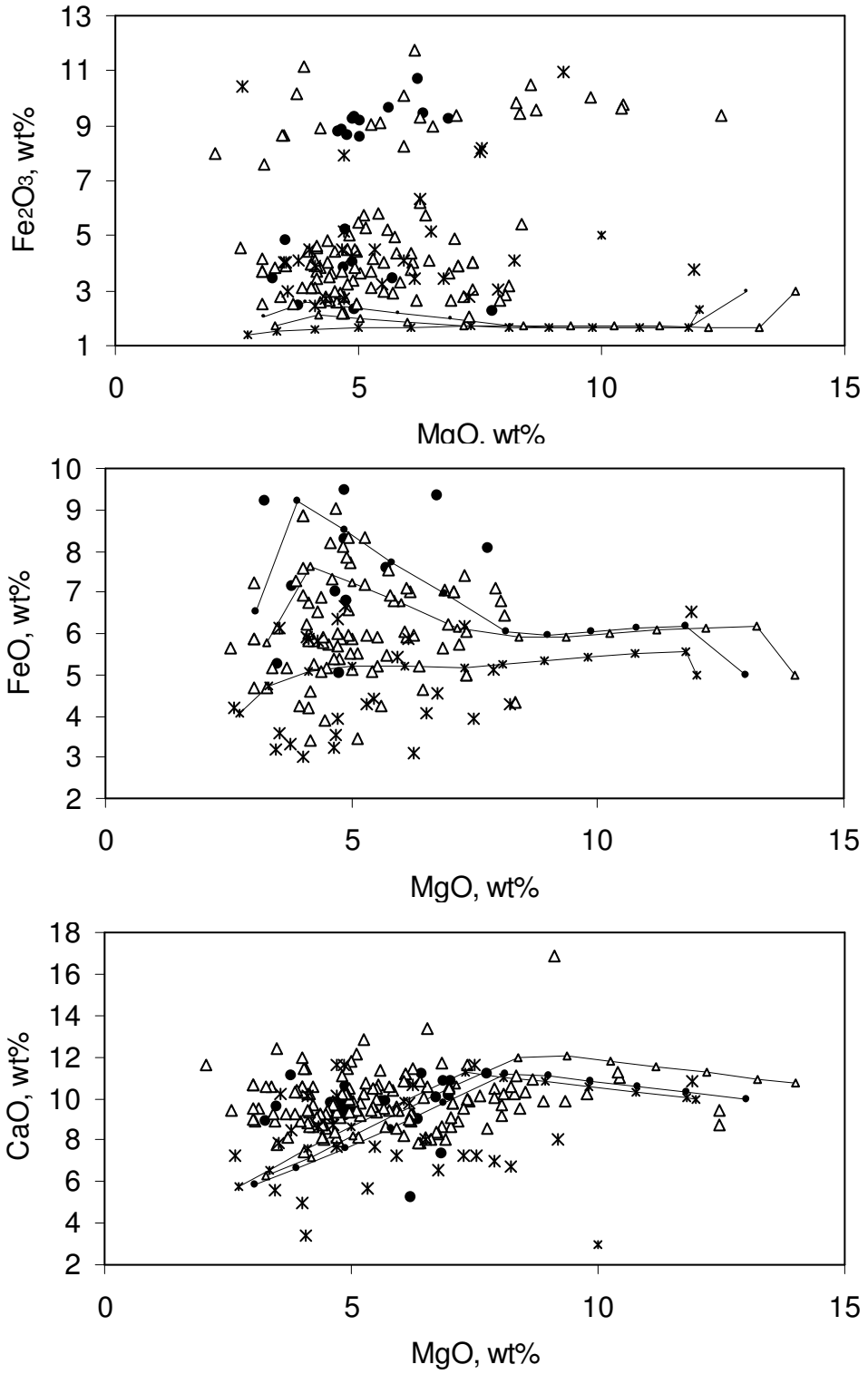

Figure B.4 (continued)

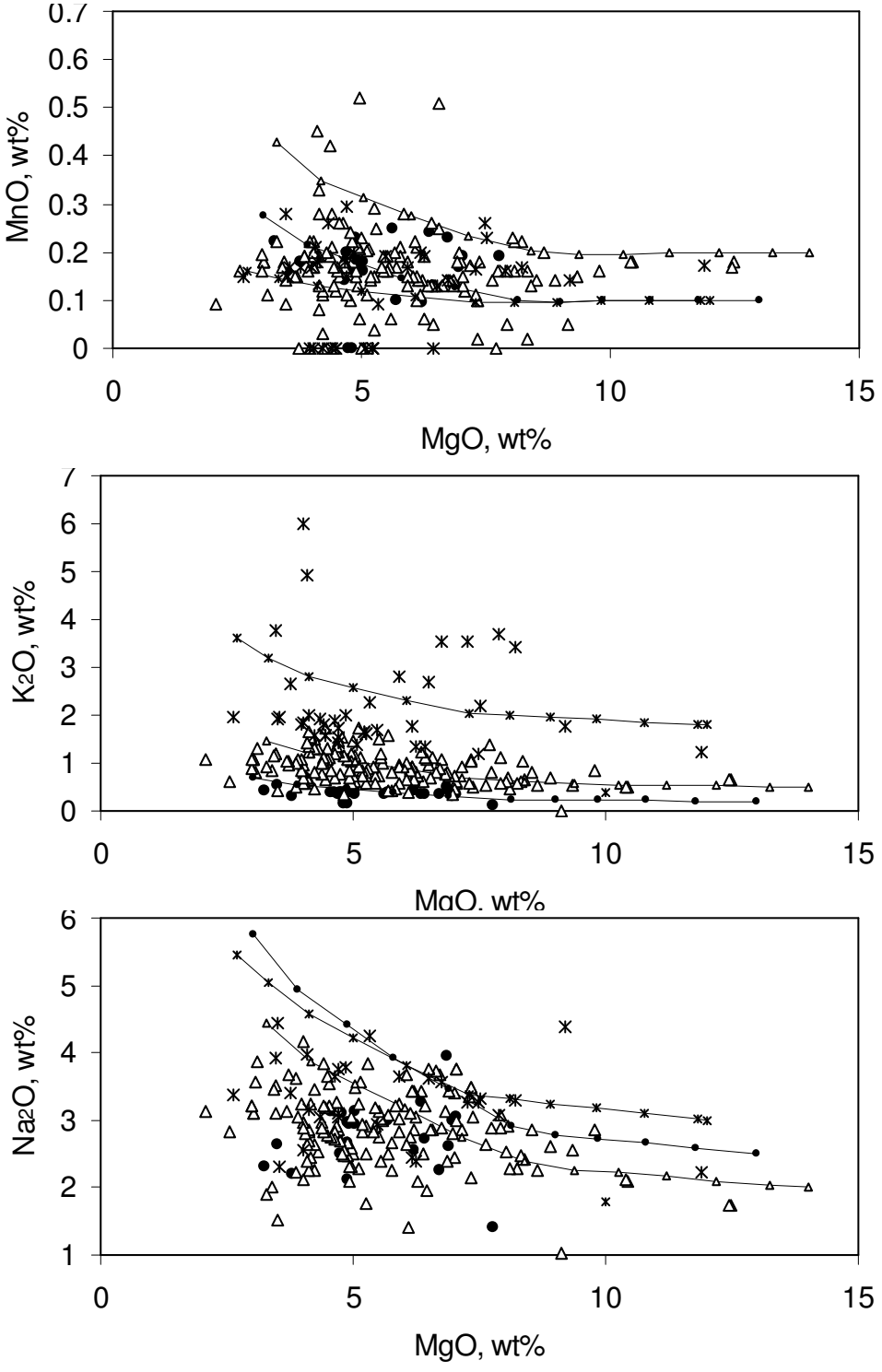

Figure B.4 (continued)

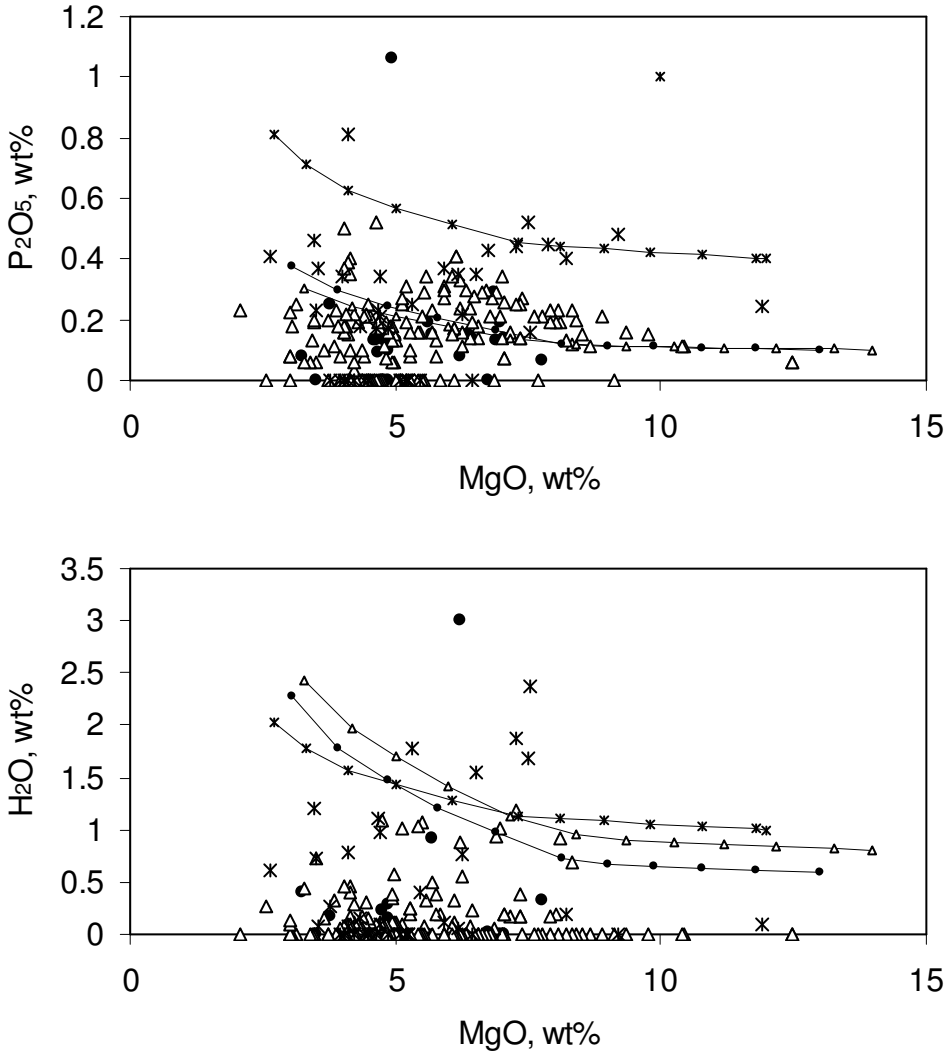

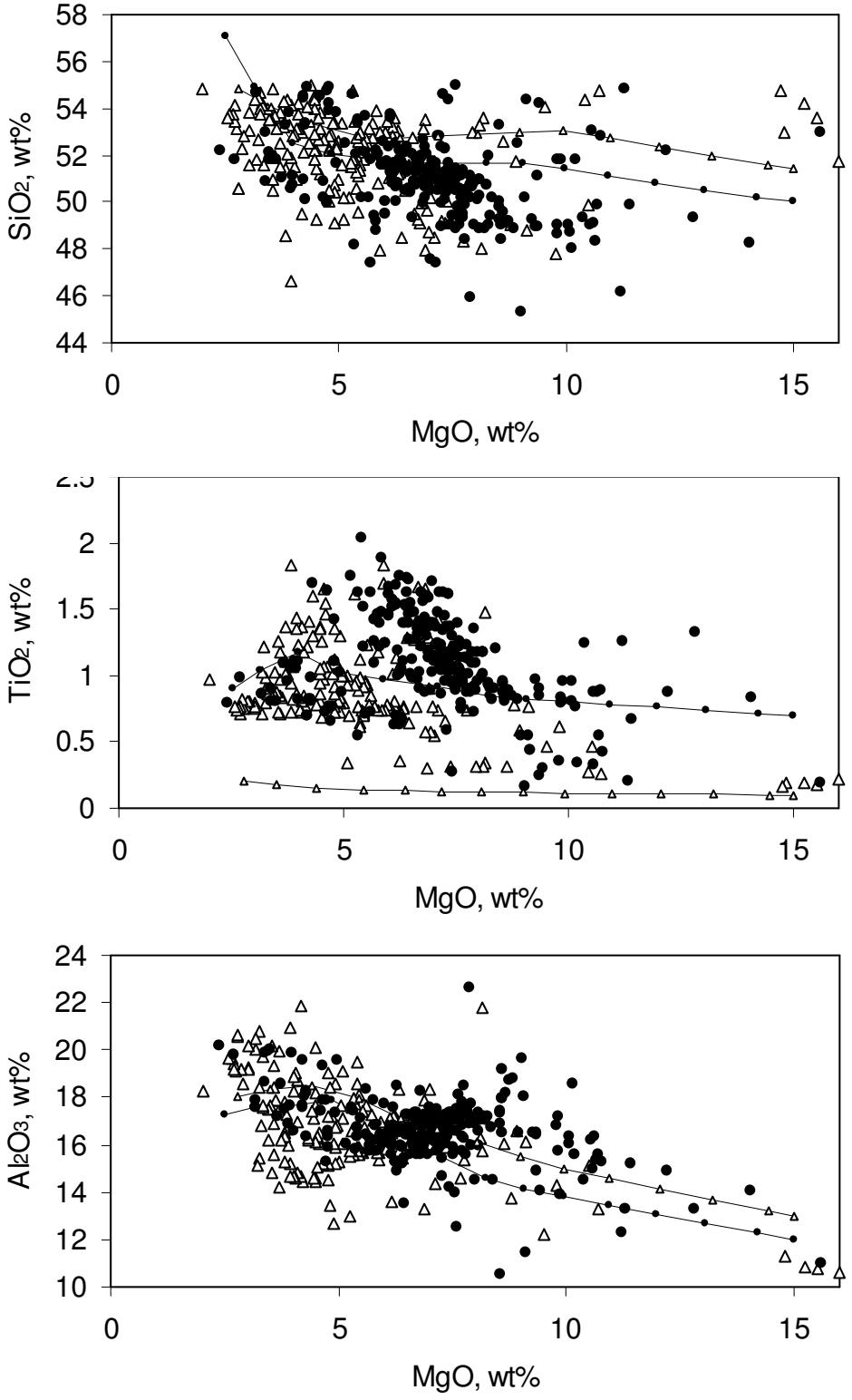

Figure B.5 Major element vs. MgO plots for the Marianas arc. Symbols as in Figure B.1.

Figure B.5 (continued)

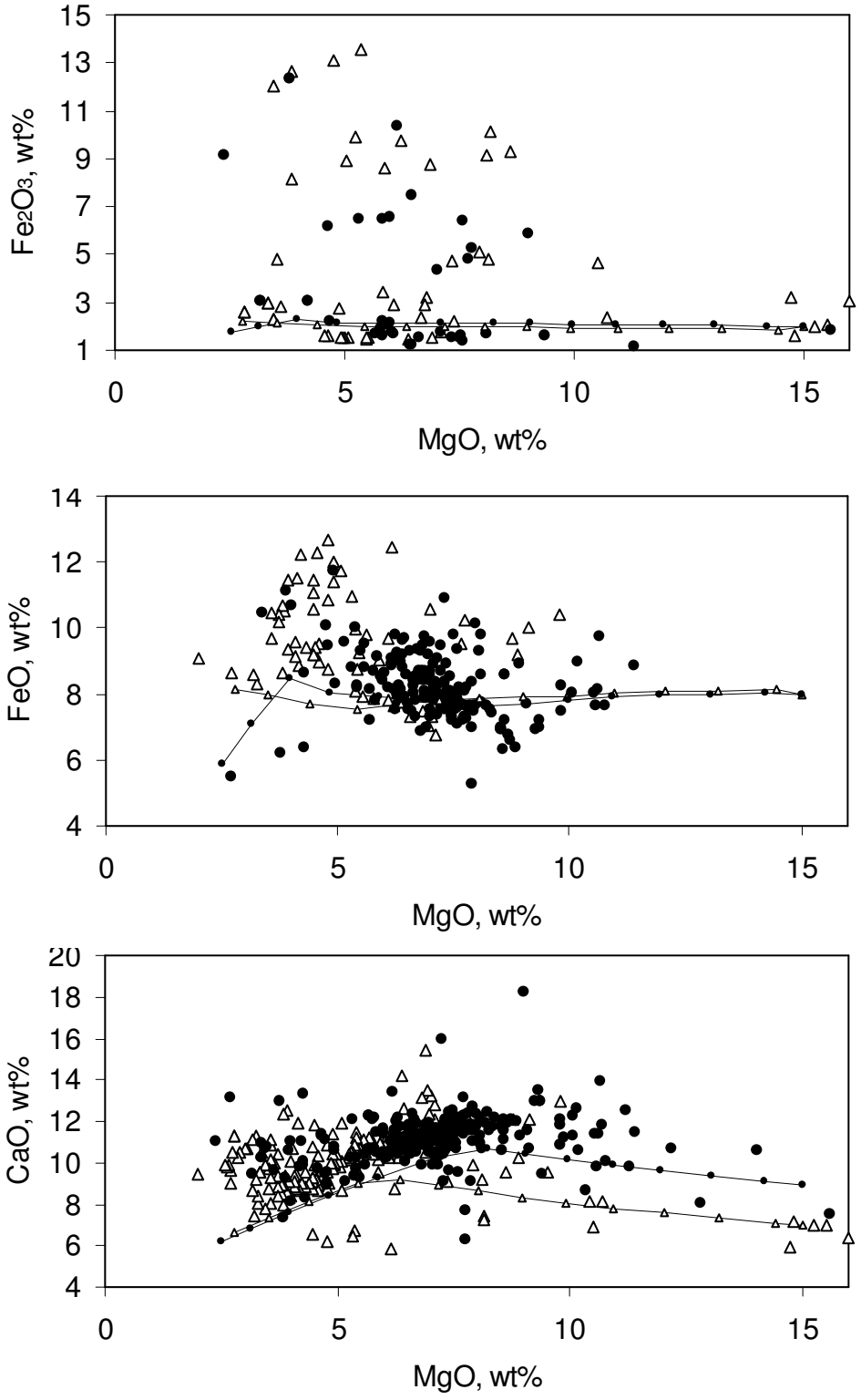

Figure B.5 (continued)

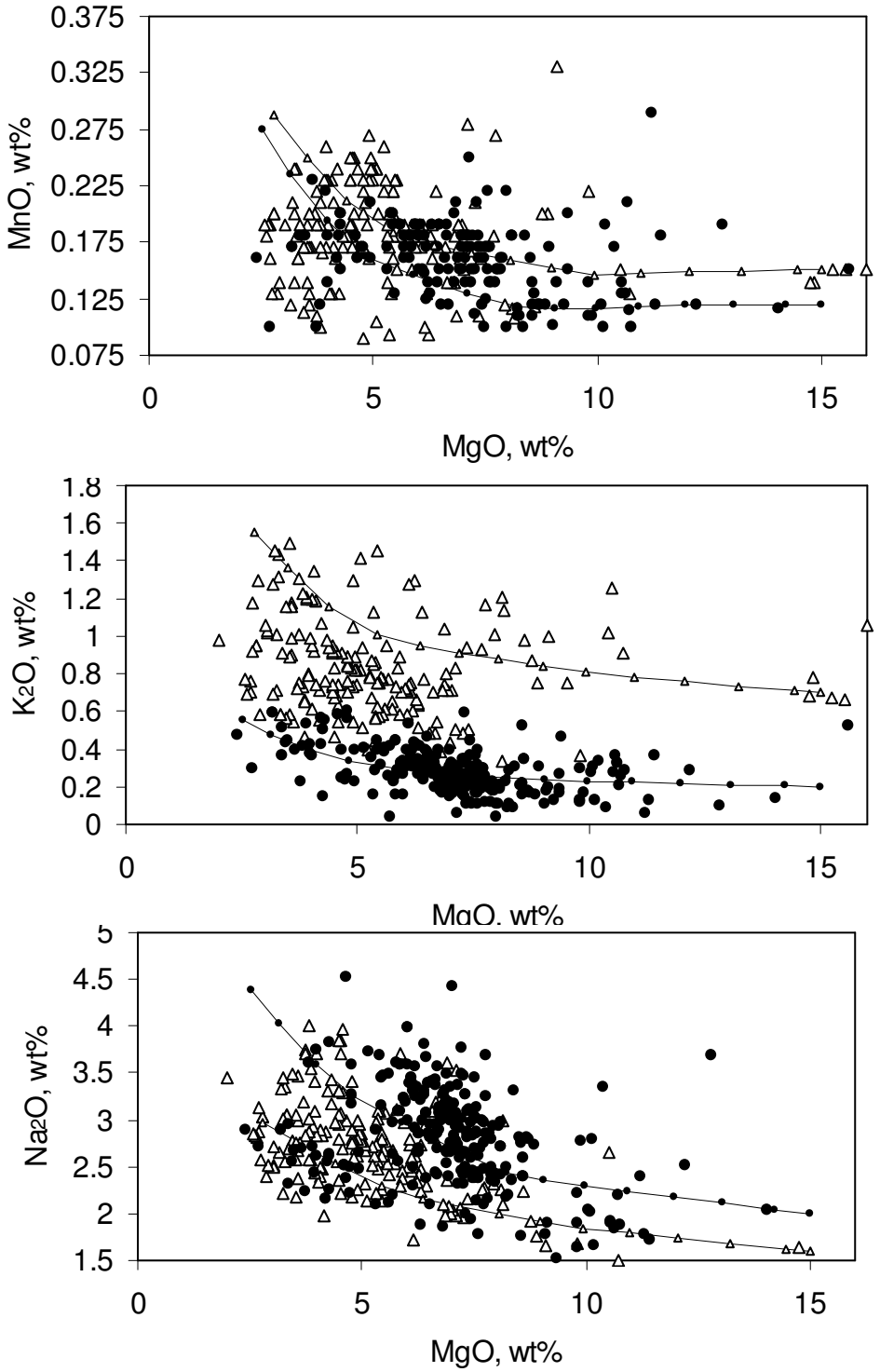

Figure B.5 (continued)

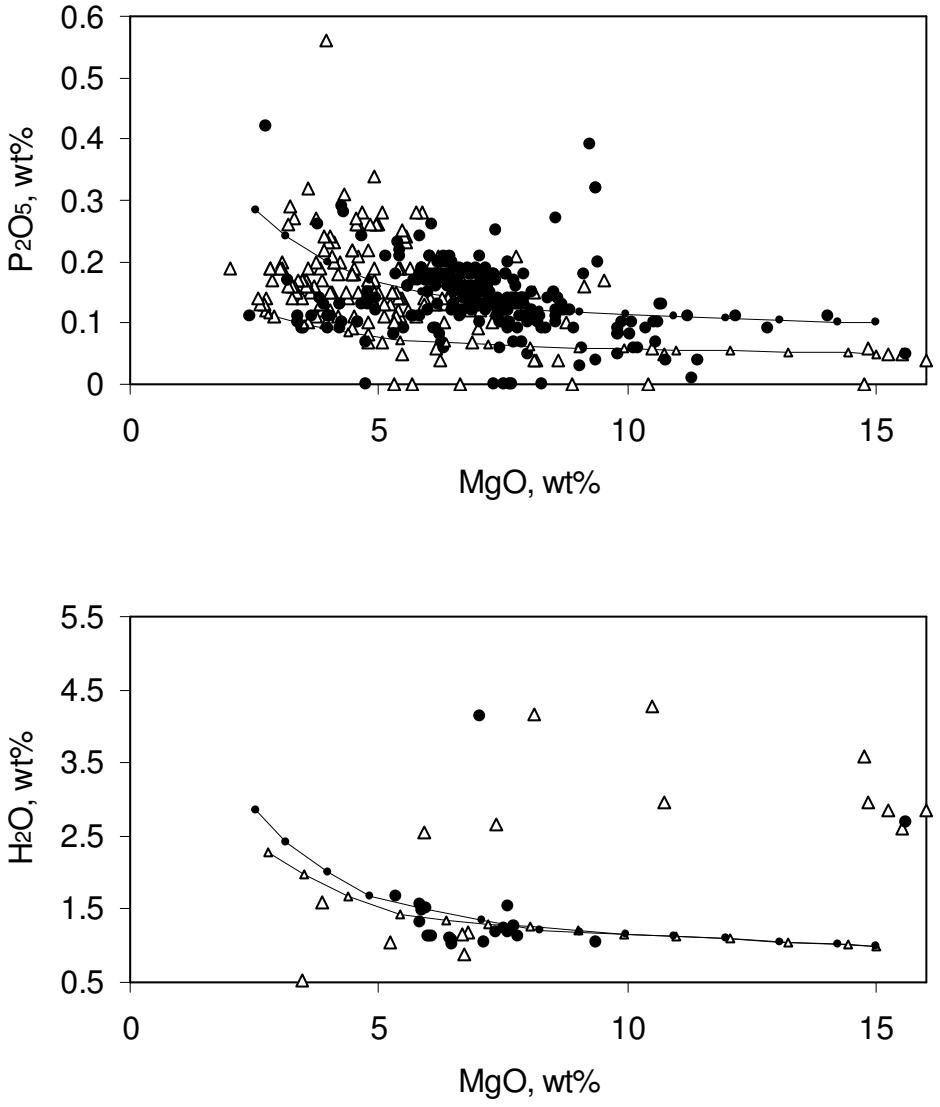

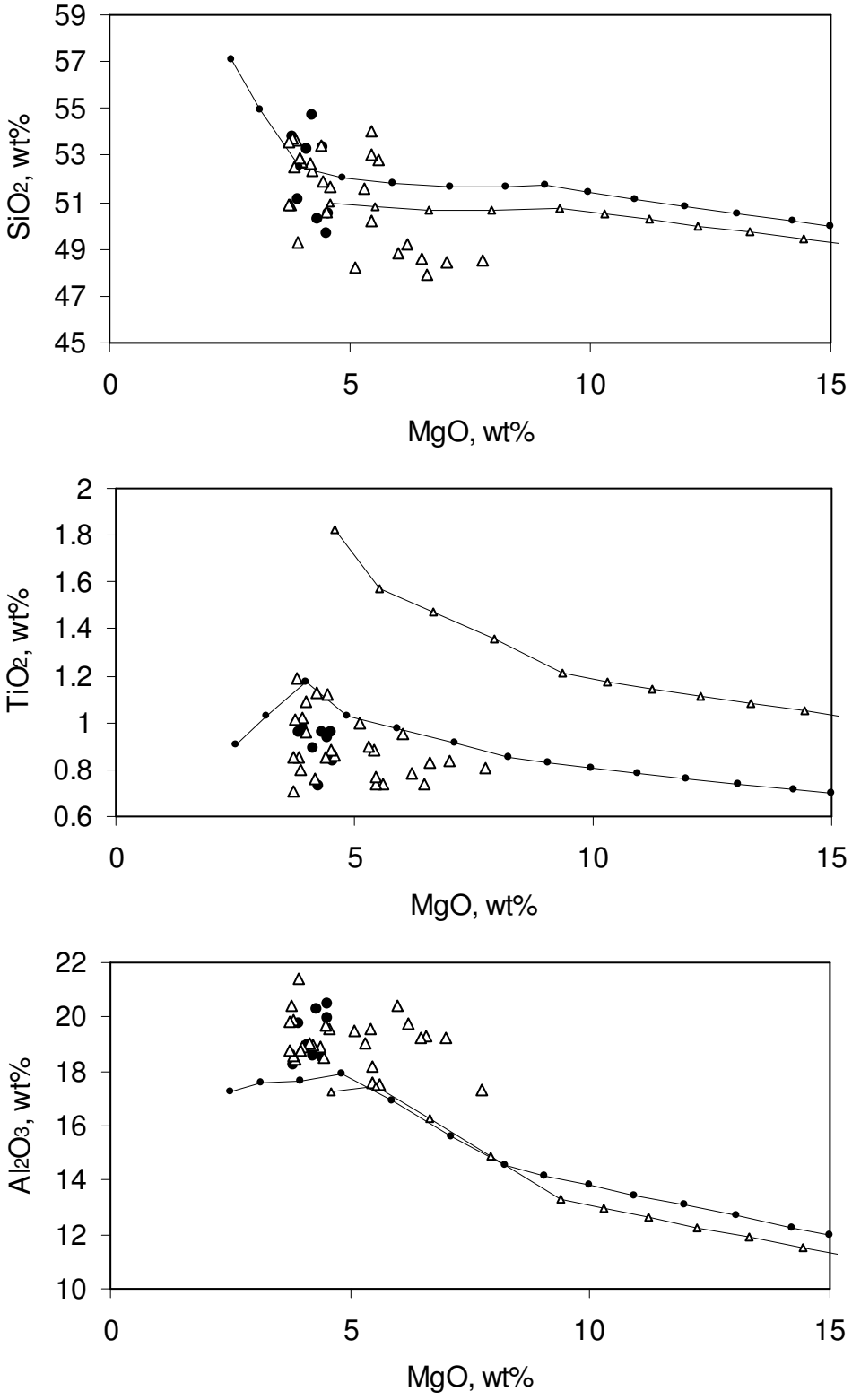

Figure B.6 Major element vs. MgO plots for the Northern Lesser Antilles arc. Symbols as in Figure B.1.

Figure B.6 (continued)

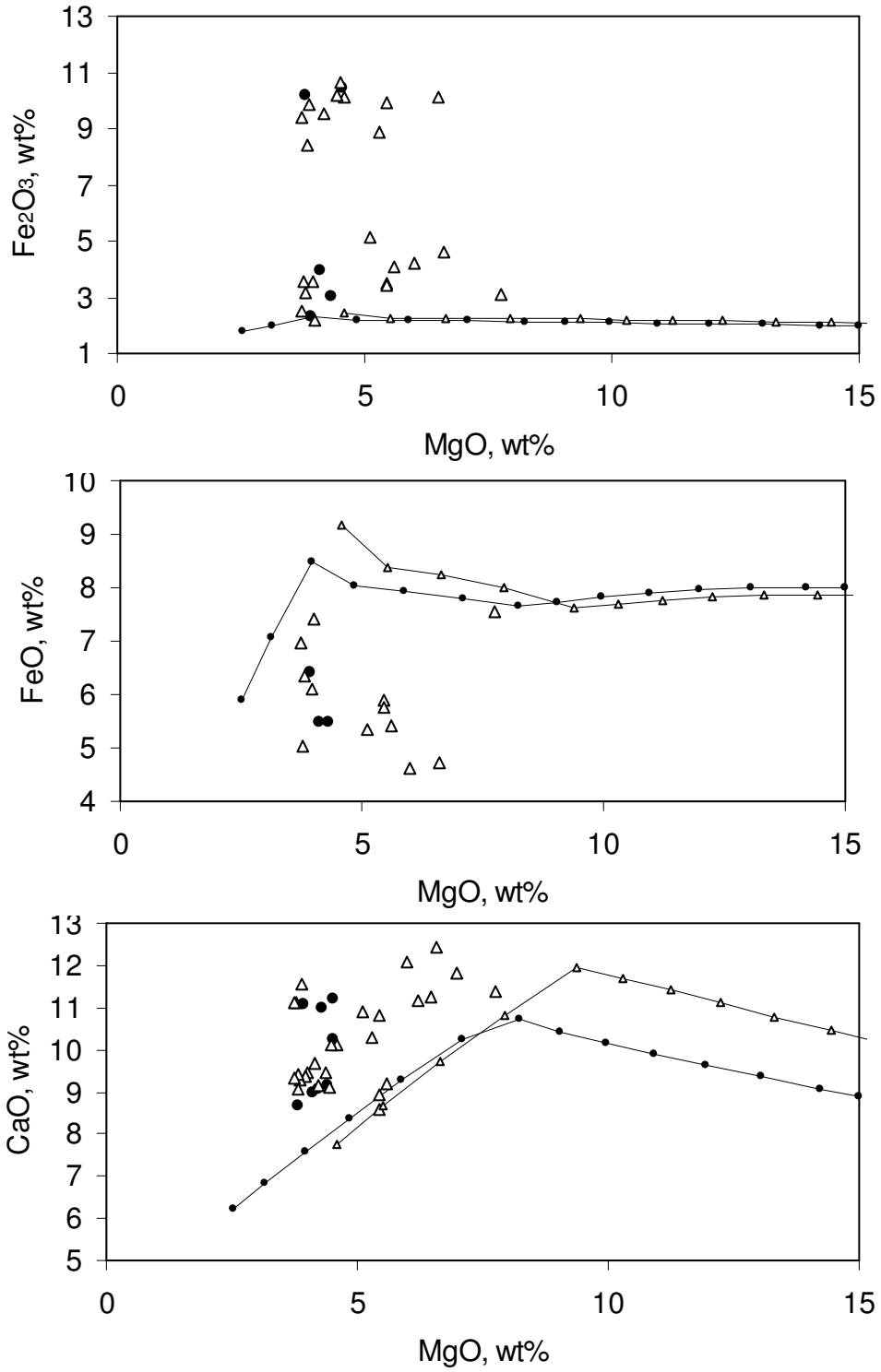

Figure B.6 (continued)

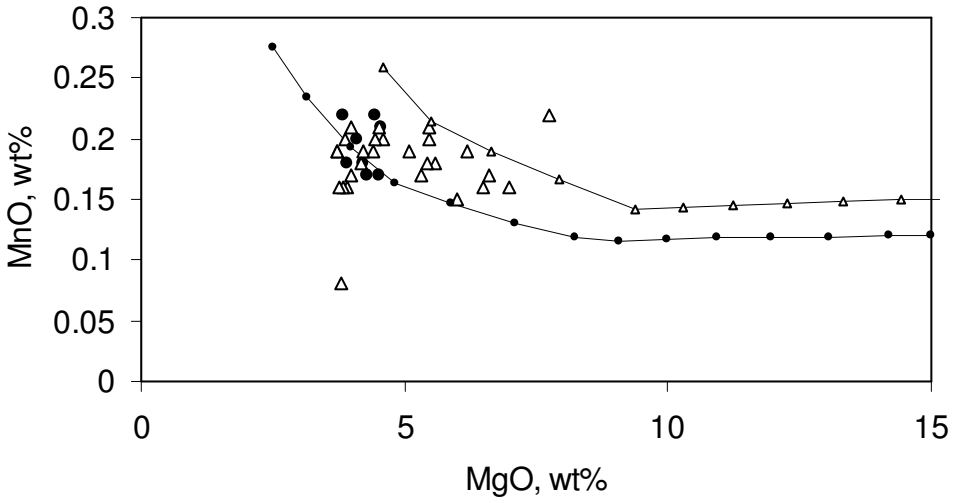

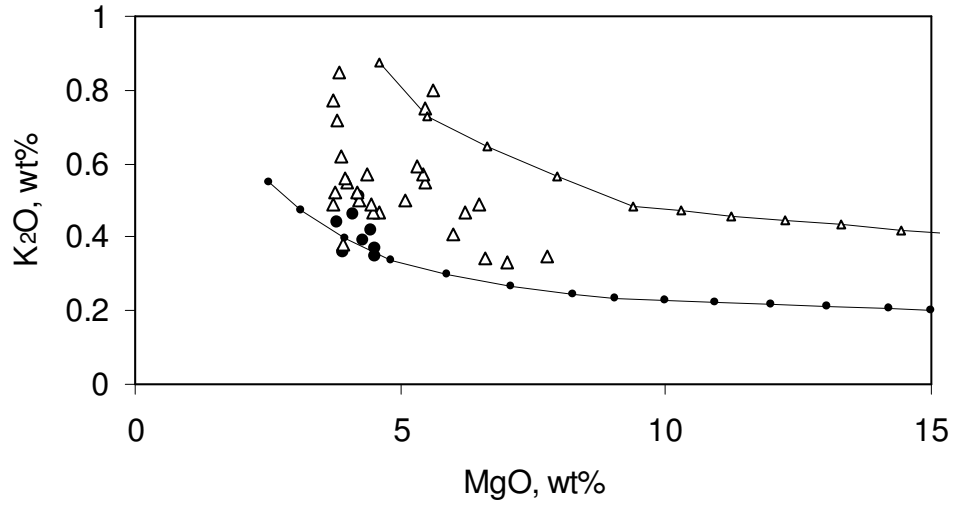

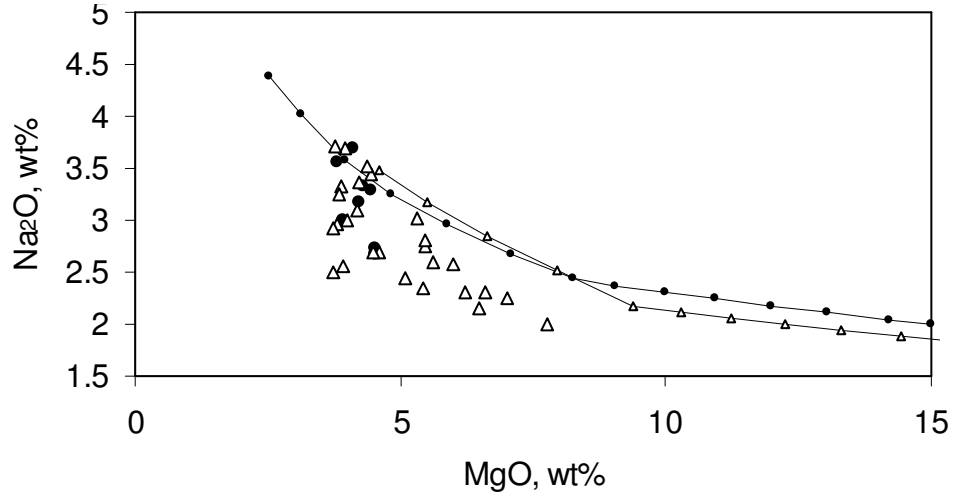

Figure B.6 (continued)

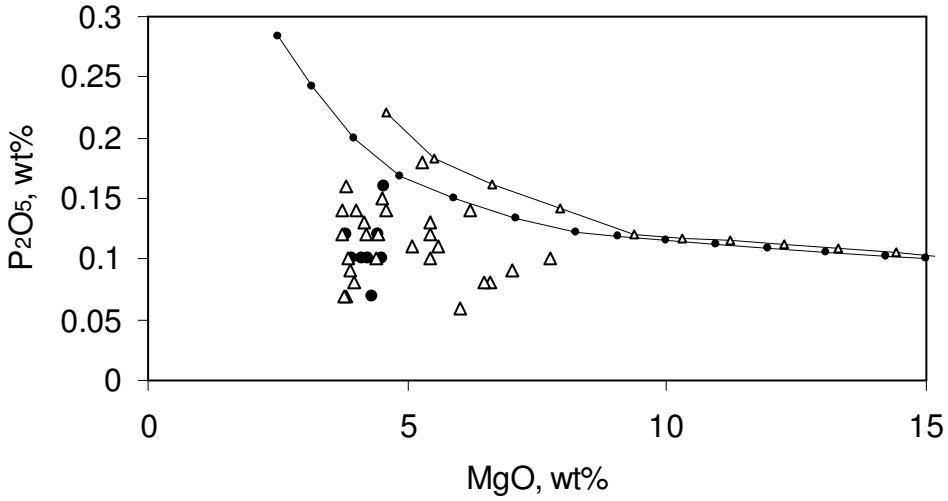

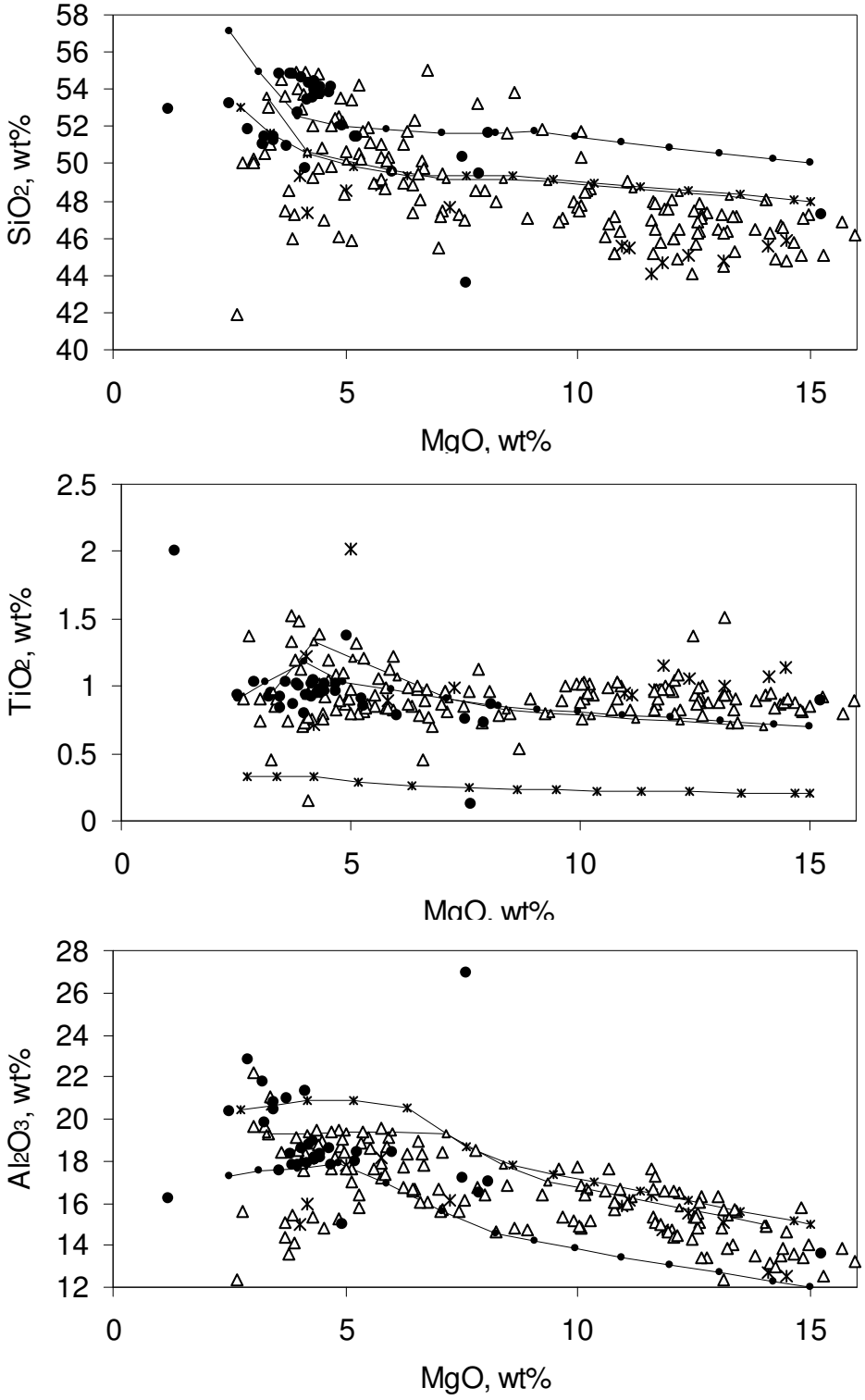

Figure B.7 Major element vs. MgO plots for the Southern Lesser Antilles arc. Symbols as in Figure B.1.

Figure B.7 (continued)

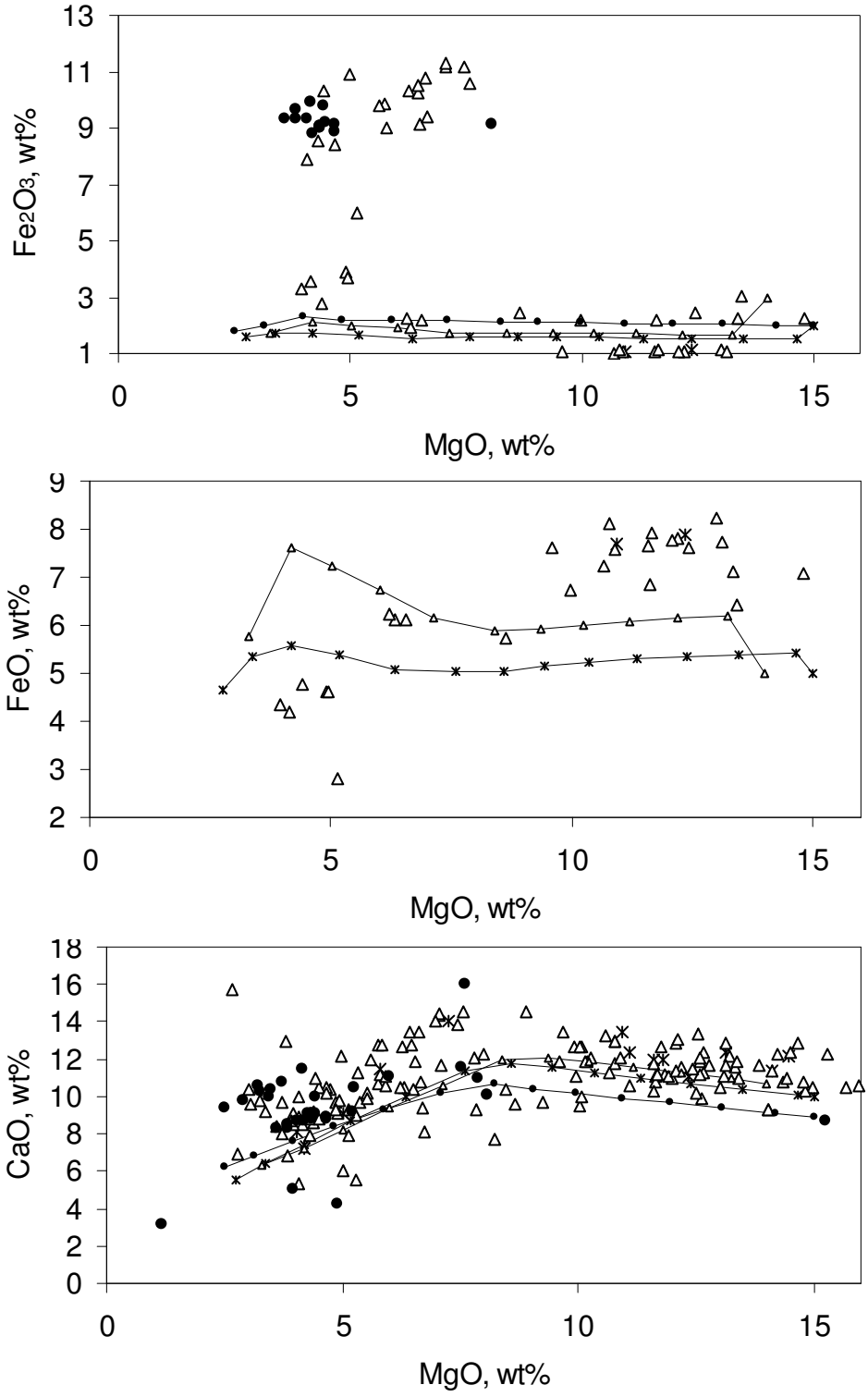

Figure B.7 (continued)

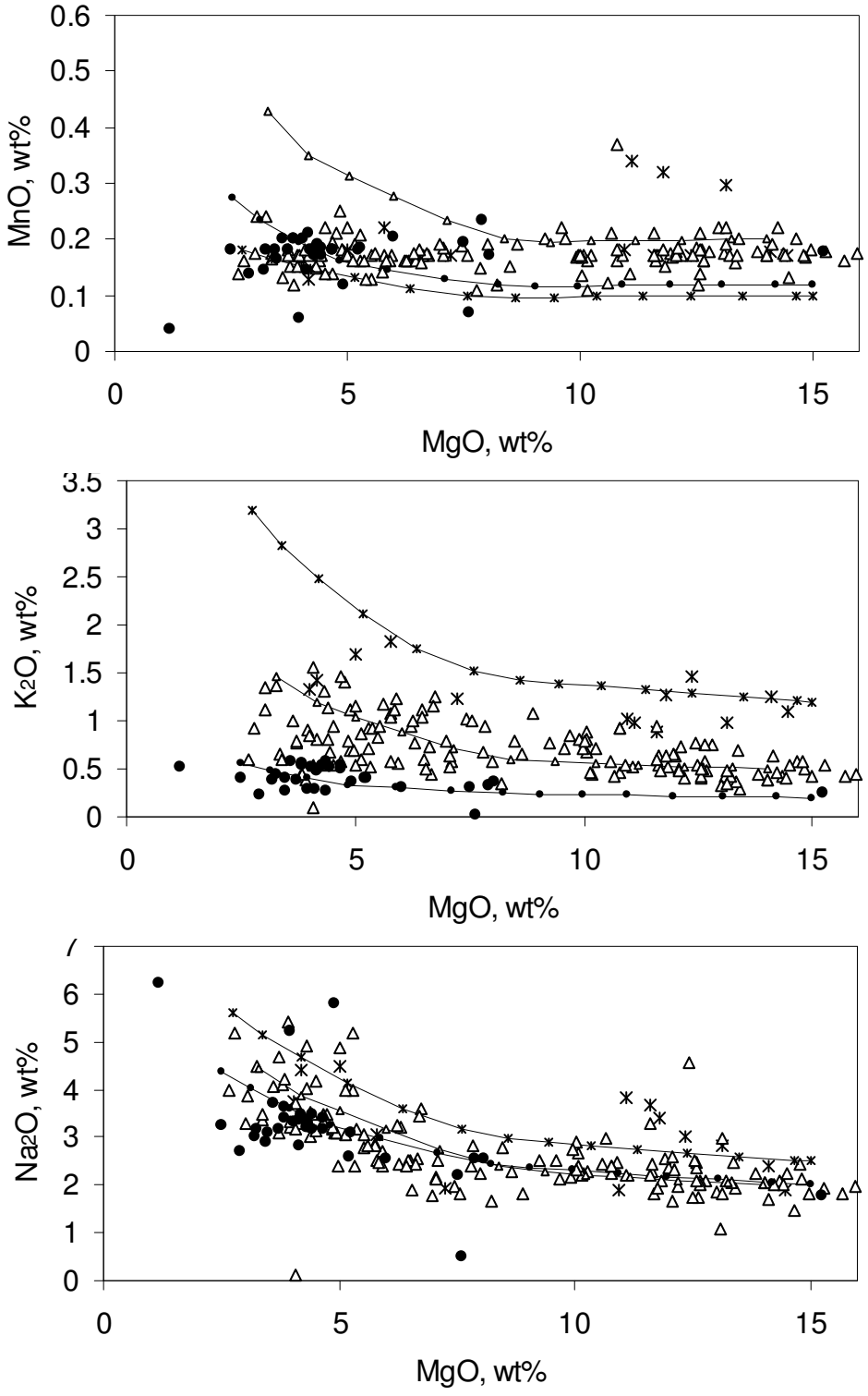

Figure B.7 (continued)

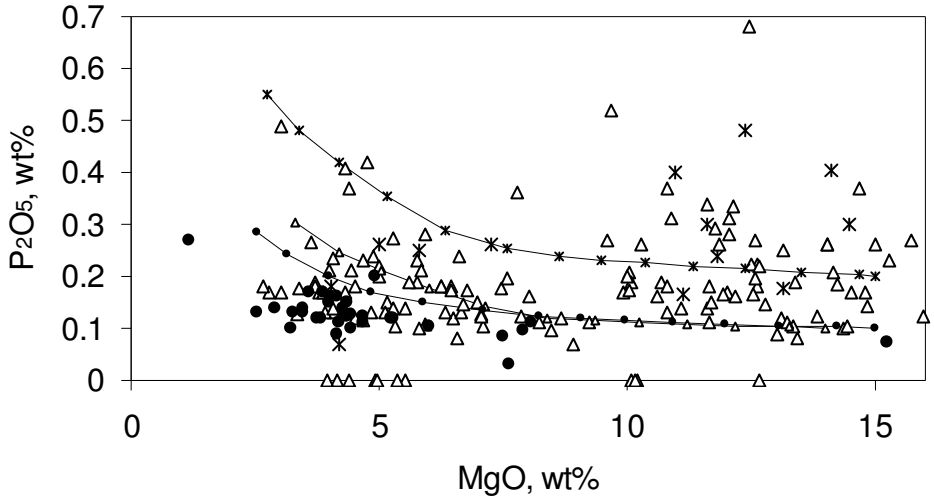

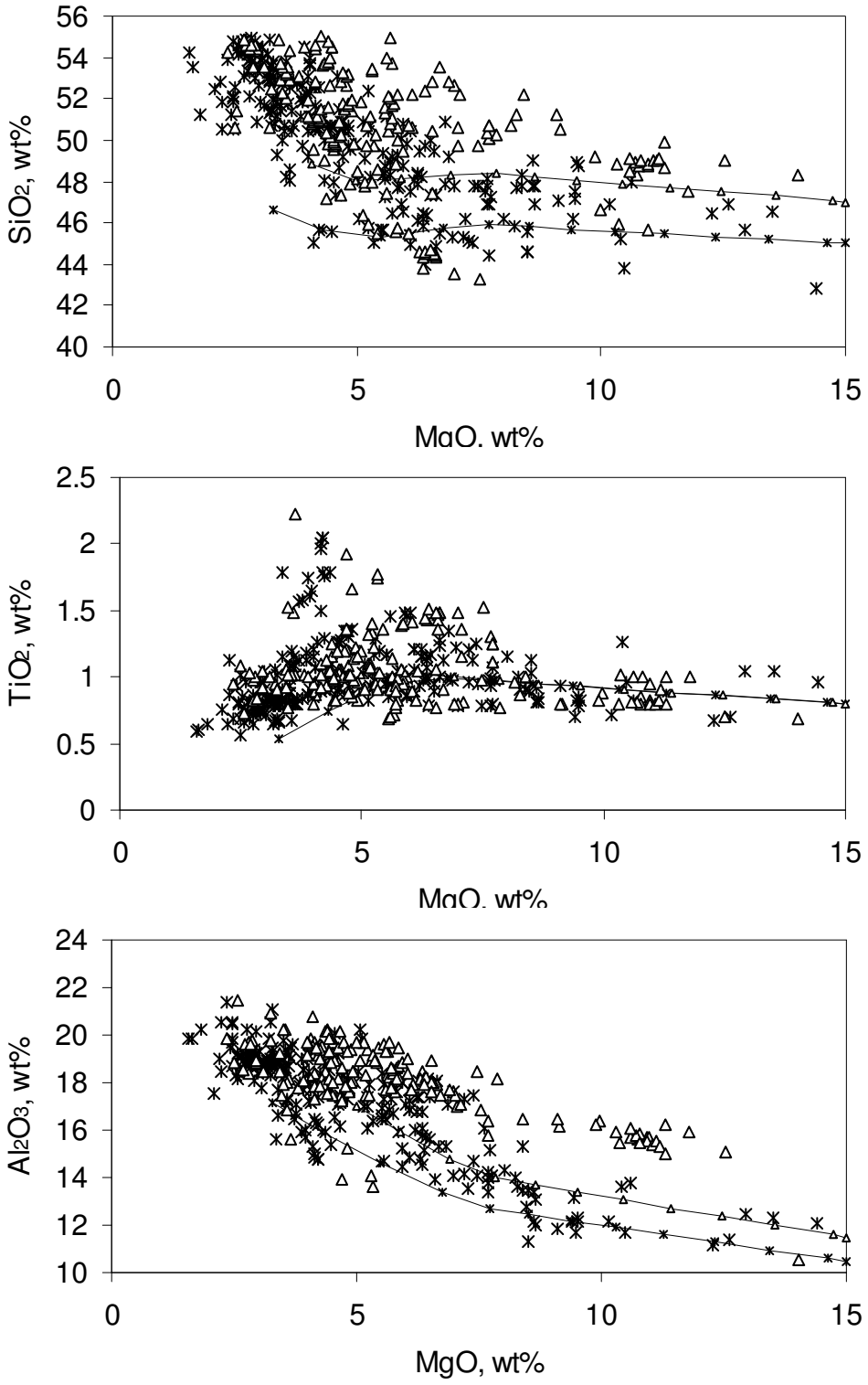

Figure B.8 Major element vs. MgO plots for the Sunda-Java arc. Symbols as in Figure B.1.

Figure B.8 (continued)

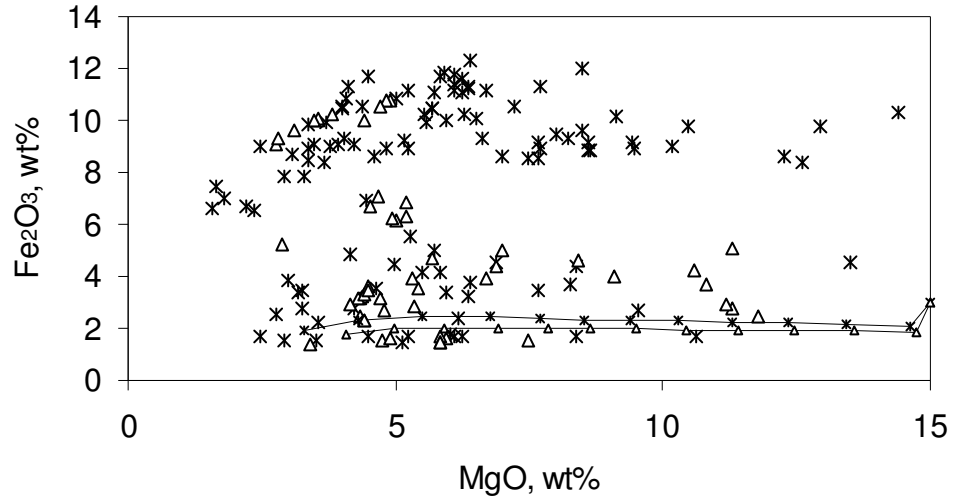

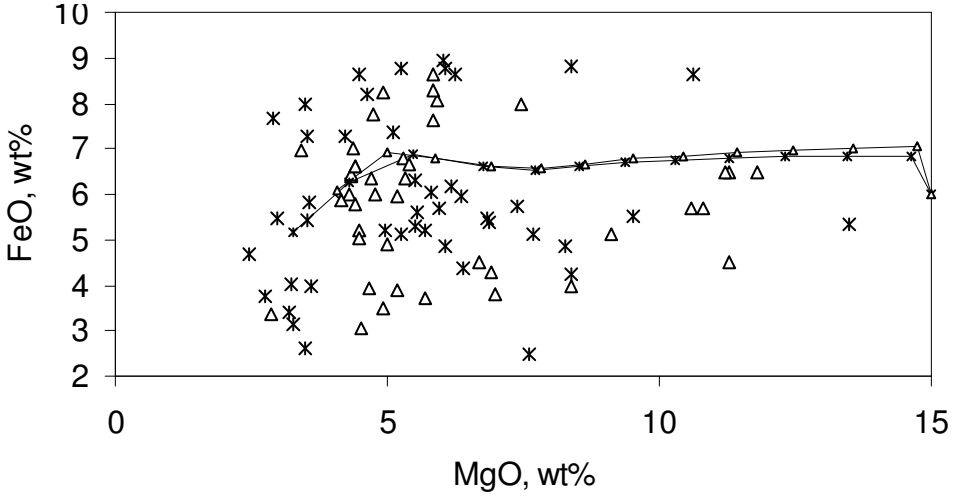

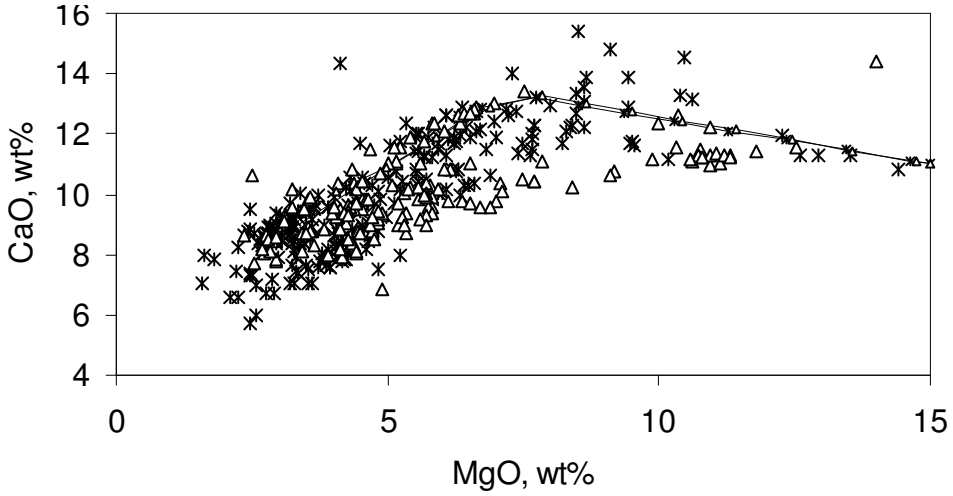

Figure B.8 (continued)

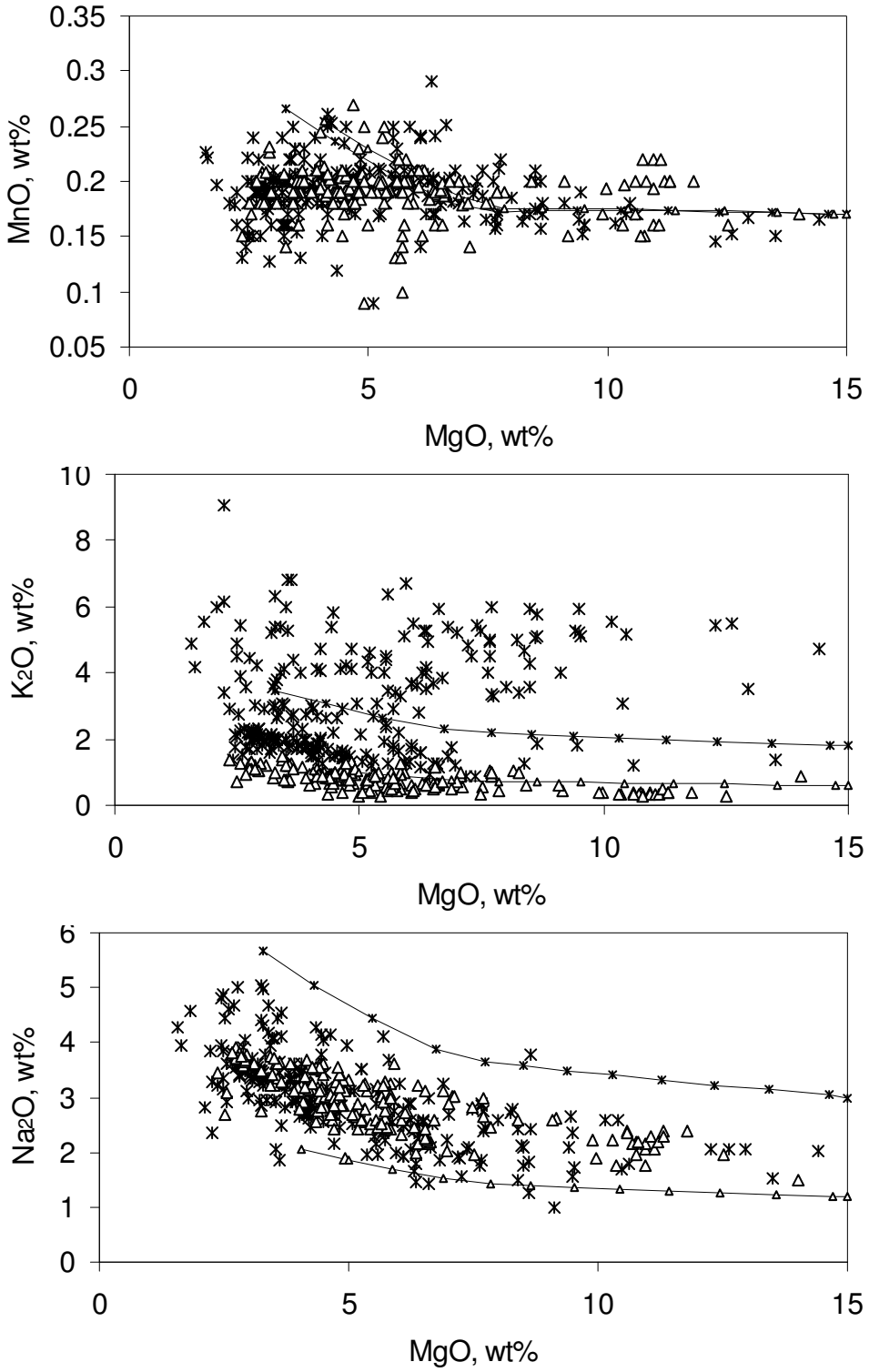

Figure B.8 (continued)

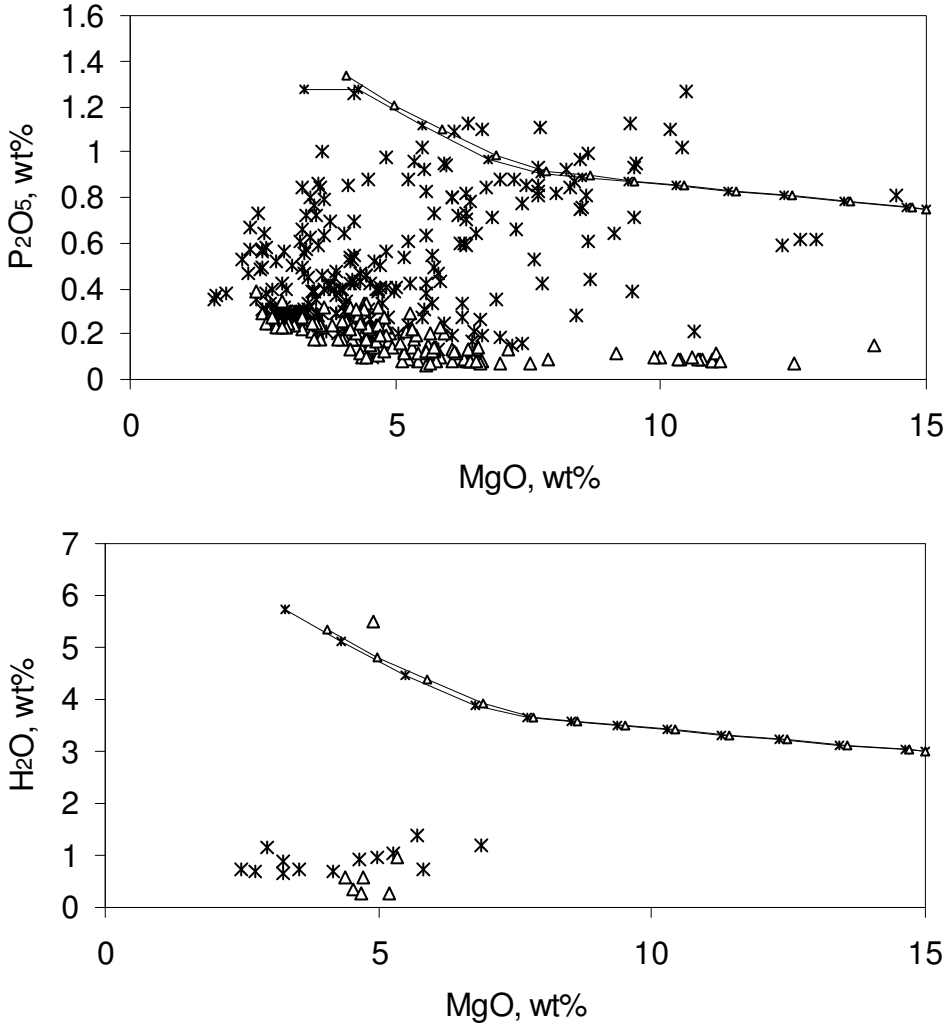

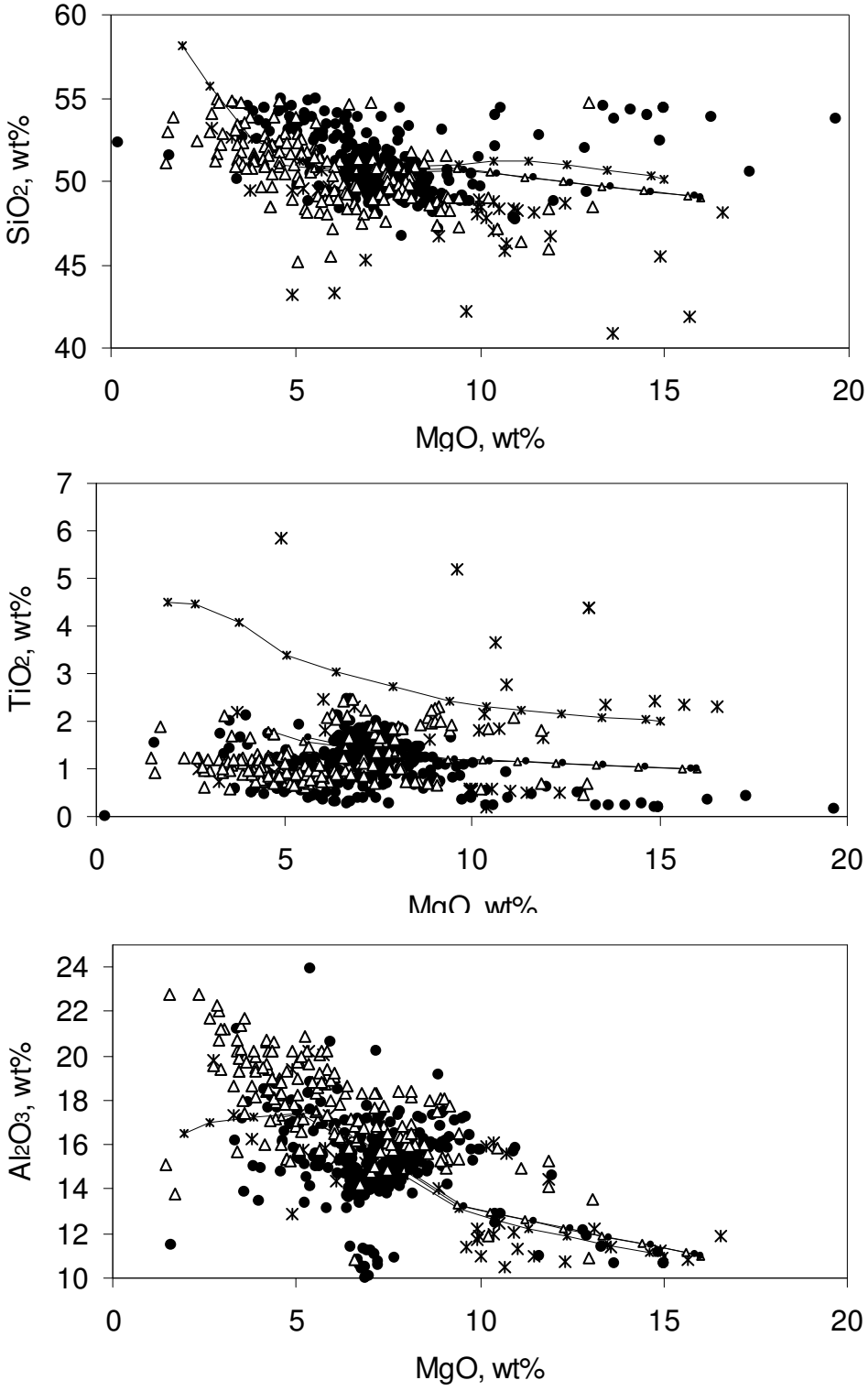

Figure B.9 Major element vs. MgO plots for the Tonga arc. Symbols as in Figure B.1.

Figure B.9 (continued)

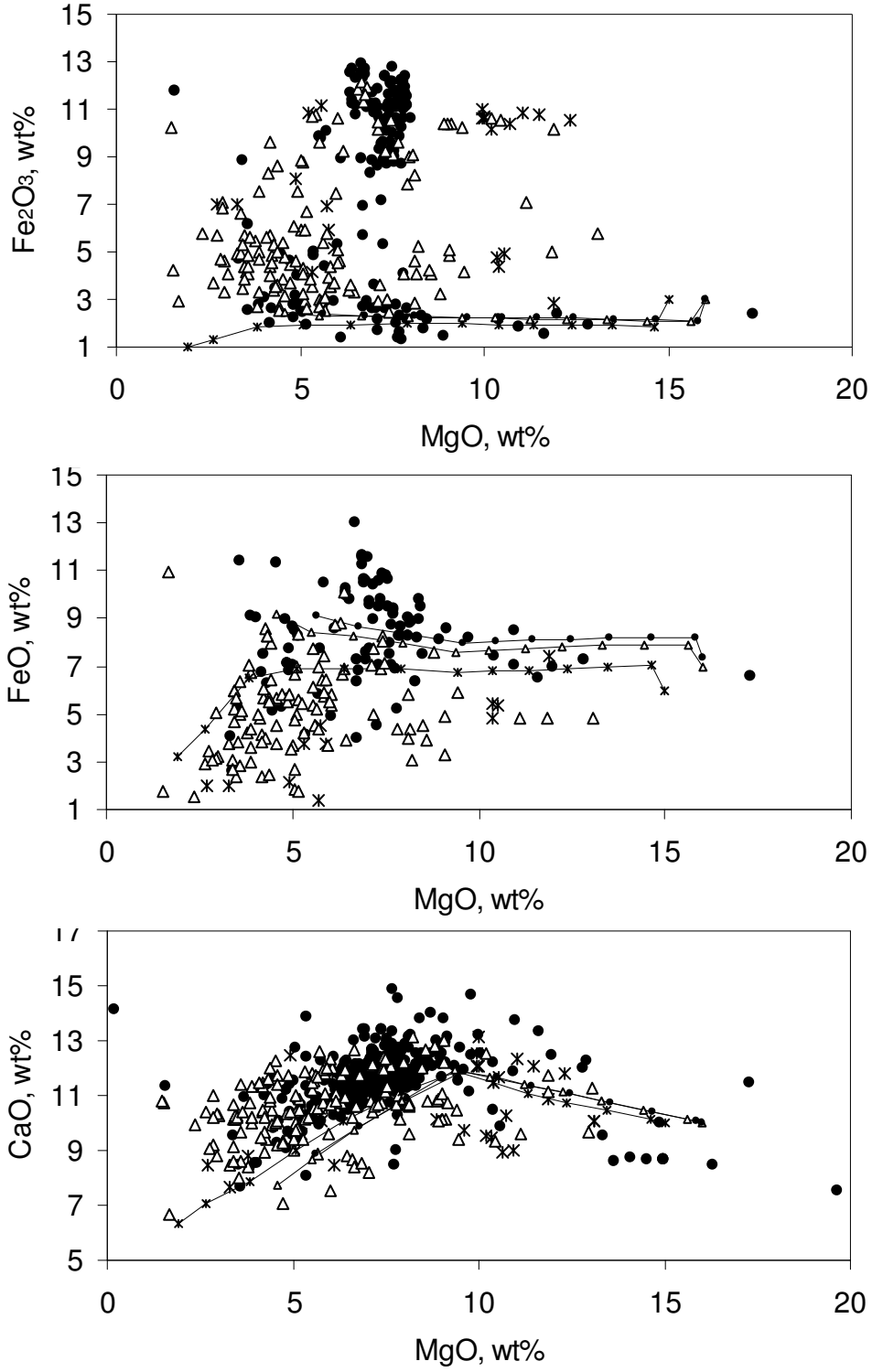

Figure B.9 (continued)

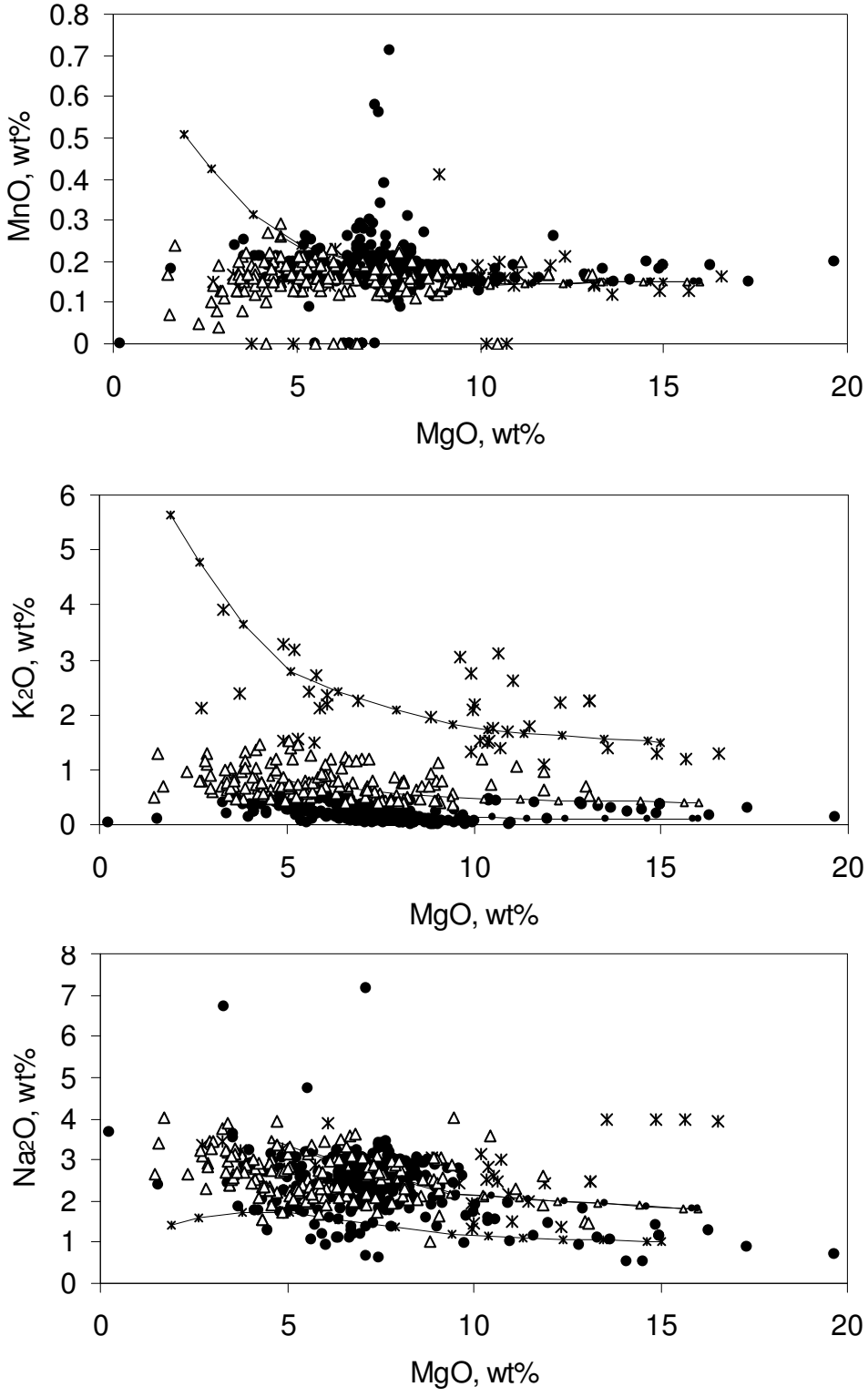

Figure B.9 (continued)

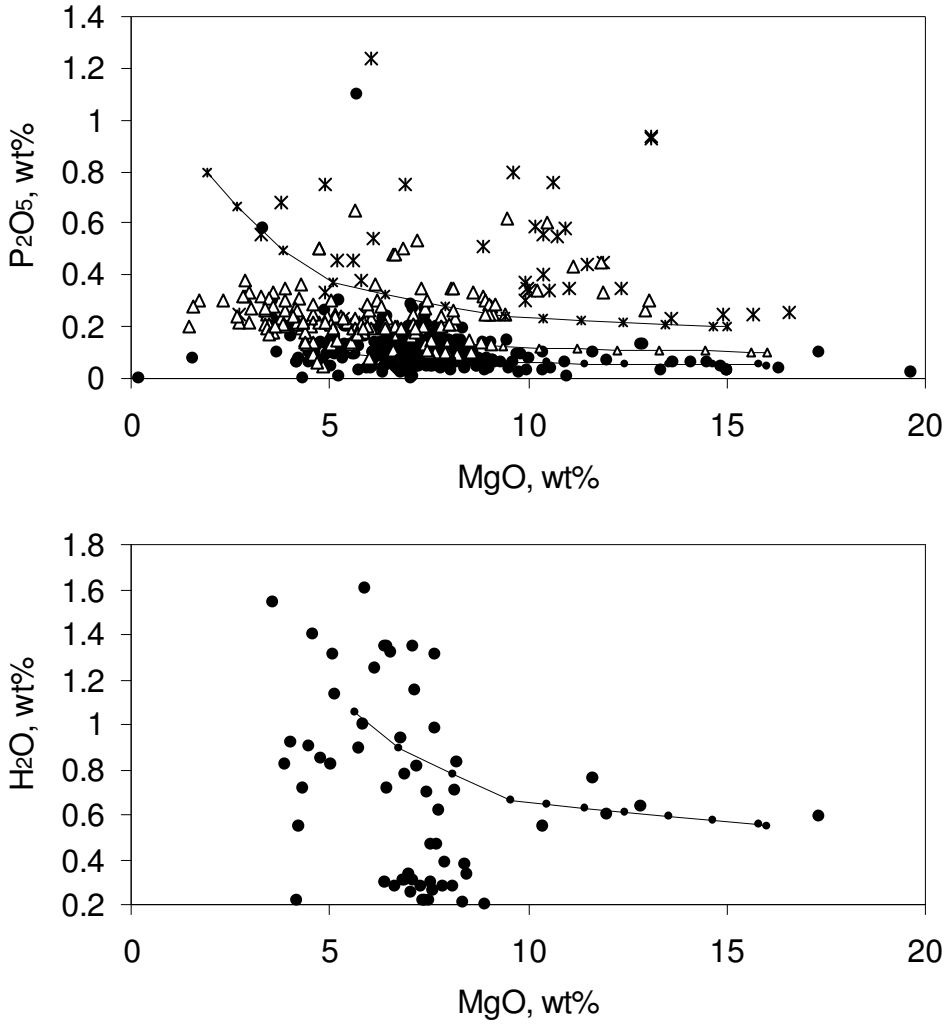

Appendix C: Fractionation-Corrected IAV Compositions

Table C.1 Fractionation-corrected IAV compositions, high –K series. Concentrations in ppm.

	Aleutians	Central America	Izu-Bonin	Kurile	Marianas	Northern Antilles	Southern Antilles	Sunda-Java	Tonga
K	3866.97	6110.90	n/a	6511.25	n/a	n/a	1447.00	10203.10	4853.31
Rb	8.11	15.94	n/a	13.85	n/a	n/a	4.10	49.78	10.93
Ba	148.35	316.34	n/a	158.33	n/a	n/a	56.70	401.55	137.89
Th	0.84	2.93	n/a	1.02	n/a	n/a	1.45	4.51	0.28
U	0.15	0.96	n/a	0.53	n/a	n/a	0.44	0.95	0.14
Nb	0.68	9.69	n/a	1.23	n/a	n/a	1.60	5.44	5.90
Ta	0.06	0.55	n/a	0.00	n/a	n/a	0.07	0.21	0.12
La	4.89	16.88	n/a	3.88	n/a	n/a	3.53	23.00	6.50
Ce	11.15	30.48	n/a	7.81	n/a	n/a	8.03	42.66	13.22
Pb	1.10	2.51	n/a	1.24	n/a	n/a	0.60	5.55	1.80
Sr	153.56	409.95	n/a	162.66	n/a	n/a	110.34	333.33	139.63
Nd	8.50	15.86	n/a	5.76	n/a	n/a	3.72	17.78	6.65
Zr	51.25	79.66	n/a	17.90	n/a	n/a	17.89	60.34	23.42
Hf	0.80	2.12	n/a	0.45	n/a	n/a	0.44	1.34	0.52
Sm	2.34	3.50	n/a	1.71	n/a	n/a	0.74	3.46	1.69
Eu	0.72	0.99	n/a	0.49	n/a	n/a	n/a	1.01	0.51
Y	14.68	16.00	n/a	9.31	n/a	n/a	3.94	15.26	7.77
Yb	1.34	1.37	n/a	0.97	n/a	n/a	0.23	1.21	0.69
Lu	0.21	0.16	n/a	0.14	n/a	n/a	0.04	0.18	0.11

Table C.2 Fractionation-corrected IAV compositions, medium-K series. Concentrations in ppm.

	Aleutians	Central America	Izu-Bonin	Kurile	Marianas	Northern Antilles	Southern Antilles	Sunda-Java	Tonga
K	4449.46	3980.47	5420.97	5989.25	2175.64	2501.60	994.59	2419.23	2805.77
Rb	9.09	8.44	5.56	16.59	5.02	5.12	2.84	5.69	5.83
Ba	186.90	279.32	84.57	147.47	64.51	63.97	41.52	105.54	76.80
Th	0.72	0.56	0.14	1.68	0.22	0.46	0.82	0.96	0.27
U	0.30	0.31	0.11	0.52	0.13	0.16	0.31	0.20	0.12
Nb	2.71	3.31	0.46	2.21	0.59	1.34	1.05	1.40	5.47
Ta	0.25	0.12	0.25	0.13	0.03	0.05	0.25	0.09	0.10
La	5.07	6.32	1.47	5.94	1.65	2.82	2.43	3.90	2.65
Ce	11.80	14.20	4.16	13.69	3.92	8.80	4.88	8.38	8.05
Pb	3.19	2.65	2.42	3.15	1.44	5.21	0.50	2.74	2.22
Sr	392.35	487.26	315.82	314.00	96.27	188.58	90.86	134.63	158.74
Nd	8.08	9.44	4.29	7.84	3.66	4.49	2.81	5.85	5.16
Zr	54.53	55.09	30.38	90.68	19.51	34.21	14.60	26.42	32.96
Hf	1.46	1.39	1.09	1.38	0.55	0.88	0.35	0.81	0.74
Sm	2.25	2.28	1.18	2.14	0.96	1.34	0.75	1.45	1.49
Eu	0.77	0.78	0.44	0.71	0.30	0.53	0.23	0.47	0.55
Y	14.85	12.37	13.33	14.11	6.68	14.51	4.80	10.55	13.29
Yb	1.55	1.28	1.28	1.61	0.80	1.34	0.46	1.00	1.30
Lu	0.27	0.19	0.21	0.23	0.12	0.21	0.07	0.17	0.20

Table C.3 Fractionation-corrected IAV compositions, low-K series. Concentrations in ppm.

	Aleutians	Central America	Izu-Bonin	Kurile	Marianas	Northern Antilles	Southern Antilles	Sunda-Java	Tonga
K	1484.19	717.73	2405.68	2714.33	936.45	1707.72	1402.18	n/a	736.13
Rb	4.69	3.39	4.19	3.23	2.49	3.49	3.46	n/a	1.88
Ba	93.38	92.99	54.08	101.95	36.63	55.29	42.92	n/a	21.20
Th	0.17	0.04	0.10	0.72	0.12	0.26	0.54	n/a	0.12
U	0.12	0.02	0.08	0.25	0.05	0.13	0.15	n/a	0.05
Nb	0.65	2.21	0.42	0.93	0.61	1.37	1.31	n/a	0.87
Ta	0.17	0.03	0.15	0.08	0.02	0.06	0.06	n/a	0.04
La	2.63	1.77	1.03	2.63	1.25	1.92	2.26	n/a	1.32
Ce	7.15	5.12	2.79	7.92	3.31	5.04	5.29	n/a	3.57
Pb	2.35	0.12	1.77	1.78	0.48	1.50	0.85	n/a	0.88
Sr	220.36	167.54	155.09	263.16	68.51	162.81	94.34	n/a	73.80
Nd	5.07	4.29	2.46	3.12	2.94	3.99	4.13	n/a	2.86
Zr	19.31	29.87	26.19	34.85	19.14	35.19	30.34	n/a	25.76
Hf	1.18	0.98	0.77	1.06	0.61	0.88	0.85	n/a	0.72
Sm	1.65	1.50	0.79	1.86	1.11	1.28	1.46	n/a	0.94
Eu	0.65	0.55	0.32	0.71	0.37	0.52	0.45	n/a	0.40
Y	5.67	11.26	12.49	12.93	10.42	14.01	12.42	n/a	13.36
Yb	1.30	1.08	0.96	1.88	1.16	1.33	1.24	n/a	1.05
Lu	0.19	0.25	0.16	0.29	0.19	0.21	0.20	n/a	0.15

Appendix D: Slab Component Fluxes, Residual Slab Fluxes, and Recycled Fractions

Table D.1 Slab-to-arc and slab-to-mantle fluxes for high-K series. Fluxes in kg/yr/km arc length.

	Aleutians		Central America		Izu-Bonin	
	F_{arc}	F_{mantle}	F_{arc}	F_{mantle}	F_{arc}	F_{mantle}
K	28585.84	1395627.90	18445.84	982198.21	n/a	n/a
Rb	64.97	3553.88	51.01	1741.24	n/a	n/a
Ba	1216.13	120248.90	1026.06	218221.70	n/a	n/a
Th	6.31	390.43	9.33	174.26	n/a	n/a
U	0.95	167.94	3.03	152.44	n/a	n/a
Nb	1.55	2134.01	25.47	2188.71	n/a	n/a
Ta	0.00	126.98	1.45	126.07	n/a	n/a
La	25.00	2810.18	48.59	3475.18	n/a	n/a
Ce	47.04	7622.10	79.67	7448.44	n/a	n/a
Pb	7.22	938.73	7.42	869.88	n/a	n/a
Sr	663.64	86245.41	1073.40	189675.45	n/a	n/a
Nd	27.63	6426.66	32.81	7518.92	n/a	n/a
Zr	57.70	61299.94	89.56	67891.75	n/a	n/a
Hf	0.12	1678.88	2.24	1884.09	n/a	n/a
Sm	5.02	2169.73	5.07	2572.07	n/a	n/a
Eu	0.88	806.60	0.95	957.03	n/a	n/a
Y	2.99	21745.12	2.35	27572.15	n/a	n/a
Yb	0.00	2355.21	0.00	2855.83	n/a	n/a
Lu	0.00	351.12	0.04	426.46	n/a	n/a

Table D.1 (continued)

	Kurile		Marianas		Northern Antilles	
	F_{arc}	F_{mantle}	F_{arc}	F_{mantle}	F_{arc}	F_{mantle}
K	113245.56	2432641.06	n/a	n/a	n/a	n/a
Rb	249.04	7381.85	n/a	n/a	n/a	n/a
Ba	2847.81	56904.20	n/a	n/a	n/a	n/a
Th	17.45	631.40	n/a	n/a	n/a	n/a
U	9.27	211.30	n/a	n/a	n/a	n/a
Nb	3.58	3272.70	n/a	n/a	n/a	n/a
Ta	n/a	183.63	n/a	n/a	n/a	n/a
La	45.39	4639.06	n/a	n/a	n/a	n/a
Ce	69.79	12892.66	n/a	n/a	n/a	n/a
Pb	19.59	2267.91	n/a	n/a	n/a	n/a
Sr	1943.82	116657.27	n/a	n/a	n/a	n/a
Nd	37.49	10496.74	n/a	n/a	n/a	n/a
Zr	31.80	94152.03	n/a	n/a	n/a	n/a
Hf	1.56	2586.04	n/a	n/a	n/a	n/a
Sm	8.24	3551.38	n/a	n/a	n/a	n/a
Eu	1.01	1274.10	n/a	n/a	n/a	n/a
Y	0.30	35298.68	n/a	n/a	n/a	n/a
Yb	0.00	3736.99	n/a	n/a	n/a	n/a
Lu	0.01	564.43	n/a	n/a	n/a	n/a

Table D.1 (continued)

	Southern Antilles		Sunda-Java		Tonga	
	F_{arc}	F_{mantle}	F_{arc}	F_{mantle}	F_{arc}	F_{mantle}
K	5695.10	1261561.37	671847.85	1556210.40	45156.69	3563624.36
Rb	16.86	5533.58	3406.15	3612.53	105.14	7280.88
Ba	233.86	14421.31	27372.31	102143.74	1329.81	73174.56
Th	6.02	479.04	304.69	437.15	2.27	623.25
U	1.83	169.30	62.72	90.69	1.18	278.60
Nb	5.30	1359.23	258.94	2338.70	48.16	5735.56
Ta	0.20	83.91	8.07	160.19	0.63	346.36
La	13.25	2223.44	1453.70	3062.44	53.30	10490.42
Ce	29.10	5643.94	2548.05	9883.50	98.83	24980.86
Pb	2.33	1005.31	366.63	1594.49	16.41	4535.89
Sr	401.35	33634.24	17842.25	94778.50	962.98	237868.41
Nd	11.28	3726.49	856.02	7397.22	36.64	23488.68
Zr	35.33	29958.40	1095.32	69488.66	18.25	186134.92
Hf	0.79	831.74	14.16	1961.47	0.05	5148.50
Sm	1.65	1118.65	116.34	2545.29	6.91	7643.82
Eu	n/a	373.50	24.65	898.76	1.52	2722.23
Y	3.47	10165.99	75.30	25147.36	2.37	74367.39
Yb	0.00	1057.35	0.00	2674.71	0.00	7858.95
Lu	0.00	160.70	0.00	404.74	0.00	1187.41

Table D.2 Slab-to-arc and slab-to-mantle fluxes for medium-K series. Fluxes in kg/yr/km arc length.

	Aleutians		Central America		Izu-Bonin	
	F_{arc}	F_{mantle}	F_{arc}	F_{mantle}	F_{arc}	F_{mantle}
K	363372.99	1060840.74	40220.90	960423.16	93398.40	2675425.85
Rb	802.59	2816.26	91.83	1700.42	96.58	7553.69
Ba	16983.76	104481.28	3155.50	216092.25	1502.76	6651.33
Th	56.94	339.80	5.33	178.27	1.15	274.78
U	24.15	144.75	3.09	152.37	1.39	258.05
Nb	81.40	2054.15	18.92	2195.25	11.15	2014.24
Ta	12.90	114.08	0.41	127.10	2.93	132.51
La	268.49	2566.69	50.63	3473.14	2.26	3969.00
Ce	509.63	7159.51	99.00	7429.11	4.58	8756.21
Pb	272.29	673.66	27.64	849.66	41.20	704.44
Sr	27972.61	58936.44	4683.78	186065.07	4493.60	72165.60
Nd	219.44	6234.85	49.06	7502.67	6.17	8495.05
Zr	498.67	60858.97	120.46	67860.85	0.38	67313.42
Hf	11.48	1667.52	2.32	1884.01	0.93	1817.67
Sm	34.59	2140.15	6.93	2570.21	0.07	2718.10
Eu	7.92	799.57	1.85	956.13	0.00	901.32
Y	2.09	21746.03	0.28	27574.21	3.13	26818.68
Yb	0.00	2355.21	0.00	2855.83	0.00	2593.11
Lu	0.43	350.70	0.00	426.50	0.02	400.69

Table D.2 (continued)

	Kurile		Marianas		Northern Antilles	
	F_{arc}	F_{mantle}	F_{arc}	F_{mantle}	F_{arc}	F_{mantle}
K	379370.04	2166516.57	167938.56	1908227.16	94155.89	923563.53
Rb	1130.18	6500.71	423.95	4744.08	218.47	2949.39
Ba	9941.23	49810.78	5487.43	18105.34	2751.22	3618.86
Th	109.58	539.26	14.76	217.66	17.19	211.85
U	33.62	186.95	9.93	132.35	5.54	75.23
Nb	30.92	3245.36	0.08	2147.31	3.45	1103.84
Ta	1.75	181.87	0.00	140.14	0.01	69.98
La	254.28	4430.17	53.85	2826.82	49.27	1418.64
Ce	489.55	12472.91	87.91	7096.03	161.73	4038.35
Pb	200.49	2087.01	115.20	435.79	232.77	269.77
Sr	15343.74	103257.35	4577.43	66394.86	5206.40	30147.09
Nd	140.95	10393.28	73.64	6447.19	16.21	3364.18
Zr	2083.62	92100.21	0.20	58023.83	3.67	31196.27
Hf	4.68	2582.92	0.06	1572.31	0.02	862.08
Sm	18.62	3540.99	7.02	2139.75	1.09	1120.60
Eu	2.89	1272.22	0.43	749.71	0.62	392.66
Y	2.46	35296.52	5.92	21227.52	14.50	11124.30
Yb	0.00	3736.99	0.00	2154.80	0.00	1152.97
Lu	0.04	564.40	0.02	329.59	0.04	176.79

Table D.2 (continued)

	Southern Antilles		Sunda-Java		Tonga	
	F_{arc}	F_{mantle}	F_{arc}	F_{mantle}	F_{arc}	F_{mantle}
K	36566.52	1230689.95	95955.51	2132102.74	99956.04	3508825.00
Rb	118.98	5431.45	250.20	6768.47	231.29	7154.73
Ba	1764.18	12890.98	4763.08	124752.96	3082.04	71422.32
Th	34.85	450.21	41.37	700.47	7.78	617.73
U	13.03	158.10	7.96	145.45	3.52	276.26
Nb	20.56	1343.98	13.70	2583.94	158.12	5625.60
Ta	9.57	74.54	1.31	166.95	0.88	346.11
La	77.25	2159.45	114.32	4401.81	40.80	10502.93
Ce	128.02	5545.01	197.25	12234.30	126.16	24953.53
Pb	18.41	989.23	119.70	1841.42	85.15	4467.16
Sr	2806.79	31228.79	3621.63	108999.12	3657.31	235174.09
Nd	45.45	3692.32	95.23	8158.01	33.86	23491.45
Zr	34.98	29958.75	8.99	70574.99	2.63	186150.54
Hf	0.23	832.29	1.13	1974.49	1.07	5147.49
Sm	7.27	1113.04	11.20	2650.43	3.87	7646.86
Eu	1.20	372.29	1.90	921.51	0.96	2722.80
Y	2.67	10166.79	8.16	25214.50	5.42	74364.34
Yb	0.00	1057.35	0.00	2674.71	0.00	7858.95
Lu	0.00	160.70	0.11	404.62	0.00	1187.41

Table D.3 Slab-to-arc and slab-to-mantle fluxes for low-K series. Fluxes in kg/yr/km arc length.

	Aleutians		Central America		Izu-Bonin	
	F_{arc}	F_{mantle}	F_{arc}	F_{mantle}	F_{arc}	F_{mantle}
K	13591.55	1410622.18	401.17	1000242.89	196590.76	2572233.50
Rb	56.46	3562.39	3.39	1788.86	370.24	7280.02
Ba	1177.91	120287.13	100.02	219147.73	4826.51	3327.58
Th	1.06	395.68	0.00	183.60	4.03	271.89
U	1.16	167.73	0.00	155.46	5.03	254.42
Nb	2.44	2133.12	0.98	2213.19	23.74	2001.66
Ta	1.01	125.97	0.01	127.51	7.62	127.82
La	12.43	2822.75	0.50	3523.27	5.46	3965.80
Ce	29.14	7640.01	1.34	7526.77	6.21	8754.58
Pb	28.10	917.85	0.00	877.29	153.04	592.60
Sr	1913.86	84995.19	117.46	190631.39	9461.13	67198.07
Nd	9.67	6444.61	0.74	7550.99	0.71	8500.51
Zr	105.26	61252.38	0.49	67980.82	29.33	67284.47
Hf	1.06	1677.95	0.07	1886.26	1.99	1816.61
Sm	2.18	2172.57	0.24	2576.90	0.23	2717.94
Eu	0.94	806.55	0.07	957.91	0.00	901.32
Y	95.59	21652.52	0.16	27574.33	100.23	26721.58
Yb	0.00	2355.21	0.00	2855.83	0.00	2593.11
Lu	0.00	351.12	0.03	426.47	0.10	400.62

Table D.3 (continued)

	Kurile		Marianas		Northern Antilles	
	F_{arc}	F_{mantle}	F_{arc}	F_{mantle}	F_{arc}	F_{mantle}
K	25216.99	2520669.62	11770.94	2064394.78	15901.64	1001817.79
Rb	32.03	7598.86	45.69	5122.34	39.20	3128.65
Ba	1173.77	58578.24	701.80	22890.97	647.38	5722.70
Th	7.16	641.69	1.10	231.32	2.09	226.95
U	2.45	218.11	0.51	141.77	1.16	79.62
Nb	3.38	3272.90	2.75	2144.63	1.20	1106.08
Ta	0.00	183.63	0.61	139.54	0.00	69.99
La	5.63	4678.82	1.58	2879.09	4.67	1463.24
Ce	17.07	12945.39	1.40	7182.54	8.08	4192.01
Pb	17.83	2269.66	6.20	544.79	16.26	486.28
Sr	1918.41	116682.68	296.38	70675.92	1132.09	34221.39
Nd	8.20	10526.03	0.14	6520.69	1.96	3378.43
Zr	41.81	94142.02	92.82	57931.22	3.24	31196.71
Hf	0.47	2587.13	1.02	1571.35	0.00	862.10
Sm	0.37	3559.24	0.23	2146.54	0.17	1121.52
Eu	0.12	1274.99	0.01	750.13	0.15	393.13
Y	19.00	35279.99	0.17	21233.27	2.84	11135.96
Yb	0.00	3736.99	0.00	2154.80	0.00	1152.97
Lu	0.00	564.44	0.02	329.58	0.01	176.81

Table D.3 (continued)

	Southern Antilles		Sunda-Java		Tonga	
	F_{arc}	F_{mantle}	F_{arc}	F_{mantle}	F_{arc}	F_{mantle}
K	10795.73	1256460.73	n.d.	n.d.	41559.96	3567221.08
Rb	34.05	5516.38	n.d.	n.d.	165.74	7220.28
Ba	427.84	14227.33	n.d.	n.d.	1862.33	72642.03
Th	5.05	480.01	n.d.	n.d.	5.89	619.62
U	1.30	169.83	n.d.	n.d.	2.65	277.13
Nb	1.13	1363.41	n.d.	n.d.	0.55	5783.17
Ta	0.01	84.11	n.d.	n.d.	0.01	346.98
La	7.68	2229.01	n.d.	n.d.	17.36	10526.37
Ce	10.67	5662.37	n.d.	n.d.	29.49	25050.20
Pb	7.05	1000.58	n.d.	n.d.	74.74	4477.56
Sr	342.53	33693.06	n.d.	n.d.	2273.93	236557.46
Nd	3.46	3734.32	n.d.	n.d.	3.60	23521.71
Zr	0.01	29993.72	n.d.	n.d.	0.14	186153.03
Hf	0.00	832.53	n.d.	n.d.	0.01	5148.54
Sm	1.16	1119.15	n.d.	n.d.	0.06	7650.67
Eu	0.02	373.47	n.d.	n.d.	0.71	2723.05
Y	0.81	10168.65	n.d.	n.d.	108.00	74261.76
Yb	0.00	1057.35	n.d.	n.d.	0.00	7858.95
Lu	0.01	160.69	n.d.	n.d.	0.05	1187.36

Table D.4 Fraction of ingoing slab material incorporated into mantle for high-K magma series.

	Aleutians	Central America	Izu-Bonin	Kurile	Marianas	Northern Antilles	Southern Antilles	Sunda-Java	Tonga
K	0.9799	0.9816	n/a	0.9555	n/a	n/a	0.9555	0.6985	0.9875
Rb	0.9820	0.9715	n/a	0.9674	n/a	n/a	0.9674	0.5147	0.9858
Ba	0.9900	0.9953	n/a	0.9523	n/a	n/a	0.9523	0.7887	0.9822
Th	0.9841	0.9492	n/a	0.9731	n/a	n/a	0.9731	0.5893	0.9964
U	0.9944	0.9805	n/a	0.9580	n/a	n/a	0.9580	0.5912	0.9958
Nb	0.9993	0.9885	n/a	0.9989	n/a	n/a	0.9989	0.9003	0.9917
Ta	1.0000	0.9887	n/a	1.0000	n/a	n/a	1.0000	0.9521	0.9982
La	0.9912	0.9862	n/a	0.9903	n/a	n/a	0.9903	0.6781	0.9949
Ce	0.9939	0.9894	n/a	0.9946	n/a	n/a	0.9946	0.7950	0.9961
Pb	0.9924	0.9915	n/a	0.9914	n/a	n/a	0.9914	0.8130	0.9964
Sr	0.9924	0.9944	n/a	0.9836	n/a	n/a	0.9836	0.8416	0.9960
Nd	0.9957	0.9957	n/a	0.9964	n/a	n/a	0.9964	0.8963	0.9984
Zr	0.9991	0.9987	n/a	0.9997	n/a	n/a	0.9997	0.9845	0.9999
Hf	0.9999	0.9988	n/a	0.9994	n/a	n/a	0.9994	0.9928	1.0000
Sm	0.9977	0.9980	n/a	0.9977	n/a	n/a	0.9977	0.9563	0.9991
Eu	0.9989	0.9990	n/a	0.9992	n/a	n/a	0.9992	0.9733	0.9994
Y	0.9999	0.9999	n/a	1.0000	n/a	n/a	1.0000	0.9970	1.0000
Yb	1.0000	1.0000	n/a	1.0000	n/a	n/a	1.0000	1.0000	1.0000
Lu	1.0000	0.9999	n/a	1.0000	n/a	n/a	1.0000	1.0000	1.0000

Table D.5 Fraction of ingoing slab material incorporated into mantle for medium-K magma series.

	Aleutians	Central America	Izu-Bonin	Kurile	Marianas	Northern Antilles	Southern Antilles	Sunda-Java	Tonga
K	0.7449	0.9598	0.9663	0.8510	0.9191	0.9075	0.9711	0.9569	0.9723
Rb	0.7782	0.9488	0.9874	0.8519	0.9180	0.9310	0.9786	0.9644	0.9687
Ba	0.8602	0.9856	0.8157	0.8336	0.7674	0.5681	0.8796	0.9632	0.9586
Th	0.8565	0.9710	0.9958	0.8311	0.9365	0.9250	0.9282	0.9442	0.9876
U	0.8570	0.9801	0.9946	0.8476	0.9302	0.9314	0.9239	0.9481	0.9874
Nb	0.9619	0.9915	0.9945	0.9906	1.0000	0.9969	0.9849	0.9947	0.9727
Ta	0.8984	0.9968	0.9784	0.9905	1.0000	0.9999	0.8862	0.9922	0.9975
La	0.9053	0.9856	0.9994	0.9457	0.9813	0.9664	0.9655	0.9747	0.9961
Ce	0.9335	0.9868	0.9995	0.9622	0.9878	0.9615	0.9774	0.9841	0.9950
Pb	0.7122	0.9685	0.9447	0.9124	0.7909	0.5368	0.9817	0.9390	0.9813
Sr	0.6781	0.9754	0.9414	0.8706	0.9355	0.8527	0.9175	0.9678	0.9847
Nd	0.9660	0.9935	0.9993	0.9866	0.9887	0.9952	0.9878	0.9885	0.9986
Zr	0.9919	0.9982	1.0000	0.9779	1.0000	0.9999	0.9988	0.9999	1.0000
Hf	0.9932	0.9988	0.9995	0.9982	1.0000	1.0000	0.9997	0.9994	0.9998
Sm	0.9841	0.9973	1.0000	0.9948	0.9967	0.9990	0.9935	0.9958	0.9995
Eu	0.9902	0.9981	1.0000	0.9977	0.9994	0.9984	0.9968	0.9979	0.9996
Y	0.9999	1.0000	0.9999	0.9999	0.9997	0.9987	0.9997	0.9997	0.9999
Yb	1.0000	1.0000	1.0000	1.0000	1.0000	1.0000	1.0000	1.0000	1.0000
Lu	0.9988	1.0000	0.9999	0.9999	0.9999	0.9998	1.0000	0.9997	1.0000

Table D.6 Fraction of ingoing slab material incorporated into mantle for low-K magma series.

	Aleutians	Central America	Izu-Bonin	Kurile	Marianas	Northern Antilles	Southern Antilles	Sunda-Java	Tonga
K	0.9905	0.9996	0.9290	0.9901	0.9943	0.9844	0.9915	n/a	0.9885
Rb	0.9844	0.9981	0.9516	0.9958	0.9912	0.9876	0.9939	n/a	0.9776
Ba	0.9903	0.9995	0.4081	0.9804	0.9703	0.8984	0.9708	n/a	0.9750
Th	0.9973	1.0000	0.9854	0.9890	0.9953	0.9909	0.9896	n/a	0.9906
U	0.9931	1.0000	0.9806	0.9889	0.9964	0.9857	0.9924	n/a	0.9905
Nb	0.9989	0.9996	0.9883	0.9990	0.9987	0.9989	0.9992	n/a	0.9999
Ta	0.9920	1.0000	0.9438	1.0000	0.9957	1.0000	0.9999	n/a	1.0000
La	0.9956	0.9999	0.9986	0.9988	0.9995	0.9968	0.9966	n/a	0.9984
Ce	0.9962	0.9998	0.9993	0.9987	0.9998	0.9981	0.9981	n/a	0.9988
Pb	0.9703	1.0000	0.7948	0.9922	0.9888	0.9676	0.9930	n/a	0.9836
Sr	0.9780	0.9994	0.8766	0.9838	0.9958	0.9680	0.9899	n/a	0.9905
Nd	0.9985	0.9999	0.9999	0.9992	1.0000	0.9994	0.9991	n/a	0.9998
Zr	0.9983	1.0000	0.9996	0.9996	0.9984	0.9999	1.0000	n/a	1.0000
Hf	0.9994	1.0000	0.9989	0.9998	0.9994	1.0000	1.0000	n/a	1.0000
Sm	0.9990	0.9999	0.9999	0.9999	0.9999	0.9998	0.9990	n/a	1.0000
Eu	0.9988	0.9999	1.0000	0.9999	1.0000	0.9996	0.9999	n/a	0.9997
Y	0.9956	1.0000	0.9963	0.9995	1.0000	0.9997	0.9999	n/a	0.9985
Yb	1.0000	1.0000	1.0000	1.0000	1.0000	1.0000	1.0000	n/a	1.0000
Lu	1.0000	0.9999	0.9998	1.0000	0.9999	0.9999	0.9999	n/a	1.0000

Appendix E: Slab Component Fluxes, Residual Slab Fluxes, and Recycled Fractions for Model Variations

Table E.1 Slab-to-arc and slab-to-mantle fluxes for high-K magma series assuming 20% partial melt of IAV source. Fluxes in kg/yr/km arc length.

	Aleutians		Central America		Izu-Bonin	
	F_{arc}	F_{mantle}	F_{arc}	F_{mantle}	F_{arc}	F_{mantle}
K	30563.79	1393649.95	573.34	1000070.72	214146.72	2150008.24
Rb	66.87	3551.98	3.59	1788.66	388.55	6117.02
Ba	1238.01	120227.03	102.35	219145.41	5040.47	2184.12
Th	6.71	390.03	0.01	183.59	6.52	262.31
U	1.10	167.79	0.01	155.45	6.21	222.67
Nb	0.20	2135.36	1.60	2212.58	0.10	1927.89
Ta	0.14	126.84	0.00	127.51	10.63	115.30
La	32.16	2803.02	1.07	3522.70	34.56	3806.40
Ce	65.29	7603.85	2.84	7525.27	70.66	8195.79
Pb	8.17	937.79	0.03	877.26	162.42	565.09
Sr	884.96	86024.09	142.98	190605.88	11501.17	62288.79
Nd	36.36	6417.93	1.39	7550.34	18.67	7988.72
Zr	91.33	61266.31	2.12	67979.20	145.66	62331.97
Hf	0.05	1678.96	0.18	1886.15	7.92	1679.52
Sm	6.09	2168.66	0.33	2576.81	0.21	2549.32
Eu	1.11	806.38	0.10	957.88	0.14	852.22
Y	2.55	21745.57	0.13	27574.37	94.11	25052.05
Yb	0.00	2355.21	0.00	2855.83	0.00	2445.21
Lu	0.01	351.12	0.03	426.47	0.11	375.43

Table E.1 (continued)

	Kurile		Marianas		Northern Antilles	
	F_{arc}	F_{mantle}	F_{arc}	F_{mantle}	F_{arc}	F_{mantle}
K	29043.43	2526369.34	15546.93	1988816.36	18675.18	1007093.27
Rb	35.69	7622.15	49.74	4915.18	41.98	3148.64
Ba	1217.87	58556.03	748.68	22679.17	679.51	5709.07
Th	7.94	641.07	1.76	229.40	2.62	226.56
U	2.76	218.53	0.78	136.08	1.37	80.01
Nb	0.35	3278.22	0.65	2129.45	6.47	1102.75
Ta	0.21	183.64	0.01	138.45	0.17	70.02
La	15.37	4672.14	9.57	2847.98	12.02	1458.48
Ce	43.37	12930.73	18.40	7077.82	25.60	4184.32
Pb	19.80	2268.12	8.10	539.67	17.73	485.17
Sr	2396.71	116271.92	649.54	69813.65	1472.19	33938.37
Nd	0.49	10545.36	4.81	6428.39	7.72	3382.49
Zr	5.96	94291.72	26.93	57139.00	21.95	31274.18
Hf	0.02	2590.67	0.01	1549.08	0.36	864.35
Sm	1.08	3562.50	0.87	2115.97	0.61	1124.43
Eu	0.29	1275.97	0.01	741.44	0.30	393.95
Y	21.15	35317.27	0.40	20935.72	2.31	11169.82
Yb	0.00	3740.47	0.00	2128.56	0.00	1155.91
Lu	0.00	565.03	0.02	325.11	0.01	177.31

Table E.1 (continued)

	Southern Antilles		Sunda-Java		Tonga	
	F_{arc}	F_{mantle}	F_{arc}	F_{mantle}	F_{arc}	F_{mantle}
K	13012.96	1257928.83	n.d.	n.d.	58037.47	3481955.51
Rb	36.32	5524.54	n.d.	n.d.	183.82	7007.62
Ba	453.79	14209.84	n.d.	n.d.	2068.03	72278.33
Th	5.53	479.59	n.d.	n.d.	9.01	615.30
U	1.48	169.92	n.d.	n.d.	3.90	270.69
Nb	5.54	1359.88	n.d.	n.d.	24.21	5742.95
Ta	0.19	84.01	n.d.	n.d.	0.93	344.44
La	14.62	2223.26	n.d.	n.d.	60.73	10460.85
Ce	26.57	5650.97	n.d.	n.d.	132.16	24863.49
Pb	8.19	999.61	n.d.	n.d.	84.30	4464.92
Sr	572.40	33489.32	n.d.	n.d.	4076.69	234266.98
Nd	9.25	3733.03	n.d.	n.d.	31.90	23409.47
Zr	7.96	30029.81	n.d.	n.d.	66.47	185264.62
Hf	0.42	833.30	n.d.	n.d.	3.19	5123.07
Sm	1.91	1119.93	n.d.	n.d.	1.58	7620.48
Eu	0.09	373.85	n.d.	n.d.	1.61	2713.82
Y	0.56	10184.16	n.d.	n.d.	99.98	73984.94
Yb	0.00	1058.70	n.d.	n.d.	0.00	7833.81
Lu	0.02	160.92	n.d.	n.d.	0.04	1183.09

Table E.2 Slab-to-arc and slab-to-mantle fluxes for medium-K magma series assuming 20% partial melt of IAV source. Fluxes in kg/yr/km arc length.

	Aleutians		**Central America**		**Izu-Bonin**	
	F_{arc}	F_{mantle}	F_{arc}	F_{mantle}	F_{arc}	F_{mantle}
K	388517.19	1035696.55	42780.52	957863.54	97676.64	2266478.32
Rb	826.77	2792.08	94.28	1697.97	100.58	6404.98
Ba	17262.15	104202.89	3183.89	216063.86	1548.78	5675.81
Th	61.90	334.84	5.83	177.77	1.79	267.03
U	26.10	142.80	3.29	152.17	1.69	227.19
Nb	149.98	1985.57	27.00	2187.17	0.18	1927.81
Ta	17.56	109.43	0.80	126.72	3.74	122.19
La	357.41	2477.77	60.36	3463.41	10.54	3830.42
Ce	735.40	6933.74	124.33	7403.78	24.91	8241.54
Pb	285.07	660.88	28.93	848.36	43.33	684.18
Sr	31254.75	55654.29	5029.49	185719.36	5040.35	68749.62
Nd	318.53	6135.76	61.12	7490.61	16.28	7991.11
Zr	876.20	60481.44	170.86	67810.45	9.09	62468.53
Hf	24.98	1654.03	4.00	1882.33	2.74	1684.70
Sm	45.77	2128.97	8.33	2568.81	0.51	2549.02
Eu	10.47	797.01	2.20	955.78	0.07	852.29
Y	0.88	21747.24	0.14	27574.36	2.46	25143.70
Yb	0.00	2355.21	0.00	2855.83	0.00	2445.21
Lu	0.45	350.67	0.00	426.50	0.02	375.51

Table E.2 (continued)

	Kurile		Marianas		Northern Antilles	
	F_{arc}	F_{mantle}	F_{arc}	F_{mantle}	F_{arc}	F_{mantle}
K	399190.52	2156222.26	180220.66	1824142.63	104740.57	921027.88
Rb	1149.20	6508.64	435.81	4529.11	228.82	2961.80
Ba	10157.00	49616.90	5622.91	17804.94	2869.56	3519.02
Th	113.60	535.42	17.07	214.08	19.29	209.89
U	35.17	186.11	10.88	125.98	6.35	75.02
Nb	76.95	3201.63	10.29	2119.81	21.86	1087.37
Ta	4.36	179.49	0.60	137.86	0.48	69.71
La	325.37	4362.14	91.35	2766.20	82.69	1387.81
Ce	671.63	12302.47	177.80	6918.42	254.27	3955.65
Pb	210.42	2077.51	121.43	426.34	238.41	264.48
Sr	17809.87	100858.76	5979.06	64484.13	6496.69	28913.86
Nd	214.36	10331.50	117.61	6315.59	42.57	3347.64
Zr	2571.82	91725.86	42.88	57123.05	56.99	31239.15
Hf	13.33	2577.36	2.44	1546.66	1.25	863.45
Sm	26.31	3537.28	11.06	2105.78	3.06	1121.99
Eu	4.40	1271.86	0.99	740.47	1.20	393.05
Y	4.15	35334.27	7.91	20928.21	12.20	11159.93
Yb	0.00	3740.47	0.00	2128.56	0.00	1155.91
Lu	0.03	565.00	0.02	325.11	0.04	177.29

Table E.2 (continued)

	Southern Antilles		Sunda-Java		Tonga	
	F_{arc}	F_{mantle}	F_{arc}	F_{mantle}	F_{arc}	F_{mantle}
K	40056.89	1230884.90	686825.18	1554070.58	109462.65	3430530.33
Rb	122.40	5438.45	3420.33	3634.66	240.53	6950.90
Ba	1803.38	12860.25	27533.66	102011.87	3187.77	71158.60
Th	35.59	449.53	307.72	434.35	9.53	614.77
U	13.32	158.09	63.89	90.48	4.22	270.36
Nb	31.36	1334.06	310.43	2290.30	192.28	5574.88
Ta	10.35	73.85	10.77	157.79	2.17	343.20
La	90.96	2146.93	1514.86	3005.41	70.07	10451.51
Ce	162.99	5514.55	2712.45	9734.78	206.25	24789.41
Pb	20.15	987.65	374.13	1587.56	90.03	4459.19
Sr	3255.30	30806.42	19745.62	92966.16	4762.25	233581.41
Nd	60.83	3681.44	938.22	7330.69	63.68	23377.69
Zr	77.49	29960.28	1423.73	69313.67	48.20	185282.88
Hf	1.34	832.39	23.92	1955.86	0.07	5126.19
Sm	9.06	1112.78	126.87	2540.12	6.68	7615.38
Eu	1.58	372.37	27.18	897.79	1.60	2713.83
Y	2.11	10182.61	69.58	25206.24	4.09	74080.83
Yb	0.00	1058.70	0.00	2679.40	0.00	7833.81
Lu	0.00	160.93	0.00	405.54	0.00	1183.13

Table E.3 Slab-to-arc and slab-to-mantle fluxes for low-K magma series assuming 20% partial melt of IAV source. Fluxes in kg/yr/km arc length.

	Aleutians		Central America		Izu-Bonin	
	F_{arc}	F_{mantle}	F_{arc}	F_{mantle}	F_{arc}	F_{mantle}
K	16351.19	1407862.54	573.34	1000070.72	214146.72	2150008.24
Rb	59.32	3559.54	3.59	1788.66	388.55	6117.02
Ba	1210.98	120254.06	102.35	219145.41	5040.47	2184.12
Th	1.54	395.20	0.01	183.59	6.52	262.31
U	1.38	167.52	0.01	155.45	6.21	222.67
Nb	0.28	2135.27	1.60	2212.58	0.10	1927.89
Ta	1.53	125.45	0.00	127.51	10.63	115.30
La	21.50	2813.68	1.07	3522.70	34.56	3806.40
Ce	52.60	7616.54	2.84	7525.27	70.66	8195.79
Pb	29.62	916.33	0.03	877.26	162.42	565.09
Sr	2284.36	84624.69	142.98	190605.88	11501.17	62288.79
Nd	18.74	6435.55	1.39	7550.34	18.67	7988.72
Zr	40.65	61316.99	2.12	67979.20	145.66	62331.97
Hf	2.55	1676.45	0.18	1886.15	7.92	1679.52
Sm	3.25	2171.49	0.33	2576.81	0.21	2549.32
Eu	1.24	806.24	0.10	957.88	0.14	852.22
Y	100.77	21647.34	0.13	27574.37	94.11	25052.05
Yb	0.00	2355.21	0.00	2855.83	0.00	2445.21
Lu	0.00	351.12	0.03	426.47	0.11	375.43

Table E.3 (continued)

	Kurile		Marianas		Northern Antilles	
	F_{arc}	F_{mantle}	F_{arc}	F_{mantle}	F_{arc}	F_{mantle}
K	29043.43	2526369.34	15546.93	1988816.36	18675.18	1007093.27
Rb	35.69	7622.15	49.74	4915.18	41.98	3148.64
Ba	1217.87	58556.03	748.68	22679.17	679.51	5709.07
Th	7.94	641.07	1.76	229.40	2.62	226.56
U	2.76	218.53	0.78	136.08	1.37	80.01
Nb	0.35	3278.22	0.65	2129.45	6.47	1102.75
Ta	0.21	183.64	0.01	138.45	0.17	70.02
La	15.37	4672.14	9.57	2847.98	12.02	1458.48
Ce	43.37	12930.73	18.40	7077.82	25.60	4184.32
Pb	19.80	2268.12	8.10	539.67	17.73	485.17
Sr	2396.71	116271.92	649.54	69813.65	1472.19	33938.37
Nd	0.49	10545.36	4.81	6428.39	7.72	3382.49
Zr	5.96	94291.72	26.93	57139.00	21.95	31274.18
Hf	0.02	2590.67	0.01	1549.08	0.36	864.35
Sm	1.08	3562.50	0.87	2115.97	0.61	1124.43
Eu	0.29	1275.97	0.01	741.44	0.30	393.95
Y	21.15	35317.27	0.40	20935.72	2.31	11169.82
Yb	0.00	3740.47	0.00	2128.56	0.00	1155.91
Lu	0.00	565.03	0.02	325.11	0.01	177.31

Table E.3 (continued)

	Southern Antilles		Sunda-Java		Tonga	
	F_{arc}	F_{mantle}	F_{arc}	F_{mantle}	F_{arc}	F_{mantle}
K	13012.96	1257928.83	n.d.	n.d.	58037.47	3481955.51
Rb	36.32	5524.54	n.d.	n.d.	183.82	7007.62
Ba	453.79	14209.84	n.d.	n.d.	2068.03	72278.33
Th	5.53	479.59	n.d.	n.d.	9.01	615.30
U	1.48	169.92	n.d.	n.d.	3.90	270.69
Nb	5.54	1359.88	n.d.	n.d.	24.21	5742.95
Ta	0.19	84.01	n.d.	n.d.	0.93	344.44
La	14.62	2223.26	n.d.	n.d.	60.73	10460.85
Ce	26.57	5650.97	n.d.	n.d.	132.16	24863.49
Pb	8.19	999.61	n.d.	n.d.	84.30	4464.92
Sr	572.40	33489.32	n.d.	n.d.	4076.69	234266.98
Nd	9.25	3733.03	n.d.	n.d.	31.90	23409.47
Zr	7.96	30029.81	n.d.	n.d.	66.47	185264.62
Hf	0.42	833.30	n.d.	n.d.	3.19	5123.07
Sm	1.91	1119.93	n.d.	n.d.	1.58	7620.48
Eu	0.09	373.85	n.d.	n.d.	1.61	2713.82
Y	0.56	10184.16	n.d.	n.d.	99.98	73984.94
Yb	0.00	1058.70	n.d.	n.d.	0.00	7833.81
Lu	0.02	160.92	n.d.	n.d.	0.04	1183.09

Table E.4 Slab-to-arc and slab-to-mantle fluxes for high-K magma series assuming 5% partial melt of IAV source. Fluxes in kg/yr/km arc length.

	Aleutians		**Central America**		**Izu-Bonin**	
	F_{arc}	F_{mantle}	F_{arc}	F_{mantle}	F_{arc}	F_{mantle}
K	24804.49	1399409.25	16894.62	983749.44	n/a	n/a
Rb	61.22	3557.63	49.50	1742.75	n/a	n/a
Ba	1172.69	120292.34	1008.66	218239.09	n/a	n/a
Th	5.55	391.19	9.01	174.59	n/a	n/a
U	0.69	168.20	2.90	152.56	n/a	n/a
Nb	21.55	2114.00	20.05	2194.12	n/a	n/a
Ta	0.31	126.68	1.14	126.37	n/a	n/a
La	14.60	2820.58	43.14	3480.62	n/a	n/a
Ce	29.31	7639.83	70.09	7458.02	n/a	n/a
Pb	5.50	940.46	6.66	870.64	n/a	n/a
Sr	476.27	86432.78	975.68	189773.17	n/a	n/a
Nd	22.34	6431.95	30.05	7521.68	n/a	n/a
Zr	41.41	61316.23	78.74	67902.57	n/a	n/a
Hf	0.51	1678.49	1.84	1884.49	n/a	n/a
Sm	4.47	2170.27	4.78	2572.36	n/a	n/a
Eu	0.77	806.72	0.88	957.10	n/a	n/a
Y	3.22	21744.89	2.47	27572.02	n/a	n/a
Yb	0.00	2355.21	0.00	2855.83	n/a	n/a
Lu	0.00	351.12	0.04	426.46	n/a	n/a

Table E.4 (continued)

	Kurile		Marianas		Northern Antilles	
	F_{arc}	F_{mantle}	F_{arc}	F_{mantle}	F_{arc}	F_{mantle}
K	106977.76	2418572.63	n/a	n/a	n/a	n/a
Rb	243.04	7330.32	n/a	n/a	n/a	n/a
Ba	2779.50	56925.80	n/a	n/a	n/a	n/a
Th	16.21	632.28	n/a	n/a	n/a	n/a
U	8.77	210.25	n/a	n/a	n/a	n/a
Nb	0.61	3270.78	n/a	n/a	n/a	n/a
Ta	n/a	n/a	n/a	n/a	n/a	n/a
La	28.48	4649.42	n/a	n/a	n/a	n/a
Ce	42.61	12895.01	n/a	n/a	n/a	n/a
Pb	16.69	2269.90	n/a	n/a	n/a	n/a
Sr	1603.13	116853.77	n/a	n/a	n/a	n/a
Nd	29.61	10479.81	n/a	n/a	n/a	n/a
Zr	59.59	93881.21	n/a	n/a	n/a	n/a
Hf	3.09	2577.92	n/a	n/a	n/a	n/a
Sm	7.36	3543.77	n/a	n/a	n/a	n/a
Eu	0.86	1271.79	n/a	n/a	n/a	n/a
Y	0.40	35214.37	n/a	n/a	n/a	n/a
Yb	0.00	3729.55	n/a	n/a	n/a	n/a
Lu	0.01	563.17	n/a	n/a	n/a	n/a

Table E.4 (continued)

	Southern Antilles		Sunda-Java		Tonga	
	F_{arc}	F_{mantle}	F_{arc}	F_{mantle}	F_{arc}	F_{mantle}
K	5355.16	1254188	642196.10	1559523.48	42751.89	3800718.25
Rb	16.53	5512.087	3377.68	3566.49	102.84	7947.05
Ba	230.11	14407.33	27048.91	102406.64	1303.55	73739.87
Th	5.95	478.9762	298.65	442.73	1.84	627.79
U	1.80	168.7421	60.38	91.04	1.01	296.50
Nb	4.15	1358.533	169.51	2421.79	39.71	5800.49
Ta	0.14	83.79174	3.87	163.77	0.29	352.21
La	12.06	2222.153	1349.26	3158.40	45.34	10573.96
Ce	26.93	5636.689	2360.31	10039.06	84.74	25281.65
Pb	2.16	1005.131	351.82	1608.12	15.23	4547.59
Sr	379.18	33601.72	16057.18	96376.83	826.01	239669.41
Nd	10.64	3717.719	801.88	7419.22	32.72	23778.98
Zr	32.56	29868.99	921.08	69348.14	11.01	188946.91
Hf	0.69	829.3402	9.28	1957.81	0.00	5224.61
Sm	1.59	1115.503	110.67	2539.98	6.48	7742.05
Eu	n/a	n/a	23.34	896.89	1.43	2750.72
Y	3.53	10133.99	78.16	25035.44	2.52	75339.04
Yb	0.00	1054.532	0.00	2665.08	0.00	7944.73
Lu	0.00	160.2218	0.00	403.10	0.00	1202.02

Table E.5 Slab-to-arc and slab-to-mantle fluxes for medium-K magma series assuming 5% partial melt of IAV source. Fluxes in kg/yr/km arc length.

	Aleutians		**Central America**		**Izu-Bonin**	
	F_{arc}	F_{mantle}	F_{arc}	F_{mantle}	F_{arc}	F_{mantle}
K	315303.50	1108910.24	35307.31	965336.75	85075.99	4129608.32
Rb	755.01	2863.84	86.98	1705.27	88.76	11651.45
Ba	16430.17	105034.87	3098.73	216149.03	1412.21	10062.91
Th	47.57	349.17	4.39	179.21	0.28	301.01
U	20.45	148.45	2.71	152.76	0.88	367.77
Nb	6.44	2129.12	7.02	2207.16	84.71	2288.68
Ta	5.82	121.16	0.02	127.50	1.62	167.79
La	142.99	2692.19	35.59	3488.18	2.43	4434.37
Ce	295.96	7373.18	72.78	7455.33	1.51	10525.56
Pb	247.54	698.41	25.13	852.17	37.09	773.35
Sr	24909.87	61999.18	4354.44	186394.41	3984.43	82926.38
Nd	162.18	6292.11	41.56	7510.17	2.02	10263.60
Zr	324.90	61032.74	94.75	67886.56	7.63	84585.55
Hf	5.60	1673.40	1.48	1884.85	0.27	2286.93
Sm	29.05	2145.69	6.20	2570.93	0.00	3320.72
Eu	6.69	800.79	1.68	956.30	0.00	1076.24
Y	2.86	21745.25	0.37	27574.12	3.48	32805.35
Yb	0.00	2355.21	0.00	2855.83	0.00	3121.55
Lu	0.41	350.71	0.00	426.50	0.02	490.66

Table E.5 (continued)

	Kurile		Marianas		Northern Antilles	
	F_{arc}	F_{mantle}	F_{arc}	F_{mantle}	F_{arc}	F_{mantle}
K	340997.93	2184552.47	144526.65	2135237.53	74556.40	923296.72
Rb	1092.38	6480.99	400.56	5343.39	198.35	2913.31
Ba	9513.86	50191.44	5219.71	18840.72	2520.55	3803.90
Th	101.73	546.76	10.60	225.39	13.32	215.37
U	30.58	188.44	8.16	149.50	4.08	75.19
Nb	0.81	3270.58	53.08	2143.31	14.51	1088.00
Ta	0.03	183.12	2.83	142.10	2.73	66.79
La	150.54	4527.36	11.82	2934.41	11.37	1450.14
Ce	311.34	12626.28	22.06	7410.60	79.22	4096.60
Pb	181.30	2105.29	103.20	456.91	221.64	280.00
Sr	13088.53	105368.37	3376.67	69039.20	4072.18	31140.45
Nd	99.51	10409.91	49.42	6719.85	5.36	3350.79
Zr	1818.67	92122.13	10.02	60447.21	2.02	30960.50
Hf	1.49	2579.52	0.34	1638.01	0.92	854.74
Sm	14.92	3536.22	5.16	2226.46	0.43	1112.98
Eu	2.21	1270.44	0.22	774.55	0.38	390.49
Y	1.80	35212.97	5.05	22071.45	15.69	11040.85
Yb	0.00	3729.55	0.00	2229.21	0.00	1145.71
Lu	0.05	563.13	0.02	342.26	0.03	175.56

Table E.5 (continued)

	Southern Antilles		Sunda-Java		Tonga	
	F_{arc}	F_{mantle}	F_{arc}	F_{mantle}	F_{arc}	F_{mantle}
K	30022.16	1229521.24	80822.36	2120897.22	82126.84	3761343.30
Rb	112.24	5416.38	234.93	6709.24	213.24	7836.65
Ba	1686.58	12950.87	4585.79	124869.75	2874.61	72168.82
Th	33.39	451.53	38.15	703.23	4.80	624.83
U	12.46	158.09	6.76	144.66	2.31	295.19
Nb	5.71	1356.97	0.17	2591.14	99.52	5740.68
Ta	8.13	75.80	0.07	167.57	0.01	352.49
La	55.87	2178.34	70.45	4437.21	8.41	10610.88
Ce	92.12	5571.49	124.22	12275.15	56.73	25309.65
Pb	15.14	992.15	111.60	1848.34	75.76	4487.06
Sr	2396.47	31584.43	2794.41	109639.59	2709.03	237786.39
Nd	36.21	3692.15	74.78	8146.32	18.82	23792.88
Zr	17.67	29883.88	0.03	70269.18	2.34	188955.59
Hf	0.00	830.03	0.19	1966.90	3.42	5221.19
Sm	6.35	1110.74	9.41	2641.24	2.64	7745.90
Eu	1.03	371.54	1.56	918.67	0.68	2751.47
Y	2.97	10134.55	8.94	25104.66	6.13	75335.43
Yb	0.00	1054.53	0.00	2665.08	0.00	7944.73
Lu	0.00	160.22	0.11	402.99	0.00	1202.02

Table E.6 Slab-to-arc and slab-to-mantle fluxes for low-K magma series assuming 5% partial melt of IAV source. Fluxes in kg/yr/km arc length.

	Aleutians		**Central America**		**Izu-Bonin**	
	F_{arc}	F_{mantle}	F_{arc}	F_{mantle}	F_{arc}	F_{mantle}
K	8808.90	1415404.84	147.55	1000496.51	167797.14	4046887.17
Rb	50.93	3567.92	3.01	1789.24	343.12	11397.08
Ba	1112.72	120352.32	95.42	219152.33	4519.75	6955.38
Th	0.36	396.38	0.04	183.56	0.88	300.42
U	0.78	168.12	0.00	155.46	3.12	365.52
Nb	33.27	2102.28	0.19	2213.98	236.20	2137.19
Ta	0.30	126.68	0.11	127.41	3.26	166.14
La	2.47	2832.71	0.02	3523.75	14.92	4421.88
Ce	10.27	7658.87	0.28	7527.83	20.05	10507.02
Pb	25.16	920.79	0.08	877.21	138.50	671.95
Sr	1580.12	85328.93	94.72	190654.14	7775.13	79135.68
Nd	5.18	6449.11	0.41	7551.32	2.35	10263.27
Zr	157.75	61199.89	0.07	67981.25	2.28	84590.91
Hf	0.45	1678.56	0.03	1886.30	0.28	2286.92
Sm	1.67	2173.07	0.20	2576.94	1.02	3319.70
Eu	0.79	806.69	0.06	957.92	0.07	1076.17
Y	93.12	21654.99	0.18	27574.31	104.47	32704.36
Yb	0.00	2355.21	0.00	2855.83	0.00	3121.55
Lu	0.00	351.12	0.03	426.47	0.09	490.59

Table E.6 (continued)

	Kurile		Marianas		Northern Antilles	
	F_{arc}	F_{mantle}	F_{arc}	F_{mantle}	F_{arc}	F_{mantle}
K	18333.03	2507217.36	5759.78	2274004.40	10993.78	986859.34
Rb	25.26	7548.11	38.06	5705.90	33.90	3077.76
Ba	1087.47	58617.84	612.03	23448.39	585.07	5739.39
Th	5.70	642.79	0.23	235.76	1.21	227.48
U	1.89	217.14	0.14	157.52	0.78	78.49
Nb	45.34	3226.05	43.78	2152.60	3.28	1099.23
Ta	0.89	182.26	4.65	140.27	0.60	68.93
La	0.12	4677.77	3.90	2942.32	0.02	1461.50
Ce	1.51	12936.10	6.20	7426.45	0.05	4175.77
Pb	14.20	2272.39	3.15	556.96	13.51	488.14
Sr	1498.25	116958.65	81.86	72334.01	840.00	34372.62
Nd	18.87	10490.54	0.77	6768.51	0.21	3355.94
Zr	78.33	93862.46	150.47	60306.75	0.01	30962.51
Hf	1.48	2579.53	2.50	1635.86	0.23	855.43
Sm	0.14	3551.00	0.05	2231.57	0.04	1113.37
Eu	0.06	1272.59	0.05	774.72	0.09	390.78
Y	17.99	35196.79	0.09	22076.41	3.12	11053.42
Yb	0.00	3729.55	0.00	2229.21	0.00	1145.71
Lu	0.00	563.18	0.02	342.25	0.01	175.58

Table E.6 (continued)

	Southern Antilles		Sunda-Java		Tonga	
	F_{arc}	F_{mantle}	F_{arc}	F_{mantle}	F_{arc}	F_{mantle}
K	6959.64	1252583.76	n.d.	n.d.	16713.05	3826757.09
Rb	29.70	5498.91	n.d.	n.d.	132.19	7917.70
Ba	377.91	14259.54	n.d.	n.d.	1480.89	73562.54
Th	4.16	480.76	n.d.	n.d.	1.62	628.01
U	0.97	169.57	n.d.	n.d.	0.87	296.64
Nb	2.36	1360.32	n.d.	n.d.	58.88	5781.33
Ta	0.33	83.60	n.d.	n.d.	4.72	347.78
La	0.85	2233.36	n.d.	n.d.	4.87	10614.42
Ce	1.07	5662.55	n.d.	n.d.	3.03	25363.35
Pb	5.03	1002.26	n.d.	n.d.	57.31	4505.52
Sr	173.12	33807.78	n.d.	n.d.	1006.37	239489.04
Nd	1.10	3727.26	n.d.	n.d.	0.45	23811.25
Zr	2.25	29899.30	n.d.	n.d.	17.83	188940.09
Hf	0.10	829.93	n.d.	n.d.	0.95	5223.66
Sm	0.82	1116.27	n.d.	n.d.	0.10	7748.44
Eu	0.00	372.56	n.d.	n.d.	0.37	2751.78
Y	0.95	10136.57	n.d.	n.d.	112.02	75229.54
Yb	0.00	1054.53	n.d.	n.d.	0.00	7944.73
Lu	0.01	160.21	n.d.	n.d.	0.06	1201.96

Table E.7 Slab-to-arc and slab-to-mantle fluxes for high-K magma series assuming doubled crustal addition rate. Fluxes in kg/yr/km arc length.

	Aleutians		**Central America**		**Izu-Bonin**	
	F_{arc}	F_{mantle}	F_{arc}	F_{mantle}	F_{arc}	F_{mantle}
K	57171.68	1367042.05	36891.69	963752.37	n/a	n/a
Rb	129.94	3488.91	102.03	1690.22	n/a	n/a
Ba	2432.27	119032.77	2052.11	217195.64	n/a	n/a
Th	12.63	384.11	18.67	164.93	n/a	n/a
U	1.91	166.99	6.06	149.41	n/a	n/a
Nb	3.10	2132.46	50.93	2163.24	n/a	n/a
Ta	0.01	126.98	2.89	124.63	n/a	n/a
La	49.99	2785.19	97.17	3426.59	n/a	n/a
Ce	94.07	7575.07	159.34	7368.77	n/a	n/a
Pb	14.44	931.51	14.83	862.46	n/a	n/a
Sr	1327.28	85581.77	2146.81	188602.05	n/a	n/a
Nd	55.26	6399.03	65.62	7486.12	n/a	n/a
Zr	115.40	61242.23	179.13	67802.18	n/a	n/a
Hf	0.25	1678.76	4.49	1881.84	n/a	n/a
Sm	10.04	2164.71	10.14	2567.00	n/a	n/a
Eu	1.76	805.72	1.89	956.09	n/a	n/a
Y	5.98	21742.13	4.70	27569.80	n/a	n/a
Yb	0.00	2355.21	0.00	2855.83	n/a	n/a
Lu	0.01	351.11	0.08	426.42	n/a	n/a

Table E.7 (continued)

	Kurile		Marianas		Northern Antilles	
	F_{arc}	F_{mantle}	F_{arc}	F_{mantle}	F_{arc}	F_{mantle}
K	226491.11	2319395.50	n/a	n/a	n/a	n/a
Rb	498.08	7132.81	n/a	n/a	n/a	n/a
Ba	5695.62	54056.39	n/a	n/a	n/a	n/a
Th	34.90	613.95	n/a	n/a	n/a	n/a
U	18.53	202.03	n/a	n/a	n/a	n/a
Nb	7.16	3269.12	n/a	n/a	n/a	n/a
Ta	n/a	n/a	n/a	n/a	n/a	n/a
La	90.77	4593.67	n/a	n/a	n/a	n/a
Ce	139.59	12822.87	n/a	n/a	n/a	n/a
Pb	39.17	2248.33	n/a	n/a	n/a	n/a
Sr	3887.63	114713.46	n/a	n/a	n/a	n/a
Nd	74.97	10459.26	n/a	n/a	n/a	n/a
Zr	63.61	94120.23	n/a	n/a	n/a	n/a
Hf	3.13	2584.47	n/a	n/a	n/a	n/a
Sm	16.47	3543.14	n/a	n/a	n/a	n/a
Eu	2.02	1273.08	n/a	n/a	n/a	n/a
Y	0.60	35298.38	n/a	n/a	n/a	n/a
Yb	0.00	3736.99	n/a	n/a	n/a	n/a
Lu	0.02	564.42	n/a	n/a	n/a	n/a

Table E.7 (continued)

	Southern Antilles		Sunda-Java		Tonga	
	F_{arc}	F_{mantle}	F_{arc}	F_{mantle}	F_{arc}	F_{mantle}
K	11390.20	1255866.26	1343695.70	884362.55	90313.37	3518467.67
Rb	33.71	5516.72	6812.29	206.38	210.28	7175.73
Ba	467.71	14187.45	54744.61	74771.43	2659.62	71844.75
Th	12.04	473.02	609.38	132.46	4.53	620.98
U	3.66	167.47	125.44	27.97	2.36	277.42
Nb	10.61	1353.93	517.87	2079.77	96.33	5687.39
Ta	0.40	83.71	16.13	152.13	1.26	345.73
La	26.50	2210.19	2907.40	1608.73	106.61	10437.12
Ce	58.20	5614.83	5096.09	7335.45	197.66	24882.03
Pb	4.65	1002.98	733.27	1227.85	32.82	4519.48
Sr	802.70	33232.89	35684.51	76936.25	1925.96	236905.43
Nd	22.57	3715.21	1712.04	6541.21	73.27	23452.04
Zr	70.65	29923.08	2190.64	68393.34	36.50	186116.67
Hf	1.58	830.95	28.31	1947.31	0.11	5148.44
Sm	3.31	1116.99	232.68	2428.96	13.82	7636.91
Eu	n/a	n/a	49.31	874.11	3.05	2720.71
Y	6.94	10162.52	150.59	25072.07	4.74	74365.02
Yb	0.00	1057.35	0.00	2674.71	0.00	7858.95
Lu	0.00	160.70	0.00	404.74	0.00	1187.41

Table E.8 Slab-to-arc and slab-to-mantle fluxes for medium-K magma series assuming doubled crustal addition rate. Fluxes in kg/yr/km arc length.

	Aleutians		**Central America**		**Izu-Bonin**	
	F_{arc}	F_{mantle}	F_{arc}	F_{mantle}	F_{arc}	F_{mantle}
K	726745.99	697467.75	80441.80	920202.26	186796.81	2733230.17
Rb	1605.19	2013.66	183.65	1608.60	193.15	7884.82
Ba	33967.52	87497.52	6311.00	212936.75	3005.51	5495.88
Th	113.88	282.87	10.66	172.94	2.29	276.29
U	48.29	120.60	6.19	149.28	2.79	268.08
Nb	162.80	1972.75	37.85	2176.33	22.29	2039.49
Ta	25.81	101.18	0.83	126.69	5.85	133.13
La	536.99	2298.19	101.25	3422.51	4.53	4015.42
Ce	1019.26	6649.89	198.01	7330.10	9.17	8936.34
Pb	544.58	401.37	55.27	822.02	82.40	670.02
Sr	55945.22	30963.83	9367.56	181381.30	8987.19	68744.08
Nd	438.87	6015.42	98.12	7453.61	12.33	8673.40
Zr	997.33	60360.30	240.93	67740.38	0.75	69120.06
Hf	22.96	1656.04	4.63	1881.70	1.85	1865.75
Sm	69.19	2105.55	13.85	2563.28	0.13	2781.05
Eu	15.84	791.65	3.71	954.27	0.01	919.61
Y	4.17	21743.94	0.56	27573.93	6.26	27441.65
Yb	0.00	2355.21	0.00	2855.83	0.00	2648.37
Lu	0.85	350.27	0.00	426.50	0.04	410.08

Table E.8 (continued)

	Kurile		Marianas		Northern Antilles	
	F_{arc}	F_{mantle}	F_{arc}	F_{mantle}	F_{arc}	F_{mantle}
K	758740.09	1787146.53	335877.11	1740288.60	188311.79	829407.64
Rb	2260.36	5370.53	847.90	4320.13	436.93	2730.92
Ba	19882.46	39869.56	10974.87	12617.90	5502.45	867.64
Th	219.17	429.68	29.51	202.91	34.38	194.66
U	67.23	153.33	19.86	122.42	11.09	69.68
Nb	61.84	3214.44	0.15	2147.23	6.90	1100.39
Ta	3.51	180.12	0.01	140.14	0.02	69.98
La	508.55	4175.89	107.70	2772.97	98.53	1369.38
Ce	979.09	11983.37	175.82	7008.12	323.47	3876.62
Pb	400.98	1886.52	230.40	320.59	465.53	37.01
Sr	30687.48	87913.61	9154.86	61817.43	10412.79	24940.69
Nd	281.89	10252.33	147.27	6373.55	32.42	3347.97
Zr	4167.24	90016.59	0.40	58023.63	7.34	31192.61
Hf	9.36	2578.24	0.12	1572.24	0.05	862.05
Sm	37.24	3522.37	14.03	2132.74	2.19	1119.50
Eu	5.78	1269.33	0.86	749.28	1.23	392.04
Y	4.93	35294.05	11.83	21221.61	29.00	11109.80
Yb	0.00	3736.99	0.00	2154.80	0.00	1152.97
Lu	0.08	564.36	0.04	329.57	0.07	176.75

Table E.8 (continued)

	Southern Antilles		Sunda-Java		Tonga	
	F_{arc}	F_{mantle}	F_{arc}	F_{mantle}	F_{arc}	F_{mantle}
K	73133.04	1194123.42	191911.02	2036147.23	199912.09	3408868.96
Rb	237.96	5312.47	500.41	6518.27	462.58	6923.43
Ba	3528.36	11126.80	9526.16	119989.88	6164.09	68340.28
Th	69.70	415.36	82.75	659.09	15.57	609.94
U	26.06	145.07	15.91	137.50	7.05	272.73
Nb	41.11	1323.42	27.39	2570.25	316.24	5467.47
Ta	19.14	64.97	2.62	165.64	1.75	345.24
La	154.50	2082.20	228.65	4287.49	81.59	10462.14
Ce	256.05	5416.99	394.50	12037.05	252.31	24827.38
Pb	36.81	970.82	239.41	1721.71	170.30	4382.01
Sr	5613.59	28422.00	7243.27	105377.49	7314.62	231516.78
Nd	90.91	3646.87	190.46	8062.79	67.72	23457.59
Zr	69.96	29923.77	17.98	70566.00	5.27	186147.90
Hf	0.47	832.06	2.26	1973.36	2.13	5146.42
Sm	14.53	1105.77	22.40	2639.23	7.74	7642.99
Eu	2.41	371.09	3.81	919.61	1.92	2721.84
Y	5.35	10164.11	16.32	25206.34	10.83	74358.93
Yb	0.00	1057.35	0.00	2674.71	0.00	7858.95
Lu	0.00	160.70	0.23	404.51	0.00	1187.41

Table E.9 Slab-to-arc and slab-to-mantle fluxes for low-K magma series assuming doubled crustal addition rate. Fluxes in kg/yr/km arc length.

	Aleutians		**Central America**		**Izu-Bonin**	
	F_{arc}	F_{mantle}	F_{arc}	F_{mantle}	F_{arc}	F_{mantle}
K	27183.11	1397030.63	802.34	999841.72	396277.43	2523749.55
Rb	112.93	3505.92	6.78	1785.47	746.32	7331.66
Ba	2355.82	119109.22	200.04	219047.71	9729.02	-1227.63
Th	2.12	394.63	0.00	183.60	8.13	270.45
U	2.32	166.57	0.01	155.46	10.14	260.73
Nb	4.87	2130.68	1.96	2212.21	47.85	2013.94
Ta	2.02	124.96	0.01	127.51	15.36	123.63
La	24.85	2810.33	1.00	3522.77	11.01	4008.93
Ce	58.27	7610.87	2.67	7525.44	12.52	8932.99
Pb	56.20	889.76	0.00	877.29	308.49	443.93
Sr	3827.72	83081.33	234.92	190513.93	19071.25	58660.02
Nd	19.35	6434.94	1.48	7550.26	1.44	8684.30
Zr	210.52	61147.12	0.98	67980.33	59.12	69061.70
Hf	2.12	1676.89	0.15	1886.18	4.01	1863.59
Sm	4.35	2170.39	0.48	2576.65	0.47	2780.71
Eu	1.88	805.61	0.15	957.83	0.00	919.61
Y	191.19	21556.93	0.32	27574.17	202.05	27245.87
Yb	0.00	2355.21	0.00	2855.83	0.00	2648.37
Lu	0.00	351.12	0.07	426.43	0.20	409.93

Table E.9 (continued)

	Kurile		Marianas		Northern Antilles	
	F_{arc}	F_{mantle}	F_{arc}	F_{mantle}	F_{arc}	F_{mantle}
K	50433.98	2495452.63	23541.88	2052623.84	31803.27	985916.15
Rb	64.06	7566.83	91.38	5076.65	78.40	3089.45
Ba	2347.54	57404.47	1403.60	22189.17	1294.76	5075.32
Th	14.32	634.53	2.19	230.23	4.19	224.85
U	4.91	215.66	1.02	141.26	2.31	78.46
Nb	6.77	3269.52	5.51	2141.88	2.41	1104.88
Ta	0.00	183.63	1.21	138.93	0.00	69.99
La	11.26	4673.19	3.15	2877.52	9.34	1458.57
Ce	34.14	12928.32	2.80	7181.14	16.16	4183.92
Pb	35.67	2251.83	12.40	538.59	32.52	470.02
Sr	3836.83	114764.26	592.75	70379.54	2264.19	33089.30
Nd	16.40	10517.83	0.28	6520.55	3.92	3376.47
Zr	83.62	94100.21	185.63	57838.40	6.48	31193.47
Hf	0.95	2586.65	2.03	1570.34	0.01	862.09
Sm	0.74	3558.87	0.46	2146.31	0.34	1121.35
Eu	0.23	1274.87	0.02	750.12	0.29	392.98
Y	37.99	35260.99	0.34	21233.10	5.68	11133.12
Yb	0.00	3736.99	0.00	2154.80	0.00	1152.97
Lu	0.01	564.44	0.04	329.56	0.03	176.80

Table E.9 (continued)

	Southern Antilles		Sunda-Java		Tonga	
	F_{arc}	F_{mantle}	F_{arc}	F_{mantle}	F_{arc}	F_{mantle}
K	21591.47	1245665.00	n.d.	n.d.	83119.93	3525661.12
Rb	68.10	5482.34	n.d.	n.d.	331.49	7054.53
Ba	855.67	13799.49	n.d.	n.d.	3724.66	70779.70
Th	10.11	474.95	n.d.	n.d.	11.79	613.72
U	2.60	168.53	n.d.	n.d.	5.30	274.48
Nb	2.26	1362.28	n.d.	n.d.	1.09	5782.63
Ta	0.02	84.10	n.d.	n.d.	0.02	346.97
La	15.37	2221.33	n.d.	n.d.	34.72	10509.00
Ce	21.33	5651.70	n.d.	n.d.	58.98	25020.71
Pb	14.11	993.53	n.d.	n.d.	149.49	4402.82
Sr	685.05	33350.54	n.d.	n.d.	4547.87	234283.53
Nd	6.91	3730.86	n.d.	n.d.	7.20	23518.12
Zr	0.02	29993.71	n.d.	n.d.	0.29	186152.88
Hf	0.01	832.52	n.d.	n.d.	0.02	5148.53
Sm	2.31	1117.99	n.d.	n.d.	0.13	7650.60
Eu	0.05	373.45	n.d.	n.d.	1.41	2722.34
Y	1.62	10167.84	n.d.	n.d.	216.01	74153.75
Yb	0.00	1057.35	n.d.	n.d.	0.00	7858.95
Lu	0.03	160.67	n.d.	n.d.	0.10	1187.31

Table E.10 Slab-to-arc and slab-to-mantle fluxes for high-K magma series assuming halved crustal addition rate. Fluxes in kg/yr/km arc length.

	Aleutians		**Central America**		**Izu-Bonin**	
	F_{arc}	F_{mantle}	F_{arc}	F_{mantle}	F_{arc}	F_{mantle}
K	14292.92	1409920.82	9222.92	991421.13	n/a	n/a
Rb	32.49	3586.37	25.51	1766.74	n/a	n/a
Ba	608.07	120856.97	513.03	218734.72	n/a	n/a
Th	3.16	393.59	4.67	178.93	n/a	n/a
U	0.48	168.42	1.51	153.95	n/a	n/a
Nb	0.78	2134.78	12.73	2201.44	n/a	n/a
Ta	0.00	126.98	0.72	126.79	n/a	n/a
La	12.50	2822.68	24.29	3499.47	n/a	n/a
Ce	23.52	7645.62	39.84	7488.27	n/a	n/a
Pb	3.61	942.34	3.71	873.58	n/a	n/a
Sr	331.82	86577.23	536.70	190212.15	n/a	n/a
Nd	13.82	6440.47	16.40	7535.33	n/a	n/a
Zr	28.85	61328.79	44.78	67936.53	n/a	n/a
Hf	0.06	1678.94	1.12	1885.21	n/a	n/a
Sm	2.51	2172.23	2.53	2574.60	n/a	n/a
Eu	0.44	807.04	0.47	957.51	n/a	n/a
Y	1.50	21746.62	1.17	27573.32	n/a	n/a
Yb	0.00	2355.21	0.00	2855.83	n/a	n/a
Lu	0.00	351.12	0.02	426.48	n/a	n/a

Table E.10 (continued)

	Kurile		Marianas		Northern Antilles	
	F_{arc}	F_{mantle}	F_{arc}	F_{mantle}	F_{arc}	F_{mantle}
K	56622.78	2489263.84	n/a	n/a	n/a	n/a
Rb	124.52	7506.37	n/a	n/a	n/a	n/a
Ba	1423.91	58328.11	n/a	n/a	n/a	n/a
Th	8.72	640.12	n/a	n/a	n/a	n/a
U	4.63	215.93	n/a	n/a	n/a	n/a
Nb	1.79	3274.49	n/a	n/a	n/a	n/a
Ta	n/a	n/a	n/a	n/a	n/a	n/a
La	22.69	4661.75	n/a	n/a	n/a	n/a
Ce	34.90	12927.56	n/a	n/a	n/a	n/a
Pb	9.79	2277.70	n/a	n/a	n/a	n/a
Sr	971.91	117629.18	n/a	n/a	n/a	n/a
Nd	18.74	10515.49	n/a	n/a	n/a	n/a
Zr	15.90	94167.93	n/a	n/a	n/a	n/a
Hf	0.78	2586.82	n/a	n/a	n/a	n/a
Sm	4.12	3555.49	n/a	n/a	n/a	n/a
Eu	0.51	1274.60	n/a	n/a	n/a	n/a
Y	0.15	35298.83	n/a	n/a	n/a	n/a
Yb	0.00	3736.99	n/a	n/a	n/a	n/a
Lu	0.01	564.44	n/a	n/a	n/a	n/a

Table E.10 (continued)

	Southern Antilles		Sunda-Java		Tonga	
	F_{arc}	F_{mantle}	F_{arc}	F_{mantle}	F_{arc}	F_{mantle}
K	2847.55	1264408.92	335923.93	1892134.33	22578.34	3586202.70
Rb	8.43	5542.00	1703.07	5315.60	52.57	7333.45
Ba	116.93	14538.24	13686.15	115829.89	664.90	73839.46
Th	3.01	482.05	152.35	589.49	1.13	624.38
U	0.91	170.21	31.36	122.05	0.59	279.19
Nb	2.65	1361.88	129.47	2468.17	24.08	5759.64
Ta	0.10	84.01	4.03	164.23	0.32	346.67
La	6.63	2230.07	726.85	3789.29	26.65	10517.08
Ce	14.55	5658.49	1274.02	11157.52	49.41	25030.27
Pb	1.16	1006.47	183.32	1777.80	8.21	4544.10
Sr	200.67	33834.91	8921.13	103699.63	481.49	238349.90
Nd	5.64	3732.13	428.01	7825.23	18.32	23507.00
Zr	17.66	29976.07	547.66	70036.32	9.12	186144.05
Hf	0.39	832.13	7.08	1968.55	0.03	5148.53
Sm	0.83	1119.48	58.17	2603.46	3.45	7647.27
Eu	n/a	n/a	12.33	911.09	0.76	2722.99
Y	1.74	10167.72	37.65	25185.01	1.18	74368.58
Yb	0.00	1057.35	0.00	2674.71	0.00	7858.95
Lu	0.00	160.70	0.00	404.74	0.00	1187.41

Table E.11 Slab-to-arc and slab-to-mantle fluxes for medium-K magma series assuming halved crustal addition rate. Fluxes in kg/yr/km arc length.

	Aleutians		Central America		Izu-Bonin	
	F_{arc}	F_{mantle}	F_{arc}	F_{mantle}	F_{arc}	F_{mantle}
K	181686.50	1242527.24	20110.45	980533.61	46699.20	2873327.77
Rb	401.30	3217.56	45.91	1746.34	48.29	8029.68
Ba	8491.88	112973.16	1577.75	217670.00	751.38	7750.01
Th	28.47	368.27	2.67	180.93	0.57	278.01
U	12.07	156.82	1.55	153.92	0.70	270.17
Nb	40.70	2094.86	9.46	2204.71	5.57	2056.21
Ta	6.45	120.53	0.21	127.31	1.46	137.52
La	134.25	2700.93	25.31	3498.45	1.13	4018.81
Ce	254.81	7414.33	49.50	7478.61	2.29	8943.21
Pb	136.15	809.81	13.82	863.47	20.60	731.82
Sr	13986.30	72922.74	2341.89	188406.96	2246.80	75484.48
Nd	109.72	6344.57	24.53	7527.20	3.08	8682.65
Zr	249.33	61108.31	60.23	67921.08	0.19	69120.63
Hf	5.74	1673.26	1.16	1885.17	0.46	1867.14
Sm	17.30	2157.45	3.46	2573.67	0.03	2781.15
Eu	3.96	803.53	0.93	957.05	0.00	919.61
Y	1.04	21747.07	0.14	27574.35	1.57	27446.35
Yb	0.00	2355.21	0.00	2855.83	0.00	2648.37
Lu	0.21	350.91	0.00	426.50	0.01	410.11

Table E.11 (continued)

	Kurile		Marianas		Northern Antilles	
	F_{arc}	F_{mantle}	F_{arc}	F_{mantle}	F_{arc}	F_{mantle}
K	189685.02	2356201.59	83969.28	1992196.44	47077.95	970641.48
Rb	565.09	7065.80	211.97	4956.05	109.23	3058.62
Ba	4970.61	54781.40	2743.72	20849.05	1375.61	4994.47
Th	54.79	594.05	7.38	225.04	8.59	220.45
U	16.81	203.76	4.97	137.32	2.77	78.00
Nb	15.46	3260.82	0.04	2147.34	1.73	1105.56
Ta	0.88	182.75	0.00	140.14	0.00	69.99
La	127.14	4557.30	26.93	2853.74	24.63	1443.28
Ce	244.77	12717.69	43.96	7139.98	80.87	4119.22
Pb	100.24	2187.25	57.60	493.39	116.38	386.15
Sr	7671.87	110929.22	2288.72	68683.58	2603.20	32750.28
Nd	70.47	10463.76	36.82	6484.01	8.11	3372.28
Zr	1041.81	93142.02	0.10	58023.94	1.83	31198.11
Hf	2.34	2585.26	0.03	1572.34	0.01	862.09
Sm	9.31	3550.30	3.51	2143.26	0.55	1121.14
Eu	1.45	1273.66	0.21	749.93	0.31	392.97
Y	1.23	35297.75	2.96	21230.48	7.25	11131.55
Yb	0.00	3736.99	0.00	2154.80	0.00	1152.97
Lu	0.02	564.42	0.01	329.59	0.02	176.81

Table E.11 (continued)

	Southern Antilles		Sunda-Java		Tonga	
	F_{arc}	F_{mantle}	F_{arc}	F_{mantle}	F_{arc}	F_{mantle}
K	18283.26	1248973.21	47977.76	2180080.50	49978.02	3558803.02
Rb	59.49	5490.94	125.10	6893.57	115.65	7270.37
Ba	882.09	13773.07	2381.54	127134.51	1541.02	72963.34
Th	17.43	467.63	20.69	721.15	3.89	621.62
U	6.51	164.61	3.98	149.43	1.76	278.02
Nb	10.28	1354.26	6.85	2590.79	79.06	5704.66
Ta	4.79	79.33	0.65	167.60	0.44	346.55
La	38.63	2198.07	57.16	4458.98	20.40	10523.33
Ce	64.01	5609.03	98.62	12332.92	63.08	25016.61
Pb	9.20	998.43	59.85	1901.27	42.57	4509.73
Sr	1403.40	32632.19	1810.82	110809.94	1828.65	237002.74
Nd	22.73	3715.05	47.61	8205.63	16.93	23508.38
Zr	17.49	29976.24	4.50	70579.49	1.32	186151.85
Hf	0.12	832.41	0.57	1975.06	0.53	5148.02
Sm	3.63	1116.67	5.60	2656.03	1.93	7648.79
Eu	0.60	372.89	0.95	922.46	0.48	2723.28
Y	1.34	10168.12	4.08	25218.58	2.71	74367.05
Yb	0.00	1057.35	0.00	2674.71	0.00	7858.95
Lu	0.00	160.70	0.06	404.68	0.00	1187.41

Table E.12 Slab-to-arc and slab-to-mantle fluxes for low-K magma series assuming halved crustal addition rate. Fluxes in kg/yr/km arc length.

	Aleutians		**Central America**		**Izu-Bonin**	
	F_{arc}	F_{mantle}	F_{arc}	F_{mantle}	F_{arc}	F_{mantle}
K	6795.78	1417417.96	200.58	1000443.47	99069.36	2820957.62
Rb	28.23	3590.62	1.70	1790.55	186.58	7891.39
Ba	588.95	120876.08	50.01	219197.74	2432.26	6069.13
Th	0.53	396.21	0.00	183.60	2.03	276.55
U	0.58	168.31	0.00	155.46	2.53	268.33
Nb	1.22	2134.34	0.49	2213.68	11.96	2049.82
Ta	0.51	126.48	0.00	127.51	3.84	135.15
La	6.21	2828.97	0.25	3523.52	2.75	4017.19
Ce	14.57	7654.57	0.67	7527.44	3.13	8942.38
Pb	14.05	931.90	0.00	877.29	77.12	675.30
Sr	956.93	85952.12	58.73	190690.12	4767.81	72963.46
Nd	4.84	6449.45	0.37	7551.36	0.36	8685.37
Zr	52.63	61305.01	0.25	67981.06	14.78	69106.04
Hf	0.53	1678.47	0.04	1886.29	1.00	1866.60
Sm	1.09	2173.66	0.12	2577.02	0.12	2781.06
Eu	0.47	807.02	0.04	957.94	0.00	919.61
Y	47.80	21700.32	0.08	27574.41	50.51	27397.40
Yb	0.00	2355.21	0.00	2855.83	0.00	2648.37
Lu	0.00	351.12	0.02	426.48	0.05	410.08

Table E.12 (continued)

	Kurile		Marianas		Northern Antilles	
	F_{arc}	F_{mantle}	F_{arc}	F_{mantle}	F_{arc}	F_{mantle}
K	12608.50	2533278.12	5885.47	2070280.25	7950.82	1009768.61
Rb	16.01	7614.88	22.84	5145.18	19.60	3148.25
Ba	586.89	59165.13	350.90	23241.87	323.69	6046.39
Th	3.58	645.27	0.55	231.87	1.05	227.99
U	1.23	219.34	0.26	142.03	0.58	80.19
Nb	1.69	3274.59	1.38	2146.01	0.60	1106.69
Ta	0.00	183.63	0.30	139.84	0.00	69.99
La	2.81	4681.63	0.79	2879.88	2.34	1465.57
Ce	8.53	12953.92	0.70	7183.24	4.04	4196.05
Pb	8.92	2278.58	3.10	547.89	8.13	494.41
Sr	959.21	117641.88	148.19	70824.10	566.05	34787.44
Nd	4.10	10530.13	0.07	6520.75	0.98	3379.41
Zr	20.91	94162.93	46.41	57977.63	1.62	31198.32
Hf	0.24	2587.36	0.51	1571.86	0.00	862.10
Sm	0.19	3559.43	0.11	2146.65	0.08	1121.61
Eu	0.06	1275.05	0.01	750.14	0.07	393.20
Y	9.50	35289.48	0.08	21233.35	1.42	11137.38
Yb	0.00	3736.99	0.00	2154.80	0.00	1152.97
Lu	0.00	564.44	0.01	329.59	0.01	176.82

Table E.12 (continued)

	Southern Antilles		Sunda-Java		Tonga	
	F_{arc}	F_{mantle}	F_{arc}	F_{mantle}	F_{arc}	F_{mantle}
K	5397.87	1261858.60	n.d.	n.d.	20779.98	3588001.06
Rb	17.02	5533.41	n.d.	n.d.	82.87	7303.15
Ba	213.92	14441.25	n.d.	n.d.	931.17	73573.20
Th	2.53	482.53	n.d.	n.d.	2.95	622.57
U	0.65	170.48	n.d.	n.d.	1.33	278.45
Nb	0.56	1363.97	n.d.	n.d.	0.27	5783.45
Ta	0.00	84.11	n.d.	n.d.	0.00	346.99
La	3.84	2232.85	n.d.	n.d.	8.68	10535.05
Ce	5.33	5667.70	n.d.	n.d.	14.74	25064.94
Pb	3.53	1004.11	n.d.	n.d.	37.37	4514.93
Sr	171.26	33864.32	n.d.	n.d.	1136.97	237694.43
Nd	1.73	3736.05	n.d.	n.d.	1.80	23523.51
Zr	0.01	29993.72	n.d.	n.d.	0.07	186153.10
Hf	0.00	832.53	n.d.	n.d.	0.00	5148.55
Sm	0.58	1119.73	n.d.	n.d.	0.03	7650.70
Eu	0.01	373.48	n.d.	n.d.	0.35	2723.40
Y	0.41	10169.06	n.d.	n.d.	54.00	74315.76
Yb	0.00	1057.35	n.d.	n.d.	0.00	7858.95
Lu	0.01	160.70	n.d.	n.d.	0.03	1187.39

Table E.13 Slab-to-arc and slab-to-mantle fluxes for high-K magma series assuming halved crustal addition rate and 5% partial melting of IAV source. Fluxes in kg/yr/km arc length.

	Aleutians		**Central America**		**Izu-Bonin**	
	F_{arc}	F_{mantle}	F_{arc}	F_{mantle}	F_{arc}	F_{mantle}
K	12402.25	1411811.49	8447.31	992196.75	n/a	n/a
Rb	30.61	3588.24	24.75	1767.50	n/a	n/a
Ba	586.35	120878.69	504.33	218743.42	n/a	n/a
Th	2.78	393.97	4.51	179.09	n/a	n/a
U	0.35	168.55	1.45	154.01	n/a	n/a
Nb	10.78	2124.78	10.03	2204.15	n/a	n/a
Ta	0.15	126.83	0.57	126.95	n/a	n/a
La	7.30	2827.88	21.57	3502.20	n/a	n/a
Ce	14.66	7654.49	35.05	7493.06	n/a	n/a
Pb	2.75	943.21	3.33	873.96	n/a	n/a
Sr	238.13	86670.91	487.84	190261.01	n/a	n/a
Nd	11.17	6443.12	15.03	7536.71	n/a	n/a
Zr	20.70	61336.94	39.37	67941.94	n/a	n/a
Hf	0.26	1678.75	0.92	1885.41	n/a	n/a
Sm	2.23	2172.51	2.39	2574.75	n/a	n/a
Eu	0.38	807.10	0.44	957.54	n/a	n/a
Y	1.61	21746.50	1.24	27573.26	n/a	n/a
Yb	0.00	2355.21	0.00	2855.83	n/a	n/a
Lu	0.00	351.12	0.02	426.48	n/a	n/a

Table E.13 (continued)

	Kurile		Marianas		Northern Antilles	
	F_{arc}	F_{mantle}	F_{arc}	F_{mantle}	F_{arc}	F_{mantle}
K	53488.88	2472061.52	n/a	n/a	n/a	n/a
Rb	121.52	7451.84	n/a	n/a	n/a	n/a
Ba	1389.75	58315.55	n/a	n/a	n/a	n/a
Th	8.11	640.38	n/a	n/a	n/a	n/a
U	4.39	214.64	n/a	n/a	n/a	n/a
Nb	0.30	3271.09	n/a	n/a	n/a	n/a
Ta	n/a	n/a	n/a	n/a	n/a	n/a
La	14.24	4663.66	n/a	n/a	n/a	n/a
Ce	21.31	12916.31	n/a	n/a	n/a	n/a
Pb	8.34	2278.24	n/a	n/a	n/a	n/a
Sr	801.57	117655.33	n/a	n/a	n/a	n/a
Nd	14.80	10494.61	n/a	n/a	n/a	n/a
Zr	29.79	93911.00	n/a	n/a	n/a	n/a
Hf	1.55	2579.46	n/a	n/a	n/a	n/a
Sm	3.68	3547.45	n/a	n/a	n/a	n/a
Eu	0.43	1272.22	n/a	n/a	n/a	n/a
Y	0.20	35214.57	n/a	n/a	n/a	n/a
Yb	0.00	3729.55	n/a	n/a	n/a	n/a
Lu	0.01	563.17	n/a	n/a	n/a	n/a

Table E.13 (continued)

	Southern Antilles		Sunda-Java		Tonga	
	F_{arc}	F_{mantle}	F_{arc}	F_{mantle}	F_{arc}	F_{mantle}
K	2677.58	1256865.82	321098.05	1880621.53	21375.94	3822094
Rb	8.26	5520.35	1688.84	5255.33	51.42	7998.468
Ba	115.06	14522.39	13524.46	115931.09	651.78	74391.65
Th	2.97	481.95	149.32	592.05	0.92	628.7122
U	0.90	169.64	30.19	121.23	0.50	297.0018
Nb	2.07	1360.61	84.75	2506.55	19.86	5820.348
Ta	0.07	83.86	1.94	165.70	0.15	352.3572
La	6.03	2228.18	674.63	3833.03	22.67	10596.62
Ce	13.46	5650.15	1180.16	11219.21	42.37	25324.02
Pb	1.08	1006.21	175.91	1784.03	7.62	4555.206
Sr	189.59	33791.31	8028.59	104405.42	413.01	240082.4
Nd	5.32	3723.04	400.94	7820.16	16.36	23795.35
Zr	16.28	29885.27	460.54	69808.67	5.51	188952.4
Hf	0.34	829.68	4.64	1962.45	0.00	5224.615
Sm	0.79	1116.30	55.34	2595.32	3.24	7745.292
Eu	n/a	n/a	11.67	908.56	0.71	2751.435
Y	1.76	10135.76	39.08	25074.52	1.26	75340.3
Yb	0.00	1054.53	0.00	2665.08	0.00	7944.729
Lu	0.00	160.22	0.00	403.10	0.00	1202.016

Table E.14 Slab-to-arc and slab-to-mantle fluxes for medium-K magma series assuming halved crustal addition rate and 5% partial melting of IAV source. Fluxes in kg/yr/km arc length.

	Aleutians		**Central America**		**Izu-Bonin**	
	F_{arc}	F_{mantle}	F_{arc}	F_{mantle}	F_{arc}	F_{mantle}
K	157651.75	1266561.99	17653.65	982990.40	42537.99	4172146.31
Rb	377.51	3241.35	43.49	1748.76	44.38	11695.82
Ba	8215.09	113249.95	1549.36	217698.39	706.11	10769.02
Th	23.79	372.96	2.20	181.40	0.14	301.15
U	10.22	158.67	1.35	154.11	0.44	368.21
Nb	3.22	2132.34	3.51	2210.67	42.36	2331.03
Ta	2.91	124.07	0.01	127.51	0.81	168.60
La	71.49	2763.69	17.80	3505.97	1.21	4435.58
Ce	147.98	7521.16	36.39	7491.72	0.75	10526.32
Pb	123.77	822.18	12.56	864.73	18.55	791.90
Sr	12454.94	74454.11	2177.22	188571.63	1992.22	84918.59
Nd	81.09	6373.20	20.78	7530.95	1.01	10264.61
Zr	162.45	61195.19	47.38	67933.93	3.82	84589.37
Hf	2.80	1676.20	0.74	1885.59	0.14	2287.07
Sm	14.52	2160.22	3.10	2574.03	0.00	3320.72
Eu	3.35	804.14	0.84	957.14	0.00	1076.24
Y	1.43	21746.68	0.18	27574.31	1.74	32807.09
Yb	0.00	2355.21	0.00	2855.83	0.00	3121.55
Lu	0.21	350.92	0.00	426.50	0.01	490.67

Table E.14 (continued)

	Kurile		Marianas		Northern Antilles	
	F_{arc}	F_{mantle}	F_{arc}	F_{mantle}	F_{arc}	F_{mantle}
K	170498.96	2355051.43	72263.33	2207500.86	37278.20	960574.92
Rb	546.19	7027.18	200.28	5543.67	99.17	3012.48
Ba	4756.93	54948.37	2609.85	21450.57	1260.28	5064.18
Th	50.86	597.62	5.30	230.69	6.66	222.03
U	15.29	203.74	4.08	153.58	2.04	77.23
Nb	0.40	3270.98	26.54	2169.85	7.25	1095.25
Ta	0.02	183.13	1.41	143.51	1.37	68.16
La	75.27	4602.63	5.91	2940.32	5.69	1455.83
Ce	155.67	12781.95	11.03	7421.63	39.61	4136.21
Pb	90.65	2195.94	51.60	508.51	110.82	390.82
Sr	6544.26	111912.64	1688.33	70727.54	2036.09	33176.54
Nd	49.75	10459.66	24.71	6744.56	2.68	3353.47
Zr	909.33	93031.46	5.01	60452.22	1.01	30961.51
Hf	0.74	2580.27	0.17	1638.18	0.46	855.20
Sm	7.46	3543.68	2.58	2229.04	0.21	1113.20
Eu	1.11	1271.54	0.11	774.66	0.19	390.68
Y	0.90	35213.87	2.53	22073.97	7.85	11048.69
Yb	0.00	3729.55	0.00	2229.21	0.00	1145.71
Lu	0.02	563.16	0.01	342.26	0.02	175.57

Table E.14 (continued)

	Southern Antilles		Sunda-Java		Tonga	
	F_{arc}	F_{mantle}	F_{arc}	F_{mantle}	F_{arc}	F_{mantle}
K	15011.08	1244532.32	40411.18	2161308.40	41063.42	3802406.72
Rb	56.12	5472.50	117.47	6826.70	106.62	7943.27
Ba	843.29	13794.16	2292.90	127162.65	1437.31	73606.12
Th	16.69	468.23	19.07	722.30	2.40	627.23
U	6.23	164.31	3.38	148.04	1.16	296.35
Nb	2.85	1359.83	0.08	2591.22	49.76	5790.44
Ta	4.07	79.87	0.04	167.61	0.01	352.50
La	27.94	2206.28	35.23	4472.43	4.21	10615.09
Ce	46.06	5617.55	62.11	12337.26	28.37	25338.02
Pb	7.57	999.72	55.80	1904.14	37.88	4524.94
Sr	1198.23	32782.66	1397.21	111036.80	1354.51	239140.90
Nd	18.11	3710.26	37.39	8183.71	9.41	23802.30
Zr	8.84	29892.72	0.02	70269.19	1.17	188956.76
Hf	0.00	830.03	0.10	1966.99	1.71	5222.90
Sm	3.18	1113.91	4.71	2645.95	1.32	7747.22
Eu	0.51	372.05	0.78	919.45	0.34	2751.81
Y	1.49	10136.03	4.47	25109.13	3.06	75338.50
Yb	0.00	1054.53	0.00	2665.08	0.00	7944.73
Lu	0.00	160.22	0.06	403.04	0.00	1202.02

Table E.15 Slab-to-arc and slab-to-mantle fluxes for low-K magma series assuming halved crustal addition rate and 5% partial melting of IAV source. Fluxes in kg/yr/km arc length.

	Aleutians		**Central America**		**Izu-Bonin**	
	F_{arc}	F_{mantle}	F_{arc}	F_{mantle}	F_{arc}	F_{mantle}
K	4404.45	1419809.29	73.77	1000570.28	83898.57	4130785.73
Rb	25.47	3593.39	1.50	1790.75	171.56	11568.64
Ba	556.36	120908.68	47.71	219200.04	2259.87	9215.25
Th	0.18	396.56	0.02	183.58	0.44	300.85
U	0.39	168.50	0.00	155.46	1.56	367.09
Nb	16.64	2118.92	0.10	2214.08	118.10	2255.29
Ta	0.15	126.83	0.05	127.46	1.63	167.77
La	1.23	2833.95	0.01	3523.76	7.46	4429.34
Ce	5.13	7664.01	0.14	7527.97	10.03	10517.05
Pb	12.58	933.37	0.04	877.25	69.25	741.19
Sr	790.06	86118.99	47.36	190701.49	3887.56	83023.24
Nd	2.59	6451.70	0.21	7551.53	1.17	10264.44
Zr	78.87	61278.76	0.03	67981.28	1.14	84592.05
Hf	0.22	1678.78	0.02	1886.31	0.14	2287.06
Sm	0.83	2173.91	0.10	2577.04	0.51	3320.21
Eu	0.40	807.09	0.03	957.95	0.04	1076.21
Y	46.56	21701.55	0.09	27574.40	52.24	32756.59
Yb	0.00	2355.21	0.00	2855.83	0.00	3121.55
Lu	0.00	351.12	0.02	426.48	0.05	490.64

Table E.15 (continued)

	Kurile		Marianas		Northern Antilles	
	F_{arc}	F_{mantle}	F_{arc}	F_{mantle}	F_{arc}	F_{mantle}
K	9166.52	2516383.88	2879.89	2276884.29	5496.89	992356.23
Rb	12.63	7560.74	19.03	5724.92	16.95	3094.71
Ba	543.73	59161.57	306.01	23754.41	292.53	6031.92
Th	2.85	645.64	0.12	235.87	0.60	228.09
U	0.95	218.08	0.07	157.59	0.39	78.88
Nb	22.67	3248.72	21.89	2174.50	1.64	1100.87
Ta	0.44	182.70	2.33	142.60	0.30	69.23
La	0.06	4677.83	1.95	2944.27	0.01	1461.50
Ce	0.76	12936.86	3.10	7429.56	0.02	4175.79
Pb	7.10	2279.49	1.58	558.54	6.75	494.89
Sr	749.13	117707.77	40.93	72374.94	420.00	34792.62
Nd	9.44	10499.98	0.38	6768.89	0.10	3356.04
Zr	39.17	93901.63	75.24	60381.99	0.00	30962.52
Hf	0.74	2580.27	1.25	1637.11	0.12	855.54
Sm	0.07	3551.07	0.03	2231.59	0.02	1113.39
Eu	0.03	1272.62	0.03	774.75	0.04	390.83
Y	8.99	35205.78	0.05	22076.45	1.56	11054.98
Yb	0.00	3729.55	0.00	2229.21	0.00	1145.71
Lu	0.00	563.18	0.01	342.26	0.01	175.58

Table E.15 (continued)

	Southern Antilles		Sunda-Java		Tonga	
	F_{arc}	F_{mantle}	F_{arc}	F_{mantle}	F_{arc}	F_{mantle}
K	3479.82	1256063.58	n.d.	n.d.	8356.53	3835113.61
Rb	14.85	5513.76	n.d.	n.d.	66.09	7983.79
Ba	188.95	14448.49	n.d.	n.d.	740.45	74302.98
Th	2.08	482.84	n.d.	n.d.	0.81	628.82
U	0.49	170.06	n.d.	n.d.	0.43	297.07
Nb	1.18	1361.50	n.d.	n.d.	29.44	5810.77
Ta	0.16	83.77	n.d.	n.d.	2.36	350.14
La	0.43	2233.79	n.d.	n.d.	2.43	10616.86
Ce	0.53	5663.08	n.d.	n.d.	1.52	25364.87
Pb	2.51	1004.78	n.d.	n.d.	28.65	4534.17
Sr	86.56	33894.34	n.d.	n.d.	503.19	239992.23
Nd	0.55	3727.81	n.d.	n.d.	0.23	23811.48
Zr	1.12	29900.43	n.d.	n.d.	8.92	188949.01
Hf	0.05	829.98	n.d.	n.d.	0.48	5224.14
Sm	0.41	1116.68	n.d.	n.d.	0.05	7748.49
Eu	0.00	372.56	n.d.	n.d.	0.19	2751.96
Y	0.48	10137.05	n.d.	n.d.	56.01	75285.55
Yb	0.00	1054.53	n.d.	n.d.	0.00	7944.73
Lu	0.01	160.22	n.d.	n.d.	0.03	1201.99

Table E.16 Slab-to-arc and slab-to-mantle fluxes for high-K magma series assuming doubled crustal addition rate and 5% partial melting of IAV source. Fluxes in kg/yr/km arc length.

	Aleutians		Central America		Izu-Bonin	
	F_{arc}	F_{mantle}	F_{arc}	F_{mantle}	F_{arc}	F_{mantle}
K	49608.98	1374604.76	33789.23	966854.82	n/a	n/a
Rb	122.45	3496.41	99.00	1693.25	n/a	n/a
Ba	2345.39	119119.65	2017.32	217230.43	n/a	n/a
Th	11.10	385.64	18.02	165.57	n/a	n/a
U	1.38	167.51	5.81	149.66	n/a	n/a
Nb	43.10	2092.45	40.10	2174.07	n/a	n/a
Ta	0.61	126.37	2.29	125.23	n/a	n/a
La	29.19	2805.99	86.29	3437.48	n/a	n/a
Ce	58.62	7610.52	140.19	7387.92	n/a	n/a
Pb	11.00	934.96	13.31	863.98	n/a	n/a
Sr	952.54	85956.51	1951.36	188797.49	n/a	n/a
Nd	44.68	6409.61	60.11	7491.63	n/a	n/a
Zr	82.81	61274.82	157.48	67823.83	n/a	n/a
Hf	1.02	1677.98	3.68	1882.65	n/a	n/a
Sm	8.94	2165.81	9.56	2567.58	n/a	n/a
Eu	1.54	805.95	1.77	956.21	n/a	n/a
Y	6.44	21741.67	4.94	27569.55	n/a	n/a
Yb	0.00	2355.21	0.00	2855.83	n/a	n/a
Lu	0.01	351.11	0.09	426.41	n/a	n/a

Table E.16 (continued)

	Kurile		Marianas		Northern Antilles	
	F_{arc}	F_{mantle}	F_{arc}	F_{mantle}	F_{arc}	F_{mantle}
K	213955.53	2311594.87	n/a	n/a	n/a	n/a
Rb	486.09	7087.28	n/a	n/a	n/a	n/a
Ba	5559.00	54146.30	n/a	n/a	n/a	n/a
Th	32.42	616.07	n/a	n/a	n/a	n/a
U	17.55	201.48	n/a	n/a	n/a	n/a
Nb	1.21	3270.18	n/a	n/a	n/a	n/a
Ta	n/a	n/a	n/a	n/a	n/a	n/a
La	56.95	4620.94	n/a	n/a	n/a	n/a
Ce	85.22	12852.40	n/a	n/a	n/a	n/a
Pb	33.38	2253.21	n/a	n/a	n/a	n/a
Sr	3206.26	115250.64	n/a	n/a	n/a	n/a
Nd	59.21	10450.20	n/a	n/a	n/a	n/a
Zr	119.18	93821.62	n/a	n/a	n/a	n/a
Hf	6.18	2574.83	n/a	n/a	n/a	n/a
Sm	14.73	3536.41	n/a	n/a	n/a	n/a
Eu	1.72	1270.93	n/a	n/a	n/a	n/a
Y	0.81	35213.96	n/a	n/a	n/a	n/a
Yb	0.00	3729.55	n/a	n/a	n/a	n/a
Lu	0.02	563.16	n/a	n/a	n/a	n/a

Table E.16 (continued)

	Southern Antilles		Sunda-Java		Tonga	
	F_{arc}	F_{mantle}	F_{arc}	F_{mantle}	F_{arc}	F_{mantle}
K	10710.33	1248833	1284392.19	917327.39	85503.78	3757966.37
Rb	33.05	5495.559	6755.36	188.81	205.68	7844.21
Ba	460.23	14177.22	54097.82	75357.73	2607.11	72436.32
Th	11.90	473.0284	597.29	144.08	3.67	625.96
U	3.60	166.9403	120.77	30.65	2.01	295.49
Nb	8.29	1354.387	339.01	2252.29	79.43	5760.78
Ta	0.28	83.64972	7.75	159.89	0.59	351.92
La	24.12	2210.094	2698.52	1809.13	90.68	10528.62
Ce	53.85	5609.764	4720.63	7678.74	169.47	25196.91
Pb	4.32	1002.972	703.65	1256.29	30.46	4532.36
Sr	758.35	33222.54	32114.35	80319.66	1652.02	238843.40
Nd	21.29	3707.074	1603.77	6617.33	65.45	23746.26
Zr	65.12	29836.43	1842.15	68427.06	22.02	188935.90
Hf	1.38	828.6512	18.56	1948.53	0.00	5224.61
Sm	3.17	1113.917	221.35	2429.31	12.97	7735.57
Eu	n/a	n/a	46.69	873.54	2.85	2749.30
Y	7.05	10130.47	156.32	24957.28	5.05	75336.51
Yb	0.00	1054.532	0.00	2665.08	0.00	7944.73
Lu	0.00	160.2213	0.00	403.10	0.00	1202.01

Table E.17 Slab-to-arc and slab-to-mantle fluxes for medium-K magma series assuming doubled crustal addition rate and 5% partial melting of IAV source. Fluxes in kg/yr/km arc length.

	Aleutians		**Central America**		**Izu-Bonin**	
	F_{arc}	F_{mantle}	F_{arc}	F_{mantle}	F_{arc}	F_{mantle}
K	630607.00	793606.74	70614.61	930029.44	170151.97	4044532.33
Rb	1510.03	2108.83	173.95	1618.30	177.51	11562.69
Ba	32860.34	88604.70	6197.45	213050.30	2824.43	8650.70
Th	95.15	301.59	8.78	174.82	0.56	300.73
U	40.89	128.00	5.42	150.05	1.76	366.89
Nb	12.87	2122.68	14.03	2200.14	169.43	2203.96
Ta	11.65	115.34	0.04	127.47	3.23	166.17
La	285.97	2549.21	71.18	3452.58	4.86	4431.94
Ce	591.93	7077.22	145.56	7382.55	3.02	10524.05
Pb	495.08	450.87	50.25	827.04	74.18	736.26
Sr	49819.74	37089.31	8708.88	182039.97	7968.87	78941.94
Nd	324.36	6129.93	83.13	7468.61	4.03	10261.58
Zr	649.80	60707.84	189.51	67791.80	15.27	84577.92
Hf	11.21	1667.80	2.97	1883.36	0.55	2286.65
Sm	58.10	2116.64	12.40	2564.73	0.00	3320.72
Eu	13.39	794.10	3.36	954.62	0.01	1076.24
Y	5.72	21742.39	0.74	27573.76	6.97	32801.86
Yb	0.00	2355.21	0.00	2855.83	0.00	3121.55
Lu	0.82	350.30	0.00	426.50	0.04	490.64

Table E.17 (continued)

	Kurile		Marianas		Northern Antilles	
	F_{arc}	F_{mantle}	F_{arc}	F_{mantle}	F_{arc}	F_{mantle}
K	681995.85	1843554.54	289053.30	1990710.88	149112.81	848740.31
Rb	2184.75	5388.61	801.12	4942.83	396.70	2714.96
Ba	19027.73	40677.58	10439.41	13621.01	5041.10	1283.35
Th	203.45	445.03	21.20	214.79	26.65	202.05
U	61.17	157.86	16.31	141.35	8.16	71.11
Nb	1.61	3269.78	106.16	2090.23	29.02	1073.49
Ta	0.07	183.08	5.66	139.27	5.47	64.06
La	301.07	4376.82	23.63	2922.59	22.75	1438.76
Ce	622.68	12314.94	44.12	7388.54	158.44	4017.38
Pb	362.60	1923.99	206.41	353.71	443.29	58.36
Sr	26177.05	92279.84	6753.34	65662.53	8144.35	27068.27
Nd	199.01	10310.40	98.85	6670.43	10.72	3345.43
Zr	3637.33	90303.46	20.04	60437.19	4.04	30958.48
Hf	2.97	2578.04	0.68	1637.67	1.84	853.82
Sm	29.83	3521.30	10.32	2221.30	0.86	1112.55
Eu	4.42	1268.22	0.45	774.33	0.76	390.11
Y	3.60	35211.17	10.10	22066.40	31.38	11025.16
Yb	0.00	3729.55	0.00	2229.21	0.00	1145.71
Lu	0.09	563.09	0.03	342.24	0.07	175.52

Table E.17 (continued)

	Southern Antilles		Sunda-Java		Tonga	
	F_{arc}	F_{mantle}	F_{arc}	F_{mantle}	F_{arc}	F_{mantle}
K	60044.32	1199499.08	161644.73	2040074.85	164253.69	3679216.45
Rb	224.47	5304.14	469.86	6474.31	426.47	7623.42
Ba	3373.15	11264.29	9171.59	120283.96	5749.22	69294.20
Th	66.78	418.15	76.29	665.08	9.60	620.03
U	24.92	145.63	13.53	137.89	4.62	292.88
Nb	11.41	1351.26	0.33	2590.97	199.04	5641.16
Ta	16.26	67.67	0.14	167.50	0.03	352.47
La	111.74	2122.47	140.90	4366.75	16.83	10602.47
Ce	184.25	5479.37	248.45	12150.92	113.46	25252.92
Pb	30.29	977.00	223.20	1736.74	151.52	4411.30
Sr	4792.94	29187.96	5588.83	106845.18	5418.05	235077.37
Nd	72.42	3655.94	149.56	8071.54	37.64	23774.06
Zr	35.34	29866.21	0.07	70269.14	4.67	188953.25
Hf	0.01	830.02	0.39	1966.70	6.84	5217.77
Sm	12.71	1104.38	18.83	2631.83	5.27	7743.26
Eu	2.05	370.51	3.11	917.12	1.36	2750.79
Y	5.95	10131.57	17.88	25095.72	12.26	75329.30
Yb	0.00	1054.53	0.00	2665.08	0.00	7944.73
Lu	0.00	160.22	0.22	402.88	0.00	1202.01

Table E.18 Slab-to-arc and slab-to-mantle fluxes for low-K magma series assuming doubled crustal addition rate and 5% partial melting of IAV source. Fluxes in kg/yr/km arc length.

	Aleutians		**Central America**		**Izu-Bonin**	
	F_{arc}	F_{mantle}	F_{arc}	F_{mantle}	F_{arc}	F_{mantle}
K	17617.80	1406595.94	295.09	1000348.96	335594.27	3879090.03
Rb	101.87	3516.99	6.02	1786.23	686.25	11053.96
Ba	2225.43	119239.61	190.84	219056.92	9039.49	2435.63
Th	0.72	396.03	0.08	183.52	1.75	299.54
U	1.56	167.34	0.01	155.46	6.24	362.40
Nb	66.54	2069.01	0.39	2213.79	472.40	1900.99
Ta	0.60	126.38	0.21	127.31	6.52	162.88
La	4.93	2830.24	0.04	3523.73	29.84	4406.96
Ce	20.54	7648.60	0.56	7527.54	40.10	10486.97
Pb	50.33	895.63	0.16	877.13	277.00	533.45
Sr	3160.24	83748.81	189.43	190559.42	15550.26	71360.55
Nd	10.36	6443.93	0.82	7550.91	4.70	10260.92
Zr	315.50	61042.14	0.13	67981.18	4.55	84588.63
Hf	0.89	1678.11	0.06	1886.27	0.56	2286.64
Sm	3.34	2171.40	0.40	2576.74	2.04	3318.68
Eu	1.58	805.90	0.13	957.85	0.14	1076.10
Y	186.25	21561.87	0.36	27574.14	208.95	32599.88
Yb	0.00	2355.21	0.00	2855.83	0.00	3121.55
Lu	0.00	351.12	0.06	426.43	0.19	490.50

Table E.18 (continued)

	Kurile		Marianas		Northern Antilles	
	F_{arc}	F_{mantle}	F_{arc}	F_{mantle}	F_{arc}	F_{mantle}
K	36666.07	2488884.33	11519.56	2268244.62	21987.57	975865.55
Rb	50.52	7522.85	76.11	5667.84	67.80	3043.86
Ba	2174.93	57530.37	1224.06	22836.37	1170.14	5154.32
Th	11.40	637.09	0.46	235.53	2.42	226.28
U	3.79	215.24	0.28	157.38	1.56	77.72
Nb	90.67	3180.72	87.56	2108.82	6.56	1095.94
Ta	1.78	181.37	9.31	135.62	1.20	68.33
La	0.24	4677.65	7.81	2938.42	0.04	1461.48
Ce	3.03	12934.59	12.40	7420.25	0.10	4175.72
Pb	28.40	2258.19	6.30	553.81	27.02	474.63
Sr	2996.50	115460.40	163.72	72252.15	1680.00	33532.62
Nd	37.75	10471.66	1.54	6767.74	0.42	3355.73
Zr	156.67	93784.13	300.95	60156.28	0.02	30962.51
Hf	2.97	2578.04	4.99	1633.36	0.47	855.19
Sm	0.27	3550.86	0.10	2231.52	0.08	1113.33
Eu	0.11	1272.54	0.10	774.67	0.17	390.70
Y	35.98	35178.80	0.19	22076.31	6.24	11050.30
Yb	0.00	3729.55	0.00	2229.21	0.00	1145.71
Lu	0.00	563.18	0.04	342.24	0.02	175.57

Table E.18 (continued)

	Southern Antilles		Sunda-Java		Tonga	
	F_{arc}	F_{mantle}	F_{arc}	F_{mantle}	F_{arc}	F_{mantle}
K	13919.28	1245624.12	n.d.	n.d.	33426.10	3810044.04
Rb	59.41	5469.21	n.d.	n.d.	264.38	7785.51
Ba	755.81	13881.64	n.d.	n.d.	2961.78	72081.65
Th	8.32	476.60	n.d.	n.d.	3.24	626.39
U	1.94	168.60	n.d.	n.d.	1.73	295.77
Nb	4.71	1357.97	n.d.	n.d.	117.75	5722.45
Ta	0.66	83.27	n.d.	n.d.	9.44	343.06
La	1.71	2232.50	n.d.	n.d.	9.74	10609.56
Ce	2.13	5661.48	n.d.	n.d.	6.06	25360.32
Pb	10.06	997.24	n.d.	n.d.	114.61	4448.21
Sr	346.23	33634.67	n.d.	n.d.	2012.74	238482.67
Nd	2.20	3726.16	n.d.	n.d.	0.90	23810.80
Zr	4.49	29897.06	n.d.	n.d.	35.67	188922.26
Hf	0.19	829.83	n.d.	n.d.	1.90	5222.71
Sm	1.64	1115.45	n.d.	n.d.	0.19	7748.34
Eu	0.01	372.55	n.d.	n.d.	0.74	2751.40
Y	1.90	10135.62	n.d.	n.d.	224.04	75117.52
Yb	0.00	1054.53	n.d.	n.d.	0.00	7944.73
Lu	0.03	160.20	n.d.	n.d.	0.11	1201.91

Table E.19 Slab-to-arc and slab-to-mantle fluxes for high-K magma series assuming doubled crustal addition rate and 20% partial melting of IAV source. Fluxes in kg/yr/km arc length.

	Aleutians		**Central America**		**Izu-Bonin**	
	F_{arc}	F_{mantle}	F_{arc}	F_{mantle}	F_{arc}	F_{mantle}
K	61127.57	1363086.17	38483.38	962160.67	n/a	n/a
Rb	133.75	3485.11	103.55	1688.70	n/a	n/a
Ba	2476.01	118989.03	2069.51	217178.25	n/a	n/a
Th	13.42	383.32	18.99	164.60	n/a	n/a
U	2.20	166.70	6.18	149.28	n/a	n/a
Nb	0.39	2135.16	56.80	2157.37	n/a	n/a
Ta	0.28	126.70	3.22	124.29	n/a	n/a
La	64.31	2770.87	103.66	3420.11	n/a	n/a
Ce	130.57	7538.57	176.50	7351.61	n/a	n/a
Pb	16.34	929.62	15.62	861.67	n/a	n/a
Sr	1769.92	85139.13	2354.21	188394.64	n/a	n/a
Nd	72.72	6381.57	74.10	7477.64	n/a	n/a
Zr	182.67	61174.97	218.83	67762.48	n/a	n/a
Hf	0.09	1678.91	5.91	1880.42	n/a	n/a
Sm	12.17	2162.57	11.22	2565.91	n/a	n/a
Eu	2.22	805.27	2.14	955.84	n/a	n/a
Y	5.09	21743.02	4.21	27570.28	n/a	n/a
Yb	0.00	2355.21	0.00	2855.83	n/a	n/a
Lu	0.01	351.11	0.08	426.42	n/a	n/a

Table E.19 (continued)

	Kurile		Marianas		Northern Antilles	
	F_{arc}	F_{mantle}	F_{arc}	F_{mantle}	F_{arc}	F_{mantle}
K	232850.42	2322562.36	n/a	n/a	n/a	n/a
Rb	504.09	7153.74	n/a	n/a	n/a	n/a
Ba	5764.10	54009.79	n/a	n/a	n/a	n/a
Th	36.16	612.85	n/a	n/a	n/a	n/a
U	19.03	202.25	n/a	n/a	n/a	n/a
Nb	20.73	3257.84	n/a	n/a	n/a	n/a
Ta	n/a	n/a	n/a	n/a	n/a	n/a
La	113.52	4573.99	n/a	n/a	n/a	n/a
Ce	196.00	12778.10	n/a	n/a	n/a	n/a
Pb	42.23	2245.69	n/a	n/a	n/a	n/a
Sr	4644.41	114024.22	n/a	n/a	n/a	n/a
Nd	101.32	10444.54	n/a	n/a	n/a	n/a
Zr	9.05	94288.62	n/a	n/a	n/a	n/a
Hf	0.41	2590.28	n/a	n/a	n/a	n/a
Sm	19.85	3543.73	n/a	n/a	n/a	n/a
Eu	2.66	1273.60	n/a	n/a	n/a	n/a
Y	0.28	35338.15	n/a	n/a	n/a	n/a
Yb	0.00	3740.47	n/a	n/a	n/a	n/a
Lu	0.02	565.02	n/a	n/a	n/a	n/a

Table E.19 (continued)

	Southern Antilles		Sunda-Java		Tonga	
	F_{arc}	F_{mantle}	F_{arc}	F_{mantle}	F_{arc}	F_{mantle}
K	11735.69	1259206.10	1373650.35	867245.41	92751.30	3447241.68
Rb	34.04	5526.82	6840.67	214.32	212.59	6978.85
Ba	471.45	14192.18	55067.32	74478.22	2685.89	71660.47
Th	12.11	473.02	615.43	126.63	4.99	619.31
U	3.69	167.72	127.79	26.59	2.54	272.04
Nb	11.87	1353.56	620.85	1979.88	105.34	5661.83
Ta	0.47	83.73	21.55	147.01	1.70	343.67
La	27.91	2209.97	3029.73	1490.55	116.25	10405.33
Ce	62.02	5615.52	5424.89	7022.34	223.19	24772.46
Pb	4.83	1002.98	748.27	1213.43	34.03	4515.19
Sr	848.88	33212.84	39491.25	73220.53	2224.75	236118.92
Nd	24.51	3717.77	1876.43	6392.48	85.49	23355.88
Zr	80.51	29957.26	2847.47	67889.94	69.18	185261.91
Hf	1.92	831.80	47.84	1931.94	0.78	5125.48
Sm	3.56	1118.27	253.73	2413.25	15.42	7606.65
Eu	n/a	n/a	54.37	870.60	3.43	2712.00
Y	6.71	10178.01	139.15	25136.67	4.13	74080.79
Yb	0.00	1058.70	0.00	2679.40	0.00	7833.81
Lu	0.00	160.93	0.00	405.53	0.00	1183.13

Table E.20 Slab-to-arc and slab-to-mantle fluxes for medium-K magma series assuming doubled crustal addition rate and 20% partial melting of IAV source. Fluxes in kg/yr/km arc length.

	Aleutians		**Central America**		**Izu-Bonin**	
	F_{arc}	F_{mantle}	F_{arc}	F_{mantle}	F_{arc}	F_{mantle}
K	777034.38	647179.36	85561.04	915083.01	195353.28	2168801.68
Rb	1653.54	1965.31	188.57	1603.68	201.16	6304.40
Ba	34524.29	86940.75	6367.79	212879.97	3097.56	4127.04
Th	123.80	272.94	11.66	171.93	3.59	265.24
U	52.20	116.70	6.59	148.88	3.39	225.50
Nb	299.97	1835.59	54.00	2160.18	0.36	1927.64
Ta	35.11	91.87	1.59	125.92	7.48	118.45
La	714.81	2120.37	120.72	3403.05	21.08	3819.88
Ce	1470.80	6198.34	248.65	7279.46	49.82	8216.63
Pb	570.15	375.80	57.86	819.43	86.66	640.85
Sr	62509.51	24399.54	10058.98	180689.87	10080.69	63709.27
Nd	637.05	5817.24	122.24	7429.50	32.57	7974.83
Zr	1752.40	59605.24	341.73	67639.58	18.18	62459.44
Hf	49.95	1629.05	8.00	1878.33	5.48	1681.96
Sm	91.54	2083.20	16.66	2560.48	1.02	2548.51
Eu	20.95	786.54	4.40	953.58	0.14	852.22
Y	1.75	21746.36	0.27	27574.22	4.93	25141.23
Yb	0.00	2355.21	0.00	2855.83	0.00	2445.21
Lu	0.90	350.22	0.00	426.50	0.05	375.49

Table E.20 (continued)

	Kurile		Marianas		Northern Antilles	
	F_{arc}	F_{mantle}	F_{arc}	F_{mantle}	F_{arc}	F_{mantle}
K	798381.03	1757031.74	360441.33	1643921.97	209481.14	816287.31
Rb	2298.39	5359.44	871.62	4093.30	457.64	2732.98
Ba	20314.00	39459.90	11245.82	12182.03	5739.11	649.46
Th	227.19	421.82	34.15	197.01	38.58	190.60
U	70.35	150.93	21.75	115.10	12.71	68.67
Nb	153.89	3124.68	20.59	2109.51	43.72	1065.51
Ta	8.72	175.13	1.20	137.26	0.96	69.23
La	650.74	4036.77	182.70	2674.85	165.39	1305.12
Ce	1343.26	11630.84	355.60	6740.63	508.55	3701.37
Pb	420.84	1867.09	242.85	304.92	476.83	26.07
Sr	35619.74	83048.89	11958.12	58505.07	12993.38	22417.17
Nd	428.72	10117.14	235.23	6197.98	85.14	3305.07
Zr	5143.64	89154.04	85.75	57080.17	113.98	31182.16
Hf	26.66	2564.03	4.87	1544.23	2.51	862.20
Sm	52.61	3510.97	22.13	2094.72	6.12	1118.93
Eu	8.79	1267.47	1.97	739.48	2.40	391.84
Y	8.31	35330.12	15.82	20920.30	24.39	11147.74
Yb	0.00	3740.47	0.00	2128.56	0.00	1155.91
Lu	0.07	564.97	0.05	325.09	0.08	177.24

Table E.20 (continued)

	Southern Antilles		Sunda-Java		Tonga	
	F_{arc}	F_{mantle}	F_{arc}	F_{mantle}	F_{arc}	F_{mantle}
K	80113.79	1190828.00	207909.74	2032986.01	218925.31	3321067.67
Rb	244.81	5316.05	515.94	6539.05	481.07	6710.37
Ba	3606.76	11056.87	9704.79	119840.75	6375.53	67970.83
Th	71.18	413.95	86.05	656.01	19.07	605.24
U	26.64	144.77	17.17	137.21	8.44	266.14
Nb	62.73	1302.70	65.97	2534.76	384.57	5382.59
Ta	20.69	63.51	5.05	163.51	4.34	341.03
La	181.91	2055.97	288.00	4232.27	140.15	10381.43
Ce	325.97	5351.56	544.28	11902.95	412.50	24583.16
Pb	40.31	967.50	247.70	1713.99	180.07	4369.15
Sr	6510.60	27551.11	9136.77	103575.01	9524.50	228819.16
Nd	121.67	3620.61	259.03	8009.88	127.37	23314.00
Zr	154.98	29882.79	120.14	70617.26	96.41	185234.68
Hf	2.67	831.05	8.39	1971.40	0.13	5126.13
Sm	18.12	1103.72	29.60	2637.38	13.36	7608.70
Eu	3.15	370.79	5.29	919.68	3.20	2712.23
Y	4.22	10180.50	13.34	25262.48	8.17	74076.75
Yb	0.00	1058.70	0.00	2679.40	0.00	7833.81
Lu	0.00	160.93	0.24	405.29	0.01	1183.13

Table E.21 Slab-to-arc and slab-to-mantle fluxes for low-K magma series assuming doubled crustal addition rate and 20% partial melting of IAV source. Fluxes in kg/yr/km arc length.

	Aleutians		**Central America**		**Izu-Bonin**	
	F_{arc}	F_{mantle}	F_{arc}	F_{mantle}	F_{arc}	F_{mantle}
K	32702.38	1391511.35	1146.68	999497.38	428293.44	1935861.52
Rb	118.64	3500.22	7.18	1785.07	777.09	5728.47
Ba	2421.96	119043.08	204.69	219043.06	10080.95	-2856.35
Th	3.09	393.66	0.02	183.57	13.03	255.79
U	2.76	166.14	0.02	155.44	12.42	216.46
Nb	0.56	2134.99	3.19	2210.98	0.20	1927.79
Ta	3.07	123.92	0.00	127.51	21.26	104.66
La	43.00	2792.17	2.14	3521.63	69.12	3771.84
Ce	105.21	7563.93	5.68	7522.43	141.32	8125.13
Pb	59.25	886.71	0.07	877.23	324.83	402.68
Sr	4568.71	82340.34	285.96	190462.90	23002.35	50787.62
Nd	37.47	6416.82	2.78	7548.96	37.35	7970.05
Zr	81.30	61276.34	4.23	67977.08	291.31	62186.31
Hf	5.11	1673.90	0.36	1885.97	15.85	1671.60
Sm	6.50	2168.24	0.66	2576.48	0.42	2549.11
Eu	2.49	805.00	0.19	957.79	0.28	852.09
Y	201.54	21546.57	0.26	27574.24	188.22	24957.94
Yb	0.00	2355.21	0.00	2855.83	0.00	2445.21
Lu	0.00	351.12	0.07	426.43	0.22	375.32

Table E.21 (continued)

	Kurile		Marianas		Northern Antilles	
	F_{arc}	F_{mantle}	F_{arc}	F_{mantle}	F_{arc}	F_{mantle}
K	58086.86	2497325.92	31093.87	1973269.43	37350.37	988418.09
Rb	71.38	7586.46	99.48	4865.44	83.95	3106.67
Ba	2435.73	57338.16	1497.35	21930.49	1359.01	5029.56
Th	15.89	633.12	3.52	227.63	5.25	223.94
U	5.52	215.77	1.56	135.30	2.74	78.64
Nb	0.70	3277.87	1.30	2128.80	12.94	1096.28
Ta	0.41	183.44	0.01	138.44	0.33	69.85
La	30.73	4656.78	19.15	2838.41	24.04	1446.46
Ce	86.74	12887.36	36.80	7059.42	51.21	4158.71
Pb	39.60	2248.32	16.20	531.57	35.45	467.44
Sr	4793.42	113875.22	1299.08	69164.11	2944.37	32466.18
Nd	0.98	10544.87	9.62	6423.58	15.43	3374.78
Zr	11.91	94285.77	53.86	57112.07	43.90	31252.23
Hf	0.04	2590.65	0.02	1549.07	0.72	863.99
Sm	2.15	3561.43	1.75	2115.10	1.23	1123.82
Eu	0.57	1275.68	0.03	741.43	0.59	393.65
Y	42.31	35296.12	0.80	20935.32	4.61	11167.52
Yb	0.00	3740.47	0.00	2128.56	0.00	1155.91
Lu	0.01	565.03	0.04	325.09	0.03	177.30

Table E.21 (continued)

	Southern Antilles		Sunda-Java		Tonga	
	F_{arc}	F_{mantle}	F_{arc}	F_{mantle}	F_{arc}	F_{mantle}
K	26025.91	1244915.88	n.d.	n.d.	116074.94	3423918.03
Rb	72.63	5488.22	n.d.	n.d.	367.64	6823.80
Ba	907.58	13756.05	n.d.	n.d.	4136.06	70210.30
Th	11.06	474.06	n.d.	n.d.	18.02	606.29
U	2.96	168.44	n.d.	n.d.	7.80	266.79
Nb	11.08	1354.34	n.d.	n.d.	48.42	5718.74
Ta	0.38	83.82	n.d.	n.d.	1.87	343.51
La	29.24	2208.65	n.d.	n.d.	121.46	10400.12
Ce	53.14	5624.40	n.d.	n.d.	264.33	24731.33
Pb	16.39	991.41	n.d.	n.d.	168.61	4380.61
Sr	1144.79	32916.92	n.d.	n.d.	8153.38	230190.29
Nd	18.49	3723.78	n.d.	n.d.	63.79	23377.58
Zr	15.93	30021.85	n.d.	n.d.	132.94	185198.15
Hf	0.84	832.89	n.d.	n.d.	6.38	5119.87
Sm	3.81	1118.03	n.d.	n.d.	3.16	7618.90
Eu	0.19	373.75	n.d.	n.d.	3.23	2712.21
Y	1.11	10183.61	n.d.	n.d.	199.96	73884.96
Yb	0.00	1058.70	n.d.	n.d.	0.00	7833.81
Lu	0.03	160.90	n.d.	n.d.	0.08	1183.05

Table E.22 Slab-to-arc and slab-to-mantle fluxes for high-K magma series assuming halved crustal addition rate and 20% partial melting of IAV source. Fluxes in kg/yr/km arc length.

	Aleutians		**Central America**		**Izu-Bonin**	
	F_{arc}	F_{mantle}	F_{arc}	F_{mantle}	F_{arc}	F_{mantle}
K	15281.89	1408931.84	9620.85	991023.21	n/a	n/a
Rb	33.44	3585.42	25.89	1766.36	n/a	n/a
Ba	619.00	120846.03	517.38	218730.38	n/a	n/a
Th	3.36	393.39	4.75	178.85	n/a	n/a
U	0.55	168.34	1.55	153.92	n/a	n/a
Nb	0.10	2135.46	14.20	2199.97	n/a	n/a
Ta	0.07	126.91	0.81	126.71	n/a	n/a
La	16.08	2819.10	25.91	3497.85	n/a	n/a
Ce	32.64	7636.50	44.12	7483.99	n/a	n/a
Pb	4.08	941.87	3.91	873.39	n/a	n/a
Sr	442.48	86466.57	588.55	190160.30	n/a	n/a
Nd	18.18	6436.11	18.52	7533.21	n/a	n/a
Zr	45.67	61311.97	54.71	67926.60	n/a	n/a
Hf	0.02	1678.98	1.48	1884.85	n/a	n/a
Sm	3.04	2171.70	2.81	2574.33	n/a	n/a
Eu	0.55	806.93	0.54	957.44	n/a	n/a
Y	1.27	21746.84	1.05	27573.44	n/a	n/a
Yb	0.00	2355.21	0.00	2855.83	n/a	n/a
Lu	0.00	351.12	0.02	426.48	n/a	n/a

Table E.22 (continued)

	Kurile		Marianas		Northern Antilles	
	F_{arc}	F_{mantle}	F_{arc}	F_{mantle}	F_{arc}	F_{mantle}
K	58212.60	2497200.17	n/a	n/a	n/a	n/a
Rb	126.02	7531.81	n/a	n/a	n/a	n/a
Ba	1441.03	58332.87	n/a	n/a	n/a	n/a
Th	9.04	639.97	n/a	n/a	n/a	n/a
U	4.76	216.53	n/a	n/a	n/a	n/a
Nb	5.18	3273.39	n/a	n/a	n/a	n/a
Ta	n/a	n/a	n/a	n/a	n/a	n/a
La	28.38	4659.13	n/a	n/a	n/a	n/a
Ce	49.00	12925.10	n/a	n/a	n/a	n/a
Pb	10.56	2277.37	n/a	n/a	n/a	n/a
Sr	1161.10	117507.53	n/a	n/a	n/a	n/a
Nd	25.33	10520.52	n/a	n/a	n/a	n/a
Zr	2.26	94295.42	n/a	n/a	n/a	n/a
Hf	0.10	2590.59	n/a	n/a	n/a	n/a
Sm	4.96	3558.62	n/a	n/a	n/a	n/a
Eu	0.67	1275.59	n/a	n/a	n/a	n/a
Y	0.07	35338.36	n/a	n/a	n/a	n/a
Yb	0.00	3740.47	n/a	n/a	n/a	n/a
Lu	0.00	565.03	n/a	n/a	n/a	n/a

Table E.22 (continued)

	Southern Antilles		Sunda-Java		Tonga	
	F_{arc}	F_{mantle}	F_{arc}	F_{mantle}	F_{arc}	F_{mantle}
K	2933.92	1268007.87	343412.59	1897483.17	23187.83	3516805.15
Rb	8.51	5552.35	1710.17	5344.82	53.15	7138.29
Ba	117.86	14545.77	13766.83	115778.70	671.47	73674.89
Th	3.03	482.10	153.86	588.21	1.25	623.06
U	0.92	170.48	31.95	122.43	0.64	273.95
Nb	2.97	1362.46	155.21	2445.52	26.33	5740.83
Ta	0.12	84.08	5.39	163.17	0.43	344.95
La	6.98	2230.90	757.43	3762.84	29.06	10492.52
Ce	15.50	5662.03	1356.22	11091.01	55.80	24939.86
Pb	1.21	1006.60	187.07	1774.63	8.51	4540.71
Sr	212.22	33849.50	9872.81	102838.97	556.19	237787.48
Nd	6.13	3736.15	469.11	7799.80	21.37	23420.00
Zr	20.13	30017.65	711.87	70025.54	17.30	185313.79
Hf	0.48	833.24	11.96	1967.83	0.19	5126.06
Sm	0.89	1120.95	63.43	2603.55	3.85	7618.21
Eu	n/a	n/a	13.59	911.38	0.86	2714.57
Y	1.68	10183.04	34.79	25241.03	1.03	74083.89
Yb	0.00	1058.70	0.00	2679.40	0.00	7833.81
Lu	0.00	160.93	0.00	405.54	0.00	1183.13

Table E.23 Slab-to-arc and slab-to-mantle fluxes for medium-K magma series assuming halved crustal addition rate and 20% partial melting of IAV source. Fluxes in kg/yr/km arc length.

	Aleutians		**Central America**		**Izu-Bonin**	
	F_{arc}	F_{mantle}	F_{arc}	F_{mantle}	F_{arc}	F_{mantle}
K	194258.59	1229955.14	21390.26	979253.80	48838.32	2315316.64
Rb	413.38	3205.47	47.14	1745.11	50.29	6455.27
Ba	8631.07	112833.97	1591.95	217655.81	774.39	6450.20
Th	30.95	365.79	2.92	180.68	0.90	267.93
U	13.05	155.84	1.65	153.82	0.85	228.04
Nb	74.99	2060.56	13.50	2200.67	0.09	1927.90
Ta	8.78	118.21	0.40	127.12	1.87	124.06
La	178.70	2656.48	30.18	3493.59	5.27	3835.69
Ce	367.70	7301.44	62.16	7465.95	12.46	8253.99
Pb	142.54	803.42	14.47	862.83	21.66	705.84
Sr	15627.38	71281.67	2514.74	188234.11	2520.17	71269.79
Nd	159.26	6295.03	30.56	7521.17	8.14	7999.26
Zr	438.10	60919.54	85.43	67895.88	4.54	62473.08
Hf	12.49	1666.52	2.00	1884.33	1.37	1686.07
Sm	22.88	2151.86	4.16	2572.97	0.26	2549.27
Eu	5.24	802.25	1.10	956.88	0.03	852.33
Y	0.44	21747.67	0.07	27574.43	1.23	25144.93
Yb	0.00	2355.21	0.00	2855.83	0.00	2445.21
Lu	0.23	350.90	0.00	426.50	0.01	375.52

Table E.23 (continued)

	Kurile		Marianas		Northern Antilles	
	F_{arc}	F_{mantle}	F_{arc}	F_{mantle}	F_{arc}	F_{mantle}
K	199595.26	2355817.52	90110.33	1914252.96	52370.29	973398.17
Rb	574.60	7083.24	217.91	4747.01	114.41	3076.21
Ba	5078.50	54695.39	2811.45	20616.39	1434.78	4953.80
Th	56.80	592.21	8.54	222.62	9.65	219.54
U	17.59	203.70	5.44	131.42	3.18	78.20
Nb	38.47	3240.10	5.15	2124.95	10.93	1098.30
Ta	2.18	181.67	0.30	138.15	0.24	69.94
La	162.68	4524.83	45.67	2811.88	41.35	1429.16
Ce	335.81	12638.28	88.90	7007.32	127.14	4082.78
Pb	105.21	2182.71	60.71	487.06	119.21	383.69
Sr	8904.94	109763.70	2989.53	67473.66	3248.34	32162.21
Nd	107.18	10438.67	58.81	6374.40	21.28	3368.92
Zr	1285.91	93011.77	21.44	57144.49	28.49	31267.64
Hf	6.67	2584.02	1.22	1547.88	0.63	864.08
Sm	13.15	3550.43	5.53	2111.31	1.53	1123.52
Eu	2.20	1274.06	0.49	740.96	0.60	393.65
Y	2.08	35336.35	3.95	20932.16	6.10	11166.03
Yb	0.00	3740.47	0.00	2128.56	0.00	1155.91
Lu	0.02	565.02	0.01	325.12	0.02	177.31

Table E.23 (continued)

	Southern Antilles		Sunda-Java		Tonga	
	F_{arc}	F_{mantle}	F_{arc}	F_{mantle}	F_{arc}	F_{mantle}
K	20028.45	1250913.34	51977.44	2188918.32	54731.33	3485261.65
Rb	61.20	5499.65	128.98	6926.00	120.27	7071.17
Ba	901.69	13761.94	2426.20	127119.34	1593.88	72752.48
Th	17.79	467.33	21.51	720.55	4.77	619.54
U	6.66	164.75	4.29	150.09	2.11	272.47
Nb	15.68	1349.74	16.49	2584.24	96.14	5671.02
Ta	5.17	79.03	1.26	167.30	1.09	344.29
La	45.48	2192.40	72.00	4448.27	35.04	10486.54
Ce	81.49	5596.05	136.07	12311.16	103.12	24892.53
Pb	10.08	997.73	61.93	1899.77	45.02	4504.20
Sr	1627.65	32434.07	2284.19	110427.59	2381.13	235962.54
Nd	30.42	3711.86	64.76	8204.15	31.84	23409.53
Zr	38.75	29999.03	30.03	70707.37	24.10	185306.99
Hf	0.67	833.05	2.10	1977.69	0.03	5126.22
Sm	4.53	1117.31	7.40	2659.58	3.34	7618.72
Eu	0.79	373.15	1.32	923.65	0.80	2714.63
Y	1.05	10183.67	3.33	25272.48	2.04	74082.88
Yb	0.00	1058.70	0.00	2679.40	0.00	7833.81
Lu	0.00	160.93	0.06	405.48	0.00	1183.13

Table E.24 Slab-to-arc and slab-to-mantle fluxes for low-K magma series assuming halved crustal addition rate and 20% partial melting of IAV source. Fluxes in kg/yr/km arc length.

	Aleutians		**Central America**		**Izu-Bonin**	
	F_{arc}	F_{mantle}	F_{arc}	F_{mantle}	F_{arc}	F_{mantle}
K	8175.60	1416038.14	286.67	1000357.39	107073.36	2257081.60
Rb	29.66	3589.19	1.80	1790.45	194.27	6311.29
Ba	605.49	120859.55	51.17	219196.58	2520.24	4704.36
Th	0.77	395.97	0.01	183.59	3.26	265.57
U	0.69	168.20	0.01	155.46	3.11	225.78
Nb	0.14	2135.41	0.80	2213.38	0.05	1927.94
Ta	0.77	126.22	0.00	127.52	5.32	120.61
La	10.75	2824.43	0.53	3523.23	17.28	3823.68
Ce	26.30	7642.84	1.42	7526.69	35.33	8231.12
Pb	14.81	931.14	0.02	877.28	81.21	646.30
Sr	1142.18	85766.87	71.49	190677.36	5750.59	68039.38
Nd	9.37	6444.92	0.69	7551.04	9.34	7998.06
Zr	20.33	61337.31	1.06	67980.25	72.83	62404.79
Hf	1.28	1677.73	0.09	1886.24	3.96	1683.48
Sm	1.63	2173.12	0.16	2576.97	0.10	2549.42
Eu	0.62	806.86	0.05	957.93	0.07	852.29
Y	50.39	21697.73	0.06	27574.43	47.05	25099.11
Yb	0.00	2355.21	0.00	2855.83	0.00	2445.21
Lu	0.00	351.12	0.02	426.48	0.05	375.48

Table E.24 (continued)

	Kurile		Marianas		Northern Antilles	
	F_{arc}	F_{mantle}	F_{arc}	F_{mantle}	F_{arc}	F_{mantle}
K	14521.71	2540891.06	7773.47	1996589.83	9337.59	1016430.86
Rb	17.84	7639.99	24.87	4940.05	20.99	3169.63
Ba	608.93	59164.96	374.34	23053.51	339.75	6048.82
Th	3.97	645.04	0.88	230.28	1.31	227.87
U	1.38	219.90	0.39	136.47	0.69	80.69
Nb	0.18	3278.40	0.32	2129.78	3.24	1105.99
Ta	0.10	183.75	0.00	138.45	0.08	70.10
La	7.68	4679.83	4.79	2852.76	6.01	1464.49
Ce	21.69	12952.41	9.20	7087.02	12.80	4197.12
Pb	9.90	2278.02	4.05	543.72	8.86	494.03
Sr	1198.35	117470.28	324.77	70138.42	736.09	34674.46
Nd	0.25	10545.61	2.41	6430.80	3.86	3386.35
Zr	2.98	94294.70	13.47	57152.46	10.98	31285.16
Hf	0.01	2590.68	0.01	1549.09	0.18	864.53
Sm	0.54	3563.04	0.44	2116.41	0.31	1124.74
Eu	0.14	1276.12	0.01	741.45	0.15	394.10
Y	10.58	35327.85	0.20	20935.92	1.15	11170.98
Yb	0.00	3740.47	0.00	2128.56	0.00	1155.91
Lu	0.00	565.04	0.01	325.12	0.01	177.32

Table E.24 (continued)

	Southern Antilles		Sunda-Java		Tonga	
	F_{arc}	F_{mantle}	F_{arc}	F_{mantle}	F_{arc}	F_{mantle}
K	6506.48	1264435	n.d.	n.d.	29018.74	3510974.24
Rb	18.16	5542.699	n.d.	n.d.	91.91	7099.53
Ba	226.89	14436.73	n.d.	n.d.	1034.01	73312.35
Th	2.77	482.3587	n.d.	n.d.	4.50	619.80
U	0.74	170.6646	n.d.	n.d.	1.95	272.63
Nb	2.77	1362.653	n.d.	n.d.	12.11	5755.06
Ta	0.09	84.10676	n.d.	n.d.	0.47	344.91
La	7.31	2230.574	n.d.	n.d.	30.37	10491.21
Ce	13.29	5664.253	n.d.	n.d.	66.08	24929.57
Pb	4.10	1003.705	n.d.	n.d.	42.15	4507.07
Sr	286.20	33775.52	n.d.	n.d.	2038.34	236305.32
Nd	4.62	3737.65	n.d.	n.d.	15.95	23425.42
Zr	3.98	30033.79	n.d.	n.d.	33.24	185297.85
Hf	0.21	833.514	n.d.	n.d.	1.60	5124.66
Sm	0.95	1120.887	n.d.	n.d.	0.79	7621.27
Eu	0.05	373.894	n.d.	n.d.	0.81	2714.63
Y	0.28	10184.44	n.d.	n.d.	49.99	74034.93
Yb	0.00	1058.698	n.d.	n.d.	0.00	7833.81
Lu	0.01	160.9237	n.d.	n.d.	0.02	1183.11

Table E.25 Fraction of ingoing slab material incorporated into mantle assuming 20% partial melting of IAV source, high –K magma series.

	Aleutians	Central America	Izu-Bonin	Kurile	Marianas	Northern Antilles	Southern Antilles	Sunda-Java	Tonga
K	0.9785	0.9808	n/a	0.9544	n/a	n/a	0.9954	0.6935	0.9869
Rb	0.9815	0.9711	n/a	0.9671	n/a	n/a	0.9969	0.5152	0.9852
Ba	0.9898	0.9953	n/a	0.9518	n/a	n/a	0.9839	0.7875	0.9819
Th	0.9831	0.9483	n/a	0.9721	n/a	n/a	0.9875	0.5853	0.9960
U	0.9935	0.9801	n/a	0.9570	n/a	n/a	0.9892	0.5861	0.9954
Nb	0.9999	0.9872	n/a	0.9968	n/a	n/a	0.9957	0.8806	0.9909
Ta	0.9989	0.9874	n/a	n/a	n/a	n/a	0.9972	0.9361	0.9975
La	0.9887	0.9853	n/a	0.9879	n/a	n/a	0.9938	0.6649	0.9945
Ce	0.9915	0.9883	n/a	0.9924	n/a	n/a	0.9945	0.7821	0.9955
Pb	0.9914	0.9911	n/a	0.9908	n/a	n/a	0.9976	0.8093	0.9963
Sr	0.9898	0.9938	n/a	0.9804	n/a	n/a	0.9875	0.8248	0.9953
Nd	0.9944	0.9951	n/a	0.9952	n/a	n/a	0.9967	0.8865	0.9982
Zr	0.9985	0.9984	n/a	1.0000	n/a	n/a	0.9987	0.9799	0.9998
Hf	1.0000	0.9984	n/a	0.9999	n/a	n/a	0.9988	0.9879	0.9999
Sm	0.9972	0.9978	n/a	0.9972	n/a	n/a	0.9984	0.9524	0.9990
Eu	0.9986	0.9989	n/a	0.9990	n/a	n/a	n/a	0.9706	0.9994
Y	0.9999	0.9999	n/a	1.0000	n/a	n/a	0.9997	0.9972	1.0000
Yb	1.0000	1.0000	n/a	1.0000	n/a	n/a	1.0000	1.0000	1.0000
Lu	1.0000	0.9999	n/a	1.0000	n/a	n/a	1.0000	1.0000	1.0000

Table E.26 Fraction of ingoing slab material incorporated into mantle assuming 20% partial melting of IAV source, medium –K magma series.

	Aleutians	Central America	Izu-Bonin	Kurile	Marianas	Northern Antilles	Southern Antilles	Sunda-Java	Tonga
K	0.7272	0.9572	0.9587	0.8438	0.9101	0.8979	0.9685	0.9536	0.9691
Rb	0.7715	0.9474	0.9845	0.8499	0.9122	0.9283	0.9780	0.9634	0.9666
Ba	0.8579	0.9855	0.7856	0.8301	0.7600	0.5508	0.8770	0.9625	0.9571
Th	0.8440	0.9682	0.9933	0.8250	0.9261	0.9158	0.9266	0.9420	0.9847
U	0.8455	0.9788	0.9926	0.8410	0.9205	0.9219	0.9223	0.9444	0.9846
Nb	0.9298	0.9878	0.9999	0.9765	0.9952	0.9803	0.9770	0.9873	0.9667
Ta	0.8617	0.9937	0.9703	0.9763	0.9957	0.9932	0.8771	0.9850	0.9937
La	0.8739	0.9829	0.9973	0.9306	0.9680	0.9438	0.9594	0.9681	0.9933
Ce	0.9041	0.9835	0.9970	0.9482	0.9749	0.9396	0.9713	0.9781	0.9917
Pb	0.6986	0.9670	0.9404	0.9080	0.7783	0.5259	0.9800	0.9369	0.9802
Sr	0.6404	0.9736	0.9317	0.8499	0.9151	0.8165	0.9044	0.9595	0.9800
Nd	0.9506	0.9919	0.9980	0.9797	0.9817	0.9874	0.9837	0.9843	0.9973
Zr	0.9857	0.9975	0.9999	0.9727	0.9992	0.9982	0.9974	0.9992	0.9997
Hf	0.9851	0.9979	0.9984	0.9949	0.9984	0.9986	0.9984	0.9979	1.0000
Sm	0.9790	0.9968	0.9998	0.9926	0.9948	0.9973	0.9919	0.9945	0.9991
Eu	0.9870	0.9977	0.9999	0.9966	0.9987	0.9970	0.9958	0.9971	0.9994
Y	1.0000	1.0000	0.9999	0.9999	0.9996	0.9989	0.9998	0.9997	0.9999
Yb	1.0000	1.0000	1.0000	1.0000	1.0000	1.0000	1.0000	1.0000	1.0000
Lu	0.9987	1.0000	0.9999	0.9999	0.9999	0.9998	1.0000	0.9997	1.0000

Table E.27 Fraction of ingoing slab material incorporated into mantle assuming 20% partial melting of IAV source, low –K magma series.

	Aleutians	Central America	Izu-Bonin	Kurile	Marianas	Northern Antilles	Southern Antilles	Sunda-Java	Tonga
K	0.9885	0.9994	0.9094	0.9886	0.9922	0.9818	0.9898	n.d.	0.9836
Rb	0.9836	0.9980	0.9403	0.9953	0.9900	0.9868	0.9935	n.d.	0.9744
Ba	0.9900	0.9995	0.3023	0.9796	0.9680	0.8936	0.9691	n.d.	0.9722
Th	0.9961	0.9999	0.9758	0.9878	0.9924	0.9886	0.9886	n.d.	0.9856
U	0.9918	0.9999	0.9729	0.9875	0.9943	0.9831	0.9914	n.d.	0.9858
Nb	0.9999	0.9993	0.9999	0.9999	0.9997	0.9942	0.9959	n.d.	0.9958
Ta	0.9879	1.0000	0.9156	0.9989	1.0000	0.9976	0.9977	n.d.	0.9973
La	0.9924	0.9997	0.9910	0.9967	0.9966	0.9918	0.9935	n.d.	0.9942
Ce	0.9931	0.9996	0.9915	0.9967	0.9974	0.9939	0.9953	n.d.	0.9947
Pb	0.9687	1.0000	0.7768	0.9913	0.9852	0.9648	0.9919	n.d.	0.9815
Sr	0.9737	0.9993	0.8441	0.9798	0.9908	0.9584	0.9832	n.d.	0.9829
Nd	0.9971	0.9998	0.9977	1.0000	0.9993	0.9977	0.9975	n.d.	0.9986
Zr	0.9993	1.0000	0.9977	0.9999	0.9995	0.9993	0.9997	n.d.	0.9996
Hf	0.9985	0.9999	0.9953	1.0000	1.0000	0.9996	0.9995	n.d.	0.9994
Sm	0.9985	0.9999	0.9999	0.9997	0.9996	0.9995	0.9983	n.d.	0.9998
Eu	0.9985	0.9999	0.9998	0.9998	1.0000	0.9992	0.9997	n.d.	0.9994
Y	0.9954	1.0000	0.9963	0.9994	1.0000	0.9998	0.9999	n.d.	0.9987
Yb	1.0000	1.0000	1.0000	1.0000	1.0000	1.0000	1.0000	n.d.	1.0000
Lu	1.0000	0.9999	0.9997	1.0000	0.9999	0.9999	0.9999	n.d.	1.0000

Table E.28 Fraction of ingoing slab material incorporated into mantle assuming 5% partial melting of IAV source, high –K magma series.

	Aleutians	Central America	Izu-Bonin	Kurile	Marianas	Northern Antilles	Southern Antilles	Sunda-Java	Tonga
K	0.9826	0.9831	n/a	0.9576	n/a	n/a	0.9957	0.7083	0.9889
Rb	0.9831	0.9724	n/a	0.9679	n/a	n/a	0.9970	0.5136	0.9872
Ba	0.9903	0.9954	n/a	0.9534	n/a	n/a	0.9843	0.7911	0.9826
Th	0.9860	0.9509	n/a	0.9750	n/a	n/a	0.9877	0.5972	0.9971
U	0.9959	0.9813	n/a	0.9599	n/a	n/a	0.9894	0.6012	0.9966
Nb	0.9899	0.9909	n/a	0.9998	n/a	n/a	0.9970	0.9346	0.9932
Ta	0.9976	0.9910	n/a	n/a	n/a	n/a	0.9983	0.9769	0.9992
La	0.9949	0.9878	n/a	0.9939	n/a	n/a	0.9946	0.7007	0.9957
Ce	0.9962	0.9907	n/a	0.9967	n/a	n/a	0.9952	0.8096	0.9967
Pb	0.9942	0.9924	n/a	0.9927	n/a	n/a	0.9979	0.8205	0.9967
Sr	0.9945	0.9949	n/a	0.9865	n/a	n/a	0.9888	0.8572	0.9966
Nd	0.9965	0.9960	n/a	0.9972	n/a	n/a	0.9971	0.9025	0.9986
Zr	0.9993	0.9988	n/a	0.9994	n/a	n/a	0.9989	0.9869	0.9999
Hf	0.9997	0.9990	n/a	0.9988	n/a	n/a	0.9992	0.9953	1.0000
Sm	0.9979	0.9981	n/a	0.9979	n/a	n/a	0.9986	0.9582	0.9992
Eu	0.9990	0.9991	n/a	0.9993	n/a	n/a	n/a	0.9746	0.9995
Y	0.9999	0.9999	n/a	1.0000	n/a	n/a	0.9997	0.9969	1.0000
Yb	1.0000	1.0000	n/a	1.0000	n/a	n/a	1.0000	1.0000	1.0000
Lu	1.0000	0.9999	n/a	1.0000	n/a	n/a	1.0000	1.0000	1.0000

Table E.29 Fraction of ingoing slab material incorporated into mantle assuming 5% partial melting of IAV source, medium –K magma series.

	Aleutians	Central America	Izu-Bonin	Kurile	Marianas	Northern Antilles	Southern Antilles	Sunda-Java	Tonga
K	0.7786	0.9647	0.9798	0.8650	0.9366	0.9253	0.9762	0.9633	0.9786
Rb	0.7914	0.9515	0.9924	0.8558	0.9303	0.9363	0.9797	0.9662	0.9735
Ba	0.8647	0.9859	0.8769	0.8407	0.7831	0.6015	0.8848	0.9646	0.9617
Th	0.8801	0.9761	0.9991	0.8431	0.9551	0.9417	0.9311	0.9485	0.9924
U	0.8789	0.9826	0.9976	0.8604	0.9483	0.9485	0.9270	0.9553	0.9922
Nb	0.9970	0.9968	0.9643	0.9998	0.9758	0.9868	0.9958	0.9999	0.9830
Ta	0.9541	0.9998	0.9905	0.9998	0.9805	0.9607	0.9031	0.9996	1.0000
La	0.9496	0.9899	0.9995	0.9678	0.9960	0.9922	0.9750	0.9844	0.9992
Ce	0.9614	0.9903	0.9999	0.9759	0.9970	0.9810	0.9837	0.9900	0.9978
Pb	0.7383	0.9714	0.9542	0.9207	0.8157	0.5582	0.9850	0.9431	0.9834
Sr	0.7134	0.9772	0.9542	0.8895	0.9534	0.8844	0.9295	0.9751	0.9887
Nd	0.9749	0.9945	0.9998	0.9905	0.9927	0.9984	0.9903	0.9909	0.9992
Zr	0.9947	0.9986	0.9999	0.9806	0.9998	0.9999	0.9994	1.0000	1.0000
Hf	0.9967	0.9992	0.9999	0.9994	0.9998	0.9989	1.0000	0.9999	0.9993
Sm	0.9866	0.9976	1.0000	0.9958	0.9977	0.9996	0.9943	0.9964	0.9997
Eu	0.9917	0.9982	1.0000	0.9983	0.9997	0.9990	0.9972	0.9983	0.9998
Y	0.9999	1.0000	0.9999	0.9999	0.9998	0.9986	0.9997	0.9996	0.9999
Yb	1.0000	1.0000	1.0000	1.0000	1.0000	1.0000	1.0000	1.0000	1.0000
Lu	0.9988	1.0000	1.0000	0.9999	1.0000	0.9998	1.0000	0.9997	1.0000

Table E.30 Fraction of ingoing slab material incorporated into mantle assuming 5% partial melting of IAV source, low –K magma series.

	Aleutians	Central America	Izu-Bonin	Kurile	Marianas	Northern Antilles	Southern Antilles	Sunda-Java	Tonga
K	0.9938	0.9999	0.9602	0.9927	0.9975	0.9890	0.9945	n.d.	0.9957
Rb	0.9859	0.9983	0.9708	0.9967	0.9934	0.9891	0.9946	n.d.	0.9836
Ba	0.9908	0.9996	0.6061	0.9818	0.9746	0.9075	0.9742	n.d.	0.9803
Th	0.9991	0.9998	0.9971	0.9912	0.9990	0.9947	0.9914	n.d.	0.9974
U	0.9954	1.0000	0.9915	0.9914	0.9991	0.9902	0.9943	n.d.	0.9971
Nb	0.9844	0.9999	0.9005	0.9861	0.9801	0.9970	0.9983	n.d.	0.9899
Ta	0.9976	0.9992	0.9808	0.9951	0.9679	0.9914	0.9961	n.d.	0.9866
La	0.9991	1.0000	0.9966	1.0000	0.9987	1.0000	0.9996	n.d.	0.9995
Ce	0.9987	1.0000	0.9981	0.9999	0.9992	1.0000	0.9998	n.d.	0.9999
Pb	0.9734	0.9999	0.8291	0.9938	0.9944	0.9731	0.9950	n.d.	0.9874
Sr	0.9818	0.9995	0.9105	0.9874	0.9989	0.9761	0.9949	n.d.	0.9958
Nd	0.9992	0.9999	0.9998	0.9982	0.9999	0.9999	0.9997	n.d.	1.0000
Zr	0.9974	1.0000	1.0000	0.9992	0.9975	1.0000	0.9999	n.d.	0.9999
Hf	0.9997	1.0000	0.9999	0.9994	0.9985	0.9997	0.9999	n.d.	0.9998
Sm	0.9992	0.9999	0.9997	1.0000	1.0000	1.0000	0.9993	n.d.	1.0000
Eu	0.9990	0.9999	0.9999	1.0000	0.9999	0.9998	1.0000	n.d.	0.9999
Y	0.9957	1.0000	0.9968	0.9995	1.0000	0.9997	0.9999	n.d.	0.9985
Yb	1.0000	1.0000	1.0000	1.0000	1.0000	1.0000	1.0000	n.d.	1.0000
Lu	1.0000	0.9999	0.9998	1.0000	0.9999	0.9999	0.9999	n.d.	1.0000

Table E.31 Fraction of ingoing slab material incorporated into mantle assuming halved crustal addition rate, high –K magma series.

	Aleutians	Central America	Izu-Bonin	Kurile	Marianas	Northern Antilles	Southern Antilles	Sunda-Java	Tonga
K	0.9900	0.9908	n/a	0.9778	n/a	n/a	0.9978	0.8492	0.9937
Rb	0.9910	0.9858	n/a	0.9837	n/a	n/a	0.9985	0.7574	0.9929
Ba	0.9950	0.9977	n/a	0.9762	n/a	n/a	0.9920	0.8943	0.9911
Th	0.9920	0.9746	n/a	0.9866	n/a	n/a	0.9938	0.7946	0.9982
U	0.9972	0.9903	n/a	0.9790	n/a	n/a	0.9947	0.7956	0.9979
Nb	0.9996	0.9942	n/a	0.9995	n/a	n/a	0.9981	0.9502	0.9958
Ta	1.0000	0.9943	n/a	n/a	n/a	n/a	0.9988	0.9760	0.9991
La	0.9956	0.9931	n/a	0.9952	n/a	n/a	0.9970	0.8391	0.9975
Ce	0.9969	0.9947	n/a	0.9973	n/a	n/a	0.9974	0.8975	0.9980
Pb	0.9962	0.9958	n/a	0.9957	n/a	n/a	0.9988	0.9065	0.9982
Sr	0.9962	0.9972	n/a	0.9918	n/a	n/a	0.9941	0.9208	0.9980
Nd	0.9979	0.9978	n/a	0.9982	n/a	n/a	0.9985	0.9481	0.9992
Zr	0.9995	0.9993	n/a	0.9998	n/a	n/a	0.9994	0.9922	1.0000
Hf	1.0000	0.9994	n/a	0.9997	n/a	n/a	0.9995	0.9964	1.0000
Sm	0.9988	0.9990	n/a	0.9988	n/a	n/a	0.9993	0.9781	0.9995
Eu	0.9995	0.9995	n/a	0.9996	n/a	n/a	n/a	0.9867	0.9997
Y	0.9999	1.0000	n/a	1.0000	n/a	n/a	0.9998	0.9985	1.0000
Yb	1.0000	1.0000	n/a	1.0000	n/a	n/a	1.0000	1.0000	1.0000
Lu	1.0000	1.0000	n/a	1.0000	n/a	n/a	1.0000	1.0000	1.0000

Table E.32 Fraction of ingoing slab material incorporated into mantle assuming halved crustal addition rate, medium –K magma series.

	Aleutians	Central America	Izu-Bonin	Kurile	Marianas	Northern Antilles	Southern Antilles	Sunda-Java	Tonga
K	0.8724	0.9799	0.9840	0.9255	0.9596	0.9537	0.9856	0.9785	0.9862
Rb	0.8891	0.9744	0.9940	0.9259	0.9590	0.9655	0.9893	0.9822	0.9843
Ba	0.9301	0.9928	0.9116	0.9168	0.8837	0.7841	0.9398	0.9816	0.9793
Th	0.9282	0.9855	0.9979	0.9156	0.9683	0.9625	0.9641	0.9721	0.9938
U	0.9285	0.9901	0.9974	0.9238	0.9651	0.9657	0.9619	0.9741	0.9937
Nb	0.9809	0.9957	0.9973	0.9953	1.0000	0.9984	0.9925	0.9974	0.9863
Ta	0.9492	0.9984	0.9895	0.9952	1.0000	0.9999	0.9431	0.9961	0.9987
La	0.9526	0.9928	0.9997	0.9729	0.9907	0.9832	0.9827	0.9873	0.9981
Ce	0.9668	0.9934	0.9997	0.9811	0.9939	0.9807	0.9887	0.9921	0.9975
Pb	0.8561	0.9842	0.9726	0.9562	0.8955	0.7684	0.9909	0.9695	0.9906
Sr	0.8391	0.9877	0.9711	0.9353	0.9678	0.9264	0.9588	0.9839	0.9923
Nd	0.9830	0.9968	0.9996	0.9933	0.9944	0.9976	0.9939	0.9942	0.9993
Zr	0.9959	0.9991	1.0000	0.9889	1.0000	0.9999	0.9994	0.9999	1.0000
Hf	0.9966	0.9994	0.9998	0.9991	1.0000	1.0000	0.9999	0.9997	0.9999
Sm	0.9920	0.9987	1.0000	0.9974	0.9984	0.9995	0.9968	0.9979	0.9997
Eu	0.9951	0.9990	1.0000	0.9989	0.9997	0.9992	0.9984	0.9990	0.9998
Y	1.0000	1.0000	0.9999	1.0000	0.9999	0.9993	0.9999	0.9998	1.0000
Yb	1.0000	1.0000	1.0000	1.0000	1.0000	1.0000	1.0000	1.0000	1.0000
Lu	0.9994	1.0000	1.0000	1.0000	1.0000	0.9999	1.0000	0.9999	1.0000

Table E.33 Fraction of ingoing slab material incorporated into mantle assuming halved crustal addition rate, low –K magma series.

	Aleutians	Central America	Izu-Bonin	Kurile	Marianas	Northern Antilles	Southern Antilles	Sunda-Java	Tonga
K	0.9952	0.9998	0.9661	0.9950	0.9972	0.9922	0.9957	n.d.	0.9942
Rb	0.9922	0.9991	0.9769	0.9979	0.9956	0.9938	0.9969	n.d.	0.9888
Ba	0.9952	0.9998	0.7139	0.9902	0.9851	0.9492	0.9854	n.d.	0.9875
Th	0.9987	1.0000	0.9927	0.9945	0.9976	0.9954	0.9948	n.d.	0.9953
U	0.9966	1.0000	0.9906	0.9944	0.9982	0.9928	0.9962	n.d.	0.9953
Nb	0.9994	0.9998	0.9942	0.9995	0.9994	0.9995	0.9996	n.d.	1.0000
Ta	0.9960	1.0000	0.9724	1.0000	0.9978	1.0000	0.9999	n.d.	1.0000
La	0.9978	0.9999	0.9993	0.9994	0.9997	0.9984	0.9983	n.d.	0.9992
Ce	0.9981	0.9999	0.9997	0.9993	0.9999	0.9990	0.9991	n.d.	0.9994
Pb	0.9851	1.0000	0.8975	0.9961	0.9944	0.9838	0.9965	n.d.	0.9918
Sr	0.9890	0.9997	0.9387	0.9919	0.9979	0.9840	0.9950	n.d.	0.9952
Nd	0.9993	1.0000	1.0000	0.9996	1.0000	0.9997	0.9995	n.d.	0.9999
Zr	0.9991	1.0000	0.9998	0.9998	0.9992	0.9999	1.0000	n.d.	1.0000
Hf	0.9997	1.0000	0.9995	0.9999	0.9997	1.0000	1.0000	n.d.	1.0000
Sm	0.9995	1.0000	1.0000	0.9999	0.9999	0.9999	0.9995	n.d.	1.0000
Eu	0.9994	1.0000	1.0000	1.0000	1.0000	0.9998	1.0000	n.d.	0.9999
Y	0.9978	1.0000	0.9982	0.9997	1.0000	0.9999	1.0000	n.d.	0.9993
Yb	1.0000	1.0000	1.0000	1.0000	1.0000	1.0000	1.0000	n.d.	1.0000
Lu	1.0000	1.0000	0.9999	1.0000	1.0000	1.0000	1.0000	n.d.	1.0000

Table E.34 Fraction of ingoing slab material incorporated into mantle assuming doubled crustal addition rate, high –K magma series.

	Aleutians	Central America	Izu-Bonin	Kurile	Marianas	Northern Antilles	Southern Antilles	Sunda-Java	Tonga
K	0.9599	0.9631	n/a	0.9110	n/a	n/a	0.9910	0.3969	0.9750
Rb	0.9641	0.9431	n/a	0.9347	n/a	n/a	0.9939	0.0294	0.9715
Ba	0.9800	0.9906	n/a	0.9047	n/a	n/a	0.9681	0.5773	0.9643
Th	0.9682	0.8983	n/a	0.9462	n/a	n/a	0.9752	0.1786	0.9928
U	0.9887	0.9610	n/a	0.9160	n/a	n/a	0.9786	0.1823	0.9916
Nb	0.9985	0.9770	n/a	0.9978	n/a	n/a	0.9922	0.8006	0.9833
Ta	0.9999	0.9773	n/a	n/a	n/a	n/a	0.9952	0.9041	0.9964
La	0.9824	0.9724	n/a	0.9806	n/a	n/a	0.9881	0.3562	0.9899
Ce	0.9877	0.9788	n/a	0.9892	n/a	n/a	0.9897	0.5901	0.9921
Pb	0.9847	0.9831	n/a	0.9829	n/a	n/a	0.9954	0.6261	0.9928
Sr	0.9847	0.9887	n/a	0.9672	n/a	n/a	0.9764	0.6831	0.9919
Nd	0.9914	0.9913	n/a	0.9929	n/a	n/a	0.9940	0.7926	0.9969
Zr	0.9981	0.9974	n/a	0.9993	n/a	n/a	0.9976	0.9690	0.9998
Hf	0.9999	0.9976	n/a	0.9988	n/a	n/a	0.9981	0.9857	1.0000
Sm	0.9954	0.9961	n/a	0.9954	n/a	n/a	0.9970	0.9126	0.9982
Eu	0.9978	0.9980	n/a	0.9984	n/a	n/a	n/a	0.9466	0.9989
Y	0.9997	0.9998	n/a	1.0000	n/a	n/a	0.9993	0.9940	0.9999
Yb	1.0000	1.0000	n/a	1.0000	n/a	n/a	1.0000	1.0000	1.0000
Lu	1.0000	0.9998	n/a	1.0000	n/a	n/a	1.0000	1.0000	1.0000

Table E.35 Fraction of ingoing slab material incorporated into mantle assuming doubled crustal addition rate, medium –K magma series.

	Aleutians	Central America	Izu-Bonin	Kurile	Marianas	Northern Antilles	Southern Antilles	Sunda-Java	Tonga
K	0.4897	0.9196	0.9360	0.7020	0.8382	0.8150	0.9423	0.9139	0.9446
Rb	0.5564	0.8975	0.9761	0.7038	0.8359	0.8621	0.9571	0.9287	0.9374
Ba	0.7204	0.9712	0.6465	0.6673	0.5348	0.1362	0.7592	0.9264	0.9173
Th	0.7130	0.9419	0.9918	0.6622	0.8730	0.8499	0.8563	0.8885	0.9751
U	0.7141	0.9602	0.9897	0.6952	0.8604	0.8627	0.8477	0.8963	0.9748
Nb	0.9238	0.9829	0.9892	0.9811	0.9999	0.9938	0.9699	0.9895	0.9453
Ta	0.7968	0.9935	0.9579	0.9809	1.0000	0.9997	0.7724	0.9844	0.9949
La	0.8106	0.9713	0.9989	0.8914	0.9626	0.9329	0.9309	0.9494	0.9923
Ce	0.8671	0.9737	0.9990	0.9245	0.9755	0.9230	0.9549	0.9683	0.9899
Pb	0.4243	0.9370	0.8905	0.8247	0.5818	0.0736	0.9635	0.8779	0.9626
Sr	0.3563	0.9509	0.8844	0.7413	0.8710	0.7055	0.8351	0.9357	0.9694
Nd	0.9320	0.9870	0.9986	0.9732	0.9774	0.9904	0.9757	0.9769	0.9971
Zr	0.9837	0.9965	1.0000	0.9558	1.0000	0.9998	0.9977	0.9997	1.0000
Hf	0.9863	0.9975	0.9990	0.9964	0.9999	0.9999	0.9994	0.9989	0.9996
Sm	0.9682	0.9946	1.0000	0.9895	0.9935	0.9980	0.9870	0.9916	0.9990
Eu	0.9804	0.9961	1.0000	0.9955	0.9989	0.9969	0.9936	0.9959	0.9993
Y	0.9998	1.0000	0.9998	0.9999	0.9994	0.9974	0.9995	0.9994	0.9999
Yb	1.0000	1.0000	1.0000	1.0000	1.0000	1.0000	1.0000	1.0000	1.0000
Lu	0.9976	1.0000	0.9999	0.9999	0.9999	0.9996	1.0000	0.9994	1.0000

Table E.36 Fraction of ingoing slab material incorporated into mantle assuming doubled crustal addition rate, low –K magma series.

	Aleutians	Central America	Izu-Bonin	Kurile	Marianas	Northern Antilles	Southern Antilles	Sunda-Java	Tonga
K	0.9809	0.9992	0.8643	0.9802	0.9887	0.9688	0.9830	n.d.	0.9770
Rb	0.9688	0.9962	0.9076	0.9916	0.9823	0.9753	0.9877	n.d.	0.9551
Ba	0.9806	0.9991	-0.1444	0.9607	0.9405	0.7967	0.9416	n.d.	0.9500
Th	0.9947	1.0000	0.9708	0.9779	0.9906	0.9817	0.9792	n.d.	0.9812
U	0.9863	1.0000	0.9626	0.9778	0.9928	0.9714	0.9848	n.d.	0.9811
Nb	0.9977	0.9991	0.9768	0.9979	0.9974	0.9978	0.9983	n.d.	0.9998
Ta	0.9841	0.9999	0.8895	1.0000	0.9914	1.0000	0.9998	n.d.	1.0000
La	0.9912	0.9997	0.9973	0.9976	0.9989	0.9936	0.9931	n.d.	0.9967
Ce	0.9924	0.9996	0.9986	0.9974	0.9996	0.9962	0.9962	n.d.	0.9976
Pb	0.9406	1.0000	0.5900	0.9844	0.9775	0.9353	0.9860	n.d.	0.9672
Sr	0.9560	0.9988	0.7547	0.9676	0.9916	0.9360	0.9799	n.d.	0.9810
Nd	0.9970	0.9998	0.9998	0.9984	1.0000	0.9988	0.9982	n.d.	0.9997
Zr	0.9966	1.0000	0.9991	0.9991	0.9968	0.9998	1.0000	n.d.	1.0000
Hf	0.9987	0.9999	0.9979	0.9996	0.9987	1.0000	1.0000	n.d.	1.0000
Sm	0.9980	0.9998	0.9998	0.9998	0.9998	0.9997	0.9979	n.d.	1.0000
Eu	0.9977	0.9998	1.0000	0.9998	1.0000	0.9993	0.9999	n.d.	0.9995
Y	0.9912	1.0000	0.9926	0.9989	1.0000	0.9995	0.9998	n.d.	0.9971
Yb	1.0000	1.0000	1.0000	1.0000	1.0000	1.0000	1.0000	n.d.	1.0000
Lu	1.0000	0.9998	0.9995	1.0000	0.9999	0.9999	0.9998	n.d.	0.9999

Table E.37 Fraction of ingoing slab material incorporated into mantle assuming halved crustal addition rate and 20% partial melting of IAV source, high –K magma series.

	Aleutians	Central America	Izu-Bonin	Kurile	Marianas	Northern Antilles	Southern Antilles	Sunda-Java	Tonga
K	0.9893	0.9904	n/a	0.9772	n/a	n/a	0.9977	0.8468	0.9934
Rb	0.9908	0.9856	n/a	0.9835	n/a	n/a	0.9985	0.7576	0.9926
Ba	0.9949	0.9976	n/a	0.9759	n/a	n/a	0.9920	0.8937	0.9910
Th	0.9915	0.9741	n/a	0.9861	n/a	n/a	0.9938	0.7927	0.9980
U	0.9967	0.9901	n/a	0.9785	n/a	n/a	0.9946	0.7931	0.9977
Nb	1.0000	0.9936	n/a	0.9984	n/a	n/a	0.9978	0.9403	0.9954
Ta	0.9994	0.9937	n/a	n/a	n/a	n/a	0.9986	0.9680	0.9988
La	0.9943	0.9926	n/a	0.9939	n/a	n/a	0.9969	0.8324	0.9972
Ce	0.9957	0.9941	n/a	0.9962	n/a	n/a	0.9973	0.8910	0.9978
Pb	0.9957	0.9955	n/a	0.9954	n/a	n/a	0.9988	0.9046	0.9981
Sr	0.9949	0.9969	n/a	0.9902	n/a	n/a	0.9938	0.9124	0.9977
Nd	0.9972	0.9975	n/a	0.9976	n/a	n/a	0.9984	0.9433	0.9991
Zr	0.9993	0.9992	n/a	1.0000	n/a	n/a	0.9993	0.9899	0.9999
Hf	1.0000	0.9992	n/a	1.0000	n/a	n/a	0.9994	0.9940	1.0000
Sm	0.9986	0.9989	n/a	0.9986	n/a	n/a	0.9992	0.9762	0.9995
Eu	0.9993	0.9994	n/a	0.9995	n/a	n/a	n/a	0.9853	0.9997
Y	0.9999	1.0000	n/a	1.0000	n/a	n/a	0.9998	0.9986	1.0000
Yb	1.0000	1.0000	n/a	1.0000	n/a	n/a	1.0000	1.0000	1.0000
Lu	1.0000	1.0000	n/a	1.0000	n/a	n/a	1.0000	1.0000	1.0000

Table E.38 Fraction of ingoing slab material incorporated into mantle assuming halved crustal addition rate and 20% partial melting of IAV source, medium –K magma series.

	Aleutians	Central America	Izu-Bonin	Kurile	Marianas	Northern Antilles	Southern Antilles	Sunda-Java	Tonga
K	0.8636	0.9786	0.9793	0.9219	0.9550	0.9489	0.9842	0.9768	0.9845
Rb	0.8858	0.9737	0.9923	0.9250	0.9561	0.9641	0.9890	0.9817	0.9833
Ba	0.9289	0.9927	0.8928	0.9150	0.8800	0.7754	0.9385	0.9813	0.9786
Th	0.9220	0.9841	0.9967	0.9125	0.9631	0.9579	0.9633	0.9710	0.9924
U	0.9227	0.9894	0.9963	0.9205	0.9603	0.9610	0.9611	0.9722	0.9923
Nb	0.9649	0.9939	1.0000	0.9883	0.9976	0.9901	0.9885	0.9937	0.9833
Ta	0.9309	0.9969	0.9852	0.9881	0.9978	0.9966	0.9386	0.9925	0.9969
La	0.9370	0.9914	0.9986	0.9653	0.9840	0.9719	0.9797	0.9841	0.9967
Ce	0.9521	0.9917	0.9985	0.9741	0.9875	0.9698	0.9856	0.9891	0.9959
Pb	0.8493	0.9835	0.9702	0.9540	0.8892	0.7630	0.9900	0.9684	0.9901
Sr	0.8202	0.9868	0.9658	0.9250	0.9576	0.9083	0.9522	0.9797	0.9900
Nd	0.9753	0.9960	0.9990	0.9898	0.9909	0.9937	0.9919	0.9922	0.9986
Zr	0.9929	0.9987	0.9999	0.9864	0.9996	0.9991	0.9987	0.9996	0.9999
Hf	0.9926	0.9989	0.9992	0.9974	0.9992	0.9993	0.9992	0.9989	1.0000
Sm	0.9895	0.9984	0.9999	0.9963	0.9974	0.9986	0.9960	0.9972	0.9996
Eu	0.9935	0.9989	1.0000	0.9983	0.9993	0.9985	0.9979	0.9986	0.9997
Y	1.0000	1.0000	1.0000	0.9999	0.9998	0.9995	0.9999	0.9999	1.0000
Yb	1.0000	1.0000	1.0000	1.0000	1.0000	1.0000	1.0000	1.0000	1.0000
Lu	0.9994	1.0000	1.0000	1.0000	1.0000	0.9999	1.0000	0.9998	1.0000

Table E.39 Fraction of ingoing slab material incorporated into mantle assuming halved crustal addition rate and 20% partial melting of IAV source, low –K magma series.

	Aleutians	Central America	Izu-Bonin	Kurile	Marianas	Northern Antilles	Southern Antilles	Sunda-Java	Tonga
K	0.9943	0.9997	0.9547	0.9943	0.9961	0.9909	0.9949	n.d.	0.9918
Rb	0.9918	0.9990	0.9701	0.9977	0.9950	0.9934	0.9967	n.d.	0.9872
Ba	0.9950	0.9998	0.6512	0.9898	0.9840	0.9468	0.9845	n.d.	0.9861
Th	0.9981	1.0000	0.9879	0.9939	0.9962	0.9943	0.9943	n.d.	0.9928
U	0.9959	1.0000	0.9864	0.9938	0.9971	0.9916	0.9957	n.d.	0.9929
Nb	0.9999	0.9996	1.0000	0.9999	0.9998	0.9971	0.9980	n.d.	0.9979
Ta	0.9940	1.0000	0.9578	0.9994	1.0000	0.9988	0.9989	n.d.	0.9986
La	0.9962	0.9998	0.9955	0.9984	0.9983	0.9959	0.9967	n.d.	0.9971
Ce	0.9966	0.9998	0.9957	0.9983	0.9987	0.9970	0.9977	n.d.	0.9974
Pb	0.9843	1.0000	0.8884	0.9957	0.9926	0.9824	0.9959	n.d.	0.9907
Sr	0.9869	0.9996	0.9221	0.9899	0.9954	0.9792	0.9916	n.d.	0.9914
Nd	0.9985	0.9999	0.9988	1.0000	0.9996	0.9989	0.9988	n.d.	0.9993
Zr	0.9997	1.0000	0.9988	1.0000	0.9998	0.9996	0.9999	n.d.	0.9998
Hf	0.9992	1.0000	0.9977	1.0000	1.0000	0.9998	0.9997	n.d.	0.9997
Sm	0.9993	0.9999	1.0000	0.9998	0.9998	0.9997	0.9992	n.d.	0.9999
Eu	0.9992	0.9999	0.9999	0.9999	1.0000	0.9996	0.9999	n.d.	0.9997
Y	0.9977	1.0000	0.9981	0.9997	1.0000	0.9999	1.0000	n.d.	0.9993
Yb	1.0000	1.0000	1.0000	1.0000	1.0000	1.0000	1.0000	n.d.	1.0000
Lu	1.0000	1.0000	0.9999	1.0000	1.0000	1.0000	1.0000	n.d.	1.0000

Table E.40 Fraction of ingoing slab material incorporated into mantle assuming halved crustal addition rate and 5% partial melting of IAV source, high –K magma series.

	Aleutians	Central America	Izu-Bonin	Kurile	Marianas	Northern Antilles	Southern Antilles	Sunda-Java	Tonga
K	0.9913	0.9916	n/a	0.9788	n/a	n/a	0.9979	0.8542	0.9944
Rb	0.9915	0.9862	n/a	0.9840	n/a	n/a	0.9985	0.7568	0.9936
Ba	0.9952	0.9977	n/a	0.9767	n/a	n/a	0.9921	0.8955	0.9913
Th	0.9930	0.9755	n/a	0.9875	n/a	n/a	0.9939	0.7986	0.9985
U	0.9980	0.9907	n/a	0.9800	n/a	n/a	0.9947	0.8006	0.9983
Nb	0.9950	0.9955	n/a	0.9999	n/a	n/a	0.9985	0.9673	0.9966
Ta	0.9988	0.9955	n/a	n/a	n/a	n/a	0.9992	0.9884	0.9996
La	0.9974	0.9939	n/a	0.9970	n/a	n/a	0.9973	0.8503	0.9979
Ce	0.9981	0.9953	n/a	0.9984	n/a	n/a	0.9976	0.9048	0.9983
Pb	0.9971	0.9962	n/a	0.9964	n/a	n/a	0.9989	0.9102	0.9983
Sr	0.9973	0.9974	n/a	0.9932	n/a	n/a	0.9944	0.9286	0.9983
Nd	0.9983	0.9980	n/a	0.9986	n/a	n/a	0.9986	0.9512	0.9993
Zr	0.9997	0.9994	n/a	0.9997	n/a	n/a	0.9995	0.9934	1.0000
Hf	0.9998	0.9995	n/a	0.9994	n/a	n/a	0.9996	0.9976	1.0000
Sm	0.9990	0.9991	n/a	0.9990	n/a	n/a	0.9993	0.9791	0.9996
Eu	0.9995	0.9995	n/a	0.9997	n/a	n/a	n/a	0.9873	0.9997
Y	0.9999	1.0000	n/a	1.0000	n/a	n/a	0.9998	0.9984	1.0000
Yb	1.0000	1.0000	n/a	1.0000	n/a	n/a	1.0000	1.0000	1.0000
Lu	1.0000	0.9999	n/a	1.0000	n/a	n/a	1.0000	1.0000	1.0000

Table E.41 Fraction of ingoing slab material incorporated into mantle assuming halved crustal addition rate and 5% partial melting of IAV source, medium –K magma series.

	Aleutians	Central America	Izu-Bonin	Kurile	Marianas	Northern Antilles	Southern Antilles	Sunda-Java	Tonga
K	0.8893	0.9824	0.9899	0.9325	0.9683	0.9626	0.9881	0.9816	0.9893
Rb	0.8957	0.9757	0.9962	0.9279	0.9651	0.9681	0.9898	0.9831	0.9868
Ba	0.9324	0.9929	0.9385	0.9203	0.8915	0.8007	0.9424	0.9823	0.9808
Th	0.9400	0.9880	0.9995	0.9216	0.9775	0.9709	0.9656	0.9743	0.9962
U	0.9395	0.9913	0.9988	0.9302	0.9741	0.9743	0.9635	0.9777	0.9961
Nb	0.9985	0.9984	0.9822	0.9999	0.9879	0.9934	0.9979	1.0000	0.9915
Ta	0.9771	0.9999	0.9952	0.9999	0.9902	0.9803	0.9516	0.9998	1.0000
La	0.9748	0.9949	0.9997	0.9839	0.9980	0.9961	0.9875	0.9922	0.9996
Ce	0.9807	0.9952	0.9999	0.9880	0.9985	0.9905	0.9919	0.9950	0.9989
Pb	0.8692	0.9857	0.9771	0.9604	0.9079	0.7791	0.9925	0.9715	0.9917
Sr	0.8567	0.9886	0.9771	0.9448	0.9767	0.9422	0.9647	0.9876	0.9944
Nd	0.9874	0.9972	0.9999	0.9953	0.9963	0.9992	0.9951	0.9955	0.9996
Zr	0.9974	0.9993	1.0000	0.9903	0.9999	1.0000	0.9997	1.0000	1.0000
Hf	0.9983	0.9996	0.9999	0.9997	0.9999	0.9995	1.0000	1.0000	0.9997
Sm	0.9933	0.9988	1.0000	0.9979	0.9988	0.9998	0.9972	0.9982	0.9998
Eu	0.9959	0.9991	1.0000	0.9991	0.9999	0.9995	0.9986	0.9992	0.9999
Y	0.9999	1.0000	0.9999	1.0000	0.9999	0.9993	0.9999	0.9998	1.0000
Yb	1.0000	1.0000	1.0000	1.0000	1.0000	1.0000	1.0000	1.0000	1.0000
Lu	0.9994	1.0000	1.0000	1.0000	1.0000	0.9999	1.0000	0.9999	1.0000

Table E.42 Fraction of ingoing slab material incorporated into mantle assuming halved crustal addition rate and 5% partial melting of IAV source, low –K magma series.

	Aleutians	Central America	Izu-Bonin	Kurile	Marianas	Northern Antilles	Southern Antilles	Sunda-Java	Tonga
K	0.9969	0.9999	0.9801	0.9964	0.9987	0.9945	0.9972	n.d.	0.9978
Rb	0.9930	0.9992	0.9854	0.9983	0.9967	0.9946	0.9973	n.d.	0.9918
Ba	0.9954	0.9998	0.8031	0.9909	0.9873	0.9537	0.9871	n.d.	0.9901
Th	0.9995	0.9999	0.9985	0.9956	0.9995	0.9974	0.9957	n.d.	0.9987
U	0.9977	1.0000	0.9958	0.9957	0.9996	0.9951	0.9972	n.d.	0.9985
Nb	0.9922	1.0000	0.9502	0.9931	0.9900	0.9985	0.9991	n.d.	0.9950
Ta	0.9988	0.9996	0.9904	0.9976	0.9839	0.9957	0.9980	n.d.	0.9933
La	0.9996	1.0000	0.9983	1.0000	0.9993	1.0000	0.9998	n.d.	0.9998
Ce	0.9993	1.0000	0.9990	0.9999	0.9996	1.0000	0.9999	n.d.	0.9999
Pb	0.9867	1.0000	0.9146	0.9969	0.9972	0.9865	0.9975	n.d.	0.9937
Sr	0.9909	0.9998	0.9553	0.9937	0.9994	0.9881	0.9975	n.d.	0.9979
Nd	0.9996	1.0000	0.9999	0.9991	0.9999	1.0000	0.9999	n.d.	1.0000
Zr	0.9987	1.0000	1.0000	0.9996	0.9988	1.0000	1.0000	n.d.	1.0000
Hf	0.9999	1.0000	0.9999	0.9997	0.9992	0.9999	0.9999	n.d.	0.9999
Sm	0.9996	1.0000	0.9998	1.0000	1.0000	1.0000	0.9996	n.d.	1.0000
Eu	0.9995	1.0000	1.0000	1.0000	1.0000	0.9999	1.0000	n.d.	0.9999
Y	0.9979	1.0000	0.9984	0.9997	1.0000	0.9999	1.0000	n.d.	0.9993
Yb	1.0000	1.0000	1.0000	1.0000	1.0000	1.0000	1.0000	n.d.	1.0000
Lu	1.0000	1.0000	0.9999	1.0000	1.0000	1.0000	1.0000	n.d.	1.0000

Table E.43 Fraction of ingoing slab material incorporated into mantle assuming doubled crustal addition rate and 20% partial melting of IAV source, high –K magma series.

	Aleutians	Central America	Izu-Bonin	Kurile	Marianas	Northern Antilles	Southern Antilles	Sunda-Java	Tonga
K	0.9571	0.9615	n/a	0.9089	n/a	n/a	0.9908	0.3870	0.9738
Rb	0.9630	0.9422	n/a	0.9342	n/a	n/a	0.9939	0.0304	0.9704
Ba	0.9796	0.9906	n/a	0.9036	n/a	n/a	0.9678	0.5749	0.9639
Th	0.9662	0.8966	n/a	0.9443	n/a	n/a	0.9750	0.1706	0.9920
U	0.9870	0.9602	n/a	0.9140	n/a	n/a	0.9785	0.1722	0.9907
Nb	0.9998	0.9743	n/a	0.9937	n/a	n/a	0.9913	0.7613	0.9817
Ta	0.9978	0.9747	n/a	n/a	n/a	n/a	0.9944	0.8722	0.9951
La	0.9773	0.9706	n/a	0.9758	n/a	n/a	0.9875	0.3297	0.9890
Ce	0.9830	0.9766	n/a	0.9849	n/a	n/a	0.9891	0.5642	0.9911
Pb	0.9827	0.9822	n/a	0.9815	n/a	n/a	0.9952	0.6186	0.9925
Sr	0.9796	0.9877	n/a	0.9609	n/a	n/a	0.9751	0.6496	0.9907
Nd	0.9887	0.9902	n/a	0.9904	n/a	n/a	0.9935	0.7731	0.9964
Zr	0.9970	0.9968	n/a	0.9999	n/a	n/a	0.9973	0.9597	0.9996
Hf	0.9999	0.9969	n/a	0.9998	n/a	n/a	0.9977	0.9758	0.9998
Sm	0.9944	0.9956	n/a	0.9944	n/a	n/a	0.9968	0.9049	0.9980
Eu	0.9973	0.9978	n/a	0.9979	n/a	n/a	n/a	0.9412	0.9987
Y	0.9998	0.9998	n/a	1.0000	n/a	n/a	0.9993	0.9945	0.9999
Yb	1.0000	1.0000	n/a	1.0000	n/a	n/a	1.0000	1.0000	1.0000
Lu	1.0000	0.9998	n/a	1.0000	n/a	n/a	1.0000	1.0000	1.0000

Table E.44 Fraction of ingoing slab material incorporated into mantle assuming doubled crustal addition rate and 20% partial melting of IAV source, medium –K magma series.

	Aleutians	Central America	Izu-Bonin	Kurile	Marianas	Northern Antilles	Southern Antilles	Sunda-Java	Tonga
K	0.4544	0.9145	0.9174	0.6876	0.8202	0.7958	0.9370	0.9072	0.9382
Rb	0.5431	0.8948	0.9691	0.6999	0.8244	0.8566	0.9560	0.9269	0.9331
Ba	0.7158	0.9710	0.5712	0.6602	0.5200	0.1017	0.7540	0.9251	0.9142
Th	0.6880	0.9365	0.9867	0.6499	0.8523	0.8317	0.8533	0.8840	0.9695
U	0.6909	0.9576	0.9852	0.6821	0.8410	0.8438	0.8446	0.8888	0.9693
Nb	0.8595	0.9756	0.9998	0.9531	0.9903	0.9606	0.9541	0.9746	0.9333
Ta	0.7235	0.9875	0.9406	0.9526	0.9914	0.9864	0.7542	0.9700	0.9874
La	0.7479	0.9657	0.9945	0.8612	0.9361	0.8875	0.9187	0.9363	0.9867
Ce	0.8082	0.9670	0.9940	0.8965	0.9499	0.8792	0.9426	0.9563	0.9835
Pb	0.3973	0.9340	0.8809	0.8161	0.5567	0.0518	0.9600	0.8737	0.9604
Sr	0.2807	0.9473	0.8634	0.6998	0.8303	0.6331	0.8089	0.9189	0.9600
Nd	0.9013	0.9838	0.9959	0.9593	0.9634	0.9749	0.9675	0.9687	0.9946
Zr	0.9714	0.9950	0.9997	0.9455	0.9985	0.9964	0.9948	0.9983	0.9995
Hf	0.9702	0.9958	0.9967	0.9897	0.9969	0.9971	0.9968	0.9958	1.0000
Sm	0.9579	0.9935	0.9996	0.9852	0.9895	0.9946	0.9838	0.9889	0.9982
Eu	0.9741	0.9954	0.9998	0.9931	0.9973	0.9939	0.9916	0.9943	0.9988
Y	0.9999	1.0000	0.9998	0.9998	0.9992	0.9978	0.9996	0.9995	0.9999
Yb	1.0000	1.0000	1.0000	1.0000	1.0000	1.0000	1.0000	1.0000	1.0000
Lu	0.9974	1.0000	0.9999	0.9999	0.9999	0.9995	1.0000	0.9994	1.0000

Table E.45 Fraction of ingoing slab material incorporated into mantle assuming doubled crustal addition rate and 20% partial melting of IAV source, low –K magma series.

	Aleutians	Central America	Izu-Bonin	Kurile	Marianas	Northern Antilles	Southern Antilles	Sunda-Java	Tonga
K	0.9770	0.9989	0.8188	0.9773	0.9845	0.9636	0.9795	n.d.	0.9672
Rb	0.9672	0.9960	0.8805	0.9907	0.9800	0.9737	0.9869	n.d.	0.9489
Ba	0.9801	0.9991	-0.3954	0.9593	0.9361	0.7873	0.9381	n.d.	0.9444
Th	0.9922	0.9999	0.9515	0.9755	0.9848	0.9771	0.9772	n.d.	0.9711
U	0.9837	0.9999	0.9457	0.9751	0.9886	0.9663	0.9827	n.d.	0.9716
Nb	0.9997	0.9986	0.9999	0.9998	0.9994	0.9883	0.9919	n.d.	0.9916
Ta	0.9759	1.0000	0.8312	0.9978	0.9999	0.9953	0.9955	n.d.	0.9946
La	0.9848	0.9994	0.9820	0.9934	0.9933	0.9836	0.9869	n.d.	0.9885
Ce	0.9863	0.9992	0.9829	0.9933	0.9948	0.9878	0.9906	n.d.	0.9894
Pb	0.9374	0.9999	0.5535	0.9827	0.9704	0.9295	0.9837	n.d.	0.9629
Sr	0.9474	0.9985	0.6883	0.9596	0.9816	0.9169	0.9664	n.d.	0.9658
Nd	0.9942	0.9996	0.9953	0.9999	0.9985	0.9954	0.9951	n.d.	0.9973
Zr	0.9987	0.9999	0.9953	0.9999	0.9991	0.9986	0.9995	n.d.	0.9993
Hf	0.9970	0.9998	0.9906	1.0000	1.0000	0.9992	0.9990	n.d.	0.9988
Sm	0.9970	0.9997	0.9998	0.9994	0.9992	0.9989	0.9966	n.d.	0.9996
Eu	0.9969	0.9998	0.9997	0.9995	1.0000	0.9985	0.9995	n.d.	0.9988
Y	0.9907	1.0000	0.9925	0.9988	1.0000	0.9996	0.9999	n.d.	0.9973
Yb	1.0000	1.0000	1.0000	1.0000	1.0000	1.0000	1.0000	n.d.	1.0000
Lu	1.0000	0.9998	0.9994	1.0000	0.9999	0.9998	0.9998	n.d.	0.9999

Table E.46 Fraction of ingoing slab material incorporated into mantle assuming doubled crustal addition rate and 5% partial melting of IAV source, high –K magma series.

	Aleutians	Central America	Izu-Bonin	Kurile	Marianas	Northern Antilles	Southern Antilles	Sunda-Java	Tonga
K	0.9652	0.9662	n/a	0.9153	n/a	n/a	0.9915	0.4166	0.9778
Rb	0.9662	0.9448	n/a	0.9358	n/a	n/a	0.9940	0.0272	0.9744
Ba	0.9807	0.9908	n/a	0.9069	n/a	n/a	0.9686	0.5821	0.9653
Th	0.9720	0.9018	n/a	0.9500	n/a	n/a	0.9755	0.1943	0.9942
U	0.9918	0.9627	n/a	0.9199	n/a	n/a	0.9789	0.2024	0.9932
Nb	0.9798	0.9819	n/a	0.9996	n/a	n/a	0.9939	0.8692	0.9864
Ta	0.9952	0.9821	n/a	n/a	n/a	n/a	0.9966	0.9538	0.9983
La	0.9897	0.9755	n/a	0.9878	n/a	n/a	0.9892	0.4013	0.9915
Ce	0.9924	0.9814	n/a	0.9934	n/a	n/a	0.9905	0.6193	0.9933
Pb	0.9884	0.9848	n/a	0.9854	n/a	n/a	0.9957	0.6410	0.9933
Sr	0.9890	0.9898	n/a	0.9729	n/a	n/a	0.9777	0.7144	0.9931
Nd	0.9931	0.9920	n/a	0.9944	n/a	n/a	0.9943	0.8049	0.9973
Zr	0.9987	0.9977	n/a	0.9987	n/a	n/a	0.9978	0.9738	0.9999
Hf	0.9994	0.9980	n/a	0.9976	n/a	n/a	0.9983	0.9906	1.0000
Sm	0.9959	0.9963	n/a	0.9959	n/a	n/a	0.9972	0.9165	0.9983
Eu	0.9981	0.9982	n/a	0.9986	n/a	n/a	n/a	0.9493	0.9990
Y	0.9997	0.9998	n/a	1.0000	n/a	n/a	0.9993	0.9938	0.9999
Yb	1.0000	1.0000	n/a	1.0000	n/a	n/a	1.0000	1.0000	1.0000
Lu	1.0000	0.9998	n/a	1.0000	n/a	n/a	1.0000	1.0000	1.0000

Table E.47 Fraction of ingoing slab material incorporated into mantle assuming doubled crustal addition rate and 5% partial melting of IAV source, medium –K magma series.

	Aleutians	Central America	Izu-Bonin	Kurile	Marianas	Northern Antilles	Southern Antilles	Sunda-Java	Tonga
K	0.5572	0.9294	0.9596	0.7300	0.8732	0.8506	0.9523	0.9266	0.9573
Rb	0.5827	0.9029	0.9849	0.7115	0.8605	0.8725	0.9594	0.9323	0.9470
Ba	0.7295	0.9717	0.7539	0.6813	0.5661	0.2029	0.7696	0.9292	0.9234
Th	0.7602	0.9522	0.9981	0.6863	0.9102	0.8835	0.8623	0.8971	0.9848
U	0.7579	0.9652	0.9952	0.7207	0.8965	0.8971	0.8539	0.9107	0.9845
Nb	0.9940	0.9937	0.9286	0.9995	0.9517	0.9737	0.9916	0.9999	0.9659
Ta	0.9083	0.9997	0.9809	0.9996	0.9610	0.9214	0.8063	0.9992	0.9999
La	0.8991	0.9798	0.9989	0.9356	0.9920	0.9844	0.9500	0.9687	0.9984
Ce	0.9228	0.9807	0.9997	0.9519	0.9941	0.9621	0.9675	0.9800	0.9955
Pb	0.4766	0.9427	0.9085	0.8414	0.6315	0.1163	0.9699	0.8861	0.9668
Sr	0.4268	0.9543	0.9083	0.7790	0.9067	0.7687	0.8590	0.9503	0.9775
Nd	0.9497	0.9890	0.9996	0.9811	0.9854	0.9968	0.9806	0.9818	0.9984
Zr	0.9894	0.9972	0.9998	0.9613	0.9997	0.9999	0.9988	1.0000	1.0000
Hf	0.9933	0.9984	0.9998	0.9988	0.9996	0.9978	1.0000	0.9998	0.9987
Sm	0.9733	0.9952	1.0000	0.9916	0.9954	0.9992	0.9886	0.9929	0.9993
Eu	0.9834	0.9965	1.0000	0.9965	0.9994	0.9981	0.9945	0.9966	0.9995
Y	0.9997	1.0000	0.9998	0.9999	0.9995	0.9972	0.9994	0.9993	0.9998
Yb	1.0000	1.0000	1.0000	1.0000	1.0000	1.0000	1.0000	1.0000	1.0000
Lu	0.9977	1.0000	0.9999	0.9998	0.9999	0.9996	1.0000	0.9995	1.0000

Table E.48 Fraction of ingoing slab material incorporated into mantle assuming doubled crustal addition rate and 5% partial melting of IAV source, low –K magma series.

	Aleutians	Central America	Izu-Bonin	Kurile	Marianas	Northern Antilles	Southern Antilles	Sunda-Java	Tonga
K	0.9876	0.9997	0.9204	0.9855	0.9949	0.9780	0.9889	n.d.	0.9913
Rb	0.9719	0.9966	0.9415	0.9933	0.9867	0.9782	0.9893	n.d.	0.9672
Ba	0.9817	0.9991	0.2123	0.9636	0.9491	0.8150	0.9484	n.d.	0.9605
Th	0.9982	0.9996	0.9942	0.9824	0.9980	0.9894	0.9828	n.d.	0.9949
U	0.9908	1.0000	0.9831	0.9827	0.9982	0.9804	0.9886	n.d.	0.9942
Nb	0.9688	0.9998	0.8010	0.9723	0.9601	0.9940	0.9965	n.d.	0.9798
Ta	0.9953	0.9983	0.9615	0.9903	0.9358	0.9828	0.9921	n.d.	0.9732
La	0.9983	1.0000	0.9933	0.9999	0.9974	1.0000	0.9992	n.d.	0.9991
Ce	0.9973	0.9999	0.9962	0.9998	0.9983	1.0000	0.9996	n.d.	0.9998
Pb	0.9468	0.9998	0.6582	0.9876	0.9888	0.9461	0.9900	n.d.	0.9749
Sr	0.9636	0.9990	0.8211	0.9747	0.9977	0.9523	0.9898	n.d.	0.9916
Nd	0.9984	0.9999	0.9995	0.9964	0.9998	0.9999	0.9994	n.d.	1.0000
Zr	0.9949	1.0000	0.9999	0.9983	0.9950	1.0000	0.9998	n.d.	0.9998
Hf	0.9995	1.0000	0.9998	0.9988	0.9970	0.9995	0.9998	n.d.	0.9996
Sm	0.9985	0.9998	0.9994	0.9999	1.0000	0.9999	0.9985	n.d.	1.0000
Eu	0.9980	0.9999	0.9999	0.9999	0.9999	0.9996	1.0000	n.d.	0.9997
Y	0.9914	1.0000	0.9936	0.9990	1.0000	0.9994	0.9998	n.d.	0.9970
Yb	1.0000	1.0000	1.0000	1.0000	1.0000	1.0000	1.0000	n.d.	1.0000
Lu	1.0000	0.9998	0.9996	1.0000	0.9999	0.9999	0.9998	n.d.	0.9999

REFERENCES

Albarede, F. (1998). The growth of continental crust. *Tectonophysics* **296**: 1-14.

Allegre, C. J., B. Hamelin, A. Provost, and B. Dupre (1986). Topology in isotopic multispace and origin of mantle chemical heterogeneities. *Earth and Planetary Science Letters* **81**: 319-337.

Alt, J. C. (1999). Hydrothermal alteration and mineralization of oceanic crust: mineralogy, geochemistry, and processes. *Reviews in Economic Geology* **8**: 133-155.

Alt, J. C., C. Laverne, and K. Muehlenbachs (1985). Alteration of the upper oceanic crust: mineralogy and processes in Deep Sea Drilling Project Hole 504B, Leg 83. *Initial Reports of the Deep Sea Drilling Project* **83**: 217-241.

Arai, S., K. Matsukage, E. Isobe, and S. Vysotskiy (1997). Concentration of incompatible elements in oceanic mantle: effect of melt/wall interaction in stagnant or failed melt conduits within peridotite. *Geochimica et Cosmochimica Acta* **61**: 671-675.

Aramaki, S., and T. Ui (1982). Japan. in *Andesites: Orogenic andesites and related rocks*. R. S. Thorpe. New York, Wiley-Interscience. 259-292.

Arnold, G. L., A. D. Anbar, J. Barling, and T. W. Lyons (2004). Molybdenum isotope evidence for widespread anoxia in Mid-Proterozoic oceans. *Science* **304**: 87-90.

Ayers, J. C. (1998). Trace element modeling of aqueous fluid-peridotite interaction in the mantle wedge of subduction zones. *Contributions to Mineralogy and Petrology* **132**: 390-404.

Ayers, J. C., and E. B. Watson (1991). Solubility of apatite, monazite, zircon, and rutile in supercritical aqueous fluids with implications for subduction zone geochemistry. *Philosophical Transactions of the Royal Society of London Series A: Physical Sciences and Engineering* **335**: 365-375.

Bach, W., J. C. Alt, Y. Niu, S. E. Humphris, J. Erzinger, and H. J. B. Dick (2001). The geochemical consequences of late-stage low-grade alteration of lower ocean crust at the SW Indian Ridge: Results from ODP Hole 735B (Leg 176). *Geochimica et Cosmochimica Acta* **65**: 3267-3287.

Becker, H., K. P. Jochum, and R. W. Carlson (2000). Trace element fractionation during dehydration of eclogites from high-pressure terranes and the implications for element fluxes in subduction zones. *Chemical Geology* **163**: 65-99.

Bindeman, I. N., and J. C. Bailey (1999). Trace elements in anorthite megacrysts from the Kurile Island Arc: a window to across-arc geochemical variations in magma compositions. *Earth and Planetary Science Letters* **169**: 209-226.

Brenan, J. M., F. J. Ryerson, and H. F. Shaw (1998). The role of aqueous fluids in the slab-to-mantle transfer of boron, beryllium, and lithium during subduction: experiments and models. *Geochimica et Cosmochimica Acta* **62**: 3337-3347.

Brenan, J. M., and E. B. Watson (1991). Partitioning of trace elements between olivine and aqueous fluids at high P-T conditions: implications for the effect of fluid composition on trace-element transport. *Earth and Planetary Science Letters* **107**: 672-688.

Canfield, D. (1998). A new model for Proterozoic ocean chemistry. *Nature* **396**: 450-453.

Carn, S. A., and D. M. Pyle (2001). Petrology and geochemistry of the Lamongan volcanic field, East Java, Indonesia: primitive Sunda Arc magmas in an extensional tectonic setting? *Journal of Petrology* **42**: 1643-1683.

Carr, M. J., W. I. J. Rose, and R. E. Stoiber (1982). Central America. in *Andesites: Orogenic andesites and related rocks*. R. S. Thorpe. New York, Wiley-Interscience. 149-166.

Chan, L. H., W. P. Leeman, and C.-F. You (1999). Lithium isotopic composition of Central American Volcanic Arc lavas: implications for modification of subarc mantle by slab-derived fluids. *Chemical Geology* **160**: 255-280.

Class, C., D. M. Miller, S. L. Goldstein, and C. H. Langmuir (2000). Distinguishing melt and fluid subduction components in Umnak volcanics, Aleutian Arc. *Geochemistry Geophysics Geosystems* **1**: paper # 1999GC000010.

Cole, J. W. (1982). Tonga-Kermadec-New Zealand. in *Andesites: Orogenic andesites and related rocks*. R. S. Thorpe. New York, Wiley-Interscience. 245-258.

Crisp, J. A. (1984). Rates of magma emplacement and volcanic output. *Journal of Volcanology and Geothermal Research* **20**: 177-211.

Deschamps, A., and S. Lallemand (2003). Geodynamic setting of Izu-Bonin-Mariana boninites. in *Intra-Oceanic Subduction Systems: Tectonic and Magmatic Processses*. R. D. Larter and P. T. Leat. London, Geological Society Special Publications. **219**: 163-185.

Dimalanta, C., A. Taira, G. P. J. Yumul, H. Tokuyama, and K. Mochizuki (2002). New rates of western Pacific island arc magmatism from seismic and gravity data. *Earth and Planetary Science Letters* **202**: 105-115.

Elderfield, H., C. G. Wheat, M. J. Mottl, C. Monnin, and B. Spiro (1999). Fluid and geochemical transport through oceanic crust: a transect across the eastern flank of the Juan de Fuca Ridge. *Earth and Planetary Science Letters* **172**: 151-165.

Elliott, T., T. Plank, A. Zindler, W. M. White, and B. Bourdon (1997). Element transport from slab to volcanic front at the Mariana Arc. *Journal of Geophysical Research B* **102**: 14991-15019.

Elliott, T., A. Zindler, and B. Bourdon (1999). Exploring the kappa conundrum: the role of recycling in the lead isotope evolution of the mantle. *Earth and Planetary Science Letters* **169**: 129-145.

Foley, S. F., S. Buhre, and D. E. Jacob (2003). Evolution of the Archean crust by delamination and shallow subduction. *Nature* **421**: 249-252.

Ghiorso, M. S. (1985). Chemical mass transfer in magmatic processes I. Thermodynamic relations and numerical algorithms. *Contributions to Mineralogy and Petrology* **90**: 107-120.

Ghiorso, M. S., and R. O. Sack (1995). Chemical mass transfer in magmatic processes IV. A revised and internally consistent thermodynamic model for the interpolation and extrapolation of liquid-solid equilibria in magmatic systems at elevated temperatures and pressures. *Contributions to Mineralogy and Petrology* **119**: 197-212.

Gillis, K. M., J. N. Ludden, T. Plank, and L. D. Hoy (1992). Low-temperature alteration and subsequent reheating of shallow oceanic crust at Hole

765D, Argo abyssal plain. *Proceedings of the Ocean Drilling Program Scientific Results* **123**: 191-199.

Hannigan, R. E., A. R. Basu, and F. Leichmann (2001). Mantle reservoir geochemistry from statistical analysis of ICP-MS trace element data of equatorial mid-Atlantic MORB glasses. *Chemical Geology* **175**: 397-428.

Harbert, W. (1987). Tectonics of Alaska, plate tectonics of the Pacific basin, and paleomagnetism of the Aleutian Arc. Stanford, California, Stanford University. 313 pp.

Hart, S. R., and H. Staudigel (1989). Isotopic characterization and identification of recycled components. in *Crust/mantle recycling at convergence zones*. S. R. Hart and L. Gulen. Boston, Massachusetts, Kluwer Academic Publishers. 15-28.

Hart, S. R., and A. Zindler (1989). Constraints on the nature and development of chemical heterogeneities in the mantle. *The Fluid Mechanics of Astrophysics and Geophysics* **4**: 261-387.

Hawkesworth, C. J., J. M. Hergt, R. M. Ellam, and F. McDermott (1991). Element fluxes associated with subduction related magmatism. *Philosophical Transactions of the Royal Society of London Series A: Physical Sciences and Engineering* **335**: 393-405.

Hawkesworth, C. J., S. P. Turner, F. McDermott, D. W. Peate, and P. van Calsteren (1997a). U-Th isotopes in arc magmas: implications for element transfer from the subducted crust. *Science* **276**: 551-555.

Hawkesworth, C. J., S. P. Turner, D. W. Peate, F. McDermott, and P. van Calsteren (1997b). Elemental U and Th variations in island arc rocks: implications for U-series isotopes. *Chemical Geology* **139**: 207-221.

Hochstaedter, A., J. Gill, R. Peters, P. Broughton, and P. Holden (2001). Across-arc geochemical trends in the Izu-Bonin arc: contributions from the subducting slab. *Geochemistry Geophysics Geosystems* **2**: paper # 2000GC000105.

Hofmann, A. W. (1988). Chemical differentiation of the Earth: the relationship between mantle, continental crust, and oceanic crust. *Earth and Planetary Science Letters* **90**: 297-314.

Holm, P. M. (2002). Data report: on the composition of the lower ocean crust -- major and trace element analyses of gabbroic rocks from Hole 735B, 500-1500 mbsf. *Proceedings of the Ocean Drilling Program Scientific Results* **176**: 1-13.

Hutchison, C. S. (1982). Indonesia. in *Andesites: Orogenic andesites and related rocks*. R. S. Thorpe. New York, John Wiley & Sons. 207-224.

Ito, E., W. M. White, and C. Gopel (1987). The O, Sr, Nd, and Pb isotope geochemistry of MORB. *Chemical Geology* **62**: 157-176.

Jacobsen, S. B. (1989). Isotopic and chemical signatures of recycled oceanic and continental crust. in *Crust/mantle recycling at convergence zones*. S. R. Hart and L. Gulen. Boston, Massachusetts, Kluwer Academic Publishers. 181-182.

Jacobsen, S. B., and A. J. Kaufman (1999). The Sr, C and O isotopic evolution of Neoproterozoic seawater. *Chemical Geology* **161**: 37-57.

Jiedong, Y., S. Weiguo, W. Zongzhe, X. Yaosong, and T. Xiancong (1999). Variations in Sr and C isotopes and Ce anomalies in successions from China: evidence for the oxygenation of Neoproterozoic seawater? *Precambrian Research* **93**: 215-233.

Johnson, M. C., and T. Plank (1999). Dehydration and melting experiments constrain the fate of subducted sediments. *Geochemistry Geophysics Geosystems* **1**: paper # 1999GC000014.

Juteau, T., and R. C. Maury (1999). *The Oceanic Crust, from Accretion to Mantle Recycling*. Chichester, U.K., Praxis Publishing/Springer-Verlag 390 pp.

Kah, L. C., T. W. Lyons, and J. T. Chesley (2001). Geochemistry of a 1.2 Ga carbonate-evaporite succession, northern Baffin and Bylot Islands: implications for Mesoproterozoic marine evolution. *Precambrian Research* **111**: 203-234.

Kamenetsky, V. S., A. J. Crawford, S. Eggins, and R. Muhe (1997). Phenocryst and melt inclusion chemistry of near-axis seamounts, Valu Fa Ridge, Lau Basin: insight into mantle wedge melting and the addition of subduction components. *Earth and Planetary Science Letters* **151**: 205-223.

Kastner, M., H. Elderfield, and J. B. Martin (1991). Fluids in convergent margins: what do we know about their composition, origin, role in diagenesis and importance for oceanic chemical fluxes? *Philosophical Transactions of the Royal Society of London Series A: Physical Sciences and Engineering* **335**: 243-259.

Kay, R. W., and S. M. Kay (1988). Crustal recycling and the Aleutian arc. *Geochimica et Cosmochimica Acta* **52**: 1351-1359.

Kay, S. M., E. Godoy, and A. Kurtz (2005). Episodic arc migration, crustal thickening, subduction erosion, and magmatism in the south-central Andes. *Geological Society of America Bulletin* **117**: 67-88.

Kelley, K. A. (2004). Trench inputs and arc outputs in the Mariana-Izu-Bonin subduction factory. Boston, Massachusetts, Boston University. 259 pp.

Kinzler, R. J., and T. L. Grove (1993). Corrections and further discussion of the primary magmas of mid-ocean ridge basalts, 1 and 2. *Journal of Geophysical Research B* **98**: 22339-22347.

Kogiso, T., Y. Tatsumi, and S. Nakano (1997). Trace element transport during dehydration processes in the subducted oceanic crust: 1. Experiments and implications for the origin of ocean island basalts. *Earth and Planetary Science Letters* **148**: 193-205.

Le Maitre, R. W. (2002). *Igneous Rocks: A Classification and Glossary of Terms*. Cambridge, UK, Cambridge University Press 236 pp.

Macpherson, C. G., and R. Hall (1999). *Tectonic controls of geochemical evolution in arc magmatism of SE Asia*. 4th PACRIM Congress, Australian Institute of Mining and Metallurgy.

Maehr, S. A. (1997). Trace element geochemistry of the arc lavas from volcanoes northwest and southeast of the Quesada Sharp Contortion, the Central American volcanic arc. Albuquerque, NM, University of New Mexico. 62 pp.

Marsh, B. D. (1982). The Aleutians. in *Andesites: Orogenic andesites and related rocks*. R. S. Thorpe. New York, Wiley-Interscience. 99-114.

Marty, B., and N. Dauphas (2003). The nitrogen record of crust-mantle interaction and mantle convection from Archean to Present. *Earth and Planetary Science Letters* **206**: 397-410.

McCulloch, M. T. (1993). The role of subducted slabs in an evolving Earth. *Earth and Planetary Science Letters* **115**: 89-100.

McCulloch, M. T., and J. Gamble (1991). Geochemical and geodynamical constraints on subduction zone magmatism. *Earth and Planetary Science Letters* **102**: 358-374.

McDonough, W. F., and S.-s. Sun (1995). The composition of the Earth. *Chemical Geology* **120**: 223-253.

Meijer, A. (1982). Mariana-Volcano Islands. in *Andesites: Orogenic andesites and related rocks*. R. S. Thorpe. New York, Wiley-Interscience. 293-306.

Morency, C., M.-P. Doin, and C. Dumoulin (2002). Convective destabilization of a thickened continental lithosphere. *Earth and Planetary Science Letters* **202**: 303-320.

Parkinson, I. J., and R. J. Arculus (1999). The redox state of subduction zones: insights from arc-peridotites. *Chemical Geology* **160**: 409-423.

Paul, D., W. M. White, and D. L. Turcotte (2002). Modelling the isotopic evolution of the Earth. *Philosophical Transactions of the Royal Society of London Series A: Physical Sciences and Engineering* **360**: 2433-2474.

Peacock, S. M. (1990). Fluid processes in subduction zones. *Science* **248**: 329-337.

Peacock, S. M., T. Rushmer, and A. B. Thompson (1994). Partial melting of subducting oceanic crust. *Earth and Planetary Science Letters* **121**: 227-244.

Pearce, J. A. (1982). Trace element characteristics of lavas from destructive plate boundaries. in *Andesites*. R. S. Thorpe. New York, New York, John Wiley & Sons. 525-548.

Plank, T. (2005). Constraints from Thorium/Lanthanum on Sediment Recycling at Subduction Zones and the Evolution of the Continents. *Journal of Petrology* doi: 10.1093/petrology/egi005.

Plank, T., and C. H. Langmuir (1998). The chemical composition of subducting sediment and its consequences for the crust and mantle. *Chemical Geology* **145**: 325-394.

Prueher, L. M., and D. K. Rea (2001). Tephrochronology of the Kamchatka-Kurile and Aleutian arcs: evidence for volcanic episodicity. *Journal of Volcanology and Geothermal Research* **106**: 67-84.

Rea, D. K., and L. J. Ruff (1996). Composition and mass flux of sediment entering the world's subduction zones: implications for global sediment budgets, great earthquakes, and volcanism. *Earth and Planetary Science Letters* **140**: 1-12.

Rea, W. J. (1982). The Lesser Antilles. in *Andesites: Orogenic andesites and related rocks*. R. S. Thorpe. New York, Wiley-Interscience. 167-186.

Sack, R. O., and M. S. Ghiorso (1994). Thermodynamics of multicomponent pyroxenes: I. Formulation of a general model. *Contributions to Mineralogy and Petrology* **116**: 277-286.

Salters, V. J. M., and A. Stracke (2004). Composition of the depleted mantle. *Geochemistry Geophysics Geosystems* **5**(Q05004): doi:10.1029/2003GC000597.

Saunders, A. D., M. J. Norry, and J. Tarney (1991). Fluid influence on the trace element compositions of subduction zone magmas. *Philosophical Transactions of the Royal Society of London Series A: Physical Sciences and Engineering* **335**: 377-392.

Shaw, A. M. (2003). Noble gas and major volatile systematics of the Manus Back-arc Basin and the Central American Arc: tracing source mixing, contamination and degassing. San Diego, CA, University of California. 210 pp.

Shen, Y., A. H. Knoll, and M. R. Walter (2003). Evidence for low sulphate and anoxia in a mid-Proterozoic marine basin. *Nature* **423**: 632-635.

Sims, K. W. W., and D. J. DePaolo (1997). Inferences about mantle magma sources from incompatible element concentration ratios in oceanic basalts. *Geochimica et Cosmochimica Acta* **61**: 765-784.

Staudigel, H., and S. D. King (1992). Ultrafast subduction: the key to slab recycling efficiency and mantle differentiation? *Earth and Planetary Science Letters* **109**: 517-530.

Staudigel, H., T. Plank, W. M. White, and H.-U. Schmincke (1996). Geochemical fluxes during seafloor alteration of the basaltic upper oceanic crust: DSDP Sites 417 and 418 (overview). in *Subduction: Top to Bottom*. G. E. Bebout, D. W. Scholl, S. H. Kirby and J. P. Platt. Washington, D.C., American Geophysical Union. **96**: 19-38.

Straub, S. M. (2003). The evolution of the Izu Bonin-Mariana volcanic arcs (NW Pacific) in terms of major element chemistry. *Geochemistry Geophysics Geosystems* **4**: doi: 10.1029/2002GC000357.

Straub, S. M., and G. D. Layne (2003). Decoupling of fluids and fluid-mobile elements during shallow subduction: evidence from halogen-rich andesite melt inclusions from the Izu arc volcanic front. *Geochemistry Geophysics Geosystems* **4**: doi: 10.1029/2002GC000349.

Straub, S. M., G. D. Layne, A. Schmidt, and C. H. Langmuir (2004). Volcanic glasses at the Izu arc volcanic front: new perspectives on fluid and

sediment melt recycling in subduction zones. *Geochemistry Geophysics Geosystems* **5**: doi: 10.1029/2002GC000408.

Sun, S.-s., and W. F. McDonough (1989). Chemical and isotopic systematics of oceanic basalts: implications for mantle composition and processes. in *Magmatism in the Ocean Basins*. A. D. Saunders and M. J. Norry. **42**: 313-345.

Tatsumi, Y. (1989). Migration of fluid phases and genesis of basalt magmas in subduction zones. *Journal of Geophysical Research B* **94**: 4697-4707.

Tatsumi, Y. (2000). Continental crust formation by crustal delamination in subduction zones and complementary accumulation of the enriched mantle I component in the mantle. *Geochemistry Geophysics Geosystems* **1**: paper# 2000GC000094.

Tatsumi, Y., and S. Eggins (1995). *Subduction Zone Magmatism*. Oxford, UK, Blackwell Science 211 pp.

Tatsumi, Y., D. L. Hamilton, and R. W. Nesbitt (1986). Chemical characteristics of fluid phase released from a subducted lithosphere and origin of arc magmas: evidence from high-pressure experiments and natural rocks. *Journal of Volcanology and Geothermal Research* **29**: 293-309.

Tatsumi, Y., M. Sakuyama, H. Fukuyama, and I. Kushiro (1983). Generation of arc basalt magmas and thermal structure of the mantle wedge in subduction zones. *Journal of Geophysical Research B* **88**: 5815-5825.

Taylor, R. N., and R. W. Nesbitt (1998). Isotopic characteristics of subduction fluids in an intra-oceanic setting, Izu-Bonin Arc, Japan. *Earth and Planetary Science Letters* **16**: 79-98.

Turner, S. P., and C. J. Hawkesworth (1997). Constraints on flux rates and mantle dynamics beneath island arcs from Tonga-Kermadec lava geochemistry. *Nature* **389**: 568-573.

Turner, S. P., C. J. Hawkesworth, N. Rogers, J. Bartlett, T. Worthington, J. M. Hergt, J. A. Pearce, and I. Smith (1997). 238U-232Th disequilibria, magma petrogenesis, and flux rates beneath the depleted Tonga-Kermadec island arc. *Geochimica et Cosmochimica Acta* **61**: 4855-4884.

Utzmann, A., T. H. Hansteen, and H.-U. Schmincke (2002). Trace element mobility during sub-seafloor alteration of basaltic glass from Ocean Drilling Program site 953 (off Gran Canaria). *International Journal of the Earth Sciences (Geologisch Rundschau)* **91**: 661-679.

van Thienen, P., A. P. van den Berg, and N. J. Vlaar (2004). Production and recycling of oceanic crust in the early Earth. *Tectonophysics* **386**: 41-65.

Veizer, J., D. Ala, K. Azmy, P. Bruckschen, D. Buhl, F. Bruhn, G. A. F. Carden, A. Diener, S. Ebneth, Y. Godderis, T. Jasper, C. Korte, F. Pawellek, O. G. Podlaha, and H. Strauss (1999). 87Sr/86Sr, [del]13C and [del]18O evolution of Phanerozoic seawater. *Chemical Geology* **161**: 59-88.

Vidal, P., C. Dupuy, R. C. Maury, and M. Richard (1989). Mantle metasomatism above subduction zones: trace-element and radiogenic isotope characteristics of peridotite xenoliths from Batan Island (Philippines). *Geology* **17**: 1115-1118.

von Huene, R., D. Klaeschen, M. Gutscher, and J. Fruehn (1998). Mass and fluid flux during accretion at the Alaskan margin. *Geological Society of America Bulletin* **110**: 468-482.

von Huene, R., C. Ranero, and P. Vannucchi (2004). Generic model of subduction erosion. *Geology* **32**: 913-916.

von Huene, R., and D. W. Scholl (1991). Observations at convergent margins concerning sediment subduction, subduction erosion, and the growth of continental crust. *Reviews of Geophysics* **29**: 279-316.

Wedepohl, K. H. (1995). The composition of the continental crust. *Geochimica et Cosmochimica Acta* **59**: 1217-1232.

Wedepohl, K. H., and G. Hartmann (1994). The composition of the primitive upper Earth's mantle. in *Kimberlites, related rocks, and mantle xenoliths: Proceedings of the 5th international kimberlite conference*. H. O. A. Meyer and O. H. Leonardo. Rio de Janeiro, Brazil, Companhia de Pesquisa de Recursos Minerais. 486-495.

White, W. M. (1989). Geochemical evidence for crust-to-mantle recycling in subduction zones. in *Crust/mantle recycling at convergence zones*. S. R. Hart and L. Gulen. Boston, Kluwer Academic Publishers. 43-58.

White, W. M. (1995). Geochemical tracers of mantle processes. *Reviews of Geophysics Supplement*: 19-24.

White, W. M., and R. A. Duncan (1996). Geochemistry and geochronology of the Society Islands: new evidence for deep mantle recycling. in *Earth Processes: reading the isotopic code*. Washington, DC, American Geophysical Union. **95**: 183-206.

White, W. M., and A. W. Hofmann (1982). Sr and Nd isotope geochemistry of oceanic basalts and mantle evolution. *Nature* **296**: 821-825.

Workman, R. K., S. R. Hart, M. Jackson, M. Regelous, K. A. Farley, J. Blusztajn, M. Kurz, and H. Staudigel (2004). Recycled metasomatized lithosphere as the origin of the Enriched Mantle II (EM2) end-member: Evidence from the Samoan volcanic chain. *Geochemistry Geophysics Geosystems* **5**: doi:10.1029/2003GC000623.

Yogodzinski, G. M., R. W. Kay, O. N. Volynets, A. V. Koloskov, and S. M. Kay (1995). Magnesian andesite in the western Aleutian Komandorsky region: implications for slab melting and processes in the mantle wedge. *Geological Society of America Bulletin* **107**: 505-519.

Yogodzinski, G. M., and P. B. Keleman (1998). Slab melting in the Aleutians: implications of an ion probe study of clinopyroxene in primitive adakite and basalt. *Earth and Planetary Science Letters* **158**: 53-65.

Yogodzinski, G. M., J. M. Lees, T. G. Churlkova, F. Dorendorf, G. Woerner, and O. N. Volynets (2001). Geochemical evidence for the melting of subducting oceanic lithosphere at plate edges. *Nature* **409**: 500-504.

You, C.-F., P. R. Castillo, J. M. Gieskes, H. L. Chan, and A. J. Spivak (1996). Trace element behavior in hydrothermal experiments: implications for fluid processes at shallow depths in subduction zones. *Earth and Planetary Science Letters* **140**: 41-52.